

โครงการ

กลศาสตร์ของท่อลำเลียงของใหลที่ยึดหดตัวได้ในสามมิติ (Mechanics of Three-Dimensional Extensible Marine Risers Transporting Fluid)

โดย ศ. ดร. สมชาย ชูชีพสกุล และคณะ

รายงานวิจัยฉบับสมบูรณ์

โครงการกลศาสตร์ของท่อลำเลียงของใหลที่ยืดหดตัวได้ในสามมิติ (MECHANICS OF THREE-DIMENSIONAL EXTENSIBLE MARINE RISERS TRANSPORTING FLUID)

	คณะผู้วิจัย	สังกัด
1.	ศ. คร. สมชาย ชูชีพสกุล	มหาวิทยาลัยเทคโนโลยีพระจอมเกล้าธนบุรี
2.	รศ. คร. นคร ภู่วโรคม	มหาวิทยาลัยธรรมศาสตร์
3.	คร. ทินกร มนฅ์ประภัสสร	มหาวิทยาลัยเอเชียอาคเนย์
4.	คร. จุลพจน์ จิรวัชรเคช	มหาวิทยาลัยเทคโนโลยีพระจอมเกล้าธนบุรี
5.	คร. หูชัย สุจิรวรกุล	มหาวิทยาลัยเทคโนโลยีพระจอมเกล้าชนบุรี
6.	นายบุญชัย ผึ้งใผ่งาม	สูนย์กลางสถาบันเทคโนโลยีราชมงคล
7.	นางสุชาคา ไวยวุทธิ	มหาวิทยาลัยเทคโนโลยีพระจอมเกล้าธนบุรี
8.	นายทวิช พูลเงิน	มหาวิทยาลัยเทคโนโลยีพระจอมเกล้าธนบุรี
9.	นายบุญมี ชินนาบุญ	มหาวิทยาลัยเทคโนโลยีพระจอมเกล้าธนบุรี
10	. นายนรากร ศรีนิล	มหาวิทยาลัยเทคโนโลยีพระจอมเกล้าชนบุรี
11	. นายชัยณรงค์ อธิสกุล	มหาวิทยาลัยเทคโนโลยีพระจอมเกล้าธนบุรี
12	. นายสุรเคช แก้วประเสริฐ	มหาวิทยาลัยเทคโนโลยีพระจอมเกล้าธนบุรี
13	. นายชัยนันทน์ มะชรา	มหาวิทยาลัยเทค ใน โลยีพระจอมเกล้าชนบุรี
14	. นาย อรุณ สุวรรณชีวะศิริ	มหาวิทยาลัยเทค โน โลยีพระจอมเกล้าธนบุรี
15	. นายยศ สมพรเจริญสุข	มหาวิทยาลัยเทค โน โลยีพระจอมเกล้าชนบุรี
16	. นายศักดิ์รัตน์ แก้วอุ่นเรือน	กรมโยชาชิการ
17	'. นายไพโรจน์ วรรณสวัสคิ้กุล	หน่วยงานเอกชน
18	. นายปริญญา แซ่อุ๋ย	หน่วยงานเอกชน

สนับสนุนโดยสำนักงานกองทุนสนับสนุนการวิจัย

19. นายสุวิทย์ รัตนศรีกูล หน่วยงานเอกชน

ABSTRACT

This research presents a three-dimensional model formulation of extensible marine risers/pipes transporting fluid and parametric studies of the effects of axial deformation and internal flow on the behaviors of risers/pipes. The variational model formulation is developed based on the new idea employing from the axially deformable elastica theory and from the view of continuum mechanics in three descriptions namely, the total Lagrangian, the updated Lagrangian, and the Eulerlian. By the principle of virtual work-energy, the governing dynamic equilibrium equations are derived in the Cartesian coordinate and are validated by the vectorial summation of forces and moments. Based on the hybrid approach and the state space formulation, the finite element method is used to solve these equations. The three-dimensional nonlinear static analysis and the two-dimensional dynamic analysis are carried out in order to explore these effects on the nonlinear static behavior, the dynamic stability, and the nonlinear oscillations of the pipe under a tidal current and a regular incoming wave, respectively. The parametric studies have demonstrated the effects of axial deformation and fluid transportation in many points of view. The results of this study show that the axial deformation reduces large deflections and nonlinear responses of the pipe, but increases the static and dynamic stabilities of the pipe, while the transported fluid affects on the contrary. The advantages of the present model are related to the flexibility offered in choosing the independent variable, and to the possibility of applying them to numerous elastica problems, including some biomechanics applications.

KEYWORDS: Three-dimensional Marine Risers / Large Strain Formulations / Variational Formulation / Elastica / Transported Fluid / Finite Element Method

บทคัดย่อ

งวนวิจัยนี้เสนอแบบจำลองของท่อลำเลียงของไหลที่ยืดตัวได้ในสามมิติและการศึกษาผล กระทบของการยืดตัวมากในแนวแกนและผลกระทบเนื่องจากของไหลภายในท่อที่มีต่อพลติกรรมของ ท่อ แบบจำลองดังกล่าวได้พัฒนาขึ้นจากวิธีการแปรผันและทฤษฎีอีลาสติคคาที่เสียรูปได้มากในแนว แกนซึ่งอยู่บนพื้นฐานกลศาสตร์วัสคุที่เสียรูปได้ โดยพิจารณามุมมองแบบโททอลลากรองจ์ อัพเคท ลากรองจ์ และออยเลอร์ จากหลักการพลังงานเสมือนทำให้ได้มาซึ่งสมการสมคุลเชิงพลศาสตร์ซึ่ง ครอบคลุมปัญหาในระบบพิกัดการ์ทีเซียน ความถูกต้องของสมการซึ่งครอบคลุมปัญหานี้ได้รับ การตรวสอบ โดยการพิจารณาสมคุลของแรงและ โมเมนต์ที่กระทำต่อชิ้นส่วนท่อลำเลียงในสภาวะการ เคลื่อนที่ซึ่งขึ้นกับเวลา การแก้สมการเหล่านี้กระทำโดยใช้วิธีการไฟในต์เอลิเมนต์ในการคำนวณและ วิเคราะห์ผลทางสถิตศาสตร์ในสามมิติ และผลทางพลศาสตร์ในสองมิติ ผลจากการวิเคราะห์ทำให้ สามารถศึกษาผลกระทบของการเสียรูปมากในแนวแกน และผลกระทบของการลำเลียงของไหลในท่อ ที่มีต่อพฤติกรรมแบบสถิตที่ไม่เป็นเชิงเส้น และเสถียรภาพเชิงพลศาสตร์ รวมถึงพฤติกรรมการสั่นแบบ ไม่เป็นเชิงเส้นของท่อลำเลียงของไหลในทะเลภายใต้กระแสน้ำและสภาวะคลื่นปกติ ผลการวิเคราะห์ สรุปได้ดังนี้ การเสียรูปในแนวแกนของท่อลำเลียงทำให้การแอ่นตัวมากมีค่าลดลง และการตอบสนอง แบบไม่เป็นเชิงเส้นต่างๆมีค่าลดลง ประกอบกับทำให้เสถียรภาพของท่อมีค่ามากขึ้น ในขณะที่การ ลำเลียงของไหลภายในท่อให้ผลกระทบในทางตรงกันข้าม แบบจำลองนี้มีจุดเด่นอยู่ที่ความสะควกใน การเลือกใช้ตัวแปรอิสระให้เข้ากับการวิเคราะห์ปัญหาในแต่ละประเภท นอกจากนี้ยังมีความเป็นไปได้ ที่จะประยุกต์ใช้กับปัญหาบางอย่างในกลศาสตร์ชีวภาพ และปัญหาแบบต่างๆอีกมากในกลศาสตร์ของ โครงสร้างอีลาสติคคา

กำลำคัญ: ท่อลำเลียงของไหลในทะเลที่เสียรูปในสามมิติ / แบบจำลองที่พิจารณาความเครียดมีค่า มาก / วิธีการแปรผัน / อีลาสติคคา / การลำเลียงของไหล / วิธีการไฟในต์เอลิเมนต์

EXECUTIVE SUMMARY

RESESEARCH SIGNIFICANCE AND PROBLEM STATEMENT

The increase of global energy consumption in recent years has urged to find the new resources and leaded to the exploration of underwater resources in the ultra deep ocean. This situation has prompted a substantial level of research activity in the fields of deep offshore engineering and marine technology. Exploration in the very deep ocean required more sophisticated equipment as well as the structural system that can withstand severe environments than those in normal condition. The exploration system, which is commonly used in the operations, is the floating structure or platform, which has marine riser as a linkage between the structure and sea floor. Thus, marine riser is the major component of the offshore/ocean drilling system and it serves two main purposes; one is to convey fluid, the other is to guide the drilling string from the platform to the wellhead at the sea floor. A failure of the riser system cause not only severe environmental pollution but also significant financial consequences. Recent offshore technology development has revealed that the marine riser has been used for water depths greater than 1000 m. This challenges the researchers and design engineers to enhance the performance of the marine riser, thus researchers and engineers must have a complete understanding of the behavior of marine riser to be operated in the ultra deep ocean.

OBJECTIVE OF RESEARCH

The objectives of this research project are as follows.

- 1. To develop a 3-D model formulation of marine riser/pipe experiencing large displacement and large axial deformation in three-dimensional space based on the virtual work-energy principle and elastica theory.
- 2. To study the effect of large strain deformation and fluid transportation on static equilibrium configurations and dynamic behaviors of the riser/pipe.
- 3. To investigate structural motion stability of the riser.
- 4. To study the response of the riser due to current and wave forces.

RESEARCH METHODOLOGY AND RESULTS

Based on the variational formulation, the total virtual work of the riser consists of the virtual work of the internal forces of the riser and the virtual work done of the external forces acting on the riser. The virtual work of the internal forces composes of the strain energies due to large axial, bending, and twisting deformations. The virtual work of the external forces composes of the virtual work of the apparent weight, hydrodynamics pressure, and inertia of the pipe and transported fluid. Large axial strain formulation is emphasized in this research study. Three deformation descriptions, namely the total Lagragian, the updated Lagragian, and the Eulerian, are used to obtain the variational formulation for three different views. The apparent tension concept and the dynamic interactions between fluid and pipe are used to derive the virtual work of the external forces of the riser pipe. The formulation is validated by the vectorial formulation, which considers the equilibrium of forces and moments of a three-dimensional riser/pipe segment.

The numerical investigation presented in this research report covers two main results; the first is of 3-D static analysis and the other is of 2-D dynamic analysis. The finite element method based on the updated Lagrangian formulation is used to solve the problem numerically for both static and dynamic analyses.

The catenary cable and the nonlinear beam problems are used to verify and validate of the model and accuracy of the computer program developed in this work. Several numerical examples of the 3-D static analysis are presented to demonstrate the significance of the large axial and nonlinear deformation of the riser. For 2-D dynamic analysis, a thorough investigation has been carried out for the effects of large axial deformation and transported fluid on the natural frequencies as well as on the nonlinear response of the riser due to current and wave forces. Stability of motion of the linearized system is explained based on the Liapunov stability definitions for the cases of stable and unstable motions.

FUTURE WORK AND RECOMMENDATION

The numerical results for 3-D marine riser have been reported only for the case of large displacement static analysis, which excludes the effect of torsional deformation. However, a thorough investigation the effects of large axial deformation and internal fluid flow on nonlinear static and nonlinear dynamic behaviors has yet to be done and will be carried out in the near future. The model formulation developed in this study can readily handle for the aforementioned cases but it requires extensive numerical investigation. Such investigation for the 3-D riser has not been reported elsewhere in the open literature. Finally, there is a possibility of applying the model formulation developed in this research study, with some modifications, to some biomechanics problems such as the three-dimensional structure of supercoiled DNA, and arteries and veins conveying fluid blood inside the human body.

กิตติกรรมประกาศ

คณะผู้วิจัยใคร่ขอขอบคุณสำนักงานกองทุนสนับสนุนการวิจัย (สกว.) ที่ให้การ สนับสนุนเงินทุนวิจัยในนามของทุนเมธีวิจัยอาวุโสภายใต้ โครงการกลศาสตร์ของท่อลำเลียงของ ไหลที่ยืดหดตัวได้ในสามมิติ โดยมี ศาสตราจารย์ คร. สมชาย ชูชีพสกุล เป็นหัวหน้าโครงการ และขอขอบคุณมหาวิทยาลัยเทคโนโลยีพระจอมเกล้าธนบุรี และภาควิชาวิศวกรรมโยธา ที่ให้การ สนับสนุนในค้านสถานที่รวมทั้งค่าสาธารณูปโภค

ภารกิจในการสร้างผลงานวิชาการรวมทั้งการสร้างนักวิจัยที่มีคุณภาพจะ ไม่สามารถ เกิดขึ้นได้ หากไม่ได้รับการสนับสนุนเงินทุนวิจัยจาก สกว. ในฐานะหัวหน้าโครงการวิจัยที่ได้รับ เกียรติและความไว้วางใจจาก สกว. จึงใคร่ขอขอบคุณ สกว. ไว้ ณ โอกาสนี้

CONTENTS

	Page
Abstract	i
บทคัดย่อ	ii
Executive Summary	iii
กิตติกรรมประกาศ	vi
Contents	vii
Introduction	1
Model Formulations of Three-Dimensional Flexible Marine Risers Transporting Fluid	1 15
Solution Methods	66
Results and Discussions	87
Conclusions	121
References	123
ผลงานที่ได้จากโครงการ	133
Appendix: Reprints and Manuscripts	139

.

1. INTRODUCTION

1.1 STATEMENT OF THE PROBLEM

In the past five decades, flexible riser pipes have been employed extensively in numerous offshore engineering applications. The most vital function of these is to transport fluids that are drilled from beneath the ocean floor such as oil, gas, hydrocarbon and other crude resources, up to the production platform or drilling ship. In the deep-ocean mining industry, flexible pipes play a role of the main module in the production system as shown in Figure 1.1(a). In moderate sea-depth applications, they are often used as the secondary part in cooperating with rigid risers as shown in Figures 1.1(b) and 1.1(c).

In the literature, there are many papers related to analysis of flexible marine riser pipes as reviewed by Chakrabarti and Frampton (1982), Ertas and Kozik (1987), Jain (1994) and Patel and Seyed (1995). The mathematical riser models have been developed continually: from two-dimensional models to three-dimensional models, from linear models to nonlinear models. However, it is remarkable that most of them omit the effects of axial deformation of the pipe and fluid transportation. Furthermore, all of them did not included the nonlinear terms of the large axial strain in their model formulations.

As will be reviewed and discussed in this work, the individual effects of axial deformations, and fluid transportation could be significant to behavior of low flexible pipes. It is therefore conceivable that the combined action of all the effects becomes more important on behavior of highly flexible pipes. In such cases, those effects should be carefully examined in three-dimensional based upon the large strain analysis.

1.2 LITERATURE REVIEW

The marine riser was first used in 1949 in the Mohole project (National Engineering and Science Company, 1965), whereas the first technical paper on riser analysis was carried out by St. Denis and Armijo (1955). The numerous research papers published on this subject since may be summarized chronologically.

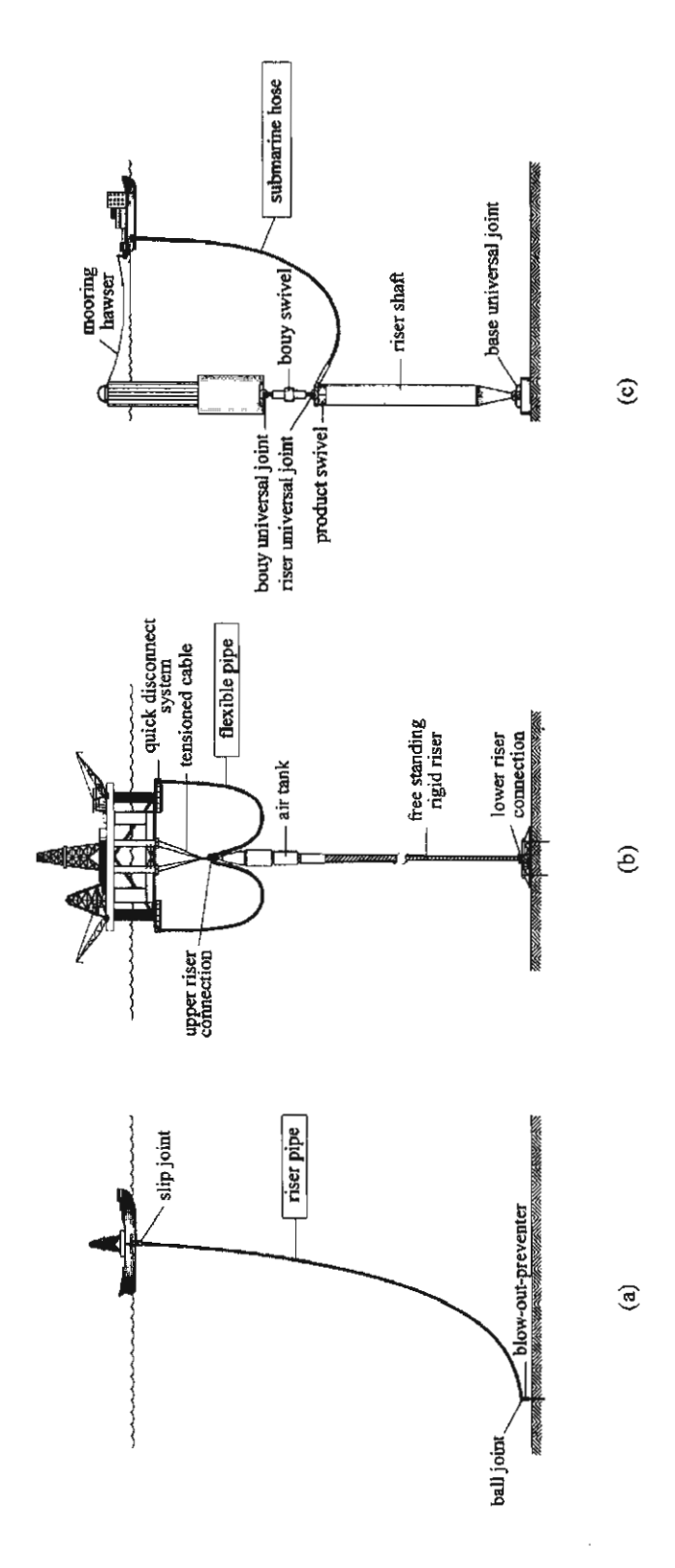


Figure 1.1 Flexible Marine Riser Pipes
(a) a Marine Riser (b) a Flexible Pipe (c) a Hoseline

In the 1960s, research work dealt predominantly with two-dimensional, linear static analysis (Fischer and Ludwig (1966), Gosse and Barksdale (1969)) and two-dimensional, linear dynamic analysis (National Engineering and Science Company (1965), Graham et al. (1965)) that did not take the relative hydrodynamic forces into consideration.

In the 1970s, the research work was escalated on various types of dynamic analyses and methods of solution as demonstrated in Table 1.1. In addition to the time domain analysis via the finite difference solution, the frequency domain analysis and the nondeterministic random vibration analysis had drawn the attention of several authors as well as the finite element method (Gardner and Kotch (1976)) and the modal analysis (Dareing and Huang (1979)). Although the paper by Bennett and Metcalf (1977) was oriented towards nonlinear dynamics, their work was still based on linear static solutions. The computer programs for the three-dimensional riser analysis, NONSAP (Bathe et al., 1974) and NASTRAN (Gnone et al., 1975) also originated in this period. Literature review on the marine riser analyses from 1950 to 1980 was given in the paper by Chakrabarti and Frampton (1982).

In the 1980s, researchers began to focus on three-dimensional large displacement analysis and nonlinear dynamic analysis. As shown in Table 1.1, most papers in this period were aimed at presenting the mathematical models for three-dimensional nonlinear analysis. Several papers were presented to indicate significances of three-dimensional analysis and nonlinear analysis (Natvig (1980), Felippa and Chung (1981), Bernitsas (1982), Safai (1983), Bernitsas et al. (1985), Huang and Chucheepsakul (1985), Owen and Qin (1987), Kokarakis and Bernitsas (1987), Bernitsas and Kokarakis (1988), O'Brien and Mcnamara (1989)). The finite element method was in widespread use for the spatial solution, whereas the numerical integration methods for time history analysis were favored as well as the modal transformation method for frequency domain analysis.

In this period, researches on the marine pipes considering the effect of axial deformation in the variational formulation were published by Felippa and Chung (1981), Irani, Modi and Weit (1987) and O'Brien and McNamara (1989). Researches that included the effect of axial deformation in the vectorial formulation were performed by Bernitsas and coauthors (Bernitsas et al. (1985), Kokarakis and

Bernitsas (1987), Bernitsas and Kokarakis (1988)). The effect of fluid transportation or internal flow were specifically studied by Irani et al. (1987), Moe and Chucheepsakul (1988) and Patel and Seyed (1989). The commercial package for the three-dimensional riser analysis, FLEXCOM-3D (Marine Computation Services International, 1989) was also launched in this period.

In the 1990s, research work on riser analysis had the trend of study of specific problems. Huang and Leonard (1990), Karamanos and Tassoulas (1991), and Hah et al. (1992) investigated the stability of the marine riser pipes. The developments of random dynamics and other types of the hydrodynamic loading were studied by Trim (1990) and Thampi and Niedzwecki (1992). A number of authors extended three-dimensional nonlinear analyses of marine risers by including accessory themes such as various types of boundary conditions (Oran (1992), Chung et al.(1994a), Chung et al. (1994b), Chung and Cheng (1996)), seabed contact problems (Tikhonov et al., 1996), as well as other coordinate systems (Huyse et al. (1997), Ngiam (1997)). In the same period, Wu and Lou (1991), Seyed and Patel (1992), Huang (1993), Chucheepsakul and Huang (1994), and Moe et al. (1994) explored the effects of internal flow. Jain (1994) and Patel and Seyed (1995) reviewed the analysis and modeling of the flexible riser.

Above is an overview of previous research work concerning marine riser pipe analysis. This research work is relevant to marine pipes that take into consideration the in-depth effects of axial deformation, radial deformation, and fluid transportation. A more detailed review of these subjects is given as follows.

1.2.1 Three-dimensional model formulation

The three-dimensional models of the marine riser have been presented in many research works. Most of them used the theory of the space curved rod that can be found in the elasticity books such as Love (1944), Antman (1991), and Atanackovic (1997), which serve as the basic theory for the three-dimensional marine riser analysis.

To obtain the governing equations or the equation of motion of the marine pipe, there are at least three difference approaches: First, the direct equilibration based on D' Alembert's principle, Second, the variational method

based on the virtual work principle. Third, the variational method based on the Hamilton's principle.

The first approach is the most favorite method that can be found in many research works, for example, Bernitsas (1982), Bernitsas, Kokarakis, and Imron (1985), Kokarakis and Bernitsas (1987), Patrikalakis and Kriezis (1987), O'Brien, McNamara and Dunne (1988), Bernitsas and Kokarakis (1988), and Bernitsas and Vlahopoulos (1989). The three-dimensional model formulation of marine riser that based on the principle of virtual work can be found in the works of Felippa and Chung (1981) and Huang and Kang (1991). The research works that used the Hamilton's principle to formulate their governing equation are found in Doll and Mote (1976), and Atadan et al. (1997).

From the literature mentioned above, most of them used the arc-length as the independent variable. Therefore, the problem is limited to the case of specified arc-length or the total arc-length known prior. In the real situation, the arc-length of the marine riser may be unknown or changed due to the large displacement or large axial deformation while the top tension is specified, therefore the formulation that use the arc-length as the independent variable may be not convenient for numerical analysis. To solve this problem, the sea depth may be used to be the independent variable. Chucheepsakul and Huang (1985) is the pioneer in using the sea depth as the independent variable in the formulation. Huang and Kang (1991) extended the model to the three-dimensional formulation including the effect of torsion. However, the effect of internal flow and the axial deformation are neglected in that work.

1.2.2 Significance of the Effect of Axial Deformation

The effect of axial deformation on marine cables was investigated by Huang (1992), Chucheepsakul et al. (1995) and Chucheepsakul and Huang (1997). On the suspended cables, they were studied by Huddleston (1981), Shih and Tadjbakhsh (1984), Burgess and Triantafyllou (1988), Lin and Perkins (1995), Triantafyllou and Yue (1994), Tjavaras and Triantafyllou (1996), and Tjavaras et al. (1998). However, for marine pipes, it is only the low flexible pipes on which the effect of axial deformation has been explored.

On static behavior, the effect of axial deformation is to increase large

displacements of low-tensioned cables due to extensibility domination, and to reduce large displacements of high-tensioned cables due to pre-stressing domination (Chucheepsakul et al. (1995), Chucheepsakul and Huang (1997)). Although Bernitsas et al. (1985) and Bernitsas and Kokarakis (1988) found that the effect of axial deformation on the static behavior of the low flexible pipes was rather small, they did not provide evidence of the same result with the highly flexible pipes.

The effect of axial deformation on the dynamic behavior is to decrease nonlinear responses as reported by Chung et al. (1994a), Chung and Cheng (1996), Chung and Whitney (1983). It reduces the natural frequencies (Chucheepsakul and Huang, 1997), and provokes the elastic mode transitions of cable vibrations (Burgess and Triantafyllou (1988), Lin and Perkins (1995)). If the stress-strain relation is hysteretic, the effect of axial deformation can amplify damping of the dynamic strain in the axial direction (Triantafyllou and Yue,1994). Several papers by Chung and coauthors (Chung et al. (1994a), Chung and Cheng (1996), Chung and Whitney (1983)) highlighted the fact that the effect of axial deformation is crucial to dynamic behavior of low flexible pipe, and should be considered in the design of the pipe.

The interesting point in all the previous research is that the effect of axial deformation has been investigated based on small strain analysis, which assumes that the strains are small, and can be approximated by the binomial expansion. However, this approach is proper if, and only if the axial strain is small compared to unity (Fung, 1965). For highly flexible pipes, such a constraint is no longer confidential. Thus, this dissertation proposes large strain modeling in which the relative elongations or the square-root expressions of large strains are adopted.

1.2.3 Significance of the Effects of Fluid Transportation

Although fluid transportation is the main function of marine riser pipes, marine riser analysis from the middle of 1950s to the end of 1970s gives little attention on the influence of fluid transportation. In the same period, research concerning mechanics of pipes conveying fluid had grown rapidly. Research work related to vibrations of straight and curved pipes can be found in the papers by Housner (1952), Gregory and Païdoussis (1966), Païdoussis (1970), Doll and Mote

(1976) and so on. It was reported that the internal flow reduced stability of the pipe and acted on the pipe like the end follower force (Thompson and Lunn, 1981). As a result, the internal flow can engender divergence instability or statical buckling of simply supported pipes (Holmes, 1978), and can induce flutter instability or snaking behavior of cantilever pipes (Gregory and Païdoussis, 1966).

The lack of connection between research work on marine pipes and pipes conveying fluid brings about a misconception by some authors. When the effects of internal flow on marine pipes were examined in the early of 1980s, it was considered that the internal flow induced only the friction force to act on the pipe wall. However, researchers concerned with pipes conveying fluid such as Gregory and Paï doussis (1966), Païdoussis (1970) and Thompson and Lunn (1981) had been well aware that the internal friction force did not act directly on the pipe, but transmitted the internal pressure into the pipe wall, which yielded tensioning and pressure drop (Païdoussis, 1998). In addition, the internal flow generated not only the effects of pressure, but also other fictitious forces such as Coriolis and centrifugal forces.

By the end of 1980s, the effects of fluid transportation on behavior of marine pipes began to draw specific interest from a number of researchers, and the misconception was dispelled. Several interesting effects of fluid transportation were reported. It was found that the internal flow reduced structural stiffness, provided negative damping (Irani et al., 1987), and induced additional large displacements of the pipes (Chucheepsakul and Huang, 1994). The natural frequencies of the pipes are slightly reduced at a low speed of internal flow, but significantly reduced at a high flow speed (Moe and Chucheepsakul (1988), Wu and Lou (1991)). The internal slug flow can induce the significant cyclic fatigue loading in deep water (Patel and Seyed, 1989). The marine riser pipe transporting fluid buckles by the divergence instability (Chucheepsakul et al., 1999).

However, the three-dimensional model formulations used in most of those works do not consider geometric nonlinearity and axial deformation of the pipes. In this research work, these objects have been taken into account in large strain analysis of marine risers. Therefore, the novelties of this work are the large strain model formulation of the three-dimensional extensible flexible marine risers/pipes transporting fluid and the unveiling of the interaction between the transported fluid and the pipe subjected to large axial deformations.

1.3 OBJECTIVES

The objectives of this research work are as follows:

- 1.3.1 To introduce and illuminate the mathematical principles for large strain analysis of the flexible marine riser pipes that are subjected to the combined action of axial and fluid transportation from viewpoints of the total Lagrangian, the updated Lagrangian and the Eulerian mechanics.
- 1.3.2 To show how to formulate large strain three-dimensional models in the Cartesian coordinates by using the axially deformable elastica theory.
- 1.3.3 To examine the in-depth effects of axial deformations and fluid transportation on behaviors of the marine pipes with large displacements.

1.4 ASSUMPTIONS AND SCOPE

The following assumptions and scope are stipulated in the present study:

- 1.4.1 The material made of the riser/pipe is linearly elastic.
- 1.4.2 At the undeformed state, the pipes are straight, and have no residual stresses.
- 1.4.3 The pipe cross sections remain circular after change of cross-sectional size due to the axial deformation effect.
- 1.4.4 Longitudinal strain is large, while the effect of shear strain is small and can be neglected, so that the Kirchhoff's rod theories can be employed.
- 1.4.5 Every cross section remains plane and remains perpendicular to the axis.
- 1.4.6 Radial lines of the sections remain straight and radial as the cross section rotates about the axis.
- 1.4.7 The internal and external fluids are inviscid, incompressible and irrotational. Their densities are uniform along arc-lengths of the riser.
 - 1.4.8 The internal flow is the one-dimensional plug laminar flow.

- 1.4.9 Morison's equation is adopted for evaluating external hydrodynamic forces of external fluid.
 - 1.4.10 The effect of rotary inertia is negligible.
- 1.4.10 The pipe connections due to construction are presumed to be homogeneous with the pipe body, and have the same properties.
- 1.4.11 The effect of wind flow over the sea surface is negligible for deep-water riser pipe analysis.
- 1.4.12 Structural model. The riser pipe is pinned at the bottom end by the ball joint of wellhead at seabed, and is held at the top end by the slip joint beneath the vessel. The slip joint allows the pipe to change its length as the vessel heaves and moves laterally. The surrounding kill and choke lines are assumed to make no contribution to the structural stiffness. The rotational stiffness at the top end of the riser and the ship motion compared to the water depth are small and negligible, so the top end could be modeled as the slip joint with hinge. The ball joint at the bottom end can not rotate freely around the tangential direction, but can rotate freely around any other direction perpendicular to the tangent.
- 1.4.13 Research methodology. The nonlinear static analysis, the natural frequency analysis and the nonlinear vibration analysis are rendered for studying the effects of axial deformation, and fluid transportation on behaviors of the pipe as shown in Figure 1.2. The nonlinearity in the vibration analysis is due to the nonlinear hydrodynamic damping. The large strains and large displacements are fully treated in the nonlinear static analysis, whereas the linear dynamic strains and the small amplitude vibrations are assumed in the natural frequency analysis and the nonlinear vibration analysis.
- 1.4.14 Current flow. The current is tidal. Its velocity profile can be expressed in form of the polynomial functions of water depth (Larsen, 1976).
- 1.4.15 Wave flow. The wave is regular incoming, and can be described by Airy's wave theory (Chen and Lin, 1989).

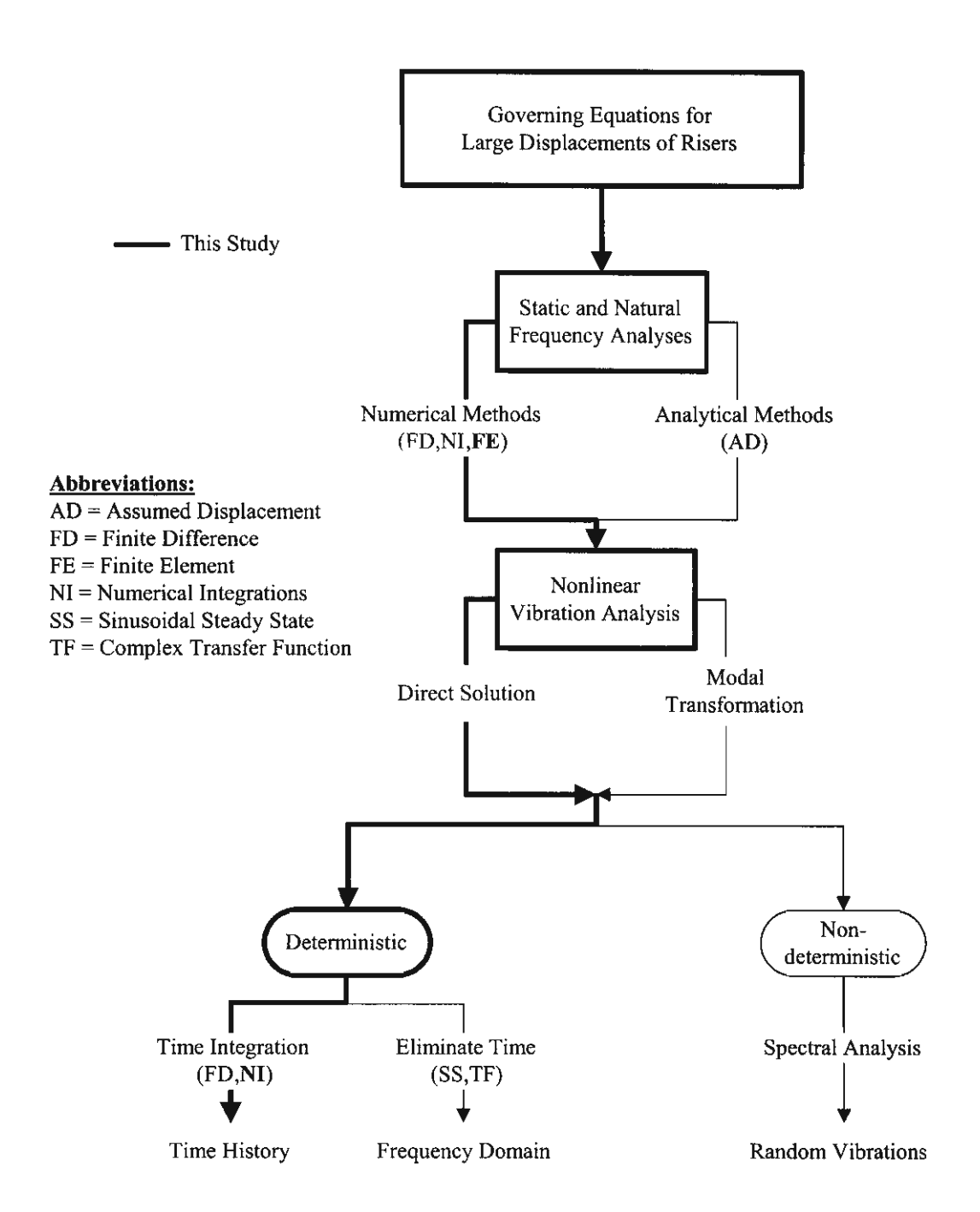


Figure 1.2 Methods of Marine Riser Analysis

Table 1.1 Summary of Paper Review on Riser Pipe Analysis

_	K
Elongation) (Tension) Radial	Bendii
(10) (11)	(6)
z	Y
z -	~
z 	٨
z	Y
z -	Y
2	, Y
z -	¥
7	¥
z -	Y
z 	>
z 	>
Z	Y
z	>
Z	гр,тн ү
	¥
Z	٨
2	>

Table 1.1 Summary of Paper Review on Riser Pipe Analysis (Continued)

			uc	noi	Sol. Technique	shnique	ədA		Deformation	nation		<u> </u>	Static loads	loads	Dynamic loads	c loads	pa	,	
Year	Reference	S=static D=dynamic	No. Dimensio	Large Deformat	Spatial	remporal	Dynamic sol	Bending.	Elongation (Tension)	Radial noilemellen	noizroT	woft Ismstri	Current	Horz. Offset	Мачея	Ship motion	ozineanil gartO	Wave theory	Boundary conditions
(E)	(2)	(3)	(4)	(5)	(9)	(3)	(8)	6)	(10)	(11)	(12)	(13)	(14)	(15)	(91)	(17)	(18)	(61)	(20)
77	Bennet and Metcaif [12]	D	2	z	FD	Z	ТН	>	I	Z		z	γ		>	>	z		Spring-Free
77	Maison and Lea [80]	Q		2	FE	FD	TH	>	_	z	z	z	*	Y2	>	>	z	S	
77	Paulling [81]	Q	3	Z	FE	SS	FD	٨	-	z	γ	z	z		*	٨	γ	Γ	Spring-Free
78	Chou et al. [82]	Ω	2	z	FD	Z	TH.	>	-	z	•	z	Y1		У3	>	z	Γ	Pinned-Free
78	Young et al. [83]	۵	2	z	FD	SS	FD	Υ	-	z		z.	Y		۲۱,3	*	Y	Г	
79	Kirk et al. [84]	SD	2	z	ΑD	MT	FD	>	ı	z		z	Y	¥1	43	>	٨	L	Pinned-Pinned
79	Dareing and Huang [11]	Q	2	z	QΥ	MT	FD	*	1	z		z	γ	Y!	Y3	*	٨	T.	Pinned-Pinned
80	Krolikowski and Gay [85]	α	2	z		SS	FD	Y	-	z		z	Y2	Ÿ	Y1,3	*	Y	Г	Ball-Ball
80	Bemitsas [86]	0	3	۲3	ΦP			٨	-	z	Y	z							
80	Natvig [15]	a	2	7.2	ž	Z	Ŧ	>	-	z		z	*		>	>	*		Forced-Forced
81	Etok and Kirk [87]	SD	2	z	Φ	TM	G	>-	-	z	$\overline{}$	z	>	Y1,2	Y3	>	>	1	Pinned-Pinned
81	Felippa and Chung [16]	s	ю	٨.	FE	,	,	>	ш	z	>	z	>			,	>		Fixed-Free
82	Bernitsas [17]	SD	3	۲3				>	-	z	>-	z						·	
83	Safai [18]	۵	ы	72	댎	Z	Ŧ	>	-	z	>	z			>	z	z		Ball-Free
85	Huang and Chuchecpsakul [20]	S	2	۲۱	Æ		٠	>	-	z	•	z	۲.	*				,	Slip-Pinned
85	Kirk [88]	۵	2	z	Ą	Ā	æ	>	~	z		z	*	Ϋ́	>	z	Y	ı	Pinned-Pinned
85	Bernitsas et al. [19]	s	m	۲۱	FE		•	>	Э	z	>	z	X	À	•	٠		•	Pinned-Pinned

Table 1.1 Summary of Paper Review on Riser Pipe Analysis (Continued)

		<u> </u>	ue		nois	Sol. Technique	mique	Abc		Deformation	nation		A	Static loads	loads	Dynamic loads	c loads	pa	A	
S-static D-dynamic No. Dimensio Large Deforma	D=dynamic No. Dimensio	D=dynamic No. Dimensio	ermolod agrad	lating2		Temporal		Dynamic sol t	Bending	Elongation (Tension)	Radial deformation	noisioT	voft lametral	Сиптері	Horz. Offset	Waves	notiom qid2	Drag lineariz	roodt ovsW	Boundary conditions (Top-Bottom)
(2) (3) (4) (5) (6) (7) ((4) (5) (6) (7)	(4) (5) (6) (7)	(5) (6) (7)	(2) (9)	(0)			(8)	(6)	(10)	(11)	(12)	(13)	(14)	(15)	(16)	(17)	(18)	(19)	(20)
Owen and Qin [21] D 3 Y3 FE NI	D 3 Y3 FE	3 Y3 FE	Y3 FE	FE		ž		TH	Υ	1	z	¥	z	Y	γ	٨	z	•••		Pinned-Pinned
Kokarakis and Bernitsas [22] D 3 Y2 FE Ni	D 3 Y2 FE	3 72 圧	72 圧	丑		ž		Ŧ	۲	I	z	*	Y.	¥	¥	.				
Irani et al. [25] D 3 N FE MT	3 N FE	3 N FE	Z H	FE		Ä		G.	>	ш	z	>	۲۱	¥	¥	>	z	>-	ı	Pinned-Pinned
Bernitsas and Kokarakis [23] S 3 YI FE -	S 3 YI FE	3 YI FE	YI FE	FE		1		1	٨	ш	z	Y	z	Y	Y					Pinned-Pinned
Moe and Chucheepsakul [26] D 2 N AD FE -	D 2 N AD,FE	2 N AD,FE	N AD,FE	AD,FE		-		•	z	-	z		١٨	Y	γ				'	Pinned-Pinned
Ahmad and Datta [89] D 2 N FE NI	D 2 N E	2 N FE	Z E	표		ž		ΗH	٧	1	z		z	γ	*	۲۱٫3	>	z	Ĺ	Spring-Spring
O'Brien and Monamara [24] SD 3 Y3 FE NI	SD 3 Y3 FE	3 Y3 FE	Y3 FE	뜐		Ē		TH	٨	Е	Z	Υ .	z	٨	Y	٨				
Patel and Seyed [27] SD 2 YI FE MT	SD 2 YI FE	2 Y1 FE	Y1 FE	FE		ΤM		FD	¥	1	z	,	Y2	٨	Υ	٨	*	>		
Spanos et al. [90] D 2 Y1 FE NI	D 2 YI FE	2 YI FE	YI FE	표		ž		FD	Y		z		z	Y		>	٨	>		Fixed-Ball
Trim [32] D 2 N FE Ni	2 N FE	2 N FE	N E	Æ		ž		RV	٨	1	z	-	z	Y	Y	¥	*		L	Pinned-Pinned
Huang and Kang [91] SD 3 Y1 FE	SD 3 Y1 FE	3 Y1 FE	Y1 FE	Æ		'		٠,	>	-	z	,	z	>	,		•	,	,	Pinned-Pinned
Wu and Lou [41] SD 2 N NI NI	SD 2 N NI	2 N NI	ž	Z		Z		ТН	>	_	z		١٨	*	*	>	>	·		Pinned-Pinned
Chung et al. [35, 36] SD 3 Y3 FE NI	SD 3 Y3 FE	3 Y3 FE	Y3 FE	표				H	¥	E	z	Α.	z	٨		*	>			Fixed-Motion
Chucheepsakul and Huang [44] S 2 Y1 FE -	S 2 Y1 FE	2 Y1 FE	Y1 FE	FE				•	Y	1	2	,	١,	>	>	•	•		,	Slip-Pinned
Tikhonov et al. [38] D 3 Y3 NI NI	D 3 Y3 NI	3 Y3 NI	Y3 NI	Z		Z		H	٨	н	z	*	z	,	>	>	z			Fixed-Fixed
Atsendan et al. [92] D 3 Y1 NI NI	D 3 Y1 NI	3 Y1 NI	Y1 NI	Z		ž		7	¥	E	z	>	۲,	>	>	>	>			Fixed-Free
Huyse et al. [39] S 3 Y1 A.D .	3 Y1 AD	3 YI AD	YI AD	Ą					z	-	z	•	2	٨	٨	•	•		,	Stip-Ball

Notes of Abbreviations in Table 1.1:

Column	1 = Random 2 = Irregular 3 = Regular		6 = Wave Elevation Record L = Linear Wave Theory S = Stoke's Fifth Order	
Colh	(16)		(19)	
	TH = Time HistoryFD = Frequency DomainRV = Random Vibration		= Extensible Analysis = Steady Flow = Slug Flow = Any Profile	= Stepwise Linear = Multidirectional = Static = Periodic
ď				2 1 3 2
Column	(8)	(10)	(13)	(15)
0	ALL Y = Yes N = No	= Static = Dynamic = Static and Dynamic	AD = Assumed Displacement FD = Finite Difference FE = Finite Element NI = Numerical Integration	= Complex Transfer Functions = Finite Difference = Numerical Integration [
	> Z	7 7 7	AD AD NI FE	TF NI WT
Column	ALL	(5)	9)	6

2. MODEL FORMULATIONS OF THREE-DIMENSIONAL FLEXIBLE MARINE RISERS TRANSPORTIG FLUID

This section presents the large strain model formulation of threedimensional flexible marine risers transporting fluid. The elastica theory of extensible rod and the kinematics theory of mass transported on the moving frame are used to obtain the model formulation.

In section 2.1, the behavior of the flexible marine risers and the physical description of the model formulation are introduced. The concept of large strain measurement in the three deformation descriptions referring to the Cartesian coordinate is discussed in section 2.2.

It is realized that the change of the large axial strain is not only effect on the differential arc-length of the riser but also effect on the property changes of the riser cross section and transporting fluid velocity, which is discussed in section 2.3. In section 2.4, the extensible elastica theorems for the Hookean material riser corresponding to the three deformation descriptors is preformed. The effect of hydrostatic pressures and hydrodynamic pressures is reviewed in section 2.5 and 2.6, respectively.

In section 2.7, the elastica theory, the apparent tension concept and the dynamic interactions between fluid and risers are used to formulate the variational formulations, which are validated by vectorial formulation in section 2.8. For the sake of generality in obtaining the model solution, the nonlinear dynamic model based on the strong form is derived in section 2.9. In section 2.10, eliminating the time-dependent terms in nonlinear dynamic model, the nonlinear static model is derived.

One conspicuous feature of the present formulation is flexibility of the model that allows users to select the independent variable to suit solution of their own problems, therefore the guideline for choosing the independent variable is discussed in section 2.11. Finally, the implementation of the present models is covered in section 2.12.

2.1 BEHAVIOR OF THE FLEXIBLE MARINE RISERS AND PHYSICAL DESCRIPTION OF THE MODEL FORMULATION

The large displacement and large deformation behaviors of a flexible marine riser transporting fluid are depicted in Figure 2.1. Firstly the riser is at rest and unstretched at the undeformed configuration. Then, the riser is subjected to the time-independent loads and its configuration changes to equilibrium configuration that is the initial condition before the dynamic actions occur. Finally, at the displaced configuration, dynamic actions such as wave, unsteady current, and unsteady internal flow disturb the riser to sustain vibration about the equilibrium configuration.

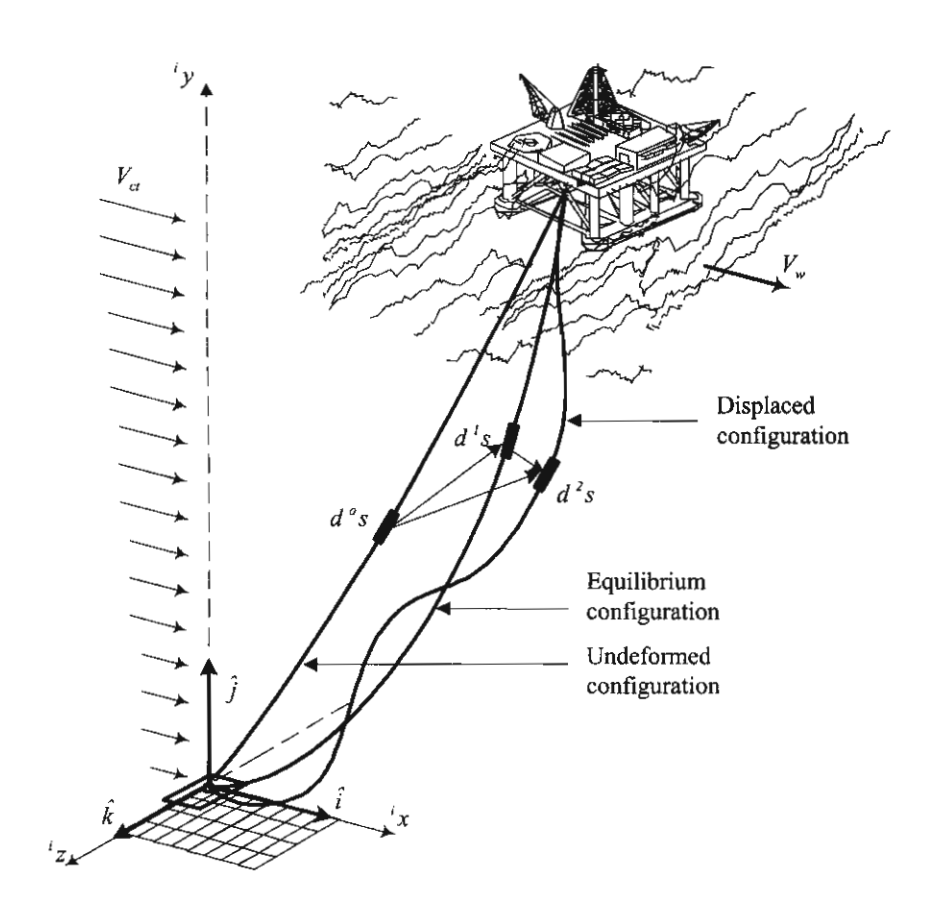


Figure 2.1 Three configurations of marine riser.

The marine riser is modeled as a three-dimensional rod with a ball joint at the bottom end and a slip joint at the top end. In this study, three orthogonal coordinate systems are used to define position, motion, and deformation of an extensible marine riser. The orthogonal triad system $\hat{t}, \hat{n}, \hat{b}$ and the cross-sectional principal axes system ${}^ix_1, {}^ix_2, {}^ix_3$ with unit normal vector ${}^ie_1, {}^ie_2, {}^ie_3$ are used as the local coordinate. The fixed cartesian system ${}^ix, {}^iy, {}^iz$ with unit normal vector $\hat{i}, \hat{j}, \hat{k}$ is used as the global coordinate. The left superscript represents the state of marine riser where 0 represents the undeformed state, 1 represents the equilibrium state and 2 represents the displaced state, therefore, $i \in (0, 1, 2)$.

Figure 2.2 shows the segments of the extensible marine riser in three states. Since the centerline of the riser at any time t is, in general, a three-dimensional curve and can be described by one parameter, the parameter α , $\alpha \in \{{}^{i}x, {}^{i}y, {}^{i}z, {}^{i}s\}$, that is employed in the formulation for the sake of generality. Therefore if ${}^{i}x, {}^{i}y$, and ${}^{i}z$ are the coordinates of a point along the marine riser at time t, then ${}^{i}x = {}^{i}x(\alpha, {}^{i}t)$, ${}^{i}y = {}^{i}y(\alpha, {}^{i}t)$, and ${}^{i}z = {}^{i}z(\alpha, {}^{i}t)$. The partial derivatives with respect to α and time ${}^{i}t$ are represented by superscripts (') and ('), respectively.

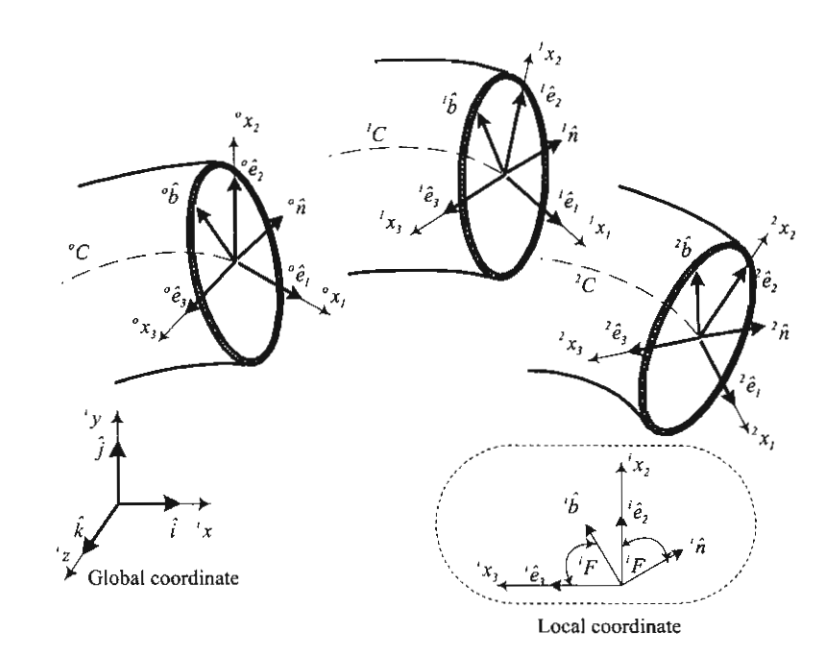


Figure 2.2 Segments of the extensible marine riser in three states.

2.2 MEASUREMENT OF LARGE AXIAL STRAINS

In Cartesian coordinate, the relations of differential arc-length at the undeformed state, the equilibrium state and the displaced state $({}^{o}s', {}^{l}s'and {}^{2}s')$ can be expressed as

$${}^{o}s' = \sqrt{{}^{o}x'^{2} + {}^{o}y'^{2} + {}^{o}z'^{2}}$$

$${}^{l}s' = \sqrt{{}^{l}x'^{2} + {}^{l}y'^{2} + {}^{l}z'^{2}} = \sqrt{({}^{o}x' + {}^{l}u')^{2} + ({}^{o}y' + {}^{l}v')^{2} + ({}^{o}z' + {}^{l}w')^{2}}$$

$${}^{2}s' = \sqrt{{}^{2}x'^{2} + {}^{2}y'^{2} + {}^{2}z'^{2}} = \sqrt{({}^{o}x' + {}^{2}u')^{2} + ({}^{o}y' + {}^{2}v')^{2} + ({}^{o}z' + {}^{2}w')^{2}}$$

$${}^{2}s' = \sqrt{({}^{o}x' + {}^{l}u' + u')^{2} + ({}^{o}y' + {}^{l}v' + v')^{2} + ({}^{o}z' + {}^{l}w' + w')^{2}}$$
(2.1 a-d)

According to the mechanics of deformable bodies, the definition of axial strain can be provided in three forms, namely the Total Lagrangian Descriptor, the Updated Lagrangian Descriptor, and the Eulerian Descriptor. Each of these forms can be demonstrated as follows.

Total Lagrangian Descriptor (TLD)

The coordinate that follows motion and deformation of a deformable body with respect to position, direction, and size of the body at the original state (or undeformed state herein) is said to be the total Lagrangian descriptor.

Total strain
$${}^{2}\overline{\varepsilon} = \frac{d^{2}s - d^{\circ}s}{d^{\circ}s} = \frac{d^{2}s}{d^{\circ}s} - 1 = \sqrt{1 + 2\binom{2}{2}L} - 1$$
Static strain
$${}^{I}\overline{\varepsilon} = \frac{d^{I}s - d^{\circ}s}{d^{\circ}s} = \frac{d^{I}s}{d^{\circ}s} - 1 = \sqrt{1 + 2\binom{2}{2}L} - 1$$
Dynamic strain
$$\overline{\varepsilon} = \frac{d^{2}s - d^{I}s}{d^{\circ}s} = \sqrt{1 + 2\binom{2}{2}L} - \sqrt{1 + 2\binom{2}{2}L}$$
(2.2 a-c)

The Green strains in each state that represents in equation (2.2) can be derived in the terms of displacements of the riser as follows.

$${}^{2}L = \frac{1}{\left({}^{o}s'\right)^{2}} \left({}^{o}x'\left({}^{2}u'\right) + {}^{o}y'\left({}^{2}v'\right) + {}^{o}z'\left({}^{2}w'\right) + \frac{\left({}^{2}u'\right)^{2}}{2} + \frac{\left({}^{2}v'\right)^{2}}{2} + \frac{\left({}^{2}w'\right)^{2}}{2}\right)$$

$${}^{1}L = \frac{1}{\left({}^{2}s'\right)^{2}} \left({}^{o}x'\left({}^{1}u'\right) + {}^{o}y'\left({}^{1}v'\right) + {}^{o}z'\left({}^{1}w'\right) + \frac{\left({}^{1}u'\right)^{2}}{2} + \frac{\left({}^{1}v'\right)^{2}}{2} + \frac{\left({}^{1}w'\right)^{2}}{2}\right)$$

$$L = {}^{2}L - {}^{1}L = \frac{1}{{}^{o}s'^{2}} \left({}^{1}x'u' + {}^{1}y'v' + {}^{1}z'w' + \frac{u'^{2}}{2} + \frac{v'^{2}}{2} + \frac{w'^{2}}{2}\right)$$

$$(2.3 \text{ a-c})$$

Updated Lagrangian Descriptor (ULD)

The coordinate that follows motion and deformation of a deformable body with respect to position, direction, and size of the body at the intermediate state (or equilibrium state, the last known deformed configuration herein) is said to be the updated Lagrangian descriptor.

Total strain
$${}^{2}\varepsilon = \frac{d^{2}s - d^{o}s}{d^{I}s} = \sqrt{1 + 2\upsilon} - \sqrt{1 - 2({}^{I}\upsilon)}$$
Static strain
$${}^{I}\varepsilon = \frac{d^{I}s - d^{o}s}{d^{I}s} = 1 - \frac{d^{o}s}{d^{I}s} = 1 - \sqrt{1 - 2({}^{I}\upsilon)}$$
Dynamic strain
$$\varepsilon = \frac{d^{2}s - d^{I}s}{d^{I}s} = \frac{d^{2}s}{d^{I}s} - 1 = \sqrt{1 + 2\upsilon} - 1 \tag{2.4 a-c}$$

The updated Green strains in each state that represents in equation (2.4) can be derived in the term of displacements of the riser which relate to the Green strains as

$${}^{2}v = {}^{1}v + v = {}^{2}L\left(\frac{{}^{o}s'}{{}^{s}s'}\right)^{2}, {}^{1}v = {}^{1}L\left(\frac{{}^{o}s'}{{}^{s}s'}\right)^{2}, \ v = {}^{2}v - {}^{1}v = L\left(\frac{{}^{o}s'}{{}^{s}s'}\right)^{2}$$
 (2.5 a-c)

Eulerian Descriptor (ED)

The coordinate that follows motion and deformation of a deformable body with respect to position, direction, and size of the body at the final state (or the displaced state herein) is said to be the Eulerian descriptor (ED).

Total strain
$${}^{2E}\varepsilon = \frac{d^2s - d^os}{d^2s} = 1 - \frac{d^os}{d^2s} = 1 - \sqrt{1 - 2\binom{2}{E}}$$
Static strain
$${}^{1E}\varepsilon = \frac{d^1s - d^os}{d^2s} = \sqrt{1 - 2E} - \sqrt{1 - 2\binom{2}{E}}$$
Dynamic strain
$${}^{E}\varepsilon = \frac{d^2s - d^1s}{d^2s} = 1 - \frac{d^1s}{d^2s} = 1 - \sqrt{1 - 2E}$$
(2.6 a-c)

The Almansi strains in each state that represents in equation (2.6) can be derived in terms of displacements of the riser which relate to the Green strains as

$${}^{2}E = {}^{2}L\left(\frac{{}^{o}S'}{{}^{2}S'}\right)^{2}, {}^{1}E = {}^{1}L\left(\frac{{}^{o}S'}{{}^{2}S'}\right)^{2}, E = {}^{2}E - {}^{1}E = L\left(\frac{{}^{o}S'}{{}^{2}S'}\right)^{2}$$
 (2.7 a-c)

From the definition of axial strain discussed above, the large axial strains are measured by mean of relative elongation that can be called as engineering strains. The square-root expressions in equations (2.2), (2.4) and (2.6) indicated that the large axial strains are function of the Green strains ^{i}L , the updated Green strains ^{i}v , and the Almansi strains ^{i}E . In nonlinear dynamic analysis with large amplitude vibrations and large strain of the flexible marine riser, the square-root expressions in the large axial strain definitions have to be included in the formulation without approximations.

In the case of the vibration problems with large amplitudes but strain is not highly large, the approximate large strain can be used in numerical analysis. By utilizing the two-term approximation of the binomial series, the approximate large total strains can be expressed as follows.

For TLD:
$${}^{2}\overline{\varepsilon} = {}^{l}\overline{\varepsilon} + \left(\frac{{}^{2}s'}{{}^{l}s'} - 1\right)\left(1 + {}^{l}\overline{\varepsilon}\right) = {}^{l}\overline{\varepsilon} + \left(\sqrt{1 + 2\upsilon} - 1\right)\left(1 + {}^{l}\overline{\varepsilon}\right) \approx {}^{l}\overline{\varepsilon} + \upsilon\left(1 + {}^{l}\overline{\varepsilon}\right)$$

For ULD: ${}^{2}\varepsilon = {}^{l}\varepsilon + \left(\sqrt{1 + 2\upsilon} - 1\right) \approx {}^{l}\varepsilon + \upsilon$

For ED: ${}^{2E}\varepsilon = {}^{lE}\varepsilon + \left(1 - \frac{{}^{l}s'}{{}^{2}s'}\right) = {}^{lE}\varepsilon + \left(1 - \frac{1}{\sqrt{1 + 2\upsilon}}\right) \approx {}^{lE}\varepsilon + \upsilon$ (2.8 a-c)

Although the approximate large dynamic strains are used, the nonlinear dynamic with large amplitude vibration is complicated and it is difficult to find the solutions. To simplify this problem to be the linear dynamic with small amplitude vibration, the total strain can be expressed same as the equation (2.8) but the updated dynamic Green strain (v) can be neglected the higher order terms as

$$\upsilon = \frac{1}{('s')^2} ('x'u' + 'y'v' + 'z'w')$$
 (2.9)

In the most research works, the large displacement analysis has been investigated by using the small strain assumption. Therefore, the engineering strains can be approximated as

$$^{2}\overline{\varepsilon} \approx ^{2}L, ^{2}\varepsilon \approx ^{2}\upsilon, ^{2E}\varepsilon \approx ^{2}E$$
 (2.10 a-c)

2.3 THE PROPERTY CHANGES OF THE RISER CROSS SECTION AND TRANSPORTING FLUID VELOCITY

The change of the large axial strain among three states leads to relations of differential arc-length of the riser, cross-sectional properties of the riser and internal flow velocity of transported fluid as shown in this section.

a) Relations of differential arc-length of the riser

TLD;
$$d^{o}s = \frac{d^{l}s}{l + l^{l}\overline{\varepsilon}} = \frac{d^{2}s}{l + e^{2}\overline{\varepsilon}}$$
ULD;
$$\frac{d^{o}s}{l - e^{l}\varepsilon} = d^{l}s = \frac{d^{2}s}{l + \varepsilon}$$
ED;
$$\frac{d^{o}s}{l - e^{2}\varepsilon} = \frac{d^{l}s}{l - e^{2}\varepsilon} = d^{2}s \qquad (2.11 \text{ a-c})$$

b) Relations of cross-sectional properties of the riser

Since the riser volume is conserved, the cross-sectional areas of the riser at the three states, ${}^{i}A_{p}$, can be related to each other as

TLD;
$${}^{\circ}A_{p} = {}^{I}A_{p} \left(1 + {}^{I}\overline{\varepsilon} \right) = {}^{2}A_{p} \left(1 + {}^{2}\overline{\varepsilon} \right)$$
ULD;
$${}^{\circ}A_{p} = \frac{{}^{I}A_{p}}{\left(1 - {}^{I}\varepsilon \right)} = \frac{{}^{2}A_{p} \left(1 + \varepsilon \right)}{\left(1 - {}^{I}\varepsilon \right)}$$
ED;
$${}^{\circ}A_{p} = \frac{{}^{I}A_{p}}{\left(1 - {}^{IE}\varepsilon \right)} = \frac{{}^{2}A_{p}}{\left(1 - {}^{2E}\varepsilon \right)}$$
 (2.12 a-c)

The relations of diameter, $\binom{i}{D_p}$, moment of inertia, $\binom{i}{I_p}$, and polar moment of inertia, $\binom{i}{J_p}$, of the circular riser among the three states determined corresponding to equations (2.12 a-c) are shown below.

TLD;
$${}^{o}D_{p} = {}^{I}D_{p}\sqrt{I + {}^{I}\overline{\varepsilon}} = {}^{2}D_{p}\sqrt{I + {}^{2}\overline{\varepsilon}}$$
, ${}^{o}I_{p} = {}^{I}I_{p}(I + {}^{I}\overline{\varepsilon})^{2} = {}^{2}I_{p}(I + {}^{2}\overline{\varepsilon})^{2}$, (2.13 a-c)

$${}^{o}J_{p} = {}^{I}J_{p}(I + {}^{I}\overline{\varepsilon})^{2} = {}^{2}J_{p}(I + {}^{2}\overline{\varepsilon})^{2} = {}^{2}I_{p}(I + {}^{2}\overline{\varepsilon})^{2},$$

$${}^{o}D_{p} = \frac{{}^{I}D_{p}}{\sqrt{I - {}^{I}\varepsilon}} = {}^{2}D_{p}\sqrt{\frac{I + \varepsilon}{I - {}^{I}\varepsilon}}, {}^{o}I_{p} = \frac{{}^{I}I_{p}}{(I - {}^{I}\varepsilon)^{2}} = {}^{2}I_{p}\frac{(I + \varepsilon)^{2}}{(I - {}^{I}\varepsilon)^{2}},$$

$${}^{o}J_{p} = \frac{{}^{I}J_{p}}{(I - {}^{I}\varepsilon)^{2}} = {}^{2}J_{p}\frac{(I + \varepsilon)^{2}}{(I - {}^{I}\varepsilon)^{2}} = \frac{{}^{2}I_{p}}{(I - {}^{2}\varepsilon)^{2}},$$

ED;
$${}^{o}D_{p} = \frac{{}^{I}D_{p}}{\sqrt{I - {}^{I}\varepsilon}\varepsilon} = \frac{{}^{2}D_{p}}{\sqrt{I - {}^{2}\varepsilon}\varepsilon}, {}^{o}I_{p} = \frac{{}^{I}I_{p}}{(I - {}^{I}\varepsilon\varepsilon)^{2}} = \frac{{}^{2}I_{p}}{(I - {}^{2}\varepsilon\varepsilon)^{2}},$$

$${}^{o}J_{p} = \frac{{}^{I}J_{p}}{(I - {}^{I}\varepsilon\varepsilon)^{2}} = \frac{{}^{2}J_{p}}{(I - {}^{2}\varepsilon\varepsilon)^{2}}$$
(2.15 a-c)

c) Relations of internal flow velocity of transported fluid

By substituting equation (2.12) into the continuity equation of the fluid flow in the control volume riser, the relationships of internal flow velocities at the three states are obtained as

TLD;
$${}^{o}V_{i} = \frac{{}^{\prime}V_{i}}{I + {}^{\prime}\overline{\varepsilon}} = \frac{{}^{2}V_{i}}{I + {}^{2}\overline{\varepsilon}}$$

ULD;
$${}^{o}V_{i} = {}^{l}V_{i} \left(1 - {}^{l}\varepsilon \right) = \frac{{}^{2}V_{i} \left(1 - {}^{l}\varepsilon \right)}{\left(1 + \varepsilon \right)}$$
ED;
$${}^{o}V_{i} = {}^{l}V_{i} \left(1 - {}^{lE}\varepsilon \right) = {}^{2}V_{i} \left(1 - {}^{2E}\varepsilon \right)$$
 (2.16 a-c)

2.4 THE EXTENSIBLE ELASTICA THEORY

The word "elastica" is the equilibrium (stable and unstable) shape of a bar with large displacement, stable, linear elasticity, no section change, axial and shear deformation neglected. In the case of extensible elastica, the material remains linearly elastic while the strain maybe large. The extensible elastica theory (Chucheepsakul et al., 2003) provided in this section is used to develop the large strain formulations of three-dimensional extensible flexible riser, which will be discussed later.

Theorem 1: When the TLD is adopted to describe deformation of the riser, the fiber strain, the constitutive relations and the virtual strain energy are expressed as follows

$${}^{2}\overline{\varepsilon}_{\zeta} = {}^{2}\overline{\varepsilon} + \zeta \left[{}^{2}\kappa \left(1 + {}^{2}\overline{\varepsilon} \right) - {}^{o}\kappa \right]$$

$${}^{2}N = E^{o}A_{p}{}^{2}\overline{\varepsilon} , {}^{2}M = E^{o}I_{p} \left[{}^{2}\kappa \left(1 + {}^{2}\overline{\varepsilon} \right) - {}^{o}\kappa \right] ,$$

$${}^{2}T = G^{o}J_{p} \left[{}^{2}\tau \left(1 + {}^{2}\overline{\varepsilon} \right) - {}^{o}\tau \right] ,$$

$$\delta U = \int_{\sigma_{s}} \left\{ {}^{2}N\delta^{2}\overline{\varepsilon} + {}^{2}M\delta \left[{}^{2}\kappa \left(1 + {}^{2}\overline{\varepsilon} \right) - {}^{o}\kappa \right] + {}^{2}T\delta \left[{}^{2}\tau \left(1 + {}^{2}\overline{\varepsilon} \right) - {}^{o}\tau \right] \right\} d^{2}s$$

$$\delta U = \int_{\alpha} \left[{}^{2}N\delta^{2}s' + {}^{2}M\delta \left({}^{2}\theta' - {}^{o}\theta' \right) + {}^{2}T\delta \left({}^{2}\phi' - {}^{o}\phi' \right) + {}^{2}T\delta \left({}^{2}\psi' - {}^{o}\psi' \right) \right] d\alpha$$

$$(2.17 a-f)$$

Theorem 2: When the ULD is adopted to describe deformation of the riser, the fiber strain, the constitutive relations and the virtual strain energy are expressed as follows

$${}^{2}\varepsilon_{\zeta} = {}^{2}\varepsilon + \zeta \left[{}^{2}\kappa (1+\varepsilon) - {}^{o}\kappa (1 - {}^{I}\varepsilon) \right]$$

$${}^{2}N = E^{I}A_{p}{}^{2}\varepsilon , {}^{2}M = E^{I}I_{p} \left[{}^{2}\kappa (1+\varepsilon) - {}^{o}\kappa (1 - {}^{I}\varepsilon) \right],$$

$${}^{2}T = G^{I}J_{p} \left[{}^{2}\tau (1+\varepsilon) - {}^{o}\tau (1 - {}^{I}\varepsilon) \right],$$

$$\delta U = \int_{s} \left\{ {}^{2}N\delta^{2}\varepsilon + {}^{2}M\delta \left[{}^{2}\kappa \left(1 + \varepsilon \right) - {}^{o}\kappa \left(1 - {}^{I}\varepsilon \right) \right] \right.$$

$$\left. + {}^{2}T\delta \left[{}^{2}\tau \left(1 + \varepsilon \right) - {}^{o}\tau \left(1 - {}^{I}\varepsilon \right) \right] \right\} d^{I}s$$

$$\delta U = \int_{\alpha} \left[{}^{2}N\delta^{2}s' + {}^{2}M\delta \left({}^{2}\theta' - {}^{o}\theta' \right) + {}^{2}T\delta \left({}^{2}\phi' - {}^{o}\phi' \right) + {}^{2}T\delta \left({}^{2}\psi' - {}^{o}\psi' \right) \right] d\alpha$$

$$(2.18 a-f)$$

Theorem 3: When the ED is adopted to describe deformation of the riser, the fiber strain, the constitutive relations and the virtual strain energy are expressed as follows

$${}^{2E}\varepsilon_{\zeta} = {}^{2E}\varepsilon + \zeta \left[{}^{2}\kappa - {}^{o}\kappa \left(I - {}^{2E}\varepsilon \right) \right]$$

$${}^{2}N = E^{2}A_{p} {}^{2E}\varepsilon , {}^{2}M = E^{2}I_{p} \left[{}^{2}\kappa - {}^{o}\kappa \left(I - {}^{2E}\varepsilon \right) \right],$$

$${}^{2}T = G^{2}J_{p} \left[{}^{2}\tau - {}^{o}\tau \left(I - {}^{2E}\varepsilon \right) \right],$$

$$\delta U = \int_{i_{s}} \left\{ {}^{2}N\delta^{2}\overline{\varepsilon} + {}^{2}M\delta \left[{}^{2}\kappa - {}^{o}\kappa \left(I - {}^{2E}\varepsilon \right) \right] \right\} d^{2}s$$

$$+ {}^{2}T\delta \left[{}^{2}\tau - {}^{o}\tau \left(I - {}^{2E}\varepsilon \right) \right] \right\} d^{2}s$$

$$\delta U = \int_{\alpha} \left[{}^{2}N\delta^{2}s' + {}^{2}M\delta \left({}^{2}\theta' - {}^{o}\theta' \right) + {}^{2}T\delta \left({}^{2}\phi' - {}^{o}\phi' \right) + {}^{2}T\delta \left({}^{2}\psi' - {}^{o}\psi' \right) \right] d\alpha$$

$$(2.19 a-f)$$

in which ε_{ζ} is the axial strain at any fiber radius (ζ) , E is the elastic modulus, G is the shear modulus, N is the axial force, M is the bending moment, T is the torque, and U is the strain energies due to axial force, bending moments, and torsion of the riser.

2.5 EFFECTS OF HYDROSTAITIC PRESSURES

Hydrostatic pressures are the pressures of still fluids. In the past, the hydrostatic pressure effects on marine riser pipe analysis were tackled via the effective tension concept proposed by Spark (1984), as will be described in section 2.5.1. However, because the effective tension concept limits $\nu = 0.5$, thus the apparent tension concept (Chucheepsakul et al., 2003) has proposed instead in order to cover all values of the Poisson's ratio, as will be explained in section 2.5.2. This research offers a more advanced technique on treating the hydrostatic pressure effects.

2.5.1 The Effective Tension Concept

First of all, the Archimedes' principle is recalled and used to explain the effective tension concept. Consider Figure 2.3(a), the equilibrium of water column element proves that the enclosing external pressure field is equivalent to the buoyancy force $\rho_w g \forall_w$ (see Figure 2.3(a3)), where ρ_w is the water density, g the gravitational acceleration, and \forall_w the volume of water column. In contrast, the enclosing internal pressure field will thus induce the weight $\rho_w g \forall_w$ against the buoyant force (see Figure 2.3(a5)). These tenets are so-called the Archimedes' principle.

It is remarkable that Archimedes' principle is usable with the enclosing pressure fields. However, unlike the water column, the pressure fields of external and internal fluids surround only the external and internal side surfaces of the riser segment, as seen in Figure 2.3(b1). Both ends cut of the riser segment are not subjected to the pressure fields, which are called the missing pressures, and thus Archimedes' principle cannot be used straightforwardly. Sparks (1984) solved this problem by proposing the superposition technique as follows:

Step 1. The first step of the superposition technique is separating all forces acting on the real system of the riser as shown in Figure 2.3(b1) into the two sets of forces as shown in Figures 2.3(b2) and 2.3(b3). The missing pressures are added in at the both ends of the riser segment in Figure 2.3(b2) to result in the pressure fields enclosing the riser segment. However, the added pressures are non-existent, so they must be removed for balance by applying the opposite pressure fields at the both ends of the riser in Figure 2.3(b3).

Step 2. Since the previous step yields the pressured fields enclosing the riser segment in Figure 2.3(b2), Archimedes's principle is now applicable. Therefore, the external pressure induces the buoyant force $-\rho_e \forall_e g$, and the internal pressure yields the internal fluid weight $\rho_i \forall_i g$ as shown in Figure 2.3(b4). Summation of these forces with the aerial weight of the riser segment produces the total weight of the effective system, which is so-called the effective weight. Therefore, the expression of the effective weight per unit length w_e is obtained as

$$w_a = (\rho_p A_p - \rho_e A_e + \rho_i A_i)g \tag{2.20}$$

Step 3. Summation between the true-wall tension and the balance forces of the missing pressures in Figure 2.3(b3) yields the total tension of the effective system, which is referred to as the effective tension, as shown in Figure 2.3(b5). Therefore, the expression of the effective tension N_a is obtained as

$$N_{e} = N + p_{e}A_{e} - p_{i}A_{i} \tag{2.21}$$

Step 4. Integrating the forces acting on Figures 2.3(b4) and 2.3(b5) together, one obtains the effective system of the riser, which is subjected to the effective weight and the effective tension as shown in Figure 2.3(b6).

Casting equations (2.20) and (2.21) into the general forms for the three deformation descriptors, one can establish Proposition 2.1.

Proposition 2.1. According to the effective tension concept, the real system of the submerged riser subjected to hydrostatic external and internal pressures is equivalent to the effective system of an empty onshore riser that is subjected to the effective weight and the effective tension

$$^{i}w_{a} = (\rho_{B}{}^{i}A_{B} - \rho_{a}{}^{i}A_{a} + \rho_{i}{}^{i}A_{i})g,$$
 (2.22)

$${}^{i}N_{e} = E^{i}A_{p}\varepsilon = N + p_{e}{}^{i}A_{e} - p_{i}{}^{i}A_{i},$$
 (2.23)

in which ${}^{i}A_{\alpha} = {}^{o}A_{\alpha}$ for TLD, ${}^{i}A_{\alpha} = {}^{l}A_{\alpha}$ for ULD, ${}^{i}A_{\alpha} = {}^{2}A_{\alpha}$ for ED when $\alpha \in \{P, e, i\}$.

2.5.2 The Apparent Tension Concept

The apparent tension concept is more accurate in undertaking the hydrostatic pressure effects on elastic body than the effective tension concept. It acknowledges that the riser is an elastic solid, and thus in the polar coordinates the enclosing pressure fields in Figure 2.3(b2) can induce the triaxial stresses: the radial stress σ_r , the circumferential stress σ_θ , and the tensile stress σ_z . From the theory of elasticity, these triaxial stresses provoke the axial strain and the tension in the form

$$\varepsilon_{tri} = \left[\sigma_z - v(\sigma_r + \sigma_\theta)\right] / E, \ N_{tri} = EA_p \varepsilon_{tri}$$
 (2.24 a,b)

In Figure 2.3(b2), the riser segment is subjected to the triaxial stresses due to the hydrostatic internal and external pressures $\sigma_z = \sigma_r = \sigma_\theta = (p_i A_i - p_e A_e)/A_P$. Consequently, equations (2.24) yield

$$N_{pj} = (2\nu - 1)(p_{e}A_{e} - p_{i}A_{j})$$
(2.24)

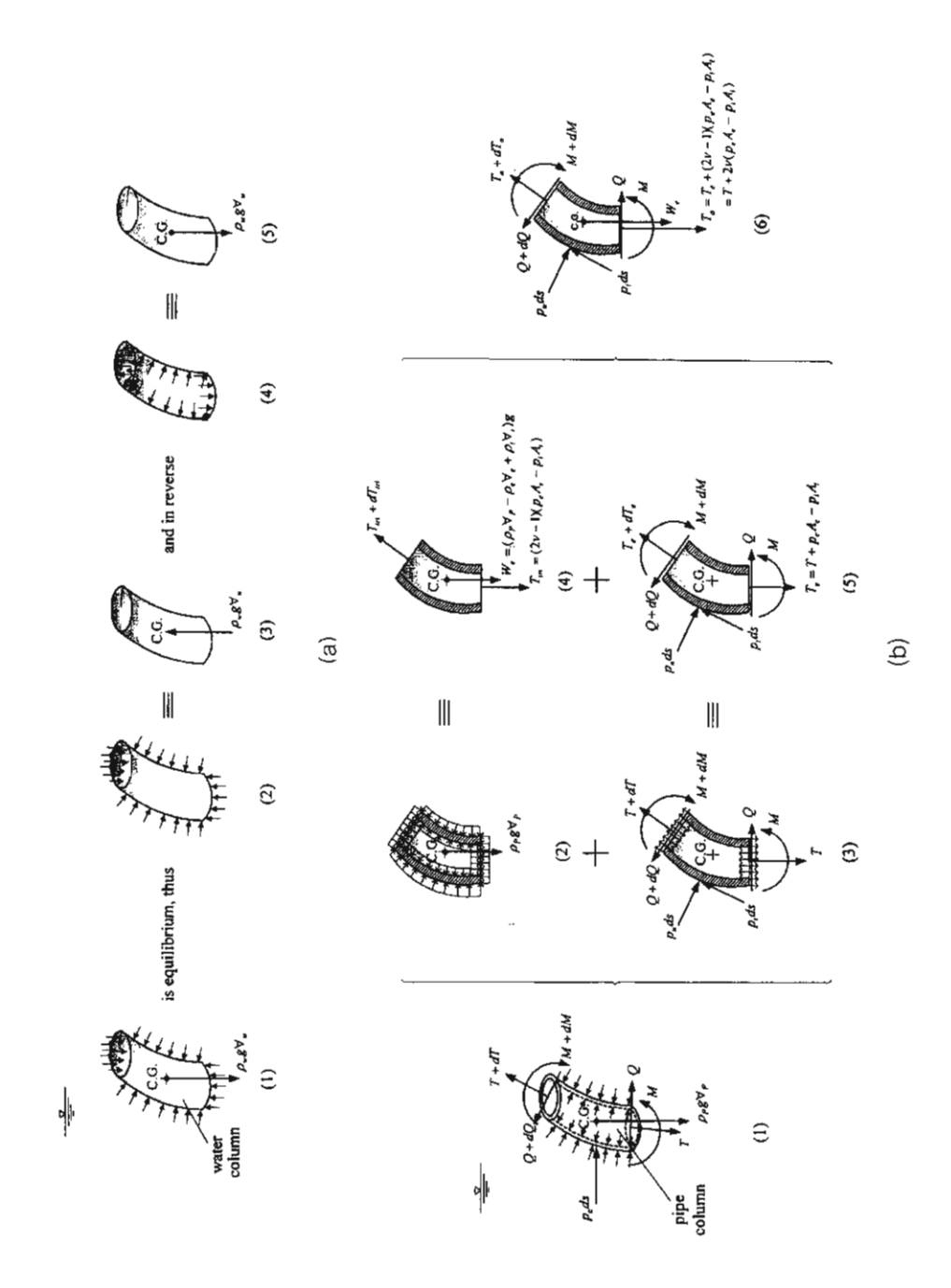


Figure 2.3 Treatments of the Hydrostatic Pressure Effects

(a) Archimedes' Principles (b) the Apparent Tension Concept

For the apparent tension concept, this tension is added into Figures 2.3(b4) and 2.3 (b6), and the system in Figure 2.3(b6) is renamed to the apparent system. The tension acting on the apparent system is called the apparent tension, of which the expression is

$$N_a = N_a + N_{tri} = N + 2\nu(p_a A_a - p_i A_i). \tag{2.25}$$

It is seen that $N_a = N_e$ if, and only if v = 0.5. This signifies that the effective tension concept is a subset of the apparent tension concept. Although the expressions of the weights acting on the effective and the apparent systems are the same, the weight acting on the apparent system is called the apparent weight.

Casting equation (2.25) into the general forms for the three deformation descriptors, one can establish Proposition 2.2.

Proposition 2.2. According to the apparent tension concept, the real system of the submerged riser subjected to hydrostatic external and internal pressures is equivalent to the apparent system of an empty onshore riser that is subjected to the apparent weight and the apparent tension

$$^{i}w_{a} = (\rho_{P}{}^{i}A_{P} - \rho_{e}{}^{i}A_{e} + \rho_{i}{}^{i}A_{i})g,$$
 (2.25)

$${}^{i}N_{a} = E^{i}A_{p}\varepsilon = N + 2\nu(p_{e}{}^{i}A_{e} - p_{i}{}^{i}A_{i})$$
 (2.25)

2.6 EFFECTS OF HYDRODYNAMIC PRESSURES

Hydrodynamic pressures occur due to steady and unsteady flows of external and internal fluids. Steady flows will cause the static forces, while unsteady flows will engender the dynamic forces acting on the riser wall. For the marine riser transporting fluid, the external flow is the horizontal cross flows of ocean current and wave, whereas the internal flow is the tangential flow of transported fluid. In this section, the hydrodynamic forces induced by the horizontal cross flows of current and wave is demonstrated in section 2.6.1, whereas the hydrodynamic forces induced by the tangential flow of transported fluid is derived in section 2.6.2.

2.6.1 <u>The Hydrodynamic Forces Due to the Horizontal Cross Flows of</u> Current and Wave

The hydrodynamic forces exerted on flexible marine risers with large displacements in the orthogonal triad system based on the coupled Morison equation (Chakrabarti, 1990) can be expressed as

$$\bar{\mathbf{F}}_{H} = \begin{cases} f_{Ht} \\ f_{Hn} \\ f_{Hbn} \end{cases} = 0.5 \rho_{e}^{2} D_{e} \begin{cases} \pi C_{Dt} \gamma_{t} | \gamma_{t} | \\ C_{Dn} \gamma_{n} | \gamma_{n} | \\ C_{Dbn} \gamma_{bn} | \gamma_{bn} | \end{cases} + \rho_{e}^{2} A_{e} C_{a} \begin{cases} \dot{\gamma}_{t} \\ \dot{\gamma}_{n} \\ \dot{\gamma}_{bn} \end{cases} + \rho_{e}^{2} A_{e} \begin{cases} \dot{V}_{Ht} \\ \dot{V}_{Hn} \\ \dot{V}_{Hbn} \end{cases}$$

$$\frac{1}{\text{Viscous drag force}} \text{ Hydrodynamic mass force mass force} \qquad (2.26)$$

where C_{Dt} , C_{Dn} , and C_{Dbn} are the tangential, normal, and binormal drag coefficients; C_a is the added mass coefficient; V_{Ht} , V_{Hn} , and V_{Hbn} are the tangential, normal and binormal velocities of currents and waves; and $\gamma_t = V_{Ht} - \dot{u}_t$, $\gamma_n = V_{Hn} - \dot{v}_n$, and $\gamma_{bn} = V_{Hbn} - \dot{w}_{bn}$ are the velocities of currents and waves relative to riser velocities \dot{u}_t , \dot{v}_n , and \dot{w}_{bn} in tangential, normal, and binormal directions, respectively. For large strain analysis, the effect of cross-sectional changes of the riser in equation (2.12) has to be applied to equation (2.26).

To eliminate the difficulty of operating with absolute function in equation (2.26), the signum function is used. Here

$$sgn(\gamma) = \begin{cases} 1 & if \gamma \ge 0 \\ -1 & if \gamma < 0. \end{cases}$$
 (2.27)

With some manipulations, equation (2.26) can be arranged into

$$\vec{F}_{H} = \begin{cases} f_{Hi} \\ f_{Hin} \\ f_{Hbn} \end{cases} = - \begin{bmatrix} C_{a}^{*} & 0 & 0 \\ 0 & C_{a}^{*} & 0 \\ 0 & 0 & C_{a}^{*} \end{bmatrix} \begin{cases} \vec{u}_{l} \\ \vec{v}_{n} \\ \vec{w}_{bn} \end{cases} - \begin{bmatrix} C_{eql}^{*} & 0 & 0 \\ 0 & C_{eqn}^{*} & 0 \\ 0 & 0 & C_{eqbn}^{*} \end{bmatrix} \begin{cases} \vec{u}_{l} \\ \vec{v}_{n} \\ \vec{w}_{bn} \end{cases} \\
+ \begin{cases} C_{Dl}^{*} V_{Hi}^{2} + C_{M}^{*} \vec{V}_{Hi} \\ C_{Dn}^{*} V_{Hin}^{2} + C_{M}^{*} \vec{V}_{Hin} \\ C_{Dbn}^{*} V_{Hin}^{2} + C_{M}^{*} \vec{V}_{Hbn} \end{cases} \tag{2.28}$$

where C_{eqt}^* , C_{eqn}^* , C_{eqbn}^* are the coefficients of equivalent tangential, normal, binormal damping, and C_{Dt}^* , C_{Dn}^* , C_{Dbn}^* are the coefficients of tangential, normal, and binormal drag forces, and C_a^* , C_M^* are the equivalent coefficients of added mass and inertia forces. They are, respectively, expressed as follows

$$C_{eat}^* = C_{Dt}^* \left[2V_{Ht} - \dot{u}_t \right], C_{Dt}^* = 0.5 \rho_e^2 D_e \pi C_{Dt} \cdot sgn(\gamma_t)$$
 (2.29 a,b)

$$C_{eqn}^* = C_{Dn}^* [2V_{Hn} - \dot{v}_n], C_{Dn}^* = 0.5 \rho_e^2 D_e C_{Dn} \cdot sgn(\gamma_n)$$
 (2.29 c,d)

$$C_{eqbn}^* = C_{Dbn}^* \left[2V_{Hbn} - \dot{w}_{bn} \right], C_{Dbn}^* = 0.5 \rho_e^2 D_e C_{Dbn} \cdot sgn(\gamma_{bn})$$
 (2.29 f,g)

$$C_a^* = \rho_e^2 A_e C_a, C_M^* = \rho_e^2 A_e C_M$$
 (2.29 h,i)

in which C_a is the added mass coefficient and $C_M = I + C_a$ is the inertia coefficient.

In order to transform hydrodynamic force in the orthogonal triad system to the fixed Cartesian coordinate system, Euler's angle (Atanackovic, 1997) is used to find the transformation matrix, which is the orthogonal matrix and can be written as

where

$$a_{1X} = \cos^2 \theta_2 \cos^2 \theta_3 \tag{2.31 a}$$

$$a_{IY} = \cos^2 \theta_2 \sin^2 \theta_3 \cos^2 \theta_1 + \sin^2 \theta_2 \sin^2 \theta_1$$
 (2.31 b)

$$a_{1Z} = \cos^2 \theta_2 \sin^2 \theta_3 \sin^2 \theta_1 - \sin^2 \theta_2 \cos^2 \theta_1$$
 (2.31 c)

$$a_{2X} = -\sin^2\theta_3 \tag{2.31 d}$$

$$a_{2Y} = \cos^2 \theta_1 \cos^2 \theta_3 \tag{2.31 e}$$

$$a_{2Z} = \sin^2 \theta_1 \cos^2 \theta_3 \tag{2.31 f}$$

$$a_{3x} = \cos^2 \theta_3 \sin^2 \theta_2 \tag{2.31 g}$$

$$a_{3Y} = \sin^2 \theta_2 \sin^2 \theta_3 \cos^2 \theta_1 - \cos^2 \theta_2 \sin^2 \theta_1 \tag{2.31 h}$$

$$a_{3Z} = \sin^2 \theta_1 \sin^2 \theta_2 \cos^2 \theta_3 + \cos^2 \theta_1 \cos^2 \theta_2 \tag{2.31 i}$$

Thus, equation (2.28) can be transformed into the fixed Cartesian coordinates system

(2.32)

where V_{Hx} , V_{Hy} and V_{Hz} are the velocities of external fluid in x, y, and z directions respectively, and

$$C_{eqx}^{*} = C_{eqt}^{*} a_{1X}^{2} + C_{eqn}^{*} a_{2X}^{2} + C_{eqbn}^{*} a_{3X}^{2}$$

$$C_{eqy}^{*} = C_{eqt}^{*} a_{1Y}^{2} + C_{eqn}^{*} a_{2Y}^{2} + C_{eqbn}^{*} a_{3Y}^{2}$$

$$C_{eqz}^{*} = C_{eqt}^{*} a_{1Z}^{2} + C_{eqn}^{*} a_{2Z}^{2} + C_{eqbn}^{*} a_{3Z}^{2}$$

$$(2.33 \text{ a-c})$$

$$C_{eqxy}^{*} = C_{eqt}^{*} a_{1X} a_{1Y} + C_{eqn}^{*} a_{2X} a_{2Y} + C_{eqbn}^{*} a_{3X} a_{3Y}$$

$$C_{eqxz}^{*} = C_{eqt}^{*} a_{1X} a_{1Z} + C_{eqn}^{*} a_{2X} a_{2Z} + C_{eqbn}^{*} a_{3X} a_{3Z}$$

$$C_{eqyz}^{*} = C_{eqt}^{*} a_{1Y} a_{1Z} + C_{eqn}^{*} a_{2Y} a_{2Z} + C_{eqbn}^{*} a_{3Y} a_{3Z}$$

$$(2.34 \text{ a-c})$$

$$C_{Dx}^{*} = C_{Dt}^{*} a_{IX}^{3} + C_{Dn}^{*} a_{2X}^{3} + C_{Dbn}^{*} a_{3X}^{3}$$

$$C_{Dy}^{*} = C_{Dt}^{*} a_{IY}^{3} + C_{Dn}^{*} a_{2Y}^{3} + C_{Dbn}^{*} a_{3Y}^{3}$$

$$C_{Dz}^{*} = C_{Dt}^{*} a_{IZ}^{3} + C_{Dn}^{*} a_{2Z}^{3} + C_{Dbn}^{*} a_{3Z}^{3}$$

$$(2.35 \text{ a-c})$$

$$C_{Dxy1}^{*} = C_{Dt}^{*} a_{1X}^{2} a_{1Y} + C_{Dn}^{*} a_{2X}^{2} a_{2Y} + C_{Dbn}^{*} a_{3X}^{2} a_{3Y}$$

$$C_{Dxz1}^{*} = C_{Dt}^{*} a_{1X}^{2} a_{1Z} + C_{Dn}^{*} a_{2X}^{2} a_{2Z} + C_{Dbn}^{*} a_{3X}^{2} a_{3Z}$$

$$C_{Dyz1}^{*} = C_{Dt}^{*} a_{1Y}^{2} a_{1Z} + C_{Dn}^{*} a_{2Y}^{2} a_{2Z} + C_{Dbn}^{*} a_{3Y}^{2} a_{3Z}$$

$$C_{Dxy2}^{*} = C_{Dt}^{*} a_{1X} a_{1Y}^{2} + C_{Dn}^{*} a_{2X} a_{2Y}^{2} + C_{Dbn}^{*} a_{3X} a_{3Y}^{2}$$

$$C_{Dxz2}^{*} = C_{Dt}^{*} a_{1X} a_{1Z}^{2} + C_{Dn}^{*} a_{2X} a_{2Z}^{2} + C_{Dbn}^{*} a_{3X} a_{3Z}^{2}$$

$$C_{Dyz2}^{*} = C_{Dt}^{*} a_{1Y} a_{1Z}^{2} + C_{Dn}^{*} a_{2Y} a_{2Z}^{2} + C_{Dbn}^{*} a_{3Y} a_{3Z}^{2}$$

$$C_{Dxyz}^{*} = C_{Dt}^{*} a_{1X} a_{1Y} a_{1Z}^{2} + C_{Dn}^{*} a_{2X} a_{2Y} a_{2Z}^{2} + C_{Dbn}^{*} a_{3X} a_{3Y}^{2} a_{3Z}$$

$$C_{Dxyz}^{*} = C_{Dt}^{*} a_{1X} a_{1Y} a_{1Z}^{2} + C_{Dn}^{*} a_{2X} a_{2Y}^{2} a_{2Z}^{2} + C_{Dbn}^{*} a_{3X}^{2} a_{3Y}^{2} a_{3Z}^{2}$$

Equations (2.33 a-c) represent the coefficients of equivalent hydrodynamic damping force in x, y, and z directions. Equations (2.34 a-c) represent the coefficients of equivalent hydrodynamic damping force in x-y, x-z, and y-z planes. Equations (2.35 a-c) represent the coefficients of drag force in x, y, and z directions. Equations (2.36 a-g) represent the coefficients of drag force in x-y, x-z, and y-z planes.

At the equilibrium state, static loading is due only to the steady flow of external fluid. Therefore, the hydrodynamic forces from equations (2.28) and (2.32) are reduced to

$${}^{1}\bar{F}_{H} = \begin{cases} {}^{I}f_{Ht} \\ {}^{I}f_{Hn} \\ {}^{I}f_{Hbn} \end{cases} = \begin{cases} {}^{I}C_{Dt}^{*} {}^{I}V_{Ht}^{2} \\ {}^{I}C_{Dn}^{*} {}^{I}V_{Hn}^{2} \\ {}^{I}C_{Dbn}^{*} {}^{I}V_{Hbn}^{2} \end{cases}$$
(2.37)

$${}^{1}\vec{F}_{H} = \begin{cases} {}^{i}f_{Hx} \\ {}^{i}f_{Hx} \end{cases} = \begin{cases} {}^{i}C_{ox}^{*} {}^{i}V_{ux}^{2} + 2{}^{i}C_{ox}^{*} {}^{i}V_{Hx} {}^{i}V_{Hy} + 2{}^{i}C_{ox}^{*} {}^{i}V_{Hx} {}^{i}V_{Hz} + 2{}^{i}C_{oxx}^{*} {}^{i}V_{Hy} {}^{i}V_{Hz} + {}^{i}C_{oxy}^{*} {}^{i}V_{Hz} + {}^{i}C_{oxy}^{*} {}^{i}V_{Hz}^{2} + {}^{i}C_{oxz}^{*} {}^{i}V_{Hz}^{2} + {}^{i}C$$

In this study, the horizontal cross flows of current and wave, in dynamic analysis, are scoped to be in-plane flows, and the dynamic pressure fields are assumed to be uniform around the cross-section of the riser, but vary along the arclength of the riser. Therefore

$${}^{2}V_{Hx} = {}^{2}V_{c} + {}^{2}V_{w}, {}^{2}V_{Hy} = 0, {}^{2}V_{Hz} = 0,$$
 (2.39 a-c)

$${}^{2}V_{Ht} = {}^{2}V_{Hx}a_{1x}, {}^{2}V_{Hn} = {}^{2}V_{Hx}a_{2x}, {}^{2}V_{Hbn} = 0$$
 (2.40 a-c)

where ${}^2V_c = {}^2V_c({}^2y)$ is the current velocity, and ${}^2V_w = {}^2V_w({}^2y,t)$ the wave velocity. The profile of the current velocity may be expressed in the form of polynomial function as

$${}^{2}V_{c} = V_{ct} \left(\frac{{}^{2}y}{{}^{o}y_{t}}\right)^{n}, \qquad (2.41)$$

where V_{ct} is the current velocity at mean sea level, and ${}^{o}y_{t}$ are surface sea level. The index n can be varied from 0 to 1 depending upon the current profile. In this study, n = 1/7 is employed for the tidal current profile (Larsen, 1976).

For the regular incoming wave, the velocity of a water particle according to Airy's wave theory may be expressed as

$$^{2}V_{w} = ^{2}V_{wa}\cos\omega_{w}t, \qquad (2.42)$$

where t is the time, and ω_w the wave frequency. For deep water (${}^o y_t / L \ge 0.5$), the velocity amplitude ${}^2V_{wa} = {}^2V_{wa}({}^2y)$ is given by

$${}^{2}V_{wa} = \varsigma_{a}\omega_{w}e^{k\left[({}^{2}y)-({}^{o}y_{t})\right]}, \tag{2.43}$$

where the wave amplitude

$$\varsigma_a = H/2, \tag{2.44 a}$$

in which H is the wave height, the wave frequency

$$\omega_{w} = 2\pi/T, \qquad (2.44 \text{ b})$$

in which T is the wave period, and the wave number

$$k = 2\pi / L \,, \tag{2.44 c}$$

in which L is the wave length.

Substituting equation (2.39) into (2.32) yields

$$f_{Hx} = -C_a^* \ddot{x} - C_{eqx}^* \dot{x} - C_{eqxy}^* \dot{y} + C_{Dx}^* V_{Hx}^2 + C_M^* \dot{V}_{Hx}, \qquad (2.45 \text{ a})$$

$$f_{Hy} = -C_a^* \ddot{y} - C_{eqy}^* \dot{y} - C_{eqxy}^* \dot{x} + C_{Dxy1}^* V_{Hx}^2 + C_M^* \dot{V}_{Hy}. \tag{2.45 b}$$

$$f_{H_2} = 0$$
 (2.45 c)

Equations (2.32) and (2.45) capture the hydrodynamic pressure effects of both steady and unsteady flows. These equations are exploited for dynamic analysis of the riser.

2.6.2 <u>The Hydrodynamic Forces Due to the Tangential Internal Flows of</u> <u>Transported Fluid</u>

Based on the control volume approach of Computational Fluid Dynamics (Shames, 1992), hydrodynamic forces due to flow of transported fluid inside extensible flexible risers with large deformation can be derived as follows. Let ${}^{i}\bar{\mathbf{V}}_{F}$ and ${}^{i}\bar{\mathbf{V}}_{P}$ represent the velocity vectors of transported fluid and the riser with respect to the fixed frame of reference, then the velocity vector of transported fluid relative to the riser velocity is given by

$${}^{i}\vec{\mathbf{V}}_{FP} = ({}^{i}V_{FP}){}^{i}\hat{\mathbf{t}} = ({}^{i}V_{FP})\partial^{i}\mathbf{\bar{\tau}}_{P} / \partial^{i}s = {}^{i}\vec{\mathbf{V}}_{F} - {}^{i}\vec{\mathbf{V}}_{P}$$

$$(2.46)$$

where ${}^{i}V_{FP}$ is the internal flow velocity function: ${}^{i}V_{FP} = {}^{o}V_{i}$, ${}^{i}V_{FP} = {}^{I}V_{i}$, and ${}^{o}V_{FP} = {}^{2}V_{i}$ at the undeformed state, the equilibrium state, and the displaced state, respectively.

From Newton's law of momentum conservation, the hydrodynamic pressures due to internal flow induce the inertial force of transported mass as

$$\int_{\forall_{i}}^{i} \mathbf{\bar{B}}_{i} d \forall_{i} = \int_{\forall_{i}}^{i} \frac{D(\rho_{i}({}^{i} \bar{\nabla}_{F}))}{Dt} d \forall_{i} = \int_{\forall_{i}}^{i} \left[\frac{D\rho_{i}}{Dt} ({}^{i} \bar{\nabla}_{F}) + \rho_{i} ({}^{i} \bar{\mathbf{a}}_{F}) \right] d \forall_{i}$$
(2.47)

where ${}^{i}\mathbf{\bar{B}_{i}}$ is the inertial force per unit control volume \forall_{i} , ${}^{i}\mathbf{\bar{a}}_{F}$ the acceleration vector of transported fluid with respect to the fixed frame of reference at each states, and

$$\frac{D()}{Dt} = \frac{\partial()}{\partial t} + (^{i}\vec{\nabla}_{FP}.\nabla)() = \frac{\partial()}{\partial t} + \frac{^{i}V_{FP}}{^{i}s'}\frac{\partial()}{\partial \alpha}$$
(2.48)

It can be proved by Lemma 2.1 that $D\rho_i/Dt$ vanishes.

Lemma 2.1. The conservative condition of transported mass yields $D\rho_i/Dt = 0$.

Proof. Utilizing equation (2.46), equation (2.47) can be written as

$$\int_{\mathbf{V}_{i}}^{t} \mathbf{\bar{B}}_{i} d \forall_{i} = \int_{\mathbf{V}_{i}}^{t} \left[\frac{D(\rho_{i}^{i} \mathbf{\bar{V}}_{p})}{Dt} \right] d \forall_{i} + \int_{\mathbf{V}_{i}}^{t} \left[\frac{D(\rho_{i}^{i} \mathbf{\bar{V}}_{FP})}{Dt} \right] d \forall_{i}$$
(2.49)

From the Reynolds transport theorem (Shames, 1992), the last integral is given by

$$\int_{\forall_{i}} \frac{D(\rho_{i}^{i} \vec{\nabla}_{FP})}{Dt} d\forall_{i} = \frac{\partial}{\partial t} \left[\int_{\forall_{i}} (\rho_{i}^{i} \vec{\nabla}_{FP}) d\forall_{i} \right] + \bigoplus_{i \neq j} {}^{i} \vec{\nabla}_{FP} (\rho_{i}({}^{i} \vec{\nabla}_{FP}) . d^{i} \vec{A}_{si}), \quad (2.50)$$

where ${}^{i}A_{si}$ is the internal control surface of the riser.

Employing the Gauss divergence theorem, one can demonstrate that

$$\bigoplus_{i_{A_{i}}} {}^{i} \vec{\nabla}_{FP} \left(\rho_{i} ({}^{i} \vec{\nabla}_{FP}) . d^{i} \vec{A}_{si} \right) = \int_{\nabla_{i}} \left[\left(\rho_{i} ({}^{i} \vec{\nabla}_{FP}) . \nabla \right)^{i} \vec{\nabla}_{FP} + \nabla . \left(\rho_{i} ({}^{i} \vec{\nabla}_{FP}) \right)^{i} \vec{\nabla}_{FP} \right] d \nabla_{i}$$
(2.51)

Substituting equations (2.51) into (2.50), one obtains

$$\int_{\forall_{i}} \frac{D(\rho_{i}({}^{i}\vec{\nabla}_{FP}))}{Dt} d\forall_{i} = \int_{\forall_{i}} \left\{ \rho_{i} \left[\frac{\partial^{i}\vec{\nabla}_{FP}}{\partial t} + ({}^{i}\vec{\nabla}_{FP}.\nabla){}^{i}\vec{\nabla}_{FP} \right] \right\}$$

$$+ \left[\frac{\partial \rho_{i}}{\partial t} + \nabla \cdot \left(\rho_{i} ({}^{i} \vec{\nabla}_{FP}) \right) \right] {}^{i} \vec{\nabla}_{FP} \right\} d \forall_{i} \qquad (2.52)$$

Refer to equation (2.48), the bracketed term (1) is known as the acceleration of transported fluid \bar{a}_{FP} , whereas following the continuity condition (Shames, 1992) the term (2) is zero due to the continuity condition of conservation of mass. Thereby, equation (2.52) yields

$$\frac{D(\rho_{i}({}^{i}\vec{\nabla}_{FP}))}{Dt} = \rho_{i}({}^{i}\vec{a}_{FP})$$
 (2.53)

But $\frac{D(\rho_i({}^i\vec{\nabla}_{FP}))}{Dt} = \frac{D\rho_i}{Dt} \cdot ({}^i\vec{\nabla}_{FP}) + \rho_i({}^i\vec{a}_{FP})$ and ${}^i\vec{\nabla}_{FP} \neq 0$, thus equation (2.53) is valid if, and only if

$$D\rho_i / Dt = 0 \tag{2.54}$$

Q.E.D.

Using Lemma 2.1 in equation (2.47), one can constitute Proposition 2.3.

Proposition 2.3. The internal flow through the moving, deforming control volume of the riser induces the inertial force per unit control volume acting on the riser wall

$${}^{t}\mathbf{\vec{B}}_{i} = \rho_{i}({}^{t}\mathbf{\vec{a}}_{F}), \tag{2.56a}$$

or the inertial force per unit riser-length

$$\overline{\mathbf{f}}_i = m_i \left({}^i \overline{\mathbf{a}}_F \right), \tag{2.56b}$$

where $\vec{\mathbf{f}}_i$ is the inertial force, and m_i the transported mass per unit riser-length.

From equation (2.56), it is seen that determining the inertial force on the transported fluid needs the expression of transported mass acceleration \bar{a}_F . Based on Eulerian mechanics (Huang, 1993), the velocity and acceleration of transported fluid can be derived as

$$\vec{V}_{F} = \vec{V}_{P} + \vec{V}_{FP} = \frac{\partial \vec{r}_{P}}{\partial t} + \frac{V_{FP}}{^{2}s'} \frac{\partial \vec{r}_{P}}{\partial \alpha}$$
(2.57)

$$\vec{a}_{F} = \vec{a}_{P} + \vec{a}_{FP} = \frac{D\vec{V}_{P}}{Dt} + \frac{D\vec{V}_{FP}}{Dt} = \frac{D}{Dt} \left(\frac{\partial \vec{r}_{p}}{\partial t} \right) + \frac{D}{Dt} \left(\frac{V_{FP}}{^{2}s'} \frac{\partial \vec{r}_{p}}{\partial \alpha} \right)$$

$$= \frac{\partial^{2}\vec{r}_{p}}{\partial t^{2}} + \left(\frac{2V_{FP}}{^{2}s'} \right) \frac{\partial^{2}\vec{r}_{p}}{\partial \alpha \partial t} + \left(\frac{V_{FP}}{^{2}s'} \right)^{2} \frac{\partial^{2}\vec{r}_{p}}{\partial \alpha^{2}} + \left(\frac{\dot{V}_{FP}}{^{2}s'} + \frac{\dot{V}_{FP}V_{FP}'}{\binom{2}s'} - \frac{\dot{V}_{FP}^{2}\dot{s}'}{\binom{2}s'}^{2} - \frac{\dot{V}_{FP}^{2}\dot{s}'}{\binom{2}s'}^{3}}{\delta \alpha} \right) \frac{\partial \vec{r}_{p}}{\partial \alpha}$$

$$(2.58)$$

in which the term (1) is the transported mass acceleration, (2) is the coriolis acceleration, (3) is the centripetal acceleration, (4) is the local acceleration due to unsteady flow, (5) is the convective acceleration due to non-uniform flow, and (6) is the relative accelerations due to local coordinate rotation and displacement.

By using the differential geometry formulas given in appendix and let V_i be the relative velocity of the transporting fluid, i.e. $V_i = V_{FP}$, the velocity and acceleration of transported fluid in the fixed Cartesian coordinate system and the orthogonal triad coordinate system can be expressed as follows

In the fixed Cartesian coordinate system, at the displaced state:

$$\bar{\mathbf{V}}_{F} = \begin{bmatrix} 2\dot{\mathbf{x}} + \frac{V_{i}^{2} 2x'}{2s'} \end{bmatrix} \hat{\mathbf{i}} + \begin{bmatrix} 2\dot{\mathbf{y}} + \frac{V_{i}^{2} 2y'}{2s'} \end{bmatrix} \hat{\mathbf{j}} + \begin{bmatrix} 2\dot{\mathbf{z}} + \frac{V_{i}^{2} 2z'}{2s'} \end{bmatrix} \hat{\mathbf{k}}$$

$$\bar{\mathbf{a}}_{F} = \begin{cases} 2\ddot{\mathbf{x}} + \left[\left(\frac{2}{2s'} - \frac{(2x')^{2}}{(2s')^{3}} \right)^{2} \dot{\mathbf{x}}' - \left(\frac{2x'^{2} 2y'}{(2s')^{3}} \right)^{2} \dot{\mathbf{y}}' - \left(\frac{2x'^{2} 2z'}{(2s')^{3}} \right)^{2} \dot{\mathbf{z}}' \right] V_{i}$$

$$+ \left[\frac{(2x''^{2} 2y' - 2x'^{2} 2y'')^{2} y' + (2x''^{2} 2z' - 2x'^{2} 2z'')^{2} z'}{(2s')^{3}} \right] V_{i}^{2} + \left(\frac{DV_{i}}{Dt} \right)^{2} \frac{2x'}{2s'} \right] \hat{\mathbf{i}}$$

$$+ \left[\frac{2\ddot{\mathbf{y}} + \left[-\left(\frac{2x'^{2} 2y'}{(2s')^{3}} \right)^{2} \dot{\mathbf{x}}' + \left(\frac{2}{2s'} - \frac{(2y')^{2}}{(2s')^{3}} \right)^{2} \dot{\mathbf{y}}' - \left(\frac{2y'^{2} 2z'}{(2s')^{3}} \right)^{2} \dot{\mathbf{z}}' \right] V_{i}$$

$$+ \left[\frac{(2y'''^{2} x' - 2y'^{2} x'')^{2} x' + (2y'''^{2} z' - 2y'^{2} z'')^{2} z'}{(2s')^{4}} \right] V_{i}^{2} + \left(\frac{DV_{i}}{Dt} \right)^{2} \frac{2y'}{s'} \right] \hat{\mathbf{j}}$$

$$+ \left\{ {}^{2}\ddot{z} + \left[-\left(\frac{{}^{2}x'^{2}z'}{\left({}^{2}s' \right)^{3}} \right)^{2}\dot{x}' - \left(\frac{{}^{2}y'^{2}z'}{\left({}^{2}s' \right)^{3}} \right)^{2}\dot{y}' + \left(\frac{2}{{}^{2}s'} - \frac{\left({}^{2}z' \right)^{2}}{\left({}^{2}s' \right)^{3}} \right)^{2}\dot{z}' \right] V_{i} \right.$$

$$+ \left[\frac{\left({}^{2}z''^{2}x' - {}^{2}z'^{2}x'' \right)^{2}x' + \left({}^{2}z''^{2}y' - {}^{2}z'^{2}y'' \right)^{2}y'}{\left({}^{2}s' \right)^{4}} \right] V_{i}^{2} + \left(\frac{DV_{i}}{Dt} \right)^{\frac{2}{2}z'} \hat{k}$$

$$(2.60)$$

in which

$$\frac{D(\)}{Dt} = \frac{\partial(\)}{\partial t} + \frac{V_i}{^2s'} \frac{\partial(\)}{\partial \alpha} \tag{2.61}$$

In the orthogonal triad coordinate system, at the displaced state:

$$\vec{\mathbf{V}}_{F} = \begin{bmatrix} {}^{2}\dot{u}_{t} + V_{i} \end{bmatrix} {}^{2}\hat{t} + \begin{bmatrix} {}^{2}\dot{v}_{n} \end{bmatrix} {}^{2}\hat{n} + \begin{bmatrix} {}^{2}\dot{w}_{bn} \end{bmatrix} {}^{2}\hat{b}$$
 (2.62)

$$\vec{a}_{F} = \left[{}^{2}\vec{u}_{i} + \frac{V_{i}({}^{2}\dot{s}')}{{}^{2}s'} + \dot{V}_{i} + \frac{V_{i}V'_{i}}{{}^{2}s'} \right] {}^{2}\hat{t} + \left[{}^{2}\ddot{v}_{n} + 2V_{i}({}^{2}\dot{s})({}^{2}\kappa) + V_{i}^{2}({}^{2}\kappa) \right] {}^{2}\hat{n} + \left[{}^{2}\ddot{w}_{bn} \right] {}^{2}\hat{b} \quad (2.63)$$

At the equilibrium state, the time-dependent terms vanish, the velocity and acceleration of transported fluid in the fixed Cartesian coordinate system and the orthogonal triad coordinate system become

In the fixed Cartesian coordinate system, at the equilibrium state:

$${}^{I}\bar{Q}_{F} = \left[\frac{{}^{I}V_{i}{}^{I}X'}{{}^{I}S'}\right]\hat{i} + \left[\frac{{}^{I}V_{i}{}^{I}y'}{{}^{I}S'}\right]\hat{j} + \left[\frac{{}^{I}V_{i}{}^{I}z'}{{}^{I}S'}\right]\hat{k}$$

$$(2.64)$$

$${}^{I}\bar{a}_{F} = \left\{ \left[\frac{\left({}^{I}X''^{I}y' - {}^{I}X'^{I}y''\right){}^{I}y' + \left({}^{I}X''^{I}z' - {}^{I}X'^{I}z''\right){}^{I}z'}}{\left({}^{I}S'\right)^{4}}\right]\left({}^{I}V_{i}\right)^{2} + \left(\frac{\left({}^{I}V_{i}\right){}^{I}V_{i}'}{{}^{I}S'}\right){}^{I}X'}{\left({}^{I}S'\right)^{4}}\hat{i} + \left\{ \left[\frac{\left({}^{I}Y''^{I}X' - {}^{I}Y'^{I}X''\right){}^{I}X' + \left({}^{I}Y''^{I}z' - {}^{I}Y'^{I}z''\right){}^{I}z'}}{\left({}^{I}S'\right)^{4}}\right]\left({}^{I}V_{i}\right)^{2} + \left(\frac{\left({}^{I}V_{i}\right){}^{I}V_{i}'}{{}^{I}S'}\right){}^{I}X' + \left({}^{I}Z''^{I}Y' - {}^{I}Z'^{I}Y''\right){}^{I}Y'}}{\left({}^{I}S'\right)^{4}}\right]\left({}^{I}V_{i}\right)^{2} + \left(\frac{\left({}^{I}V_{i}\right){}^{I}V_{i}'}{{}^{I}S'}}\right){}^{I}Z'}{\left({}^{I}S'\right)^{4}}\hat{k}$$

$$(2.65)$$

In the orthogonal triad coordinate system, at the equilibrium state:

$${}^{I}\vec{\mathbf{V}}_{F} = \left({}^{I}V_{i}\right){}^{I\partial}\hat{t} \tag{2.66}$$

$$\vec{\mathbf{a}}_{F} = \left[\frac{\left({}^{\prime}V_{i} \right) {}^{\prime}V_{i}^{\prime}}{{}^{\prime}S^{\prime}} \right] {}^{\prime}\hat{t} + \left[\left({}^{\prime}V_{i} \right)^{2} \left({}^{\prime}\kappa \right) \right] {}^{\prime}\hat{n}$$
(2.67)

2.7 VIRTUAL WORK FORMULATIONS

Based on the elastica theory, the apparent tension concept and dynamic interactions between fluid and riser, the internal virtual work and external virtual work can be obtained.

2.7.1 Internal Virtual Work

For the overall apparent system, the riser is subjected to the apparent tension N_a in place of the axial force of the real system. Therefore, applying equations (2.17-2.19) (the extensible elastica theory) to the apparent system yields the stiffness equation of the initially straight riser:

$$\delta({}^{2}U) = \int_{\alpha} {}^{2}N_{a}\delta({}^{2}s') + {}^{2}M\delta({}^{2}\theta') + {}^{2}T\delta({}^{2}\phi') + {}^{2}T\delta({}^{2}\psi') d\alpha \qquad (2.68)$$

where

$${}^{2}N_{a} = \begin{cases} E^{o}A_{p}{}^{2}\overline{\varepsilon} & (\text{TLD}) \\ E^{l}A_{p}{}^{2}\varepsilon & (\text{ULD}), {}^{2}M = {}^{2}B({}^{2}\kappa), {}^{2}B = \begin{cases} E({}^{o}I_{p})(1 + {}^{2}\overline{\varepsilon}) & (\text{TLD}) \\ E({}^{l}I_{p})(1 + \varepsilon) & (\text{ULD}) \end{cases} \\ E({}^{2}I_{p}) & (\text{ED}) \end{cases}$$

$${}^{2}T = {}^{2}C({}^{2}\tau), {}^{2}C = \begin{cases} G({}^{o}J_{p})(1 + {}^{2}\overline{\varepsilon}) & (\text{TLD}) \\ G({}^{I}J_{p})(1 + \varepsilon) & (\text{ULD}) \end{cases}$$

$$G({}^{2}J_{p}) \qquad (\text{ED})$$
(2.69 a-c)

By utilizing the differential geometry expressions and integrating by parts equation (2.68) three times, obtain the four forms of the internal virtual work can be expressed as follows:

Form 1:

$$\begin{split} \delta\left({}^{2}U\right) &= \int_{a}^{1} \left[\left[{}^{2}N_{a} \left(\frac{{}^{2}x'}{{}^{2}s'} \right) - {}^{2}M_{a} \left(\frac{{}^{2}\kappa\left({}^{2}x'\right)}{{}^{2}s'} + \frac{{}^{2}s''}{{}^{2}\kappa\left({}^{2}s'\right)^{3}} \frac{\partial}{\partial\alpha} \left(\frac{{}^{2}x'}{{}^{2}s'} \right) \right] \delta\left({}^{2}u'\right) \right. \\ &+ \left[{}^{2}N_{a} \left(\frac{{}^{2}y'}{{}^{2}s'} \right) - {}^{2}M_{a} \left(\frac{{}^{2}\kappa\left({}^{2}y'\right)}{{}^{2}s'} + \frac{{}^{2}s''}{{}^{2}\kappa\left({}^{2}s'\right)^{3}} \frac{\partial}{\partial\alpha} \left(\frac{{}^{2}y'}{{}^{2}s'} \right) \right] \delta\left({}^{2}v'\right) \right. \\ &+ \left[{}^{2}N_{a} \left(\frac{{}^{2}z'}{{}^{2}s'} \right) - {}^{2}M_{a} \left(\frac{{}^{2}\kappa\left({}^{2}z'\right)}{{}^{2}s'} + \frac{{}^{2}s''}{{}^{2}\kappa\left({}^{2}s'\right)^{3}} \frac{\partial}{\partial\alpha} \left(\frac{{}^{2}z'}{{}^{2}s'} \right) \right] \delta\left({}^{2}w'\right) \right\} d\alpha \\ &+ \int_{a}^{1} \left\{ \left[\frac{{}^{2}M_{a}}{{}^{2}\kappa\left({}^{2}s'\right)^{3}} \frac{\partial}{\partial\alpha} \left(\frac{{}^{2}x'}{{}^{2}s'} \right) \right] \delta\left({}^{2}u''\right) + \left[\frac{{}^{2}M_{a}}{{}^{2}\kappa\left({}^{2}s'\right)^{3}} \frac{\partial}{\partial\alpha} \left(\frac{{}^{2}z'}{{}^{2}s'} \right) \right] \delta\left({}^{2}w''\right) \right\} d\alpha \\ &+ \int_{a}^{1} \left\{ {}^{2}T \left[\frac{{}^{2}T\left({}^{2}x'\right)}{{}^{2}s'} + \frac{{}^{2}s'}{{}^{2}3} \left({}^{2}y''\left({}^{2}z''\right) - {}^{2}y''\left({}^{2}z''\right) \right) \right. \\ &+ \left. \left(\frac{{}^{2}M_{a}}{{}^{2}\kappa\left({}^{2}s'\right)^{3}} \frac{\partial}{\partial\alpha} \left(\frac{{}^{2}x'}}{{}^{2}s'} \right) \right] \delta\left({}^{2}w''\right) \right\} d\alpha \\ &+ \int_{a}^{1} \left\{ {}^{2}T\left({}^{2}T\left({}^{2}x''\right) + \frac{{}^{2}s'}{{}^{2}3} \left({}^{2}y''\left({}^{2}z''\right) - {}^{2}y''\left({}^{2}z''\right) \right) \right. \\ &+ \left. \left({}^{2}T\left({}^{2}T\left({}^{2}x''\right) + \frac{{}^{2}s'}{{}^{2}3} \left({}^{2}x''\left({}^{2}x''\right) - {}^{2}x''\left({}^{2}x''\right) \right) \right) \right. \\ &+ \left. \left({}^{2}T\left({}^{2}T\left({}^{2}T\right) + \frac{{}^{2}S}{{}^{2}3} \left({}^{2}T\left({}^{2}T\left({}^{2}T\right) - {}^{2}T\left({}^{2}T\left({}^{2}T\right) \right) \right) \right. \right] \delta\left({}^{2}u'\right) \right. \\ &+ \left. \left({}^{2}T\left({}^{2}T\left({}^{2}T\right) - {}^{2}T\left({}^{2}T\left({}^{2}T\left({}^{2}T\right) - {}^{2}T\left({}^{2}T\left({}^{2}T\right) \right) \right) \right] \delta\left({}^{2}T\left({}^{2}T\right) \right) \right] \delta\left({}^{2}T\left({}^{2}T\left({}^{2}T\left({}^{2}T\right) - {}^{2}T\left({}^{2}T\left({}^{2}T\left({}^{2}T\right) - {}^{2}T\left({}^{2}T\left({}^{2}T\right) \right) \right) \right] \delta\left({}^{2}T\left({}^{2}T\left({}^{2}T\left({}^{2}T\left({}^{2}T\right) - {}^{2}T\left({}^{2}T\left({}^{2}T\left({}^{2}T\right) - {}^{2}T\left({}^{2}T\left({}^{2}T\left({}^{2}T\right) - {}^{2}T\left({}^{2}T\left({}^{2}T\left({}^{2}T\left({}^{2}T\left({}^{2}T\right) - {}^{2}T\left({}^{2}T\left({}^{2}T\left({}^{2}T\left({}^{2}T\left({}^{2}T\left({}^{2}T\left({}^{2}T\left({}^{2}T\left({}^{2}T\left({}^{2}T$$

$$-2\left(2^{2}\tau\right)\left\{\left(2^{2}x''(2^{2}y')-2^{2}x'(2^{2}y'')\right)\left(2^{2}y'\right)+\left(2^{2}x''(2^{2}z')-2^{2}x'(2^{2}z'')\right)\left(2^{2}z'\right)\right\}\right]\delta\left(2^{2}u''\right)$$

$$+\frac{2^{2}T\left(2^{2}s'\right)}{2}\left[\left(2^{2}x'(2^{2}z'')-2^{2}z'(2^{2}x'')\right)\right]$$

$$-2\left(2^{2}\tau\right)\left\{\left(2^{2}y''(2^{2}z')-2^{2}y'(2^{2}z'')\right)\left(2^{2}z'\right)-\left(2^{2}x''(2^{2}y')-2^{2}x'(2^{2}y'')\right)\left(2^{2}x'\right)\right\}\right]\delta\left(2^{2}v''\right)$$

$$+\frac{2^{2}T\left(2^{2}s'\right)}{2}\left[\left(2^{2}y'(2^{2}x''')-2^{2}x'(2^{2}y''')\right)$$

$$-2\left(2^{2}\tau\right)\left\{-\left(2^{2}x''(2^{2}z')-2^{2}x'(2^{2}z'')\right)\left(2^{2}x'\right)-\left(2^{2}y''(2^{2}z')-2^{2}y'(2^{2}x'')\right)\left(2^{2}y'\right)\right\}\right]\delta\left(2^{2}w''\right)\right\}d\alpha$$

$$+\int_{a}\left\{\frac{2^{2}T\left(2^{2}s'\right)}{2}\left(2^{2}y'(2^{2}z'')-2^{2}z'(2^{2}y'')\right)\delta\left(2^{2}w'''\right)+\frac{2^{2}T\left(2^{2}s'\right)}{2}\left(2^{2}z'(2^{2}x'')-2^{2}x'(2^{2}z'')\right)\delta\left(2^{2}w'''\right)\right\}d\alpha$$

$$+\frac{2^{2}T\left(2^{2}s'\right)}{2}\left(2^{2}x'(2^{2}y'')-2^{2}y'(2^{2}x'')\right)\delta\left(2^{2}w'''\right)\right\}d\alpha$$

$$+\frac{2^{2}T\left(2^{2}s'\right)}{2}\left(2^{2}x'(2^{2}y'')-2^{2}y'(2^{2}x'')\right)\delta\left(2^{2}w'''\right)\right\}d\alpha$$

$$+\frac{2^{2}T\left(2^{2}s'\right)}{2}\left(2^{2}x'(2^{2}y'')-2^{2}y'(2^{2}x'')\right)\delta\left(2^{2}w'''\right)\right\}d\alpha$$

$$+\frac{2^{2}T\left(2^{2}s'\right)}{2}\left(2^{2}x'(2^{2}y'')-2^{2}y'(2^{2}x'')\right)\delta\left(2^{2}w'''\right)\right\}d\alpha$$

$$+\frac{2^{2}T\left(2^{2}s'\right)}{2}\left(2^{2}x'(2^{2}y'')-2^{2}y'(2^{2}x'')\right)\delta\left(2^{2}w'''\right)\right\}d\alpha$$

$$+\frac{2^{2}T\left(2^{2}s'\right)}{2}\left(2^{2}x'(2^{2}y'')-2^{2}y'(2^{2}x'')\right)\delta\left(2^{2}w''\right)\right\}d\alpha$$

$$+\frac{2^{2}T\left(2^{2}s'\right)}{2}\left(2^{2}x'(2^{2}y'')-2^{2}y'(2^{2}x'')\right)\delta\left(2^{2}w'''\right)$$

Form 2: After a first integration by part

$$\delta({}^{2}U) = \left[\frac{{}^{2}T({}^{2}s')}{{}^{2}\mathfrak{I}}({}^{2}y'({}^{2}z'') - {}^{2}z'({}^{2}y''))\delta({}^{2}u'')\right]_{\alpha_{o}}^{\alpha_{i}} + \left[\frac{{}^{2}T({}^{2}s')}{{}^{2}\mathfrak{I}}({}^{2}z'({}^{2}x'') - {}^{2}x'({}^{2}z''))\delta({}^{2}v'')\right]_{\alpha_{o}}^{\alpha_{i}} + \left[\frac{{}^{2}T({}^{2}s')}{{}^{2}\mathfrak{I}}({}^{2}x'({}^{2}y'') - {}^{2}y'({}^{2}x''))\delta({}^{2}w'')\right]_{\alpha_{o}}^{\alpha_{i}} + \int_{\alpha}^{2}\left[\frac{{}^{2}X'}{{}^{2}S'}\right] - {}^{2}M_{a}\left(\frac{{}^{2}K({}^{2}x')}{{}^{2}S'} + \frac{{}^{2}S''}{{}^{2}K({}^{2}S')}^{3}\frac{\partial}{\partial\alpha}(\frac{{}^{2}X'}{{}^{2}S'})\right)\right]\delta({}^{2}u')$$

$$+ \left[{}^{2}N_{a} \left(\frac{{}^{2}y'}{{}^{2}s'} \right) - {}^{2}M_{a} \left(\frac{{}^{2}\kappa \left({}^{2}y' \right)}{{}^{2}s'} + \frac{{}^{2}s''}{{}^{2}\kappa \left({}^{2}s' \right)^{3}} \frac{\partial}{\partial \alpha} \left(\frac{{}^{2}y'}{{}^{2}s'} \right) \right] \right] \delta \left({}^{2}v' \right)$$

$$+ \left[{}^{2}N_{a} \left(\frac{{}^{2}z'}{{}^{2}s'} \right) - {}^{2}M_{a} \left(\frac{{}^{2}\kappa \left({}^{2}z' \right)}{{}^{2}s'} + \frac{{}^{2}s''}{{}^{2}\kappa \left({}^{2}s' \right)^{3}} \frac{\partial}{\partial \alpha} \left(\frac{{}^{2}z'}{{}^{2}s'} \right) \right] \delta \left({}^{2}w' \right) \right\} d\alpha$$

$$+ \int_{a} \left\{ \left[\frac{{}^{2}M}{{}^{2}\kappa \left({}^{2}s' \right)^{2}} \frac{\partial}{\partial \alpha} \left(\frac{{}^{2}x'}{{}^{2}s'} \right) \right] \delta \left({}^{2}u'' \right) + \left[\frac{{}^{2}M}{{}^{2}\kappa \left({}^{2}s' \right)^{2}} \frac{\partial}{\partial \alpha} \left(\frac{{}^{2}y'}{{}^{2}s'} \right) \right] \delta \left({}^{2}v'' \right) \right\} d\alpha$$

$$+ \left[\frac{{}^{2}M}{{}^{2}\kappa \left({}^{2}s' \right)^{2}} \frac{\partial}{\partial \alpha} \left(\frac{{}^{2}z'}{{}^{2}s'} \right) \right] \delta \left({}^{2}w'' \right) + \mathbb{F}_{2z} \delta \left({}^{2}w'' \right) + \mathbb{F}_{2z} \delta \left({}^{2}w'' \right) \right\} d\alpha$$

$$+ \int_{a} \left\{ \left\{ \mathbb{F}_{Ix} \delta \left({}^{2}u' \right) + \mathbb{F}_{Iz} \delta \left({}^{2}w' \right) + \mathbb{F}_{2z} \delta \left({}^{2}w'' \right) + \mathbb{F}_{2z} \delta \left({}^{2}w'' \right) \right\} d\alpha \right\} d\alpha$$

$$+ \int_{a} \left\{ \mathbb{F}_{Ix} \delta \left({}^{2}w' \right) \right\} d\alpha d\alpha$$

$$+ \int_{a} \left\{ \mathbb{F}_{Ix} \delta \left({}^{2}w' \right) \right\} d\alpha d\alpha$$

$$(2.71)$$

where

$$\mathbb{F}_{lx} = {}^{2}T \left[\frac{{}^{2}\tau({}^{2}x')}{{}^{2}s'} + \frac{{}^{2}s'}{{}^{2}\mathfrak{F}} ({}^{2}y''({}^{2}z''') - {}^{2}y'''({}^{2}z'')) + \frac{2({}^{2}s')({}^{2}\tau)}{{}^{2}\mathfrak{F}} (({}^{2}x''({}^{2}y') - {}^{2}x'({}^{2}y''))({}^{2}y'') + ({}^{2}x''({}^{2}z') - {}^{2}x'({}^{2}z''))({}^{2}z'')) \right]$$
(2.72 a)

$$\mathbb{F}_{2x} = \frac{{}^{2}T({}^{2}s')}{{}^{2}\mathfrak{F}} ({}^{2}z'({}^{2}y''') - {}^{2}y'({}^{2}z'''))
-2({}^{2}\tau) \{ ({}^{2}x''({}^{2}y') - {}^{2}x'({}^{2}y'')) ({}^{2}y') + ({}^{2}x''({}^{2}z') - {}^{2}x'({}^{2}z'')) ({}^{2}z') \} \frac{{}^{2}T({}^{2}s')}{{}^{2}\mathfrak{F}}
- \left[\frac{{}^{2}T({}^{2}s')}{{}^{2}\mathfrak{F}} ({}^{2}y'({}^{2}z'') - {}^{2}z'({}^{2}y'')) \right]^{\prime}$$
(2.72 b)

$$\mathbb{F}_{2x} = \frac{-^{2}T(^{2}y'(^{2}z'') - ^{2}z'(^{2}y''))(^{2}s'')}{(^{2}s')^{6}(^{2}\kappa)^{2}}$$
(2.72 c)

$$\mathbb{F}_{Iy} = {}^{2}T \left[\frac{{}^{2}\tau({}^{2}y')}{{}^{2}s'} - \frac{{}^{2}s'}{{}^{2}\mathfrak{F}} ({}^{2}x''({}^{2}z''') - {}^{2}x'''({}^{2}z'')) \right] \\
+ \frac{2({}^{2}s')({}^{2}\tau)}{{}^{2}\mathfrak{F}} (({}^{2}y''({}^{2}z') - {}^{2}y'({}^{2}z''))({}^{2}z'') - ({}^{2}x''({}^{2}y') - {}^{2}x'({}^{2}y''))({}^{2}x'')) \right] \\
\mathbb{F}_{2y} = \frac{{}^{2}T({}^{2}s')}{{}^{2}\mathfrak{F}} ({}^{2}x'({}^{2}z''') - {}^{2}z'({}^{2}x''')) \tag{2.72 d}$$

$$\mathbb{F}_{2y} = \frac{{}^{2}T\binom{2}{s'}}{{}^{2}\mathfrak{F}} \binom{2}{x'} \binom{2}{z''} - {}^{2}z'\binom{2}{x''}$$

$$-2\binom{2}{t} \left\{ \binom{2}{t}y''\binom{2}{t} - {}^{2}y'\binom{2}{t}y'' \right\} \binom{2}{t} - \binom{2}{t}x''\binom{2}{t}y' - {}^{2}x'\binom{2}{t}y''$$

$$- \left[\frac{{}^{2}T\binom{2}{s'}}{{}^{2}\mathfrak{F}} \binom{2}{t}z'\binom{2}{t}x'' - {}^{2}x'\binom{2}{t}x'' \right]$$

$$- \left[\frac{2}{t}\binom{2}{t}x'' - {}^{2}x'\binom{2}{t}x'' - {}^{2}x'\binom{2}{t}x'' \right]$$

$$(2.72 e)$$

$$\mathbb{F}_{2y} = \frac{-^{2}T(^{2}z'(^{2}x'') - ^{2}x'(^{2}z''))(^{2}s'')}{(^{2}s')^{6}(^{2}\kappa)^{2}}$$
(2.72 f)

$$\mathbb{F}_{Iz} = {}^{2}T \left[\frac{{}^{2}\tau({}^{2}z')}{{}^{2}s'} + \frac{{}^{2}s'}{{}^{2}\mathfrak{F}} ({}^{2}x''({}^{2}y''') - {}^{2}x'''({}^{2}y'')) - \frac{{}^{2}x'''({}^{2}y'')}{{}^{2}\mathfrak{F}} (({}^{2}y''({}^{2}z') - {}^{2}y'({}^{2}z''))({}^{2}y'') + ({}^{2}x''({}^{2}z') - {}^{2}x'({}^{2}z''))({}^{2}x'')) \right]$$
(2.72 g)

$$\mathbb{F}_{2z} = \frac{{}^{2}T({}^{2}s')}{{}^{2}\mathfrak{F}}({}^{2}y'({}^{2}x''') - {}^{2}x'({}^{2}y'''))
-2({}^{2}\tau)\{-({}^{2}x''({}^{2}z') - {}^{2}x'({}^{2}z''))({}^{2}x') - ({}^{2}y''({}^{2}z') - {}^{2}y'({}^{2}z''))({}^{2}y')\}\frac{{}^{2}T({}^{2}s')}{{}^{2}\mathfrak{F}}
-\left[\frac{{}^{2}T({}^{2}s')}{{}^{2}\mathfrak{F}}({}^{2}x'({}^{2}y'') - {}^{2}y'({}^{2}x''))\right]'$$
(2.72 h)

$$\mathbb{F}_{2z} = \frac{-^{2}T(^{2}x'(^{2}y'') - ^{2}y'(^{2}x''))(^{2}s'')}{(^{2}s')^{6}(^{2}\kappa)^{2}}$$
(2.72 i)

Form 3: After a second integration by part

$$\delta \begin{pmatrix} {}^{2}U \end{pmatrix} = \begin{bmatrix} {}^{2}T \left(\frac{{}^{2}b_{x}}{\left({}^{2}s' \right)^{2} {}^{2}K} \delta \left({}^{2}u'' \right) + \frac{{}^{2}b_{y}}{\left({}^{2}s' \right)^{2} {}^{2}K} \delta \left({}^{2}w'' \right) + \frac{{}^{2}b_{z}}{\left({}^{2}s' \right)^{2} {}^{2}K} \delta \left({}^{2}w'' \right) \end{bmatrix} \right]_{a_{x}}^{a_{x}}$$

$$+ \begin{bmatrix} \frac{{}^{2}M}{{}^{2}s'} \left({}^{2}n_{x}\delta \left({}^{2}u' \right) + {}^{2}n_{y}\delta \left({}^{2}v' \right) + {}^{2}n_{z}\delta \left({}^{2}x' \right) \right) \right]_{a_{x}}^{a_{x}}$$

$$+ \int_{a} \left[\left\{ \left({}^{2}N_{a} - {}^{2}B \left({}^{2}K \right)^{2} \right) \left(\frac{{}^{2}x'}{{}^{2}s'} \right) - \frac{{}^{2}B \left({}^{2}s'' \right)}{\left({}^{2}s' \right)^{3}} \frac{\partial}{\partial \alpha} \left(\frac{{}^{2}x'}{{}^{2}s'} \right) + \left(\mathbb{F}_{Ix} - \mathbb{F}'_{Ix} \right) \right.$$

$$- \left[\frac{{}^{2}B}{\left({}^{2}s' \right)^{2}} \frac{\partial}{\partial \alpha} \left(\frac{{}^{2}x'}{{}^{2}s'} \right) \right] \right] \delta \left({}^{2}u' \right)$$

$$+ \left\{ \left({}^{2}N_{a} - {}^{2}B \left({}^{2}K \right)^{2} \right) \left(\frac{{}^{2}y'}{{}^{2}s'} \right) - \frac{{}^{2}B \left({}^{2}s'' \right)}{\left({}^{2}s' \right)^{3}} \frac{\partial}{\partial \alpha} \left(\frac{{}^{2}y'}{{}^{2}s'} \right) + \left(\mathbb{F}_{Iy} - \mathbb{F}'_{2y} \right) \right.$$

$$- \left[\frac{{}^{2}B}{\left({}^{2}s' \right)^{2}} \frac{\partial}{\partial \alpha} \left(\frac{{}^{2}y'}{{}^{2}s'} \right) \right] \right\} \delta \left({}^{2}v' \right)$$

$$+ \left\{ \left({}^{2}N_{a} - {}^{2}B \left({}^{2}K \right)^{2} \right) \left(\frac{{}^{2}z'}{{}^{2}s'} \right) - \frac{{}^{2}B \left({}^{2}s'' \right)}{\left({}^{2}s' \right)^{3}} \frac{\partial}{\partial \alpha} \left(\frac{{}^{2}z'}{{}^{2}s'} \right) + \left(\mathbb{F}_{Iz} - \mathbb{F}'_{2z} \right) \right.$$

$$- \left[\frac{{}^{2}B}{\left({}^{2}s' \right)^{2}} \frac{\partial}{\partial \alpha} \left(\frac{{}^{2}z'}{{}^{2}s'} \right) \right] \right\} \delta \left({}^{2}w' \right) d\alpha + \int_{\alpha} \left\{ {}^{2}T\delta \left({}^{2}w' \right) \right\} d\alpha$$

$$(2.73)$$

Form 4: After a third integration by part

$$\delta({}^{2}U) = \begin{bmatrix} {}^{2}T\left(\frac{{}^{2}b_{x}}{\left({}^{2}s'\right)^{2}{}^{2}\kappa}\delta({}^{2}u'') + \frac{{}^{2}b_{y}}{\left({}^{2}s'\right)^{2}{}^{2}\kappa}\delta({}^{2}v'') + \frac{{}^{2}b_{z}}{\left({}^{2}s'\right)^{2}{}^{2}\kappa}\delta({}^{2}w'') \end{bmatrix} \right]_{\alpha_{x}}^{\alpha_{t}}$$

$$+ \mathbb{E}_{2x}\delta({}^{2}u') + \mathbb{E}_{2y}\delta({}^{2}v') + \mathbb{E}_{2z}\delta({}^{2}z') + {}^{2}T\delta({}^{2}\psi)$$

$$+\left[\frac{{}^{2}M}{{}^{2}S'}\left({}^{2}n_{x}\delta\left({}^{2}u'\right)+{}^{2}n_{y}\delta\left({}^{2}v'\right)+{}^{2}n_{z}\delta\left({}^{2}w'\right)\right)\right]_{\alpha_{o}}^{\alpha_{i}}$$

$$+\left[{}^{2}R_{x}\delta\left({}^{2}u\right)+{}^{2}R_{y}\delta\left({}^{2}v\right)+{}^{2}R_{z}\delta\left({}^{2}w\right)\right]_{\alpha_{o}}^{\alpha_{i}}$$

$$+\int_{\alpha}\left[\left\{-{}^{2}R'_{x}\right\}\delta\left({}^{2}u\right)+\left\{-{}^{2}R'_{y}\right\}\delta\left({}^{2}v\right)+\left\{-{}^{2}R'_{z}\right\}\delta\left({}^{2}w\right)+\left\{-{}^{2}T'\right\}\delta\left({}^{2}\psi\right)\right]d\alpha \quad (2.74)$$

where

$$\mathbb{F}_{lx} - \mathbb{F}'_{2x} = {}^{2}T({}^{2}\kappa)({}^{2}b_{x}) \qquad (2.75 \text{ a})$$

$$\mathbb{F}_{ly} - \mathbb{F}'_{2y} = {}^{2}T({}^{2}\kappa)({}^{2}b_{y}) \qquad (2.75 \text{ b})$$

$$\mathbb{F}_{lz} - \mathbb{F}'_{2z} = {}^{2}T({}^{2}\kappa)({}^{2}b_{y}) \qquad (2.75 \text{ b})$$

$$\mathbb{F}_{lz} - \mathbb{F}'_{2z} = {}^{2}T({}^{2}\kappa)({}^{2}b_{z}) \qquad (2.75 \text{ c})$$

$${}^{2}R_{x} = \left[\left({}^{2}N_{a} - {}^{2}B({}^{2}\kappa)^{2}\right)\left({}^{2}\frac{2x'}{2s'}\right) - \frac{{}^{2}B({}^{2}s'')}{({}^{2}s')^{3}}\frac{\partial}{\partial\alpha}\left({}^{2}\frac{2x'}{2s'}\right)\right] + {}^{2}T({}^{2}\kappa)({}^{2}b_{x})$$

$$-\left[\frac{{}^{2}B}{({}^{2}s')^{2}}\frac{\partial}{\partial\alpha}\left({}^{2}\frac{2x'}{2s'}\right) - \frac{{}^{2}B({}^{2}s'')}{({}^{2}s')^{3}}\frac{\partial}{\partial\alpha}\left({}^{2}\frac{2y'}{2s'}\right)\right] + {}^{2}T({}^{2}\kappa)({}^{2}b_{y})$$

$$-\left[\frac{{}^{2}B}{({}^{2}s')^{2}}\frac{\partial}{\partial\alpha}\left({}^{2}\frac{2y'}{2s'}\right) - \frac{{}^{2}B({}^{2}s'')}{({}^{2}s')^{3}}\frac{\partial}{\partial\alpha}\left({}^{2}\frac{2z'}{2s'}\right)\right] + {}^{2}T({}^{2}\kappa)({}^{2}b_{z})$$

$$-\left[\frac{{}^{2}B}{({}^{2}s')^{2}}\frac{\partial}{\partial\alpha}\left({}^{2}\frac{2z'}{2s'}\right) - \frac{{}^{2}B({}^{2}s'')}{({}^{2}s')^{3}}\frac{\partial}{\partial\alpha}\left({}^{2}\frac{2z'}{2s'}\right)\right] + {}^{2}T({}^{2}\kappa)({}^{2}b_{z})$$

$$-\left[\frac{{}^{2}B}{({}^{2}s')^{2}}\frac{\partial}{\partial\alpha}\left({}^{2}\frac{2z'}{2s'}\right) - \frac{{}^{2}B({}^{2}s'')}{({}^{2}s')^{3}}\frac{\partial}{\partial\alpha}\left({}^{2}\frac{2z'}{2s'}\right)\right] + {}^{2}T({}^{2}\kappa)({}^{2}b_{z})$$

$$-\left[\frac{{}^{2}B}{({}^{2}s')^{2}}\frac{\partial}{\partial\alpha}\left({}^{2}\frac{2z'}{2s'}\right) - \frac{{}^{2}B({}^{2}s'')}{({}^{2}s')^{3}}\frac{\partial}{\partial\alpha}\left({}^{2}\frac{2z'}{2s'}\right)\right] + {}^{2}T({}^{2}\kappa)({}^{2}b_{z})$$

2.7.2 External Virtual Work

The external forces exert upon the marine risers are the effective weight, hydrodynamic loading, and inertial forces which depend on deformation of the riser. Therefore, an evaluation of these forces should be done with respect to the current

configuration of the riser. Then the variation of external virtual work evaluating from the free bodies at displaced state is

$$\delta W = \delta W_{w} + \delta W_{H} + \delta W_{I} \tag{2.76}$$

where δW_w , δW_H and δW_I are the virtual work of the apparent weight, hydrodynamic pressure, and inertial forces of the riser and transported fluid respectively. In the Cartesian coordinates, these expressions are written as follows,

$$\delta W_{w} = -\int_{\alpha} w_{a} \left({}^{2}s' \right) \delta \left({}^{2}v \right) d\alpha \tag{2.77}$$

$$\delta W_{H} = \int_{\alpha} \left[f_{Hx} \left({}^{2}s' \right) \delta \left({}^{2}u \right) + f_{Hy} \left({}^{2}s' \right) \delta \left({}^{2}v \right) + f_{Hz} \left({}^{2}s' \right) \delta \left({}^{2}w \right) \right] d\alpha \tag{2.78}$$

$$\delta W_{I} = - \iint_{a} \left(m_{p} a_{px} + m_{i} a_{Fx} \right) \left({^{2}s'} \right) \delta \left({^{2}u} \right) + \left(m_{p} a_{py} + m_{i} a_{Fy} \right) \left({^{2}s'} \right) \delta \left({^{2}v} \right)$$

$$+\left(m_{p}a_{pz}+m_{i}a_{Fz}\right)\left({}^{2}s'\right)\delta\left({}^{2}w\right)+m_{p}\left({}^{2}J_{p}\right)\left({}^{2}s'\right)\left({}^{2}\ddot{\psi}\right)\delta\left({}^{2}\psi\right)\right]d\alpha \qquad (2.79)$$

in which $\vec{a}_p = a_{px}\hat{i} + a_{py}\hat{j} + a_{pz}\hat{k} = \ddot{r} = {}_2\ddot{u}\hat{i} + {}_2\ddot{v}\hat{j} + {}_2\ddot{w}\hat{k}$ and the expressions of hydrodynamic force, $\vec{F}_H = f_{Hx}\hat{i} + f_{Hy}\hat{j} + f_{Hz}\hat{k}$, and the accelerate of transporting fluid, $\vec{a}_F = a_{Fx}\hat{i} + a_{Fy}\hat{j} + a_{Fz}\hat{k}$, are given by equations (2.32) and (2.60) respectively. Substituting equations (2.77)-(2.79) into equation (2.76) yields

$$\delta W = \int_{\alpha} \left\{ {}^{2}s' \left[f_{Hx} - m_{p} a_{px} - m_{i} a_{Fx} \right] \delta^{2} u \right\} d\alpha$$

$$+ \int_{\alpha} \left\{ {}^{2}s' \left[-w_{a} + f_{Hy} - m_{p} a_{py} - m_{i} a_{Fy} \right] \delta^{2} v \right\} d\alpha$$

$$+ \int_{\alpha} \left\{ {}^{2}s' \left[f_{Hz} - m_{p} a_{pz} - m_{i} a_{Fz} \right] \delta^{2} w \right\} d\alpha$$

$$- \int_{\alpha} \left\{ {}^{2}s' \left[m_{p} \left({}^{2}J_{p} \right) \left({}^{2}\ddot{\psi} \right) \right] \delta \left({}^{2}\psi \right) \right\} d\alpha$$

$$(2.80)$$

2.7.3 Total Virtual Work

From the principle of virtual work, the total virtual work of the effective system is zero:

$$\delta \pi = \delta U - \delta W = 0 \tag{2.81}$$

Substituting equations (2.70) and (2.80) into equation (2.81) and utilizing the differential geometry expressions in appendix yields the first weak form of the total virtual work expressed in the fixed Cartesian coordinate.

$$\begin{split} \delta\left({}^{2}\pi\right) &= \int_{a}^{\left\{\left[{}^{2}N_{a}\left(\frac{{}^{2}x'}{{}^{2}s'}\right) - {}^{2}M_{a}\left(\frac{{}^{2}\kappa\left({}^{2}x'\right)}{{}^{2}s'} + \frac{{}^{2}s''}{{}^{2}\kappa\left({}^{2}s'\right)^{3}}\frac{\partial}{\partial\alpha}\left(\frac{{}^{2}x'}{{}^{2}s'}\right)\right]\right\} \delta\left({}^{2}u'\right)} \\ &+ \left[{}^{2}N_{a}\left(\frac{{}^{2}y'}{{}^{2}s'}\right) - {}^{2}M_{a}\left(\frac{{}^{2}\kappa\left({}^{2}x'\right)}{{}^{2}s'} + \frac{{}^{2}s''}{{}^{2}\kappa\left({}^{2}s'\right)^{3}}\frac{\partial}{\partial\alpha}\left(\frac{{}^{2}x'}{{}^{2}s'}\right)\right]\right] \delta\left({}^{2}v'\right)} \\ &+ \left[{}^{2}N_{a}\left(\frac{{}^{2}z'}{{}^{2}s'}\right) - {}^{2}M_{a}\left(\frac{{}^{2}\kappa\left({}^{2}z'\right)}{{}^{2}s'} + \frac{{}^{2}s''}{{}^{2}\kappa\left({}^{2}s'\right)^{3}}\frac{\partial}{\partial\alpha}\left(\frac{{}^{2}z'}{{}^{2}s'}\right)\right]\right] \delta\left({}^{2}w'\right)\right\} d\alpha} \\ &+ \int_{a}^{\left\{\left[\frac{{}^{2}M}{{}^{2}\kappa\left({}^{2}s'\right)^{2}}\frac{\partial}{\partial\alpha}\left(\frac{{}^{2}x'}{{}^{2}s'}\right)\right] \delta\left({}^{2}u''\right) + \left[\frac{{}^{2}M}{{}^{2}\kappa\left({}^{2}s'\right)^{2}}\frac{\partial}{\partial\alpha}\left(\frac{{}^{2}y'}{{}^{2}s'}\right)\right] \delta\left({}^{2}w''\right)\right\} d\alpha} \\ &+ \int_{a}^{\left\{{}^{2}T\left[\frac{{}^{2}\tau\left({}^{2}x'\right)}{{}^{2}s'} + \frac{{}^{2}s'}{{}^{2}\Im}\left({}^{2}y''\left({}^{2}z''\right) - {}^{2}y''\left({}^{2}z''\right)\right)\right.} + \left({}^{2}x''\left({}^{2}z'\right) - {}^{2}x'\left({}^{2}z''\right)\right)\right\} \delta\left({}^{2}u'\right)} \\ &+ \frac{{}^{2}\left\{{}^{2}T\left[\frac{{}^{2}\tau\left({}^{2}x'\right)}{{}^{2}s'} + \frac{{}^{2}s'}{{}^{2}\Im}\left({}^{2}x''\left({}^{2}x''\right) - {}^{2}y''\left({}^{2}z''\right)\right)\right.} + \left({}^{2}x''\left({}^{2}z'\right) - {}^{2}x'\left({}^{2}z''\right)\right)\right\} \delta\left({}^{2}u'\right)} \\ &+ \frac{{}^{2}T\left[\frac{{}^{2}\tau\left({}^{2}x'\right)}{{}^{2}s'} - \frac{{}^{2}s'}{{}^{2}\Im}\left({}^{2}x''\left({}^{2}z''\right) - {}^{2}x''\left({}^{2}z''\right)\right)\right.} + \left({}^{2}x''\left({}^{2}z'\right) - {}^{2}x'\left({}^{2}x''\right)\right) \left({}^{2}x''\right)\right] \delta\left({}^{2}u'\right)} \\ &+ \frac{{}^{2}T\left[\frac{{}^{2}\tau\left({}^{2}z'\right)}{{}^{2}s'} - \frac{{}^{2}s'}{{}^{2}\Im}\left({}^{2}x''\left({}^{2}z''\right) - {}^{2}x''\left({}^{2}z''\right)\right)\right] \delta\left({}^{2}u'\right)} + \left({}^{2}x''\left({}^{2}x''\right) - {}^{2}x'\left({}^{2}x''\right)\right) \left({}^{2}x''\right)\right] \delta\left({}^{2}u'\right)} \right] \delta\left({}^{2}u'\right)} \\ &+ \frac{{}^{2}T\left[\frac{{}^{2}\tau\left({}^{2}z'\right)}{{}^{2}S'} - \frac{{}^{2}S'}{{}^{2}\Im}\left({}^{2}x''\left({}^{2}z''\right) - {}^{2}x''\left({}^{2}z''\right)\right) \left({}^{2}x''\right) - {}^{2}x'\left({}^{2}x''\right)\right) \left({}^{2}x''\right)} \right] \delta\left({}^{2}u'\right)} \\ &+ \frac{{}^{2}T\left[\frac{{}^{2}\tau\left({}^{2}x'\right)}{{}^{2}S'} - \frac{{}^{2}S'}{{}^{2}\Im}\left({}^{2}x''\left({}^{2}x''\right) - {}^{2}x''\left({}^{2}x''\right) - {}^{2}x''\left({}^{2}x''\right)\right) \left({}^{2}x''\right)} - {}^{2}x''\left({}^{2}x''\right) - {}^{2}x''\left({}^{2}x''\right) -$$

$$-2\left(2^{2}\tau\right)\left\{\left(2^{2}x''(2^{2}y')-2^{2}x'(2^{2}y'')\right)\left(2^{2}y'\right)+\left(2^{2}x''(2^{2}z')-2^{2}x'(2^{2}y')\right)\left(2^{2}z'\right)\right\}\right]\delta\left(2^{2}u''\right)$$

$$+\frac{2^{2}T\left(2^{2}s'\right)}{2\Im}\left[\left(2^{2}x'(2^{2}z'')-2^{2}y'(2^{2}z'')\right)\left(2^{2}z'\right)-\left(2^{2}x''(2^{2}y')-2^{2}x'(2^{2}y'')\right)\left(2^{2}x'\right)\right\}\right]\delta\left(2^{2}v''\right)$$

$$+\frac{2^{2}T\left(2^{2}s'\right)}{2\Im}\left[\left(2^{2}y'(2^{2}x''')-2^{2}x'(2^{2}y''')\right)$$

$$-2\left(2^{2}\tau\right)\left\{-\left(2^{2}x''(2^{2}z')-2^{2}x'(2^{2}z'')\right)\left(2^{2}x'\right)-\left(2^{2}y''(2^{2}z'')-2^{2}y'(2^{2}z'')\right)\left(2^{2}y'\right)\right\}\right]\delta\left(2^{2}w''\right)\right\}d\alpha$$

$$+\int_{a}\left\{\frac{2^{2}T\left(2^{2}s'\right)}{2\Im}\left(2^{2}y'(2^{2}z'')-2^{2}z'(2^{2}y'')\right)\delta\left(2^{2}w'''\right)+\frac{2^{2}T\left(2^{2}s'\right)}{2\Im}\left(2^{2}z'(2^{2}x'')-2^{2}x'(2^{2}x'')\right)\delta\left(2^{2}w'''\right)$$

$$+\frac{2^{2}T\left(2^{2}s'\right)}{2\Im}\left(2^{2}x'(2^{2}y'')-2^{2}y'(2^{2}x'')\right)\delta\left(2^{2}w'''\right)\right\}d\alpha$$

$$-\int_{a}\left\{2^{2}s'\left[f_{Hx}-m_{p}a_{px}-m_{i}a_{Fx}\right]\delta\left(2^{2}u\right)\right\}d\alpha$$

$$-\int_{a}\left\{2^{2}s'\left[-w_{a}+f_{Hy}-m_{p}a_{py}-m_{i}a_{Fy}\right]\delta\left(2^{2}v\right)\right\}d\alpha$$

$$-\int_{a}\left\{2^{2}s'\left[f_{Hx}-m_{p}a_{px}-m_{i}a_{Fx}\right]\delta\left(2^{2}w\right)\right\}d\alpha$$

$$-\int_{a}\left\{2^{2}s'\left[f_{Hx}-m_{p}a_{px}-m_{i}a_{Fx}\right]\delta\left(2^{2}w\right)\right\}d\alpha$$

$$+\int_{a}\left\{2^{2}s'\left[m_{p}\left(2^{2}J_{p}\right)\left(2^{2}\psi'\right)\right]\delta\left(2^{2}\psi'\right)\right\}d\alpha$$

$$+\int_{a}\left\{2^{2}s'\left[m_{p}\left(2^{2}J_{p}\right)\left(2^{2}\psi'\right)\right]\delta\left(2^{2}w'\right)\right\}d\alpha$$

$$+\int_{a}\left\{2^{2}s'\left[m_{p}\left(2^{2}J_{p}\right)\left(2^{2}\psi'\right)\right]\delta\left(2^{2}w'\right)\right\}d\alpha$$

$$+\int_{a}\left\{2^{2}s'\left[m_{p}\left(2^{2}J_{p}\right)\left(2^{2}\psi'\right)\right]\delta\left(2^{2}w'\right)\right\}d\alpha$$

$$+\int_{a}\left\{2^{2}s'\left[m_{p}\left(2^{2}J_{p}\right)\left(2^{2}\psi'\right)\right]\delta\left(2^{2}w'\right)\right\}d\alpha$$

$$+\int_{a}\left\{2^{2}s'\left[m_{p}\left(2^{2}J_{p}\right)\left(2^{2}\psi'\right)\right]\delta\left(2^{2}w'\right)\right\}d\alpha$$

$$+\int_{a}\left\{2^{2}s'\left[m_{p}\left(2^{2}J_{p}\right)\left(2^{2}\psi'\right)\right]\delta\left(2^{2}w'\right)\right\}d\alpha$$

$$+\int_{a}\left\{2^{2}s'\left[m_{p}\left(2^{2}J_{p}\right)\left(2^{2}\psi'\right)\right]\delta\left(2^{2}w'\right)\right\}d\alpha$$

Integrating by part three times, one obtains the last weak form of the total virtual work as follows.

$$\delta\left({}^{2}\pi\right) = \begin{bmatrix} {}^{2}T\left(\frac{{}^{2}b_{x}}{\left({}^{2}s'\right)^{2}{}^{2}\kappa}\delta\left({}^{2}u''\right) + \frac{{}^{2}b_{y}}{\left({}^{2}s'\right)^{2}{}^{2}\kappa}\delta\left({}^{2}v''\right) + \frac{{}^{2}b_{z}}{\left({}^{2}s'\right)^{2}{}^{2}\kappa}\delta\left({}^{2}w''\right) \end{bmatrix} \right]_{\alpha_{0}}^{\alpha_{1}} + \mathbb{E}_{2x}\delta\left({}^{2}u'\right) + \mathbb{E}_{2y}\delta\left({}^{2}v'\right) + \mathbb{E}_{2z}\delta\left({}^{2}z'\right) + {}^{2}T\delta\left({}^{2}\psi\right)$$
Torque boundary condition (term 4)

$$+ \left[\frac{{}^{2}M}{{}^{2}s'}\left({}^{2}n_{x}\delta\left({}^{2}u'\right) + {}^{2}n_{y}\delta\left({}^{2}v'\right) + {}^{2}n_{z}\delta\left({}^{2}w'\right)\right)\right]_{\alpha_{o}}^{\alpha_{i}}$$

$$+ \left[\frac{{}^{2}R_{x}\delta\left({}^{2}u\right) + {}^{2}R_{y}\delta\left({}^{2}v\right) + {}^{2}R_{z}\delta\left({}^{2}w\right)\right]_{\alpha_{o}}^{\alpha_{i}}$$

$$+ \left[\frac{{}^{2}R_{x}\delta\left({}^{2}u\right) + {}^{2}R_{y}\delta\left({}^{2}v\right) + {}^{2}R_{z}\delta\left({}^{2}w\right)\right]_{\alpha_{o}}^{\alpha_{i}}$$

$$+ \int_{\alpha} \left\{\left\{-{}^{2}R'_{x} - {}^{2}s'\left({}^{2}q_{x}\right)\right\}\delta\left({}^{2}u\right) + \left\{-{}^{2}R'_{y} - {}^{2}s'\left({}^{2}q_{y}\right)\right\}\delta\left({}^{2}v\right) + \left\{-{}^{2}R'_{z} - {}^{2}s'\left({}^{2}q_{y}\right)\right\}\delta\left({}^{2}w\right)\right\} d\alpha (2.83)$$

$$+ \int_{\alpha} \left\{\left\{-{}^{2}R'_{z} - {}^{2}s'\left({}^{2}q_{z}\right)\right\}\delta\left({}^{2}w\right) + \left\{-{}^{2}T' + {}^{2}s'\left[m_{p}\left({}^{2}J_{p}\right)\left({}^{2}\ddot{\psi}\right)\right]\right\}\delta\left({}^{2}\psi\right)\right\} d\alpha (2.83)$$

where

$$^{2}q_{x} = \left[f_{Hx} - m_{p} a_{px} - m_{i} a_{Fx} \right]$$
 (2.84 a)

$$^{2}q_{y} = \left[-w_{a} + f_{Hy} - m_{p}a_{py} - m_{i}a_{Fy}\right]$$
 (2.84 b)

$$^{2}q_{z} = \left[f_{Hz} - m_{p} a_{pz} - m_{i} a_{Fz} \right]$$
 (2.84 c)

2.7.4 Euler Equations and Boundary Conditions

Considering the boundary conditions of the problem, two classes of boundary conditions are identified, called essential and natural boundary conditions. The essential boundary conditions are also called geometric boundary conditions and correspond to prescribe displacements and rotations. The natural boundary conditions are also called the force boundary conditions and correspond to prescribe boundary forces and moments. In this problem, the hinge support is applied on top and bottom end, therefore, the essential boundary condition are

$${}^{2}u(\alpha_{o}, {}^{2}t) = 0, {}^{2}u(\alpha_{t}, {}^{2}t) = 0$$
 (2.85 a)

$$^{2}v(\alpha_{\alpha},^{2}t) = 0,^{2}v(\alpha_{t},^{2}t) = 0$$
 (2.85 b)

$$^{2}w(\alpha_{o},^{2}t) = 0,^{2}w(\alpha_{t},^{2}t) = 0$$
 (2.85 c)

To extract from the variational equation, equation (2.83), the governing differential equations and natural boundary conditions can be obtained. One uses the argument that the variations on 2u , 2v , and 2w are completely arbitrary, except that there can be no variations on the prescribed essential boundary conditions. Hence, because ${}^2u(\alpha_o, {}^2t)$, ${}^2u(\alpha_t, {}^2t)$, ${}^2v(\alpha_o, {}^2t)$, ${}^2v(\alpha_o, {}^2t)$, ${}^2w(\alpha_o, {}^2t)$, and ${}^2w(\alpha_t, {}^2t)$ are prescribed one has $\delta({}^2u(\alpha_o, {}^2t))$, $\delta({}^2u(\alpha_t, {}^2t))$, $\delta({}^2v(\alpha_o, {}^2t))$, $\delta({}^2v(\alpha_o, {}^2t))$, and $\delta({}^2w(\alpha_t, {}^2t))$ are equal to zero and term 2 in equation (2.83) vanishes. Then

$$\left[{}^{2}R_{x}\delta^{2}u + {}^{2}R_{y}\delta^{2}v + {}^{2}R_{z}\delta^{2}w\right]_{\alpha}^{\alpha_{i}} = 0$$
 (2.86)

Considering term 3 in equation (2.83), since the variations on ${}^{2}u'$, ${}^{2}v'$, and ${}^{2}w'$ are completely arbitrary at any point, that means

$$\left[\frac{{}^{2}M}{{}^{2}s'}\left({}^{2}n_{x}\right)\right]_{\alpha_{o}}^{\alpha_{i}} = \left[\frac{{}^{2}B\left({}^{2}\kappa\right)}{{}^{2}s'}\left({}^{2}n_{x}\right)\right]_{\alpha_{i}}^{\alpha_{i}} = 0$$
 (2.87 a)

$$\left[\frac{{}^{2}M}{{}^{2}S'}\left({}^{2}n_{y}\right)\right]_{\alpha_{o}}^{\alpha_{i}} = \left[\frac{{}^{2}B\left({}^{2}\kappa\right)}{{}^{2}S'}\left({}^{2}n_{y}\right)\right]_{\alpha}^{\alpha_{i}} = 0$$
 (2.87 b)

$$\left[\frac{{}^{2}M}{{}^{2}S'}\left({}^{2}n_{z}\right)\right]_{\alpha_{o}}^{\alpha_{i}} = \left[\frac{{}^{2}B\left({}^{2}\kappa\right)}{{}^{2}S'}\left({}^{2}n_{z}\right)\right]_{\alpha_{o}}^{\alpha_{i}} = 0$$
 (2.87 c)

Considering term 4 in equation (2.83), one has

$$\frac{{}^{2}T\left({}^{2}b_{x}\right)}{\left({}^{2}s'\right)^{2}{}^{2}\kappa}\delta\left({}^{2}u''\left(\alpha_{o},{}^{2}t\right)\right) = 0, \frac{{}^{2}T\left({}^{2}b_{y}\right)}{\left({}^{2}s'\right)^{2}{}^{2}\kappa}\delta\left({}^{2}v''\left(\alpha_{o},{}^{2}t\right)\right) = 0,$$

$$\frac{{}^{2}T\left({}^{2}b_{z}\right)}{\left({}^{2}s'\right)^{2}{}^{2}\kappa}\delta\left({}^{2}w''\left(\alpha_{o},{}^{2}t\right)\right) = 0, {}^{2}T\delta\left({}^{2}\psi\left(\alpha_{o},{}^{2}t\right)\right)$$

$$\frac{{}^{2}T\left({}^{2}b_{x}\right)}{\left({}^{2}s'\right)^{2}{}^{2}\kappa}\delta\left({}^{2}u''\left(\alpha_{t},{}^{2}t\right)\right) = 0, \frac{{}^{2}T\left({}^{2}b_{y}\right)}{\left({}^{2}s'\right)^{2}{}^{2}\kappa}\delta\left({}^{2}v''\left(\alpha_{t},{}^{2}t\right)\right) = 0,$$

$$(2.88 a-d)$$

$$\frac{{}^{2}T\left({}^{2}b_{z}\right)}{\left({}^{2}s'\right)^{2}{}^{2}\kappa}\delta\left({}^{2}w''\left(\alpha_{t},{}^{2}t\right)\right) = 0, {}^{2}T\delta\left({}^{2}\psi\left(\alpha_{t},{}^{2}t\right)\right) \tag{2.89 a-d}$$

$$\left[\mathbb{F}_{2x} \right]_{\alpha_{0}}^{\alpha_{1}} = \left[\left[\frac{-^{2}T(^{2}y'^{2}z'' - ^{2}z'^{2}y'')^{2}s''}{(^{2}s')^{6}(^{2}\kappa)^{2}} \right] \right]_{\alpha}^{\alpha_{1}} = 0$$
 (2.90 a)

$$\left[\mathbb{F}_{2y}\right]_{\alpha_{0}}^{\alpha_{1}} = \left[\left(\frac{-^{2}T\left(\frac{^{2}z'^{2}x'' - \frac{^{2}x'^{2}z''}}{\left(\frac{^{2}s'}{\right)^{6}\left(\frac{^{2}\kappa}{\right)^{2}}}\right)^{2}s''}\right)\right]_{\alpha}^{\alpha_{1}} = 0$$
 (2.90 b)

$$\left[\mathbb{F}_{2z} \right]_{\alpha_{o}}^{\alpha_{i}} = \left[\left(\frac{-^{2}T \left({^{2}x'} {^{2}y''} - {^{2}y'} {^{2}x''} \right) {^{2}s''}}{\left({^{2}s'} \right)^{6} \left({^{2}\kappa} \right)^{2}} \right) \right]_{\alpha}^{\alpha_{i}} = 0$$
 (2.90 c)

It is true that equation (2.88) will be exact by two arguments. First, the variation of the second derivative of displacements or the variation the twisting angle are equal to zero, i.e. $\delta\left({}^2u''(\alpha_o,{}^2t)\right) = 0$, $\delta\left({}^2v''(\alpha_o,{}^2t)\right) = 0$, $\delta\left({}^2w''(\alpha_o,{}^2t)\right) = 0$, and $\delta\left({}^2\psi\left(\alpha_o,{}^2t\right)\right) = 0$. Second, the torque at the bottom end is equal to zero, i.e. ${}^2T\left(\alpha_o,{}^2t\right) = 0$. In this study, the bottom end of the riser can not rotate around the tangential direction freely, but can rotate freely around any other direction perpendicular to the tangent. Therefore, the second argument can not occur because the torque reaction is not equal to zero, i.e. ${}^2T\left(\alpha_o,{}^2t\right) \neq 0$. Consequently, the first argument has been adopted and it can be concluded that the second derivative of the displacement is a constant or equal to zero, i.e.

$$^{2}u''(\alpha_{o},^{2}t) = Const$$
, or $^{2}u''(\alpha_{o},^{2}t) = 0$
 $^{2}v''(\alpha_{o},^{2}t) = Const$, or $^{2}v''(\alpha_{o},^{2}t) = 0$
 $^{2}w''(\alpha_{o},^{2}t) = Const$, or $^{2}w''(\alpha_{o},^{2}t) = 0$

In the same manner, the equation (2.89) will be exact by two arguments in the same manner as equation (2.88). At the top end, however, the riser can rotate

freely around in every direction. Therefore, the first argument can not occur because the torsion at the top end is not equal to zero, i.e. ${}^2\tau(\alpha_o,{}^2t)\neq 0$. Since the torsion is function of the second derivative of the displacement, they and their variation are not equal to zero, i.e.

$${}^{2}u''(\alpha_{t}, {}^{2}t) \neq 0$$
, and $\delta({}^{2}u''(\alpha_{t}, {}^{2}t)) \neq 0$
 ${}^{2}v''(\alpha_{t}, {}^{2}t) \neq 0$, and $\delta({}^{2}v''(\alpha_{t}, {}^{2}t)) \neq 0$
 ${}^{2}w''(\alpha_{t}, {}^{2}t) \neq 0$, and $\delta({}^{2}w''(\alpha_{t}, {}^{2}t)) \neq 0$

Consequently, the second argument has been adopted and it can be concluded that, the torque at the top end is equal to zero in the case of no applied external torque. For the most general problem, the external torque may be applied from the environment of the riser. Thus, the natural boundary condition of torque at the top end becomes ${}^2T(\alpha_t, {}^2t) = T_{ex}$.

Considering equation (2.90), each term is composed of the second derivative of displacement and torque. From this reason, this condition corresponds to the conditions of equation (2.88) and (2.89).

Since the variations on ${}^{2}u$, ${}^{2}v$, and ${}^{2}w$ are completely arbitrary at any point except at the essential boundary, the governing differential equations are shown in term 1 of equation (2.83) and can be called Euler's equations. By substituting equations (2.75 d)-(2.75 f) into term 1 of equation (2.83), one obtain the governing differential equations in three directions of the fixed cartesian coordinate system as follows.

In x direction:

$$\left[\frac{{}^{2}B}{\left({}^{2}s'\right)^{2}}\frac{\partial}{\partial\alpha}\left({}^{2}x'\right)\right]^{n} - \left[\left({}^{2}N_{a} - {}^{2}B\left({}^{2}\kappa\right)^{2}\right)\frac{{}^{2}x'}{{}^{2}s'} - {}^{2}B\left(\frac{{}^{2}s''}{\left({}^{2}s'\right)^{3}}\right)\frac{\partial}{\partial\alpha}\left(\frac{{}^{2}x'}{{}^{2}s'}\right)\right]^{n} - \left[{}^{2}T\left({}^{2}\kappa\right)\left({}^{2}b_{x}\right)\right]^{n} - \left({}^{2}s'\right)\left({}^{2}q_{x}\right) = 0$$
(2.91)

In y direction:

$$\left[\frac{{}^{2}B}{\left({}^{2}s'\right)^{2}}\frac{\partial}{\partial\alpha}\left({}^{2}\frac{y'}{{}^{2}s'}\right)\right]'' - \left[\left({}^{2}N_{a} - {}^{2}B\left({}^{2}\kappa\right)^{2}\right)\frac{{}^{2}y'}{{}^{2}s'} - {}^{2}B\left(\frac{{}^{2}s''}{\left({}^{2}s'\right)^{3}}\right)\frac{\partial}{\partial\alpha}\left({}^{2}\frac{y'}{{}^{2}s'}\right)\right]' - \left[{}^{2}T\left({}^{2}\kappa\right)\left({}^{2}b_{y}\right)\right]' - \left({}^{2}s'\right)\left({}^{2}q_{y}\right) = 0$$
(2.92)

In z direction:

$$\left[\frac{{}^{2}B}{\left(\frac{2}{s'}\right)^{2}}\frac{\partial}{\partial\alpha}\left(\frac{2}{s'}\right)\right]^{n} - \left[\left(\frac{2}{s}N_{a} - \frac{2}{s}B\left(\frac{2}{s}\kappa\right)^{2}\right)\frac{2}{s'} - \frac{2}{s}B\left(\frac{2}{s'}\right)^{3}\right]\frac{\partial}{\partial\alpha}\left(\frac{2}{s'}\right)^{3} - \left[\left(\frac{2}{s}\kappa\right)\left(\frac{2}{s}\kappa\right)\left(\frac{2}{s}\kappa\right)\right]^{2} - \left(\frac{2}{s}\kappa\right)\left(\frac{2}{s}\kappa\right)\left(\frac{2}{s}\kappa\right) - \left(\frac{2}{s}\kappa\right)\left(\frac{2}{s}\kappa\right)\left(\frac{2}{s}\kappa\right) = 0$$
(2.93)

In twisting rotation

$${}^{2}T' = {}^{2}s' \left[m_{p} \left({}^{2}J_{p} \right) \left({}^{2}\ddot{\psi} \right) \right] \tag{2.94}$$

By using the differential geometry of space curve, equations (2.91)-(2.93) can be written in the vector form as

$$\left[\frac{{}^{2}B}{\left({}^{2}s'\right)^{2}}\frac{\partial}{\partial\alpha}\left({}^{2}\vec{r}'\right)\right]'' - \left[\left({}^{2}N_{a} - {}^{2}B\left({}^{2}\kappa\right)^{2}\right)\frac{{}^{2}\vec{r}'}{{}^{2}s'} - {}^{2}B\left(\frac{{}^{2}s''}{\left({}^{2}s'\right)^{3}}\right)\frac{\partial}{\partial\alpha}\left(\frac{{}^{2}\vec{r}'}{{}^{2}s'}\right)\right]''$$

$$-\left[\frac{^{2}T}{^{2}s'}\left(\frac{^{2}\vec{r}'}{^{2}s'}\times\frac{\partial}{\partial\alpha}\left(\frac{^{2}\vec{r}'}{^{2}s'}\right)\right)\right]'-\left(^{2}s'\right)\left(^{2}\vec{q}\right)=0$$
(2.95)

Note that

$$\frac{{}^{2}\vec{r}'}{{}^{2}s'} = \frac{{}^{2}x'}{{}^{2}s'}\hat{i} + \frac{{}^{2}y'}{{}^{2}s'}\hat{j} + \frac{{}^{2}z'}{{}^{2}s'}\hat{k}$$
 (2.96 a)

$$\frac{\partial}{\partial \alpha} \left(\frac{{}^{2}\vec{r}'}{{}^{2}s'} \right) = \frac{\partial}{\partial \alpha} \left(\frac{{}^{2}x'}{{}^{2}s'} \right) \hat{i} + \frac{\partial}{\partial \alpha} \left(\frac{{}^{2}y'}{{}^{2}s'} \right) \hat{j} + \frac{\partial}{\partial \alpha} \left(\frac{{}^{2}z'}{{}^{2}s'} \right) \hat{k}$$
 (2.96 b)

$$\left(\frac{{}^{2}\vec{r}'}{{}^{2}s'} \times \frac{\partial}{\partial \alpha} \left(\frac{{}^{2}\vec{r}'}{{}^{2}s'}\right)\right) = \left({}^{2}s'\right) \left({}^{2}\kappa\right) \left({}^{2}b_{x}\right) \hat{i} + \left({}^{2}s'\right) \left({}^{2}\kappa\right) \left({}^{2}b_{y}\right) \hat{j} + \left({}^{2}s'\right) \left({}^{2}\kappa\right) \left({}^{2}b_{y}\right) \hat{k} \qquad (2.96 c)$$

If $\alpha = {}^2s$, equations (2.94)-(2.95) become

$$^{2}T' = \left\lceil m_{p} \left(^{2}J_{p} \right) \left(^{2}\ddot{\psi} \right) \right\rceil \tag{2.97 a}$$

$$\left[{}^{2}B^{2}\bar{r}''\right]'' - \left[\left({}^{2}N_{a} - {}^{2}B\left({}^{2}\kappa\right)^{2}\right){}^{2}\bar{r}'\right]' - \left[{}^{2}T\left({}^{2}\bar{r}'\times{}^{2}\bar{r}''\right)\right]' - {}^{2}\bar{q} = 0$$
 (2.97 b)

which is compatible with the nonlinear dynamic equation given by Kokarakis and Bernitsas (1987).

2.8 VECTORIAL FORMULATION

To validate equation (2.94)-(2.95), one has to use the relation between three orthogonal coordinate systems and two moment differential equations to eliminate shear forces. As a result, it is found that the six equilibrium equations are reduced to three equations and can be arranged in vectorial form as equation (2.95).

Figure 3. shows the riser element of the length d^2s in displaced state loaded by forces and couples in the cross-sectional principal axes system. Let ${}^2\bar{R}$ be the vector of an internal force such that ${}^2\bar{R} = {}^2R_1{}^2\hat{e}_1 + {}^2R_2{}^2\hat{e}_2 + {}^2R_3{}^2\hat{e}_3$ where 2R_1 is an axial force, 2R_2 and 2R_3 are shear forces; let ${}^2\bar{M}$ be the vector of an internal moment such that ${}^2\bar{M} = {}^2M_1{}^2\hat{e}_1 + {}^2M_2{}^2\hat{e}_2 + {}^2M_3{}^2\hat{e}_3$ where 2M_1 is a twisting moment, 2M_2 and 2M_3 are bending moments. The vector of an external load, i.e., current and wave force, effective weight, inertial force, is represented by ${}^2\bar{q} = {}^2q_1{}^2\hat{e}_1 + {}^2q_2{}^2\hat{e}_2 + {}^2q_3{}^2\hat{e}_3$ and the vector of an external distributed moment is represented by ${}^2\bar{m} = {}^2m_1{}^2\hat{e}_1 + {}^2m_2{}^2\hat{e}_2 + {}^2m_3{}^2\hat{e}_3$.

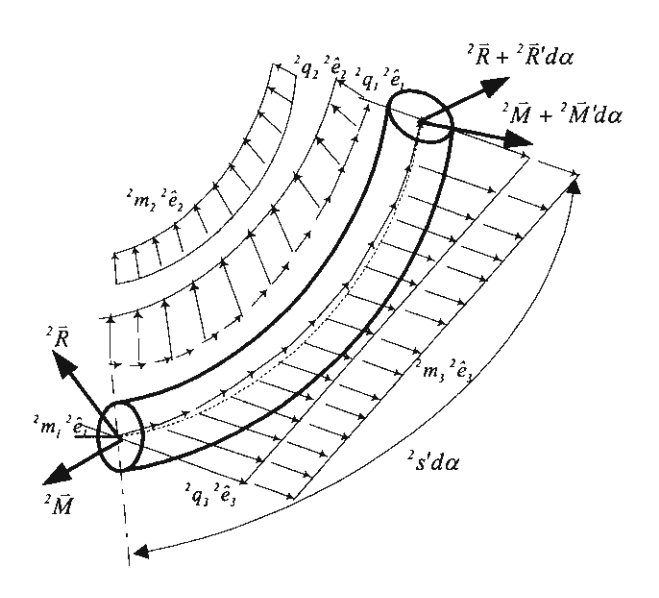


Figure 2.3 Riser differential segment.

Since the riser element is in equilibrium, therefore the sum of forces and the sum of moments equal to zero. Hence, the equilibrium equations in the crosssectional principal axes system are

$$\frac{{}^{2}R'_{1}}{{}^{2}s'} + {}^{2}R_{3}{}^{2}\omega_{2} - {}^{2}R_{2}{}^{2}\omega_{3} = -{}^{2}q_{1}$$
 (2.98 a)

$$\frac{{}^{2}R'_{2}}{{}^{2}s'} + {}^{2}R_{I}{}^{2}\omega_{3} - {}^{2}R_{3}{}^{2}\omega_{I} = -{}^{2}q_{2}$$
 (2.98 b)

$$\frac{{}^{2}R'_{3}}{{}^{2}S'} + {}^{2}R_{2}{}^{2}\omega_{1} - {}^{2}R_{1}{}^{2}\omega_{2} = -{}^{2}q_{3}$$
 (2.98 c)

$$\frac{{}^{2}M'_{I}}{{}^{2}S'} + {}^{2}M_{3}{}^{2}\omega_{2} - {}^{2}M_{2}{}^{2}\omega_{3} = -{}^{2}m_{I} + \left[m_{p}\left({}^{2}J_{p}\right)\left({}^{2}\ddot{\psi}\right)\right]$$
(2.98 d)

$$\frac{{}^{2}M_{2}'}{{}^{2}S'} + {}^{2}M_{1}{}^{2}\omega_{3} - {}^{2}M_{3}{}^{2}\omega_{1} = {}^{2}R_{3} - {}^{2}m_{2}$$
 (2.98 e)

$$\frac{{}^{2}M_{3}'}{{}^{2}s'} + {}^{2}M_{2}{}^{2}\omega_{1} - {}^{2}M_{1}{}^{2}\omega_{2} = -{}^{2}R_{2} - {}^{2}m_{3}$$
 (2.98 f)

It is worth noticing in this formulation that the external forces are assumed to act on the centerline of the riser, therefore the distributed external moments are equal to zero.

By coordinate transformation and shear force elimination, the components of internal force vector in fixed Cartesian coordinate can be derived and written in vectorial form as follows

$${}^{i}\bar{R} = \left[{}^{i}N_{a} - {}^{i}B({}^{i}\kappa)^{2} \right)^{i}\frac{\vec{r}'}{{}^{i}s'} - {}^{i}B\left(\frac{{}^{i}s''}{\left({}^{i}s'\right)^{3}}\right) \frac{\partial}{\partial\alpha} \left(\frac{{}^{i}\vec{r}'}{{}^{i}s'}\right) \right] - \left[\frac{{}^{i}B}{\left({}^{i}s'\right)^{2}} \frac{\partial}{\partial\alpha} \left(\frac{{}^{i}\vec{r}'}{{}^{i}s'}\right) \right]' + \left[\frac{{}^{i}T}{{}^{i}s'} \left(\frac{{}^{i}\vec{r}'}{{}^{i}s'}\right) \frac{\partial}{\partial\alpha} \left(\frac{{}^{i}\vec{r}'}{{}^{i}s'}\right) \right]$$

$$(2.99)$$

Since, the summation of forces in fixed Cartesian coordinate and the summation of moments in tangential axis are

$${}^{2}\vec{R}' + {}^{2}s'({}^{2}\vec{q}') = 0$$
 (2.100 a)

$${}^{2}T' = {}^{2}s' \left[m_{p} \left({}^{2}J_{p} \right) \left({}^{2}\ddot{\psi} \right) \right]$$
 (2.100 b)

therefore, it is confirmed that exact agreement is achieved among the vectorial formulation and the variational formulation.

2.9 NONLINEAR DYNAMIC AND LARGE AMPLITUDE VIBRATION MODELS

Based on the variational formulation, the governing equation describing nonlinear dynamics of the flexible marine riser have been achived in the four weak forms and in the one strong form. For the sake of generality in obtaining the finite element model, however, the strong form is used to generate the large amplitude vibration models. The governing equation in displacement-based strong form can be expressed as follows

$${}^{2}s'\left(m_{p}-m_{i}\right)\left\{\frac{\partial^{2}\left(^{2}\bar{r}\right)}{\partial t^{2}}\right\}+{}^{2}s'm_{p}\left\{\begin{pmatrix}0\\2J_{p}\right)\left(^{2}\bar{\psi}'\right)\right\}+{}^{2}s'm_{i}\left(\frac{2V_{i}}{2s'}\right)\left\{\frac{\partial^{2}\left(^{2}\bar{r}\right)}{\partial \alpha \partial t}\right\}$$

$$+\left[\frac{^{2}B}{\left(^{2}s'\right)^{2}}\left\{\frac{\partial}{\partial \alpha}\left(^{2}\frac{\bar{r}'}{2s'}\right)\right\}\right]^{"}-\left[\left(^{2}N_{a}-^{2}B\left(^{2}\kappa\right)^{2}\right)\left\{\frac{^{2}\bar{r}'}{^{2}s'}\right\}-^{2}B\left(\frac{^{2}s''}{^{2}s'}\right)\right\}\left\{\frac{\partial}{\partial \alpha}\left(^{2}\frac{\bar{r}'}{^{2}s'}\right)\right\}\right]^{'}$$

$$-\left[\frac{^{2}T}{^{2}s'}\left\{\left(\frac{^{2}\bar{r}'}{^{2}s'}\times\frac{\partial}{\partial \alpha}\left(^{2}\frac{\bar{r}'}{^{2}s'}\right)\right)\right\}+\left\{0\\^{2}T\right\}\right]^{'}$$

$$+^{2}s'm_{i}\left(\frac{V_{i}}{^{2}s'}\right)^{2}\left\{\frac{\partial^{2}\left(^{2}\bar{r}\right)}{\partial \alpha^{2}}\right\}+^{2}s'm_{i}\left[\frac{V_{i}V_{i}'}{\left(^{2}s'\right)^{2}}-\frac{V_{i}\left(^{2}s'\right)}{\left(^{2}s'\right)^{2}}-\frac{V_{i}^{2}\left(^{2}s''\right)}{\left(^{2}s'\right)^{3}}\right]\left\{\frac{\partial\left(^{2}\bar{r}\right)}{\partial \alpha}\right\}$$

$$=^{2}s'\left\{\frac{^{2}\bar{F}_{H}}{0}\right\}-^{2}s'^{2}w_{a}\hat{J}-^{2}s'm_{i}\left[\frac{\dot{V}_{i}}{^{2}s'}\right]\left\{\frac{\partial\left(^{2}\bar{r}\right)}{\partial \alpha}\right\}$$

$$=^{2}s'\left\{\frac{^{2}\bar{F}_{H}}{0}\right\}-^{2}s'^{2}w_{a}\hat{J}-^{2}s'm_{i}\left[\frac{\dot{V}_{i}}{^{2}s'}\right]\left\{\frac{\partial\left(^{2}\bar{r}\right)}{\partial \alpha}\right\}$$

$$=^{2}s'\left\{\frac{^{2}\bar{F}_{H}}{0}\right\}-^{2}s'^{2}w_{a}\hat{J}-^{2}s'm_{i}\left[\frac{\dot{V}_{i}}{^{2}s'}\right]\left\{\frac{\partial\left(^{2}\bar{r}\right)}{\partial \alpha}\right\}$$

By utilizing the differential geometry of a space curve, each term in equation (2.101 a) are expanded by

$$\begin{split} & {}^{2}s'(m_{p}+m_{i}) \begin{cases} \frac{\partial^{2}(^{2}\bar{r})}{\partial t^{2}} \\ 0 \end{cases} + {}^{2}s'm_{p} \begin{cases} 0 \\ (^{2}J_{p})(^{2}\bar{\psi}) \end{cases} \\ & = \begin{bmatrix} {}^{2}s'(m_{p}+m_{i}) & 0 & 0 & 0 \\ 0 & {}^{2}s'(m_{p}+m_{i}) & 0 & 0 \\ 0 & 0 & {}^{2}s'(m_{p}+m_{i}) & 0 \\ 0 & 0 & 0 & {}^{2}s'(m_{p}+m_{i}) & 0 \\ 0 & 0 & 0 & {}^{2}s'(m_{p}+m_{i}) & 0 \end{cases} \\ & = \begin{bmatrix} {}^{2}\frac{B}{3} & \partial \alpha \begin{pmatrix} {}^{2}\bar{r}' \\ {}^{2}\bar{s}' \end{pmatrix} = \frac{2}{3} & \left[{}^{2}y')^{2} + {}^{2}(z')^{2} & {}^{2}-z'^{2}y' & {}^{2}-z'^{2}z' \\ {}^{2}z'' & {}^{2}z'' & {}^{2}z'' & {}^{2}z''^{2}z' \\ {}^{2}z'' & {}^{2}z'' & {}^{2}z''^{2}z' & {}^{2}z'^{2}z' \\ {}^{2}z'' & {}^{2}z'' & {}^{2}z''^{2}z' & {}^{2}z''^{2}z' \\ {}^{2}z'' & {}^{2}z'' & {}^{2}z''^{2}z' & {}^{2}z'^{2}z' \\ {}^{2}z'' & {}^{2}z'' & {}^{2}z''^{2}z' & {}^{2}z''^{2}z' \\ {}^{2}z'' & {}^{2}z'' & {}^{2}z''^{2}z' & {}^{2}z'^{2}z' \\ {}^{2}z'' & {}^{2}z'' & {}^{2}z'^{2}z' & {}^{2}z'^{2}z' \\ {}^{2}z'' & {}^{2}z'' & {}^{2}z''^{2}z' & {}^{2}z''^{2}z' \\ {}^{2}z'' & {}^{2}z'' & {}^{2}z'' & {}^{2}z'' \\ {}^{2}z'' & {}^{2}z'' & {}^{2}z''^{2}z' & {}^{2}z'^{2}z' \\ {}^{2}z'' & {}^{2}z'' & {}^{2}z'' & {}^{2}z'' \\ {}^{2}z'' & {}^{2}z'' & {}^{2}z''^{2}z' & {}^{2}z'^{2}z' \\ {}^{2}z'' & {}^{2}z'' & {}^{2}z'' & {}^{2}z'' & {}^{2}z'' \\ {}^{2}z'' & {}^{2}z'' & {}^{2}z'' & {}^{2}z'' & {}^{2}z'' \\ {}^{2}z'' & {}^{2}z'' & {}^{2}z'' & {}^{2}z'' & {}^{2}z'' \\ {}^{2}z'' & {}^{2}z'' & {}^{2}z'' & {}^{2}z'' & {}^{2}z'' \\ {}^{2}z'' & {}^{2}z'' & {}^{2}z'' & {}^{2}z'' & {}^{2}z'' \\ {}^{2}z'' & {}^{2}z'' & {}^{2}z'' & {}^{2}z'' & {}^{2}z'' \\ {}^{2}z'' & {}^{2}z'' & {}^{2}z'' & {}^{2}z'' & {}^{2}z'' \\ {}^{2}z'' & {}^{2}z'' & {}^{2}z'' & {}^{2}z'' & {}^{2}z'' & {}^{2}z'' \\ {}^{2}z'' & {}^{2}z'' & {}^{2}z'' & {}^{2}z'' & {}^{2}z'' & {}^{2}z'' \\ {}^{2}z'' & {}^{2}z'' \\ {}^{2}z'' & {}^{2}z$$

$$= \frac{m_{i}V_{i}^{2}}{\left(\frac{2}{s'}\right)^{3}} \begin{bmatrix} \left(\frac{2}{y'}\right)^{2} + \left(\frac{2}{z'}\right)^{2} & -\frac{2}{x'^{2}}y' & -\frac{2}{x'^{2}}z' \\ -\frac{2}{x'^{2}}y' & \left(\frac{2}{x'}\right)^{2} + \left(\frac{2}{z'}\right)^{2} & -\frac{2}{y'^{2}}z' \\ -\frac{2}{x'^{2}}z' & -\frac{2}{y'^{2}}z' & \left(\frac{2}{x'}\right)^{2} + \left(\frac{2}{y'}\right)^{2} \end{bmatrix} \begin{cases} \frac{2}{2}x'' \\ \frac{2}{2}z'' \end{bmatrix}$$

$$= \frac{2}{s'}m_{i}\left(\frac{V_{i}V_{i}'}{2s'}\right) \frac{\partial \left(\frac{2}{r}\right)}{\partial \alpha} = \frac{m_{i}V_{i}V'}{2s'} \begin{bmatrix} 1 & 0 & 0 \\ 0 & 1 & 0 \\ 0 & 0 & 1 \end{bmatrix} \begin{bmatrix} \frac{2}{x'} \\ \frac{2}{y'} \\ \frac{2}{z'} \end{bmatrix}$$

$$= \frac{m_{i}V_{i}}{\left(\frac{2}{s'}\right)^{2}} \begin{bmatrix} 2\left(\frac{2}{s'}\right)^{2} + \left(\frac{2}{s'}\right)^{2} - \frac{2}{x'^{2}}y' & -\frac{2}{x'^{2}}z' \\ -\frac{2}{x'^{2}}y' & 2\left(\frac{2}{s'}\right)^{2} + \left(\frac{2}{y'}\right)^{2} & -\frac{2}{y'^{2}}z' \\ -\frac{2}{x'^{2}}z' & -\frac{2}{y'^{2}}z' & \left(\frac{2}{s'}\right)^{2} + \left(\frac{2}{z'}\right)^{2} \end{bmatrix} \begin{cases} \frac{2}{x'} \\ \frac{2}{y'} \\ \frac{2}{z'} \end{cases}$$

$$= \frac{m_{i}V_{i}}{\left(\frac{2}{s'}\right)^{2}} \begin{bmatrix} 2\left(\frac{2}{s'}\right)^{2} + \left(\frac{2}{x'}\right)^{2} & -\frac{2}{x'^{2}}y' & -\frac{2}{x'^{2}}z' \\ -\frac{2}{x'^{2}}z' & -\frac{2}{y'^{2}}z' & \left(\frac{2}{s'}\right)^{2} + \left(\frac{2}{z'}\right)^{2} \end{bmatrix} \begin{cases} \frac{2}{s'} \\ \frac{2}{s'} \\ \frac{2}{s'} \end{cases}$$

$$= \frac{2}{s'}m_{i}\left(\frac{\dot{V}_{i}}{\left(\frac{2}{s'}\right)}\right) \frac{\partial \left(\frac{2}{r}\right)}{\partial \alpha} = \frac{2}{s'} \begin{cases} \frac{m_{i}\dot{V}_{i}\left(\frac{2}{s'}\right)}{\frac{2}{s'}} \\ \frac{m_{i}\dot{V}_{i}\left(\frac{2}{s'}\right)}{\frac{2}{s'}} \end{cases}$$

$$(2.102 i)$$

By substituting equations (2.32) and (2.102) into (2.101) together with some manipulation. The nonlinear dynamic, large amplitude model in the Cartesian coordinate system is obtained as

$$\begin{bmatrix}
\mathbf{M} & \mathbf{0} \\
\mathbf{0} & m_{p} \begin{pmatrix} {}^{2}s' \end{pmatrix} \begin{pmatrix} {}^{2}J_{p} \end{pmatrix} \end{bmatrix} \begin{Bmatrix} {}^{2}\ddot{r} \\ {}^{2}\ddot{\psi} \end{Bmatrix} + \begin{bmatrix} \mathbf{C} & \mathbf{0} \\ \mathbf{0} & \mathbf{0} \end{bmatrix} \begin{Bmatrix} {}^{2}\dot{r} \\ {}^{2}\psi \end{Bmatrix} + \begin{bmatrix} \mathbf{G} & \mathbf{0} \\ \mathbf{0} & \mathbf{0} \end{bmatrix} \begin{Bmatrix} {}^{2}\dot{r}' \\ {}^{2}\psi' \end{Bmatrix}$$

$$+ \begin{bmatrix}
 {}^{2}\mathbf{K} & \mathbf{0} \\
 {}^{1}\mathbf{I}^{2}\mathbf{K} & \mathbf{0} \\
 {}^{2}\psi'' \end{Bmatrix} + \begin{bmatrix}
 {}^{2}\mathbf{K} & \mathbf{0} \\
 {}^{2}\mathbf{I}^{2}\mathbf{K} \\
 {}^{2}\psi'' \end{Bmatrix} + \begin{bmatrix}
 {}^{2}\mathbf{K} & \mathbf{0} \\
 {}^{2}\mathbf{I}^{2}\mathbf{K} \\
 {}^{2}\psi'' \end{Bmatrix} + \begin{bmatrix}
 {}^{2}\mathbf{K} & \mathbf{0} \\
 {}^{2}\mathbf{I}^{2}\mathbf{K} \\
 {}^{2}\psi'' \end{Bmatrix} \end{bmatrix} \begin{pmatrix} {}^{2}\ddot{r}' \\ {}^{2}\psi'' \end{Bmatrix} + \begin{bmatrix}
 {}^{2}\mathbf{K} & \mathbf{0} \\
 {}^{2}\mathbf{I}^{2}\mathbf{K} \\
 {}^{2}\mathbf{I}^{2}\mathbf{K} \end{bmatrix} \begin{pmatrix} {}^{2}\ddot{r}' \\ {}^{2}\psi'' \end{Bmatrix} + \begin{bmatrix}
 {}^{2}\mathbf{K} & \mathbf{0} \\
 {}^{2}\mathbf{I}^{2}\mathbf{K} \\
 {}^{2}\mathbf{I}^{2}\mathbf{K} \end{bmatrix} \begin{pmatrix} {}^{2}\ddot{r}' \\ {}^{2}\psi'' \end{Bmatrix} + \begin{bmatrix}
 {}^{2}\mathbf{I}^{2}\mathbf{K} & \mathbf{0} \\
 {}^{2}\mathbf{I}^{2}\mathbf{K} \end{bmatrix} \begin{pmatrix} {}^{2}\ddot{r}' \\ {}^{2}\psi' \end{Bmatrix} = \begin{Bmatrix} {}^{2}\mathbf{I} \\
 {}^{2}\mathbf{I}^{2}\mathbf{I} \\
 {}^{2}\mathbf{I}^{2}\mathbf{I}^{2}\mathbf{I} \\
 {}^{2}\mathbf{I}^{$$

where the total mass matrix is

$$\mathbf{M} = {}^{2}s' \Big(m_{p} + m_{i} + C_{a}^{*} \Big) \begin{bmatrix} I & 0 & 0 \\ 0 & I & 0 \\ 0 & 0 & I \end{bmatrix}$$
 (2.104)

the hydrodynamic damping matrix is

$$\mathbf{C} = {}^{2}S' \begin{bmatrix} C_{eqx}^{*} & C_{eqxy}^{*} & C_{eqxz}^{*} \\ C_{eqxy}^{*} & C_{eqy}^{*} & C_{eqyz}^{*} \\ C_{eqxz}^{*} & C_{eqyz}^{*} & C_{eqz}^{*} \end{bmatrix}$$
(2.105)

the gyroscopic matrix is

$$\mathbf{G} = \frac{m_i V_i}{\binom{2}{s'}^2} \begin{bmatrix} 2\binom{2}{s'}^2 + \binom{2}{x'}^2 & -\frac{2}{x'}^2 y' & -\frac{2}{x'}^2 z' \\ -\frac{2}{x'}^2 y' & 2\binom{2}{s'}^2 + \binom{2}{y'}^2 & -\frac{2}{y'}^2 z' \\ -\frac{2}{x'}^2 z' & -\frac{2}{y'}^2 z' & \binom{2}{s'}^2 + \binom{2}{z'}^2 \end{bmatrix}$$
(2.106)

the torsion stiffness matrix is

$${}_{\mathbf{T}}^{2}\mathbf{K} = \begin{bmatrix} {}_{71}^{2}k_{11} & {}_{71}^{2}k_{12} & {}_{71}^{2}k_{13} & 0 \\ {}_{71}^{2}k_{12} & {}_{71}^{2}k_{22} & {}_{71}^{2}k_{23} & 0 \\ {}_{271}^{2}k_{13} & {}_{71}^{2}k_{23} & {}_{71}^{2}k_{33} & 0 \\ 0 & 0 & 0 & 0 \end{bmatrix} + \begin{bmatrix} 0 & 0 & 0 & {}_{72}^{2}k_{14} \\ 0 & 0 & 0 & {}_{72}^{2}k_{24} \\ 0 & 0 & 0 & {}_{72}^{2}k_{34} \\ 0 & 0 & 0 & {}_{72}^{2}k_{44} \end{bmatrix}$$
(2.107 a)

in which

$${}_{TI}^{2}k_{II} = -\frac{{}^{2}C({}^{2}s')^{6}}{({}^{2}\kappa)^{2}}({}^{2}y'{}^{2}z'' - {}^{2}z'{}^{2}y'')^{2}$$
(2.107 b)

$${}_{TI}^{2}k_{22} = -\frac{{}^{2}C({}^{2}s')^{6}}{({}^{2}\kappa)^{2}}({}^{2}z'{}^{2}x'' - {}^{2}x'{}^{2}z'')^{2}$$
(2.107 c)

$${}_{T_{I}}^{2}k_{33} = -\frac{{}^{2}C({}^{2}s')^{6}}{({}^{2}\kappa)^{2}}({}^{2}x'{}^{2}y'' - {}^{2}y'{}^{2}x'')^{2}$$
(2.107 d)

$${}_{T_{I}}^{2}k_{I2} = {}_{T}^{2}k_{2I} = -\frac{{}^{2}C({}^{2}s')^{6}}{({}^{2}\kappa)^{2}}({}^{2}y'{}^{2}z'' - {}^{2}z'{}^{2}y'')({}^{2}z'{}^{2}x'' - {}^{2}x'{}^{2}z'') \quad (2.107 e)$$

$${}_{T_{I}}^{2}k_{I3} = {}_{T}^{2}k_{3I} = -\frac{{}^{2}C({}^{2}s')^{6}}{({}^{2}\kappa)^{2}}({}^{2}y'{}^{2}z'' - {}^{2}z'{}^{2}y'')({}^{2}x'{}^{2}y'' - {}^{2}y'{}^{2}x'') \quad (2.107 \text{ f})$$

$${}_{T_{1}}^{2}k_{23} = {}_{T}^{2}k_{32} = -\frac{{}^{2}C({}^{2}s')^{6}}{({}^{2}\kappa)^{2}}({}^{2}z'{}^{2}x'' - {}^{2}x'{}^{2}z'')({}^{2}x'{}^{2}y'' - {}^{2}y'{}^{2}x'') \quad (2.107 \text{ g})$$

$${}_{T2}^{2}k_{14} = \frac{{}^{2}C}{\left({}^{2}s'\right)^{2}} \left[\frac{\left({}^{2}y'\right)\left({}^{2}z''\right) - \left({}^{2}z'\right)\left({}^{2}y''\right)}{\left({}^{2}s'\right)^{2}} \right]$$
(2.107 h)

$${}_{T_2}^2 k_{24} = \frac{{}^2 C}{\left({}^2 s'\right)^2} \left[\frac{\left({}^2 z'\right) \left({}^2 x''\right) - \left({}^2 x'\right) \left({}^2 z''\right)}{\left({}^2 s'\right)^2} \right]$$
(2.107 i)

$${}_{T2}^{2}k_{34} = \frac{{}^{2}C}{\left({}^{2}s'\right)^{2}} \left[\frac{\left({}^{2}x'\right)\left({}^{2}y''\right) - \left({}^{2}y'\right)\left({}^{2}x''\right)}{\left({}^{2}s'\right)^{2}} \right]$$
(2.107 j)

$${}_{T2}^{2}k_{44} = {}^{2}C\left(\frac{{}^{2}\tau_{I}}{\left({}^{2}\psi'\right)} + \frac{1}{\left({}^{2}s'\right)}\right)$$
(2.107 k)

the bending stiffness matrices are

$${}_{b1}^{2}\mathbf{K} = \frac{{}^{2}B}{\left({}^{2}s'\right)^{5}} \begin{bmatrix} \left({}^{2}y'\right)^{2} + \left({}^{2}z'\right)^{2} & -{}^{2}x'{}^{2}y' & -{}^{2}x'{}^{2}z' \\ -{}^{2}x'{}^{2}y' & \left({}^{2}x'\right)^{2} + \left({}^{2}z'\right)^{2} & -{}^{2}y'{}^{2}z' \\ -{}^{2}x'{}^{2}z' & -{}^{2}y'{}^{2}z' & \left({}^{2}x'\right)^{2} + \left({}^{2}y'\right)^{2} \end{bmatrix}$$
(2.108 a)

$${}_{\mathbf{b}2}^{2}\mathbf{K} = \begin{bmatrix} {}_{b2}^{2}k_{11} & {}_{b2}^{2}k_{12} & {}_{b2}^{2}k_{13} \\ {}_{b2}^{2}k_{21} & {}_{b2}^{2}k_{22} & {}_{b2}^{2}k_{32} \\ {}_{b2}^{2}k_{13} & {}_{b2}^{2}k_{32} & {}_{b2}^{2}k_{33} \end{bmatrix}$$
(2.108 b)

in which

$${}_{b2}^{2}k_{II} = \frac{{}^{2}B}{\left({}^{2}s'\right)^{7}} \left[2\left({}^{2}x''^{2}y' - {}^{2}x'^{2}y''\right){}^{2}x'^{2}y' + 2\left({}^{2}x''^{2}z' - {}^{2}x'^{2}z''\right){}^{2}x'^{2}z'\right]$$
(2.108 c)

$${}_{b2}^{2}k_{22} = \frac{{}^{2}B}{\left({}^{2}s'\right)^{7}} \left[2\left({}^{2}y''^{2}z' - {}^{2}y'^{2}z''\right){}^{2}y'^{2}z' - 2\left({}^{2}x''^{2}y' - {}^{2}x'^{2}y''\right){}^{2}x'^{2}y'\right]$$
(2.108 d)

$$_{b2}^{2}k_{33} = \frac{^{2}B}{\left(^{2}s'\right)^{7}} \left[-2\left(^{2}x''^{2}z' - ^{2}x'^{2}z''\right)^{2}x'^{2}z' - 2\left(^{2}y''^{2}z' - ^{2}y'^{2}z''\right)^{2}y'^{2}z' \right]$$
 (2.108 e)

$${}_{b2}^{2}k_{12} = \frac{{}^{2}B}{\left({}^{2}s'\right)^{7}} \left[\left({}^{2}x''^{2}y' - {}^{2}x'^{2}y''\right) \left(\left({}^{2}y'\right)^{2} - \left({}^{2}x'\right)^{2}\right) + \left({}^{2}y''^{2}z' - {}^{2}y'^{2}z''\right)^{2}x'^{2}z'\right]$$

$$+ \left({}^{2}x''^{2}z' - {}^{2}x'^{2}z'' \right) {}^{2}y'^{2}z' \right]$$

$$+ \left({}^{2}x''^{2}z' - {}^{2}x'^{2}z'' \right) {}^{2}y'^{2}z' \right]$$

$$+ \left({}^{2}x''^{2}z' - {}^{2}x'^{2}z'' \right) \left(\left({}^{2}z' \right)^{2} - \left({}^{2}x' \right)^{2} \right) - \left({}^{2}y''^{2}z' - {}^{2}y'^{2}z'' \right) {}^{2}x'^{2}y'$$

$$+ \left({}^{2}x''^{2}y' - {}^{2}x'^{2}y'' \right) {}^{2}y'^{2}z' \right]$$

$$+ \left({}^{2}x''^{2}y' - {}^{2}x'^{2}y'' \right) {}^{2}y'^{2}z' \right]$$

$$+ \left({}^{2}x''^{2}y' - {}^{2}x'^{2}y'' \right) {}^{2}y'^{2}z' \right]$$

$$+ \left({}^{2}x''^{2}z' - {}^{2}x'^{2}z'' \right) {}^{2}x'^{2}z'$$

$$- \left({}^{2}x''^{2}y' - {}^{2}x'^{2}y'' \right) {}^{2}x'^{2}z' \right]$$

$$+ \left({}^{2}x''^{2}z' - {}^{2}x'^{2}z'' \right) {}^{2}x'^{2}z'$$

$$+ \left({}^{2}x''^{2}y' - {}^{2}x'^{2}y'' \right) {}^{2}x'^{2}z' \right]$$

$$+ \left({}^{2}x''^{2}y' - {}^{2}x'^{2}y'' \right) {}^{2}x'^{2}z'$$

$$+ \left({}^{2}x''^{2}y' - {}^{2}x'^{2}y'' \right) {}^{2}x'^{2}z' \right]$$

$$+ \left({}^{2}x''^{2}y' - {}^{2}x'^{2}y'' \right) {}^{2}x'^{2}z'$$

the axial stiffness matrices are

$${}_{NI}^{2}\mathbf{K} = \frac{\left({}^{2}N'_{a} - m_{i}V_{i}^{2}\right)}{\left({}^{2}s'\right)^{3}} \begin{bmatrix} -\left(\left({}^{2}y'\right)^{2} + \left({}^{2}z'\right)^{2}\right) & {}^{2}x'^{2}y' & {}^{2}x'^{2}z' \\ & {}^{2}x'^{2}y' & -\left(\left({}^{2}x'\right)^{2} + \left({}^{2}z'\right)^{2}\right) & {}^{2}y'^{2}z' \\ & {}^{2}x'^{2}z' & {}^{2}y'^{2}z' & -\left(\left({}^{2}y'\right)^{2} + \left({}^{2}x'\right)^{2}\right) \end{bmatrix}$$

$$-\left({}^{2}N'_{a} - m_{i}V_{i}V'_{i}\right) \begin{bmatrix} 1 & 0 & 0 \end{bmatrix}$$

$$(2.109)$$

$${}_{N2}^{2}\mathbf{K} = \frac{-\binom{2}{N_{a}'} - m_{i}V_{i}V_{i}'}{\binom{2}{S'}} \begin{bmatrix} I & 0 & 0 \\ 0 & I & 0 \\ 0 & 0 & I \end{bmatrix}$$
(2.110)

$$\frac{2\bar{\mathbf{f}}}{} = {}^{2}S' \left\{ C_{M}^{*}\dot{V}_{Hx} + C_{Dx}^{*}V_{Hx}^{2} + 2C_{Dxyz}^{*}V_{Hx}V_{Hy} + 2C_{Dxyz}^{*}V_{Hx}V_{Hz} \right.$$

$$\frac{2\bar{\mathbf{f}}}{} = {}^{2}S' \left\{ C_{M}^{*}\dot{V}_{Hy} + C_{Dy}^{*}V_{Hy}^{2} + 2C_{Dxyz}^{*}V_{Hx}V_{Hy} + 2C_{Dxyz}^{*}V_{Hx}V_{Hz} \right.$$

$$\frac{2\bar{\mathbf{f}}}{} = {}^{2}S' \left\{ C_{M}^{*}\dot{V}_{Hy} + C_{Dy}^{*}V_{Hy}^{2} + 2C_{Dxyz}^{*}V_{Hx}V_{Hy} + 2C_{Dxyz}^{*}V_{Hx}V_{Hz} \right.$$

$$\frac{2\bar{\mathbf{f}}}{} = {}^{2}S' \left\{ C_{M}^{*}\dot{V}_{Hy} + C_{Dy}^{*}V_{Hy}^{2} + 2C_{Dxyz}^{*}V_{Hx}V_{Hz} \right.$$

$$\frac{2\bar{\mathbf{f}}}{} = {}^{2}S' \left\{ C_{M}^{*}\dot{V}_{Hy} + C_{Dy}^{*}V_{Hx}V_{Hy} + 2C_{Dxyz}^{*}V_{Hx}V_{Hz} \right.$$

$$\frac{2\bar{\mathbf{f}}}{} = {}^{2}S' \left\{ C_{M}^{*}\dot{V}_{Hy}V_{Hz} + C_{Dxyz}^{*}V_{Hx}V_{Hy} + 2C_{Dxyz}^{*}V_{Hx}V_{Hz} - m_{i}\dot{V}_{i}\left(\frac{2\chi'}{2S'}\right) \right.$$

$$\frac{2\bar{\mathbf{f}}}{} = {}^{2}S' \left\{ C_{M}^{*}\dot{V}_{Hy}V_{Hz} + C_{Dxyz}^{*}V_{Hy}V_{Hz} + C_{Dxyz}^{*}V_{Hy}V_{Hz} - m_{i}\dot{V}_{i}\left(\frac{2\chi'}{2S'}\right) \right.$$

$$\frac{2\bar{\mathbf{f}}}{} = {}^{2}S' \left\{ C_{M}^{*}\dot{V}_{Hy}V_{Hz} + C_{Dxyz}^{*}V_{Hx}V_{Hy} + 2C_{Dxyz}^{*}V_{Hx}V_{Hz} - m_{i}\dot{V}_{i}\left(\frac{2\chi'}{2S'}\right) \right.$$

$$\frac{2\bar{\mathbf{f}}}{} = {}^{2}S' \left\{ C_{M}^{*}\dot{V}_{Hy}V_{Hz} + C_{Dxyz}^{*}V_{Hx}V_{Hy} + 2C_{Dxyz}^{*}V_{Hx}V_{Hz} - m_{i}\dot{V}_{i}\left(\frac{2\chi'}{2S'}\right) \right.$$

$$\frac{2\bar{\mathbf{f}}}{} = {}^{2}S' \left[C_{M}^{*}\dot{V}_{Hy}V_{Hz} + C_{Dxyz}^{*}V_{Hx}V_{Hy} + 2C_{Dxyz}^{*}V_{Hx}V_{Hz} - m_{i}\dot{V}_{i}\left(\frac{2\chi'}{2S'}\right) \right.$$

$$\frac{2\bar{\mathbf{f}}}{} = {}^{2}S' \left[C_{M}^{*}\dot{V}_{Hy}V_{Hz} + C_{Dxyz}^{*}V_{Hx}V_{Hy} + 2C_{Dxyz}^{*}V_{Hx}V_{Hz} - m_{i}\dot{V}_{i}\left(\frac{2\chi'}{2S'}\right) \right.$$

$$\frac{2\bar{\mathbf{f}}}{} = {}^{2}S' \left[C_{M}^{*}\dot{V}_{Hy}V_{Hz} + C_{Dxyz}^{*}V_{Hx}V_{Hy} + 2C_{Dxyz}^{*}V_{Hx}V_{Hz} + C_{Dxyz}^{*}V_{Hx}V_{Hz} - m_{i}\dot{V}_{i}\left(\frac{2\chi'}{2S'}\right) \right.$$

$$\frac{2\bar{\mathbf{f}}}{} = {}^{2}S' \left[C_{M}^{*}\dot{V}_{Hy}V_{Hz} + C_{Dxyz}^{*}V_{Hx}V_{Hy} + 2C_{Dxyz}^{*}V_{Hx}V_{Hz} + C_{Dxyz}^{*}V_{Hx}V_{Hz} + C_{Dxyz}^{*}V_{Hx}V_{Hz} \right.$$

$$\frac{2\bar{\mathbf{f}}}{} = {}^{2}S' \left[C_{M}^{*}\dot{V}_{Hy}V_{Hz} + C_{Dxyz}^{*}V_{Hx}V_{Hz} + C_{Dxyz}^{*}V_{Hx}V_{Hz} + C_{Dxyz}^{*}V_{Hx}V_{Hz} \right]$$

$$\frac{2\bar{\mathbf{f}}}{} = {}^{2}S' \left[C_{M}^{*}\dot{V}_{Hy}V_{Hz} + C_{Dxyz}^{*}V_{Hx}V$$

.

2.10 NONLINEAR STATIC EQUILIBRIUM MODEL

The nonlinear static model is obtained by eliminating the time-dependent terms in the nonlinear dynamic equation (2.102) and replacing the variables at the displaced state by ones at the equilibrium state. Therefore, the nonlinear static model can be expressed as follows.

$$+\left[\begin{bmatrix} {}_{11}^{l}\mathbf{K} & \mathbf{0} \\ \mathbf{0} & \mathbf{0} \end{bmatrix} \begin{Bmatrix} {}_{1}\vec{r}'' \\ {}_{1}\psi''' \end{Bmatrix} + \begin{bmatrix} \mathbf{0} & {}_{12}^{l}k_{14} \\ 0 & {}_{12}^{l}k_{24} \\ {}_{12}^{l}k_{34} \\ 0 & 0 & {}_{12}^{l}k_{44} \end{bmatrix} \begin{Bmatrix} {}_{1}\vec{r}' \\ {}_{1}\psi' \end{Bmatrix} \right] + \left[\begin{bmatrix} {}_{\mathbf{b}_{1}}^{l}\mathbf{K} & \mathbf{0} \\ \mathbf{0} & \mathbf{0} \end{bmatrix} \begin{Bmatrix} {}_{1}\vec{r}'' \\ {}_{1}\psi'' \end{Bmatrix} \right] + \left[\begin{bmatrix} {}_{\mathbf{b}_{1}}^{l}\mathbf{K} & \mathbf{0} \\ \mathbf{0} & \mathbf{0} \end{bmatrix} \begin{Bmatrix} {}_{1}\vec{r}'' \\ {}_{1}\psi'' \end{Bmatrix} \right] + \left[\begin{bmatrix} {}_{\mathbf{b}_{1}}^{l}\mathbf{K} & \mathbf{0} \\ \mathbf{0} & \mathbf{0} \end{bmatrix} \begin{Bmatrix} {}_{1}\vec{r}' \\ {}_{1}\psi'' \end{Bmatrix} + \left[\begin{bmatrix} {}_{\mathbf{b}_{1}}^{l}\mathbf{K} & \mathbf{0} \\ \mathbf{0} & \mathbf{0} \end{bmatrix} \begin{Bmatrix} {}_{1}\vec{r}' \\ {}_{1}\psi'' \end{Bmatrix} = \begin{Bmatrix} {}_{1}\vec{\mathbf{f}} \\ \mathbf{0} \end{Bmatrix}$$

$$(2.112)$$

the torsion stiffness matrix is

$${}_{\mathbf{T}}^{I}\mathbf{K} = \begin{bmatrix} {}_{1}{}^{I}k_{11} & {}_{1}{}^{I}k_{12} & {}_{1}{}^{I}k_{13} & 0 \\ {}_{1}{}^{I}k_{12} & {}_{1}{}^{I}k_{22} & {}_{1}{}^{I}k_{23} & 0 \\ {}_{1}{}^{I}k_{13} & {}_{1}{}^{I}k_{23} & {}_{1}{}^{I}k_{33} & 0 \\ 0 & 0 & 0 & 0 \end{bmatrix} + \begin{bmatrix} 0 & 0 & 0 & {}_{1}{}^{I}k_{14} \\ 0 & 0 & 0 & {}_{1}{}^{I}k_{24} \\ 0 & 0 & 0 & {}_{1}{}^{I}k_{24} \\ 0 & 0 & 0 & {}_{1}{}^{I}k_{34} \\ 0 & 0 & 0 & {}_{1}{}^{I}k_{34} \end{bmatrix}$$
 (2.113 a)

in which

 ${}_{T}^{I}k_{II} = -\frac{{}^{I}C({}^{I}s')^{6}}{({}^{I}\kappa)^{2}}({}^{I}y'{}^{I}z'' - {}^{I}z'{}^{I}y'')^{2}$ (2.113 b)

$${}_{T}^{I}k_{22} = -\frac{{}^{I}C({}^{I}s')^{6}}{({}^{I}\kappa)^{2}}({}^{I}z'{}^{I}x'' - {}^{I}x'{}^{I}z'')^{2}$$
(2.113 c)

$${}_{T}^{I}k_{33} = -\frac{{}^{I}C({}^{I}s')^{6}}{({}^{I}\kappa)^{2}}({}^{I}x'{}^{I}y'' - {}^{I}y'{}^{I}x'')^{2}$$
 (2.113 d)

$${}_{T}^{l}k_{l2} = {}_{T}^{l}k_{2l} = -\frac{{}^{l}C({}^{l}s')^{6}}{({}^{l}\kappa)^{2}}({}^{l}y'{}^{l}z'' - {}^{l}z'{}^{l}y'')({}^{l}z'{}^{l}x'' - {}^{l}x'{}^{l}z'') \qquad (2.113 e)$$

$${}_{T}^{l}k_{l3} = {}_{T}^{l}k_{3l} = -\frac{{}^{l}C({}^{l}s')^{6}}{({}^{l}\kappa)^{2}}({}^{l}y'{}^{l}z'' - {}^{l}z'{}^{l}y'')({}^{l}x'{}^{l}y'' - {}^{l}y'{}^{l}x'') \qquad (2.113 f)$$

$${}_{T}^{l}k_{23} = {}_{T}^{l}k_{32} = -\frac{{}_{C}^{l}({}_{s}^{l})^{6}}{({}_{K}^{l})^{2}}({}_{z}^{l}x'' - {}_{x}^{l}x'' z'')({}_{x}^{l}x'' y'' - {}_{y}^{l}x'') \qquad (2.113 g)$$

$${}_{T_{2}}{}^{J}k_{J4} = \frac{{}^{J}C}{\left({}^{J}s'\right)^{2}} \left[\frac{\left({}^{J}y'\right)\left({}^{J}z''\right) - \left({}^{J}z'\right)\left({}^{J}y''\right)}{\left({}^{J}s'\right)^{2}} \right]$$
(2.113 h)

$${}_{T_{2}}{}^{I}k_{24} = \frac{{}^{I}C}{\left({}^{I}s'\right)^{2}} \left[\frac{\left({}^{I}z'\right)\left({}^{I}x''\right) - \left({}^{I}x'\right)\left({}^{I}z''\right)}{\left({}^{I}s'\right)^{2}} \right]$$
(2.113 i)

$${}_{T_{2}}{}^{l}k_{34} = \frac{{}^{l}C}{\left({}^{l}s'\right)^{2}} \left[\frac{\left({}^{l}x'\right)\left({}^{l}y''\right) - \left({}^{l}y'\right)\left({}^{l}x''\right)}{\left({}^{l}s'\right)^{2}} \right]$$
(2.113 j)

$$T_{2}^{I}k_{44} = {}^{I}C\left(\frac{{}^{I}\tau_{I}}{\left({}^{I}\psi'\right)} + \frac{I}{\left({}^{I}s'\right)}\right)$$
 (2.113 k)

the bending stiffness matrices are

$${}_{\mathbf{b}\mathbf{i}}^{I}\mathbf{K} = \frac{{}^{I}B}{\left({}^{I}s'\right)^{5}} \begin{bmatrix} \left({}^{I}y'\right)^{2} + \left({}^{I}z'\right)^{2} & -{}^{I}x'{}^{I}y' & -{}^{I}x'{}^{I}z' \\ -{}^{I}x'{}^{I}y' & \left({}^{I}x'\right)^{2} + \left({}^{I}z'\right)^{2} & -{}^{I}y'{}^{I}z' \\ -{}^{I}x'{}^{I}z' & -{}^{I}y'{}^{I}z' & \left({}^{I}x'\right)^{2} + \left({}^{I}y'\right)^{2} \end{bmatrix} (2.114 \text{ a})$$

$${}_{\mathbf{b2}}^{I}\mathbf{K} = \begin{bmatrix} {}_{b2}^{I}k_{1l} & {}_{b2}^{I}k_{12} & {}_{b2}^{I}k_{13} \\ {}_{b2}^{I}k_{2l} & {}_{b2}^{I}k_{22} & {}_{b2}^{I}k_{32} \\ {}_{b2}^{I}k_{13} & {}_{b2}^{I}k_{32} & {}_{b2}^{I}k_{33} \end{bmatrix}$$
(2.114 b)

in which

$${}_{b2}{}^{l}k_{II} = \frac{{}^{l}B}{\left({}^{l}s'\right)^{7}} \left[2\left({}^{l}x''^{I}y' - {}^{l}x'^{I}y''\right){}^{l}x'^{I}y' + 2\left({}^{l}x''^{I}z' - {}^{l}x'^{I}z''\right){}^{l}x'^{I}z'\right]$$
(2.114 c)

$${}_{b2}{}^{l}k_{22} = \frac{{}^{l}B}{\left({}^{l}s'\right)^{7}} \left[2\left({}^{l}y'''z' - {}^{l}y''z''\right){}^{l}y'{}^{l}z' - 2\left({}^{l}x'''y' - {}^{l}x''^{l}y''\right){}^{l}x'{}^{l}y'\right]$$
(2.114 d)

$${}_{b2}{}^{l}k_{33} = \frac{{}^{l}B}{\left({}^{l}s'\right)^{2}} \left[-2\left({}^{l}x''^{l}z' - {}^{l}x'^{l}z''\right){}^{l}x'^{l}z' - 2\left({}^{l}y''^{l}z' - {}^{l}y'^{l}z''\right){}^{l}y'^{l}z'\right]$$
(2.114 e)

$${}_{b2}{}^{I}k_{I2} = \frac{{}^{I}B}{\left({}^{I}s'\right)^{7}} \left[\left({}^{I}x''^{I}y' - {}^{I}x'^{I}y''\right) \left(\left({}^{I}y'\right)^{2} - \left({}^{I}x'\right)^{2}\right) + \left({}^{I}y''^{I}z' - {}^{I}y'^{I}z''\right) {}^{I}x'^{I}z' + \left({}^{I}x''^{I}z' - {}^{I}x'^{I}z''\right) {}^{I}y'^{I}z'\right]$$

$$(2.114 f)$$

$${}_{b2}{}^{l}k_{l3} = \frac{{}^{l}B}{\left({}^{l}s'\right)^{7}} \left[\left({}^{l}x'''^{l}z' - {}^{l}x'^{l}z''\right) \left(\left({}^{l}z'\right)^{2} - \left({}^{l}x'\right)^{2}\right) - \left({}^{l}y''^{l}z' - {}^{l}y'^{l}z''\right){}^{l}x'^{l}y'\right]$$

$$+ \left({}^{I}x''^{I}y' - {}^{I}x'^{I}y'' \right) {}^{I}y'^{I}z' \right]$$

$$= \frac{{}^{I}B}{\left({}^{I}s' \right)^{2}} \left[\left({}^{I}y''^{I}z' - {}^{I}y'^{I}z'' \right) \left(\left({}^{I}z' \right)^{2} - \left({}^{I}y' \right)^{2} \right) - \left({}^{I}x''^{I}z' - {}^{I}x'^{I}z'' \right) {}^{I}x'^{I}y' \right]$$

$$- \left({}^{I}x''^{I}y' - {}^{I}x'^{I}y'' \right) {}^{I}x'^{I}z' \right]$$
(2.114 h)

the axial stiffness matrices are

$$\mathbf{N}_{\mathbf{I}}^{I}\mathbf{K} = \frac{\left({}^{I}N_{a}^{\prime} - m_{i}V_{i}^{2}\right)}{\left({}^{\prime}s^{\prime}\right)^{3}} \begin{bmatrix} -\left(\left({}^{\prime}y^{\prime}\right)^{2} + \left({}^{\prime}z^{\prime}\right)^{2}\right) & {}^{I}x^{\prime I}y^{\prime} & {}^{I}x^{\prime I}z^{\prime} \\ {}^{I}x^{\prime I}y^{\prime} & -\left(\left({}^{I}x^{\prime}\right)^{2} + \left({}^{I}z^{\prime}\right)^{2}\right) & {}^{I}y^{\prime I}z^{\prime} \\ {}^{I}x^{\prime I}z^{\prime} & {}^{I}y^{\prime I}z^{\prime} & -\left(\left({}^{I}y^{\prime}\right)^{2} + \left({}^{I}x^{\prime}\right)^{2}\right) \end{bmatrix} \tag{2.115}$$

$$\mathbf{N}_{\mathbf{I}}^{I}\mathbf{K} = \frac{-\left({}^{I}N_{a}^{\prime} - m_{i}V_{i}V_{i}^{\prime}\right)}{{}^{I}s^{\prime}} \begin{bmatrix} I & 0 & 0 \\ 0 & I & 0 \\ 0 & 0 & I \end{bmatrix} \tag{2.116}$$

$$\mathbf{I}_{\mathbf{I}}^{I}\mathbf{f} = {}^{I}s^{\prime} \begin{cases} {}^{I}C_{bx}^{*} {}^{I}V_{a}^{2} + 2{}^{I}C_{bxy}^{*} {}^{I}V_{Hx} {}^{I}V_{Hy} + 2{}^{I}C_{bxy}^{*} {}^{I}V_{Hx} {}^{I}V_{Hz} \\ {}^{I}C_{by}^{*} {}^{I}V_{by}^{2} + 2{}^{I}C_{bxy}^{*} {}^{I}V_{Hx} {}^{I}V_{Hy} + 2{}^{I}C_{bxy}^{*} {}^{I}V_{Hx} {}^{I}V_{Hz} \\ {}^{I}C_{bx}^{*} {}^{I}V_{By}^{2} + 2{}^{I}C_{bxy}^{*} {}^{I}V_{Hx} {}^{I}V_{Hy} + 2{}^{I}C_{bxy}^{*} {}^{I}V_{Hx} {}^{I}V_{Hz} \\ {}^{I}C_{bx}^{*} {}^{I}V_{Hy}^{2} {}^{I}V_{Hy} + 2{}^{I}C_{bxy}^{*} {}^{I}V_{Hx} {}^{I}V_{Hz} \\ {}^{I}V_{hy}^{2} {}^{I}V_{Hz} + {}^{I}C_{bxy}^{*} {}^{I}V_{Hz} + {}^{I}C_{bxy}^{*} {}^{I}V_{Hz}^{2} \\ {}^{I}V_{by}^{2} {}^{I}V_{Hz} + {}^{I}C_{bxy}^{*} {}^{I}V_{Hz}^{2} + {}^{I}C_{bxy}^{*} {}^{I}V_{Hz}^{2} - {}^{I}V_{a} \\ {}^{I}V_{hy}^{2} {}^{I}V_{Hz} + {}^{I}C_{bxy}^{*} {}^{I}V_{Hz}^{2} + {}^{I}C_{bxz}^{*} {}^{I}V_{Hz}^{2} \\ {}^{I}V_{hy}^{2} {}^{I}V_{Hz} + {}^{I}C_{bxz}^{*} {}^{I}V_{Hz}^{2} + {}^{I}C_{bxz}^{*} {}^{I}V_{Hy}^{2} \\ {}^{I}V_{Hz}^{2} + {}^{I}C_{bxz}^{*} {}^{I}V_{Hy}^{2} \\ {}^{I}V_{Hz}^{2} + {}^{I}C_{bxz}^{*} {}^{I}V_{Hy}^{2} + {}^{I}C_{bxz}^{*} {}^{I}V_{Hy}^{2} \\ {}^{I}V_{Hz}^{2} + {}^{I}C_{bxz}^{*} {}^{I}V_{Hy}^{2} + {}^{I}C_{bxz}^{*} {}^{I}V_{Hy}^{2} \\ {}^{I}V_{Hz}^{2} + {}^{I}C_{bxz}^{*} {}^{I}V_{Hy}^{2} \\ {}^{I}V$$

2.11 CHOICES OF THE INDEPENDENT VARIABLE α

One salient feature of the large strain formulations presented in this work is that the independent variable α used in the formulations provides flexibility in the choice of parameters defining elastic curves. The formulations therefore allow users to select the independent variable that is most efficient for their own problem solution. For example, analysis of flexible marine risers as shown in Figure 2.1, has at least four alternatives for the independent variable α such as the vertical coordinate y, the in-plane offset distance x, the out-of-plane offset distance z, and the arc length s.

The advantage of using $\alpha = y$ is that the total water depth or the boundary condition is known initially. While using $\alpha = x$ or $\alpha = z$ the boundary condition is known if the offset at the top end of the riser can be assumed to be static, and is unknown if the offset is dynamic. If one uses $\alpha = s$, the boundary condition is always unknown, because the total arc-length changes after deformation. The problem for which the boundary condition is unknown, becomes much more difficult, and requires specific treatment.

However, the disadvantage of using $\alpha = y$ is that if elastic curves after large displacements form like the U-shape or the semi U-shape as shown in Figures 1 (b) and 1(c), the vertical position is no longer a one to one function for all points on the elastic curves. Consequently, $\alpha = y$ is not an effective choice in this case. Likewise, using $\alpha = x$ or $\alpha = z$ encounter the same difficulty when the elastic curves after large displacements develop akin to the C-shape or the semi C-shape. In these troublesome cases, using $\alpha = s$ becomes the best way, because arc-length is an intrinsic property, and thus is always a one to one function for all points of the elastic curves.

Therefore for flexible marine risers which do not face the problem of elastic curves having a U-shape, such as the high-tensioned risers, using $\alpha = y$ is sufficient. However, if the risers confront the problem that occurs in the case of low-tensioned risers, $\alpha = s$ should be employed. It should be noted that in addition to the four alternatives of α as exemplified earlier, there are still other choices of α such as the span length, the rotational angle, and so on, which may be employed if efficient.

2.12 IMPLEMENTATION OF THE MODEL FORMULATION TO PRACTICAL ENGINEERING PROBLEMS

The present formulations are applicable to large strain analysis not only of flexible marine risers, but also of any kind of engineering structures, which may have the elastica's behavior. The examples of these are listed as follows.

(a) Onshore pipes. The effect of external fluid would be excluded from the present models.

- (b) Submerged pipes. The hydrodynamic pressure effect of external fluid would be excluded.
- (c) Marine cables. Bending rigidity, Torsion rigidity and influence of internal fluid would be excluded.
- (d) Submerged cables. Bending rigidity, Torsion rigidity, influence of internal fluid, and hydrodynamic pressure effect of external fluid would be excluded from the present models.
- (e) Onshore cables and strings. Bending rigidity, Torsion rigidity, and influences of internal and external fluids would be excluded from the present models.
- (g) Elastic rods, long columns, and long beams. Influences of external and internal fluids would be excluded from the present models.

Even though the present models are intended for engineering structures with environment-induced initial curvatures, the models can still be extended to the structures with man-made initial curvatures such as curved beams and arches by considering $\vec{k} \neq 0$ in application of the extensible elastica theory developed in this study.

3. SOLUTION METHODS

In this chapter, the updated Lagrangian descriptor (ULD) is employed for describing the nonlinear behaviors of the riser, and the independent variable $\alpha = {}^{I}y$ is adopted. For the 3-D nonlinear static analysis, the weak formulation $\delta^{I}\pi = 0$ is derived and solved by the hybrid finite element method as will be elaborated in section 3.1. For the 2-D dynamic analysis, the ordinary differential equations of motion are derived from the weak formulation $\delta^{2}\pi = 0$ by the finite element method as will be shown in section 3.2. Based on the state-space formulation obtained from section 3.2, the natural frequency analysis and the time history analysis of the nonlinear vibrations will be carried out in sections 3.3 and 3.4, respectively.

3.1 THREE-DIMENSIONAL NONLINEAR STATIC ANALYSIS VIA THE HYBRID FINITE ELEMENT METHOD

The hybrid finite element method herein refers to the finite element solution of the weak formulation that is mixed with the strong formulation. One may question why this method is essential for the nonlinear static analysis of the marine riser. The answer is as follows. For the extensible analysis of most structures, the static axial strain in the weak formulation is determined from the strain-displacement relation such as

$${}^{I}\varepsilon = (d^{I}s - d^{o}s)/d^{I}s. \tag{3.1}$$

However, for extensible marine risers with large displacements this approach may not be applicable, because in practices, marine risers do not have the undeformed configuration as for reference. In other words, for marine risers $d^{\circ}s$ is nonexistence for use in equation (3.1). The equilibrium state is the only initial state or the first state of marine risers, which is unknown initially, while the undeformed state is the ideal state, which never appears in the real situation. The way to solve this problem is to establish the static axial strain from the constitutive equation

$${}^{l}\varepsilon = {}^{l}N_{a} / E^{l}A_{p}, \qquad (3.2)$$

where the apparent axial force ${}^{I}N_{a}$ is determined from the equilibrium equations. This approach is called the hybrid method (O'Brien and Mcnamara, 1989).

It should be noted that this problem would not be encountered in the dynamic analysis of the marine riser, because the dynamic axial strain can be determined from the strain-displacement relation

$$\varepsilon = (d^2s - d^1s)/d^1s, \qquad (3.3)$$

where the reference configuration d's in equation (3.3) refers to the equilibrium configuration, which is known from static analysis. Therefore, the hybrid method is not needed for dynamic analysis.

In section 2.7, there are at least four forms of the weak variational formulations to be used. In this study, the second weak formulation is employed. With application of $\alpha = {}^{t}y$, and neglecting the time-dependent terms in equation (2.71) and (2.80), the hybrid formulation for nonlinear static analysis is obtained as

$$\delta({}^{l}\pi) = \int_{y_{a}}^{y_{B}} \left\{ \left[{}^{l}N_{a} \left(\frac{{}^{l}x'}{{}^{l}s'} \right) - {}^{l}B \left(\frac{{}^{l}\kappa}{{}^{l}s'} + \frac{{}^{l}s''}{{}^{l}s'} + \frac{{}^{l}s''}{{}^{l}s'} - \frac{{}^{l}x''({}^{l}s'')}{{}^{l}s'} - \frac{{}^{l}x'({}^{l}s'')}{{}^{l}s'} \right] \right] \delta({}^{l}u')$$

$$+ \left[{}^{l}N_{a} \left(\frac{{}^{l}z'}{{}^{l}s'} \right) - {}^{l}B \left(\frac{{}^{l}\kappa}{{}^{l}s'} + \frac{{}^{l}s''}{{}^{l}s'} + \frac{{}^{l}s''}{{}^{l}s'} - \frac{{}^{l}z'({}^{l}s'')}{{}^{l}s'} - \frac{{}^{l}z'({}^{l}s'')}{{}^{l}s'} \right] \right] \delta({}^{l}w')$$

$$+ \frac{{}^{l}B}{{}^{l}({}^{l}s')^{2}} \left(\frac{{}^{l}x'''}{{}^{l}s'} - \frac{{}^{l}x'({}^{l}s'')}{{}^{l}(s')^{2}} \right) \delta({}^{l}u'') + \frac{{}^{l}B}{{}^{l}s'} - \frac{{}^{l}z'({}^{l}s'')}{{}^{l}(s')^{2}} \right] \delta({}^{l}w')$$

$$+ {}^{l}\mathbb{F}_{lx}\delta({}^{l}u') + {}^{l}\mathbb{F}_{lz}\delta({}^{l}w') + {}^{l}\mathbb{F}_{lz}\delta({}^{l}u'') + {}^{l}\mathbb{F}_{2z}\delta({}^{l}u'') + {}^{l}\mathbb{F}_{2z}\delta({}^{l}w'') + {}^{l}T\delta({}^{l}\psi')$$

$$+ {}^{l}s'(-{}^{l}f_{Hx} + m_{i}({}^{l}a_{Fx}))\delta({}^{l}u) + {}^{l}s'(-{}^{l}f_{Hz} + m_{i}({}^{l}a_{Fz}))\delta({}^{l}w)$$

$$+ {}^{l}s'(-{}^{l}f_{Hx} + m_{i}({}^{l}a_{Fx}))\delta({}^{l}u) + {}^{l}s'(-{}^{l}f_{Hz} + m_{i}({}^{l}a_{Fz}))\delta({}^{l}w)$$

where

$${}^{I}N_{a}({}^{I}y) = {}^{I}N_{a}({}^{I}y_{H}) + \int_{y}^{y_{H}} \left[\left({}^{I}B({}^{I}\kappa) \right)'({}^{I}\kappa) + {}^{I}s'({}^{I}q_{I}) \right] d({}^{I}y), \qquad (3.5 \text{ a})$$

$${}^{\prime}T\left({}^{\prime}y\right) = {}^{\prime}T\left({}^{\prime}y_{H}\right),\tag{3.5 b}$$

$${}^{I}q_{I} = {}^{I}f_{Ht} - {}^{I}m_{i}({}^{I}a_{Ft}) - {}^{I}w_{a}(\frac{{}^{I}y'}{{}^{I}s'}),$$
 (3.5 c)

$${}^{1}f_{Ht} = 0.5 \rho_{e} ({}^{1}D_{e}) \pi C_{Dt} ({}^{1}V_{Ht})^{2},$$
 (3.5 d)

$${}^{I}f_{Hn} = 0.5 \rho_{e} \left({}^{I}D_{e} \right) C_{Dn} \left({}^{I}V_{Hn} \right)^{2},$$
 (3.5 e)

$${}^{1}f_{Hbn} = 0.5 \rho_{e} ({}^{1}D_{e}) C_{Dn} ({}^{1}V_{Hbn})^{2},$$
 (3.5 f)

$${}^{1}f_{Hx} = {}^{1}f_{Ht} \left(\frac{{}^{1}x'}{{}^{1}S'} \right) + {}^{1}f_{Hn} \left({}^{1}n_{x} \right) + {}^{1}f_{Hbn} \left({}^{1}b_{x} \right), \tag{3.5 g}$$

$${}^{I}f_{Hz} = {}^{I}f_{Ht} \left(\frac{{}^{I}z'}{{}^{I}s'} \right) + {}^{I}f_{Hn} \left({}^{I}n_{z} \right) + {}^{I}f_{Hbn} \left({}^{I}b_{z} \right), \tag{3.5 h}$$

$${}^{\prime}a_{Fi} = \frac{{}^{\prime}V_{i}({}^{\prime}V_{i}')}{{}^{\prime}S'},$$
 (3.5 i)

$${}^{I}a_{Fx} = {}^{I}\kappa \left({}^{I}n_{x}\right)\left({}^{I}V_{i}\right)^{2} + \frac{\left({}^{I}V_{i}\right)\left({}^{I}V_{i}'\right)\left({}^{I}x'\right)}{\left({}^{I}s'\right)^{2}},$$
(3.5 j)

$${}^{\prime}a_{Fz} = {}^{\prime}\kappa \left({}^{\prime}n_{z}\right)\left({}^{\prime}V_{i}\right)^{2} + \frac{\left({}^{\prime}V_{i}\right)\left({}^{\prime}V_{i}^{\prime}\right)\left({}^{\prime}z^{\prime}\right)}{\left({}^{\prime}s^{\prime}\right)^{2}}, \tag{3.5 k}$$

$${}^{I}V_{Ht} = {}^{I}V_{Hx} \left(\frac{{}^{I}x'}{{}^{I}s'} \right) + {}^{I}V_{Hz} \left(\frac{{}^{I}z'}{{}^{I}s'} \right), \tag{3.5 l}$$

$${}^{I}V_{Hn} = {}^{I}V_{Hx} \left({}^{I}n_{x}\right) + {}^{I}V_{Hz} \left({}^{I}n_{z}\right),$$
 (3.5 m)

$${}^{1}V_{Hbn} = {}^{1}V_{Hx} ({}^{1}b_{x}) + {}^{1}V_{Hz} ({}^{1}b_{z}),$$
 (3.5 n)

Note that for $\alpha = {}^{1}y$,

$${}^{I}B = E({}^{I}I_{p}), {}^{I}B' = 2E({}^{0}I_{p})(1 + {}^{I}\varepsilon){}^{I}\varepsilon', \qquad (3.6 \text{ a,b})$$

$${}^{\prime}s' = \sqrt{1 + \left({}^{\prime}x'\right)^{2} + \left({}^{\prime}z'\right)^{2}}, \ {}^{\prime}s'' = \frac{{}^{\prime}x'\left({}^{\prime}u''\right) + {}^{\prime}z'\left({}^{\prime}w''\right)}{{}^{\prime}s'}, \tag{3.6 c,d}$$

$${}^{I}\kappa = \frac{I}{\left({}^{I}s'\right)^{3}} \sqrt{\left({}^{I}u''\right)^{2} + \left({}^{I}w''\right)^{2} + \left(\left({}^{I}u''\right)\left({}^{I}z'\right) - \left({}^{I}x'\right)\left({}^{I}w''\right)\right)^{2}} , \qquad (3.6 e)$$

$${}^{I}\kappa' = \frac{1}{\left({}^{I}s'\right)^{6}\left({}^{I}\kappa\right)}\left\{ \left({}^{I}u''\right)\left({}^{I}u'''\right) + \left({}^{I}w'''\right)\left({}^{I}w''''\right)\right\}$$

$$+\left[\left({}^{\prime}u''\right)\left({}^{\prime}z'\right)-\left({}^{\prime}x'\right)\left({}^{\prime}w''\right)\right]\left[\left({}^{\prime}u'''\right)\left({}^{\prime}z'\right)-\left({}^{\prime}x'\right)\left({}^{\prime}w'''\right)\right]\right] -\frac{3\left({}^{\prime}\kappa\right)\left({}^{\prime}s''\right)}{{}^{\prime}s'} \quad (3.6 \text{ f})$$

$${}^{l}\tau = {}^{l}\tau_{I} + \frac{{}^{l}\psi'}{{}^{l}s'}, {}^{l}\tau_{I} = \frac{{}^{(l}w'')({}^{l}u''') - {}^{(l}w''')({}^{l}u'')}{{}^{(l}u'') + {}^{(l}w'')^{2} + {}^{(l}u''')({}^{l}z') - {}^{(l}x')({}^{l}w'')]^{2}}, \quad (3.6 \text{ g,h})$$

$${}^{l}\mathfrak{F}_{lx} = {}^{l}T \left[\frac{{}^{l}\tau_{I}({}^{l}x')}{{}^{l}s'} + \frac{2({}^{l}s')({}^{l}\tau_{I})}{{}^{l}\mathfrak{I}} \left({}^{(l}u'')({}^{l}z') - {}^{(l}x')({}^{l}w'') \right) ({}^{l}w'') \right] \quad (3.6 \text{ j})$$

$${}^{l}\mathfrak{F}_{lz} = {}^{l}T \left[\frac{{}^{l}\tau_{I}({}^{l}z')}{{}^{l}s'} - \frac{2({}^{l}s')({}^{l}\tau_{I})}{{}^{l}\mathfrak{I}} \left({}^{(l}u'')({}^{l}z') - {}^{(l}x')({}^{l}w'') \right) ({}^{l}u'') \right] \quad (3.6 \text{ k})$$

$${}^{l}\mathfrak{F}_{lz} = \frac{-{}^{l}T({}^{(l}w'')({}^{l}s'')}{{}^{l}\mathfrak{I}} + \frac{{}^{l}T({}^{(l}w'')({}^{l}s'')}{{}^{l}\mathfrak{I}} + \frac{{}^{l}T({}^{(l}u'')({}^{l}s'')}{{}^{l}\mathfrak{I}} + \frac{{}^{l}T({}^{(l}u'')({}^{(l}s''))}{{}^{(l}s'')} + \frac{{}^{l}T({}^{(l}u'')({}^{(l}s'$$

In large strain analysis, the axial strain is one of degree of freedom and the axial force can be derived from constitutive equation.

$${}^{I}N_{a}({}^{I}y) = E({}^{I}A_{p})({}^{I}\varepsilon({}^{I}y))$$
(3.7)

To satisfy both equilibrium equation and constitutive equation, equation (3.7) has to be equal to equation (3.5 a), the constrain equation of this condition may be written as

$$\delta w_c = \int_{y_a}^{y_H} \left\{ E(^{\prime}A_p)^{\prime} \varepsilon(^{\prime}y) - ^{\prime}N_a(^{\prime}y) \right\} \delta(^{\prime}\varepsilon) = 0$$
 (3.8)

This constrain equation may be considered as an equivalent work term and is added directly to the standard virtual work statement; equation (3.4).

From equations (3.4)-(3.8), it is seen that there are four dependent variables (${}^{1}u$, ${}^{1}w$, ${}^{1}\psi$, and ${}^{1}\varepsilon$) and one independent variable (${}^{1}y$). Along with the essential and the natural boundary conditions of the riser that has the slip joint at top and the ball joint that can not rotate in tangential direction at the bottom end.

at
$${}^{1}y = 0$$
: ${}^{1}u = 0$, ${}^{1}w = 0$, ${}^{1}\psi = 0$, (essential) (3.9 a, b)

$${}^{1}u'' = 0, {}^{1}w'' = 0$$
 (natural) (3.9 c,d)

and at
$$y = y_t$$
: $u = 0$, $w = 0$, $\varepsilon = (N_{aH}) / E(A_{pH})$ (essential) (3.10 a-c)

$$^{I}T = {}^{I}T_{H}$$
 (essential) (3.10 d)

$${}^{l}u'' = \theta, {}^{l}w'' = \theta$$
 (natural), (3.10 e,f)

the system of equations (3.4)-(3.10) is the boundary value problem that should be discretized by using the C² finite elements so that all the boundary conditions are constrained. Note that the C^m finite elements are the elements of which derivatives of displacement field through order 'm' are continuous.

However, the higher derivatives of the twisting rotation ${}^{l}\psi$ and the strain ${}^{l}\varepsilon$ are equal to order one, thus it is sufficient to approximate the twisting rotation and the strain by the C^{1} element. Therefore, in this study the elements mixed between the C^{1} and the C^{2} elements are used for approximating the displacement vector of ${}^{l}\psi$, ${}^{l}\varepsilon$, ${}^{l}u$ and ${}^{l}w$.

For ease, the third and the fifth order polynomial shape functions are employed to correspond the C^1 and the C^2 finite elements, respectively. Therefore, the displacement vector is expressed as

$$\{ \vec{d} \} = \{ u^{-1} w^{-1} \psi^{-1} \varepsilon \}^{T} = [N] \{ \vec{d}_{n} \},$$
 (3.11)

where the generalized coordinates of the nodal displacements of each element are

and the shape function matrix at the equilibrium state

$$\begin{bmatrix} {}^{I}\mathbf{N} \end{bmatrix} = \begin{bmatrix} {}^{I}N_{51} & {}^{I}N_{52} & {}^{I}N_{53} & 0 & 0 & 0 & 0 & 0 & 0 & 0 \\ \hline 0 & 0 & 0 & {}^{I}N_{51} & {}^{I}N_{52} & {}^{I}N_{53} & 0 & 0 & 0 & 0 \\ \hline 0 & 0 & 0 & 0 & 0 & 0 & {}^{I}N_{31} & {}^{I}N_{32} & 0 & 0 \\ \hline 0 & 0 & 0 & 0 & 0 & 0 & 0 & 0 & {}^{I}N_{31} & {}^{I}N_{32} \end{bmatrix}$$

$$\frac{\begin{vmatrix}
^{1}N_{54} & ^{1}N_{55} & ^{1}N_{56} & 0 & 0 & 0 & 0 & 0 & 0 & 0 \\
\hline
0 & 0 & 0 & ^{1}N_{54} & ^{1}N_{55} & ^{1}N_{56} & 0 & 0 & 0 & 0 \\
\hline
0 & 0 & 0 & 0 & 0 & 0 & ^{1}N_{33} & ^{1}N_{34} & 0 & 0 \\
\hline
0 & 0 & 0 & 0 & 0 & 0 & 0 & 0 & ^{1}N_{33} & ^{1}N_{34}
\end{vmatrix}$$
(3.13)

Note that ${}^{I}N_{3i}$ and ${}^{I}N_{5i}$ are the coefficients of the third and the fifth order polynomial shape functions, respectively.

From equation (3.13), the number of degrees of freedom per element is 20. From equation (2.81) and the calculus of variation, one has

$$\delta\left({}^{I}\pi^{(e)}\right) = \sum_{i=1}^{20} \left[\frac{\partial\left({}^{I}\pi^{(e)}\right)}{\partial\left({}^{I}d_{ni}\right)}\right] \delta\left({}^{I}d_{ni}\right) = 0. \tag{3.14}$$

Equation (3.14) yields the twenty equilibrium equations of each element

$$\frac{\partial \binom{1}{\pi^{(e)}}}{\partial \binom{1}{d_{ni}}} = 0, \text{ for } i = 1, 2, \dots, 20.$$

$$(3.15)$$

Substituting equation (3.11) into equations (3.4) and (3.8), the matrix form of equation (3.15) can be obtained as

$$\int_{0}^{h} \left\{ \left[{}^{l}N_{x} \left(\frac{{}^{l}X'}{{}^{l}S'} \right) - {}^{l}B \left(\frac{{}^{l}K'}{{}^{l}S'} + \frac{{}^{l}S''}{{}^{l}S'} + \frac{{}^{l}S''}{{}^{l}S'} - \frac{{}^{l}X'({}^{l}S'')}{{}^{l}S'} \right] \right\} + {}^{l}\mathbb{F}_{lx} \right] \left[{}^{l}N'\right]^{T} \begin{cases} l \\ 0 \\ 0 \\ 0 \end{cases}$$

$$+ \left[{}^{l}N_{x} \left(\frac{{}^{l}Z'}{{}^{l}S'} \right) - {}^{l}B \left(\frac{{}^{l}K'}{{}^{l}S'} + \frac{{}^{l}S''}{{}^{l}S'} + \frac{{}^{l}S''}{{}^{l}S''} - \frac{{}^{l}Z'({}^{l}S'')}{{}^{l}S'} - \frac{{}^{l}Z'({}^{l}S'')}{{}^{l}S'} \right] \right] + {}^{l}\mathbb{F}_{lx} \left[{}^{l}N'\right]^{T} \begin{cases} 0 \\ l \\ 0 \\ 0 \end{cases}$$

$$+ \left[\frac{{}^{l}B}{{}^{l}S'} \left(\frac{{}^{l}X''}{{}^{l}S'} - \frac{{}^{l}X'({}^{l}S'')}{{}^{l}(S')^{2}} \right) + {}^{l}\mathbb{F}_{2x} \right] \left[{}^{l}N''\right]^{T} \begin{cases} 0 \\ 0 \\ 0 \\ 0 \end{cases}$$

$$+ \left[\frac{{}^{l}B}{{}^{l}S'} \left(\frac{{}^{l}Z''}{{}^{l}S'} - \frac{{}^{l}Z'({}^{l}S'')}{{}^{l}(S')^{2}} \right) + {}^{l}\mathbb{F}_{2x} \right] \left[{}^{l}N''\right]^{T} \begin{cases} 0 \\ l \\ 0 \\ 0 \end{cases}$$

$$+ \left[\frac{{}^{l}B}{{}^{l}S'} \left(\frac{{}^{l}Z''}{{}^{l}S'} - \frac{{}^{l}Z'({}^{l}S'')}{{}^{l}(S')^{2}} \right) + {}^{l}\mathbb{F}_{2x} \right] \left[{}^{l}N''\right]^{T} \begin{cases} 0 \\ l \\ 0 \\ 0 \end{cases}$$

$$+ {}^{l}S'(-{}^{l}f_{hx} + m_{l}({}^{l}a_{Fx})) \left[{}^{l}N\right]^{T} \begin{cases} 0 \\ 0 \\ 0 \\ 0 \end{cases}$$

$$+ \left[({}^{l}A_{p})({}^{l}S) - {}^{l}N_{x} \right] \left[{}^{l}N\right]^{T} \left[{}^{l}S' \right] \right] \begin{cases} 0 \\ 0 \\ 0 \end{cases}$$

$$+ \left[({}^{l}A_{p})({}^{l}S) - {}^{l}N_{x} \right] \left[{}^{l}N\right]^{T} \left[{}^{l}S' \right] \end{cases} \begin{cases} 0 \\ 0 \\ 0 \end{cases}$$

$$+ \left[({}^{l}A_{p})({}^{l}S) - {}^{l}N_{x} \right] \left[{}^{l}N\right]^{T} \left[{}^{l}S' \right] \end{cases} \begin{cases} 0 \\ 0 \\ 0 \end{cases}$$

$$+ \left[({}^{l}A_{p})({}^{l}S) - {}^{l}N_{x} \right] \left[{}^{l}N\right] \left[{}^{l}N\right] \right] \begin{cases} 0 \\ 0 \\ 0 \end{cases} \end{cases} \end{cases} \begin{cases} 0 \\ 0 \\ 0 \end{cases}$$

The Fortran-90 codes for solving the system of equation (3.16) has been developed based on the aforementioned finite element method. The solution steps used in the codes can be summarized as follows.

- Step 1 Read the usual data from the data file.
- Step 2 Set the values of constants.
- Step 3 Determine the values of the constant.
- Step 4 Label the node number of all elements.
- Step 5 Initialize the guessed values of all degrees of freedom.
- Step 6 Form the system of finite element equations, in which the procedures are as follows:
- Step 6.1 Calculate the nodal axial forces and the nodal axial strains based on equation (3.5a).
- Step 6.2 Create the element equations based on equation (3.16). The numerical integration is performed by using the fourth-order Gaussian quadrature. The global degrees of freedom are transformed to the local. The third and the fifth order polynomial shape functions are calculated. The shape function matrices are formed. The generalized coordinates of displacements are evaluated. The effects of radial deformation on the changes of cross-sectional properties and velocity of transported fluid are treated. The external loads due to the effects of the hydrostatic and the hydrodynamic pressures are evaluated. The axial and shear forces at the depth 'y are computed.
- Step 6.3 Assemble the element equations obtained from step 6.2 to generate the global system of finite element equations.

Step 6.4 Impose the boundary conditions from equations (3.9) and (3.10).

Step 7 Solve the system of the finite element equations obtained from step 6 by numerical methods. This study utilizes the modified Powell hybrid algorithm based on the MINPACK subroutine HYBRD1 (More et al., 1980) which will correct and update the guessed values of degrees of freedom, and repeat steps 4-7 until the stopping error criterion is satisfied.

Step 8 Save the numerical results in the result files.

3.2 TWO-DIMENSIONAL DYNAMIC ANALYSIS

The second weak formulation is employed for the dynamic analysis as well. From equation (2.81) $\delta \pi = 0$, hence the second weak formulation may be decomposed into the following four nonlinear dynamic equilibrium equations.

$$\int_{\alpha} \left\{ \left[\frac{{}^{2}M}{{}^{2}\kappa \left({}^{2}s' \right)^{2}} \frac{\partial}{\partial \alpha} \left(\frac{{}^{2}x'}{{}^{2}s'} \right) + {}^{2}\mathbb{F}_{2x} \right] \delta \left({}^{2}u'' \right) \right. \\
+ \left[{}^{2}N_{a} \left(\frac{{}^{2}x'}{{}^{2}s'} \right) - {}^{2}M_{a} \left(\frac{{}^{2}\kappa \left({}^{2}x' \right)}{{}^{2}s'} + \frac{{}^{2}s''}{{}^{2}\kappa \left({}^{2}s' \right)^{3}} \frac{\partial}{\partial \alpha} \left(\frac{{}^{2}x'}{{}^{2}s'} \right) \right) + {}^{2}\mathbb{F}_{1x} \right] \delta \left({}^{2}u' \right) \right. \\
+ \left[{}^{2}N_{a} \left(\frac{{}^{2}y'}{{}^{2}s'} \right) + {}^{2}\mathbb{F}_{2y} \right] \delta \left({}^{2}v'' \right) \\
+ \left[{}^{2}N_{a} \left(\frac{{}^{2}y'}{{}^{2}s'} \right) - {}^{2}M_{a} \left(\frac{{}^{2}\kappa \left({}^{2}y' \right)}{{}^{2}s'} + \frac{{}^{2}s''}{{}^{2}\kappa \left({}^{2}s' \right)^{3}} \frac{\partial}{\partial \alpha} \left(\frac{{}^{2}y'}{{}^{2}s'} \right) + {}^{2}\mathbb{F}_{1y} \right] \delta \left({}^{2}v' \right) \\
+ \left[{}^{2}N_{a} \left(\frac{{}^{2}y'}{{}^{2}s'} \right) - {}^{2}M_{a} \left(\frac{{}^{2}\kappa \left({}^{2}y' \right)}{{}^{2}s'} + \frac{{}^{2}s''}{{}^{2}\kappa \left({}^{2}s' \right)^{3}} \frac{\partial}{\partial \alpha} \left(\frac{{}^{2}y'}{{}^{2}s'} \right) \right] + {}^{2}\mathbb{F}_{1y} \right] \delta \left({}^{2}v' \right) \right.$$

$$\int_{\alpha}^{2} \left\{ \left[-w_{a} - f_{Hy} - m_{p} a_{py} - m_{i} a_{Fy} \right] \delta\left(^{2}v\right) \right\} d\alpha = 0, \qquad (3.17 \text{ b})$$

$$\int_{\alpha}^{2} \left\{ \left[\frac{^{2}M}{^{2}\kappa\left(^{2}s'\right)^{2}} \frac{\partial}{\partial\alpha} \left(\frac{^{2}z'}{^{2}s'}\right) + {}^{2}\mathbb{F}_{2w} \right] \delta\left(^{2}w''\right) + \left[{}^{2}N_{a} \left(\frac{^{2}z'}{^{2}s'}\right) - {}^{2}M_{a} \left(\frac{^{2}\kappa\left(^{2}z'\right)}{^{2}s'} + \frac{^{2}s''}{^{2}\kappa\left(^{2}s'\right)^{3}} \frac{\partial}{\partial\alpha} \left(\frac{^{2}z'}{^{2}s'}\right) \right) + {}^{2}\mathbb{F}_{1z} \right] \delta\left(^{2}w'\right)$$

$${}^{2}s' \left[f_{Hz} - m_{p} a_{pz} - m_{i} a_{Fz} \right] \delta\left(^{2}w\right) \right\} d\alpha = 0, \qquad (3.17 \text{ c})$$

$$\int_{\alpha}^{2} \left\{ {}^{2}T\delta\left(^{2}\psi'\right) - {}^{2}s'\left(-m_{p}\left(^{2}J_{p}\right)\left(^{2}\ddot{\psi}\right)\right) \delta\left(^{2}\psi\right) \right\} d\alpha = 0, \qquad (3.17 \text{ d})$$

By neglecting the out-of-plane motion and the effect of torsion, the two nonlinear dynamic equilibrium equations for two-dimensional analysis can be expressed as follows

$$\int_{a}^{\left\{\frac{B(^{2}\kappa)}{^{2}s'}\left(\frac{^{2}y'}{^{2}s'}\right)\delta(^{2}u'')\right\} d\alpha = 0, \qquad (3.18 a)$$

$$\int_{a}^{-2s'}\left[f_{Hx} - m_{p}a_{px} - m_{i}a_{Fx}\right]\delta(^{2}u) d\alpha = 0, \qquad (3.18 a)$$

$$\int_{a}^{-2s'}\left[f_{Hx} - m_{p}a_{px} - m_{i}a_{Fx}\right]\delta(^{2}u) d\alpha = 0, \qquad (3.18 b)$$

$$\int_{a}^{-2s'}\left[f_{Hx} - a_{p}a_{px} - a_{px} - a_{px}\right]\delta(^{2}u) d\alpha = 0, \qquad (3.18 b)$$

$$\int_{a}^{-2s'}\left[f_{Hx} - a_{p}a_{px} - a_{px} - a_{px}\right]\delta(^{2}u) d\alpha = 0, \qquad (3.18 b)$$

From the assumption of the linear dynamic strain of the vibrations with infinitesimal amplitudes in equation (2.8) and (2.9), one has

$${}^{2}N_{a} \approx {}^{1}N_{a} + E({}^{1}A_{P})\left(\frac{{}^{1}x'u' + {}^{1}y'v'}{({}^{1}s')^{2}}\right).$$
 (3.19)

By substituting equations (2.45), (2.65), and (3.19) into equations (3.18 a-b) together with neglecting the higher order terms of the vibrations with infinitesimal amplitudes, equations (3.18 a-b) can be expressed as

$$\left\{ \frac{{}^{1}B}{({}^{'}s')^{2}} \left[({}^{1}y')^{2} ({}^{2}x'') - (({}^{1}x')({}^{1}y'))({}^{2}y'') \right] \delta({}^{2}u'') \right. \\
+ \left[\frac{({}^{1}N_{a} - {}^{1}m_{i}({}^{1}V_{i})^{2})({}^{2}x')}{{}^{i}s'} \right] \delta({}^{2}u') \\
+ E({}^{1}A_{p}) \left[\frac{({}^{1}x')^{2}u' + (({}^{1}x')({}^{1}y'))v'}{({}^{1}s')^{3}} \right] \delta({}^{2}u') \\
- \frac{{}^{1}B({}^{1}K)}{({}^{1}s')^{4}} \left[(2({}^{1}x')({}^{1}y'))({}^{2}x'') + (({}^{1}y')^{2} - ({}^{1}x')^{2})({}^{2}y'') \right] \delta({}^{2}u') \\
- {}^{1}s' \left[-{}^{1}C_{a}^{*}({}^{2}\ddot{x}) - {}^{1}C_{eqx}^{*}({}^{2}\dot{x}) - {}^{1}C_{eqxy}^{*}({}^{2}\dot{y}) + {}^{1}C_{Dx}^{*}V_{Hx}^{2} + {}^{1}C_{M}^{*}\dot{V}_{Hx} \right] \delta({}^{2}u) \right\} d\alpha \\
+ {}^{1}s' \left[({}^{1}m_{p} + {}^{1}m_{i})({}^{2}\ddot{x}) + {}^{1}m_{i}({}^{1}V_{i}) \left(\frac{2}{s'} - \frac{({}^{1}x')^{2}}{({}^{1}s')^{3}} \right)({}^{2}\dot{x}') \right] \\
+ {}^{1}s' \left[\left({}^{1}m_{i}({}^{1}V_{i})({}^{1}V_{i}') \right] ({}^{2}x') + \frac{{}^{1}m_{i}({}^{1}x')}{s'} \frac{DV_{td}}{Dt} \right] \delta({}^{2}u) \right] \\
+ \left[{}^{1}m_{i}({}^{1}V_{i})({}^{1}V_{i}') \left({}^{1}s')^{2} \right] ({}^{2}x') + \frac{{}^{1}m_{i}({}^{1}x')}{s'} \frac{DV_{td}}{Dt} \right] \delta({}^{2}u) \right]$$

$$(3.20 a)$$

$$\frac{\frac{i_{B}}{\left(i's'\right)^{2}}\left[-\left(\left(i'x'\right)\left(i'y'\right)\right)\left(i'x''\right)+\left(i'x'\right)^{2}\left(i'y''\right)\right]\delta\left(i'y''\right)}{+\left[\frac{\left(i'N_{a}-i'm_{i}\left(i'V_{i}\right)^{2}\right)\left(i'y'\right)}{i's'}\right]\delta\left(i'y'\right)} + \left[\frac{\left(i'X'\right)\left(i'y'\right)\left(i'y'\right)}{i's'}\right]\delta\left(i'y'\right) + \left[\left(i'y'\right)^{2}\right]v'\right]}\delta\left(i'y'\right) + \left[\frac{i'B\left(i'K\right)}{\left(i's'\right)^{3}}\left[\left(\left(i'y'\right)^{2}-\left(i'x'\right)^{2}\right)\left(i'x'\right)-\left(i'x'\right)\left(i'y'\right)\right)\left(i'y'\right)\right]\delta\left(i'y'\right)}{\left(i's'\right)^{3}}\left[\left(i'y'\right)^{2}-i'C_{eqy}^{*}\left(i'y'\right)-i'C_{eqy}^{*}\left(i'x'\right)+i'C_{Dsy}^{*}V_{ffx}^{*}\right]\delta\left(i'y'\right) + \left[\frac{i'M_{i}\left(i'V_{i}\right)\left(i'x'\right)\left(i'y'\right)}{\left(i's'\right)^{3}}\left(i'x'\right)\right]\delta\left(i'y'\right) + \left[\frac{i'M_{i}\left(i'V_{i}\right)\left(i'Y_{i}\right)\left(i'x'\right)\left(i'y'\right)}{\left(i's'\right)^{3}}\left(i'y'\right)\right]\delta\left(i'y'\right) + \left[\frac{i'M_{i}\left(i'V_{i}\right)\left(i'Y_{i}\right)\left(i'y'\right)}{\left(i's'\right)^{3}}\left(i'y'\right)\right]\delta\left(i'y'\right) + \left[\frac{i'M_{i}\left(i'V_{i}\right)\left(i'Y_{i}\right)\left(i'Y_{i}\right)\left(i'y'\right)}{i's'}\left(i'y'\right)\right]\delta\left(i'y'\right) + \left[\frac{i'M_{i}\left(i'V_{i}\right)\left(i'Y_{i$$

Note that the following relations are used in the derivation of equations (3.20 a,b):

$$-{}^{2}B({}^{2}\kappa)^{2}\left(\frac{{}^{2}x'}{{}^{2}s'}\right) - \frac{{}^{2}B({}^{2}\kappa)({}^{2}s'')}{({}^{2}s')^{2}}\left(\frac{{}^{2}y'}{{}^{2}s'}\right)$$

$$= -\frac{{}^{2}B({}^{2}\kappa)}{({}^{2}s')^{4}}\left[\left(2({}^{2}x')({}^{2}y')\right)({}^{2}x'') + \left(({}^{2}y')^{2} - ({}^{2}x')^{2}\right)({}^{2}y'')\right] \qquad (3.21 \text{ a})$$

$$-{}^{2}B({}^{2}\kappa)^{2}\left(\frac{{}^{2}y'}{{}^{2}s'}\right) + \frac{{}^{2}B({}^{2}\kappa)({}^{2}s'')}{({}^{2}s')^{2}}\left(\frac{{}^{2}x'}{{}^{2}s'}\right)$$

$$= \frac{{}^{2}B({}^{2}\kappa)}{({}^{2}s')^{4}}\left[\left(({}^{2}y')^{2} - ({}^{2}x')^{2}\right)({}^{2}x'') - \left(2({}^{2}x')({}^{2}y')\right)({}^{2}y'')\right] \qquad (3.21 \text{ b})$$

$$\int \left[{}^{4}s'({}^{4}m_{i})({}^{2}V_{i})^{2}\frac{({}^{2}\kappa)({}^{2}y')}{{}^{2}s'}}\right]\delta({}^{2}u)d\alpha$$

$$= \left[\frac{{}^{4}s'}{{}^{2}s'}{}^{4}m_{i}({}^{2}V_{i})^{2}\delta({}^{2}u)\frac{{}^{2}x'}{{}^{2}s'}\right]\delta({}^{2}u)d\alpha$$

$$= \left[\frac{{}^{4}s'}{{}^{2}s'}{}^{4}m_{i}({}^{2}V_{i})^{2}\left(-\frac{({}^{2}\kappa)({}^{2}x')}{{}^{2}s'}\right)\right]\delta({}^{2}v)d\alpha$$

$$= \left[\frac{{}^{4}s'}{{}^{2}s'}{}^{4}m_{i}({}^{2}V_{i})^{2}\delta({}^{2}v)\frac{{}^{2}y'}{{}^{2}s'}\right]_{a_{a_{i}}}^{a_{i}} - \frac{a_{i}}{a_{s}}\left[\left(\frac{{}^{4}s'}{{}^{2}s'}{}^{4}m_{i}({}^{2}V_{i})^{2}\delta({}^{2}v)\right)\frac{{}^{2}\frac{y'}{{}^{2}s'}}\right]d\alpha \qquad (3.21 \text{ d})$$

$${}^{2}s' = \frac{({}^{2}x')({}^{2}u') + ({}^{2}y')({}^{2}v')}{{}^{2}s'}}, \qquad (3.21 \text{ e})$$

$${}^{2}\kappa = \frac{({}^{2}x'')({}^{2}y') - ({}^{2}x')({}^{2}y')}{({}^{2}s')^{3}}. \qquad (3.21 \text{ f})$$

When the time-independent terms in equations (3.17a-c) are eliminated, the equations of the vibrations with infinitesimal amplitudes can be obtained as

$$\left\{ \frac{\frac{i}{B}}{\left(\frac{i}{s'}\right)^{2}} \left[\left(\frac{i}{y'}\right)^{2} u'' - \left(\left(\frac{i}{x'}\right)\left(\frac{i}{y'}\right)\right) v'' \right] \delta u'' \right. \\
+ \left[\frac{\left(\frac{i}{N_{a}} - i m_{i} \left(\frac{i}{V_{i}}\right)^{2}\right) \left(u'\right)}{i's'} \right] \delta u' \\
+ E \left(\frac{i}{A_{p}}\right) \left[\frac{\left(\frac{i}{x'}\right)^{2} u' + \left(\left(\frac{i}{x'}\right)\left(\frac{i}{y'}\right)\right) v'}{\left(\frac{i}{s'}\right)^{3}} \right] \delta u' \\
- \frac{\frac{i}{B} \left(\frac{i}{K}\right)}{\left(\frac{i}{s'}\right)^{4}} \left[\left(2\left(\frac{i}{x'}\right)\left(\frac{i}{y'}\right)\right) \left(u''\right) + \left(\left(\frac{i}{y'}\right)^{2} - \left(\frac{i}{x'}\right)^{2}\right) \left(v''\right) \right] \delta u' \\
- \frac{i}{s'} \left[-\frac{i}{C_{a}} \ddot{u} - i C_{eqx}^{*} \dot{u} - i C_{eqxy}^{*} \dot{v} + i C_{Dx}^{*} \left(2V_{c}V_{w} + V_{w}^{2}\right) + i C_{M}^{*} \dot{V}_{w} \right] \delta u \\
+ \frac{i}{s'} \left[\left(\frac{i}{m_{p}} + i m_{i}\right) \ddot{u} + i m_{i} \left(\frac{i}{V_{i}}\right) \left(\frac{2}{is'} - \frac{\left(\frac{i}{x'}\right)^{2}}{\left(\frac{i}{s'}\right)^{3}}\right) \dot{u}' \right] \delta u \\
+ \frac{i}{s'} \left[\left(\frac{i}{m_{i}} \left(\frac{i}{V_{i}}\right) \left(\frac{i}{V_{i}}\right)\right] u' + \frac{i}{i} m_{i} \left(\frac{i}{x'}\right) \frac{DV_{id}}{Dt} \right] \delta u \\
+ \left[\frac{i}{m_{i}} \left(\frac{i}{V_{i}}\right)^{2} u' \right] \delta u \right]^{a_{i}} = 0, \tag{3.22 a}$$

$$\frac{\frac{i}{B}}{\left(\frac{i}{S'}\right)^{2}} \left[-\left(\left(\frac{i}{X'}\right)\left(\frac{i}{Y'}\right)\right)u'' + \left(\frac{i}{X'}\right)^{2}v'' \right] \delta v'' \\
+ \left[\frac{\left(\frac{i}{N_{a}} - im_{i}\left(\frac{i}{V_{i}}\right)^{2}\right)v'}{i_{S'}} \right] \delta v' \\
+ E\left(\frac{i}{A_{p}}\right) \left[\frac{\left(\left(\frac{i}{X'}\right)\left(\frac{i}{Y'}\right)\right)u' + \left(\left(\frac{i}{Y'}\right)^{2}\right)v'}{\left(\frac{i}{S'}\right)^{3}} \right] \delta v' \\
- \frac{\frac{i}{B}\left(\frac{i}{K}\right)}{\left(\frac{i}{S'}\right)^{4}} \left[\left(\left(\frac{i}{Y'}\right)^{2} - \left(\frac{i}{X'}\right)^{2}\right)u'' - \left(2\left(\frac{i}{X'}\right)\left(\frac{i}{Y'}\right)\right)v'' \right] \delta v' \\
- \frac{i}{S'} \left[-iC_{a}^{*}\ddot{v} - iC_{eqy}^{*}\dot{v} - iC_{eqy}^{*}\dot{u} + iC_{Dsyl}^{*}\left(2V_{c}V_{w} + V_{w}^{2}\right)\right] \delta v \\
+ \frac{i}{S'} \left[\left(\frac{i}{m_{p}} + im_{i}\right)\ddot{v} - im_{i}\left(\frac{i}{V_{i}}\right)\left(\frac{i}{S'}\right)^{3}\right) \dot{v}' \\
+ \frac{i}{m_{i}}\left(\frac{i}{V_{i}}\right)\left(\frac{2}{i_{S'}} - \frac{\left(\frac{i}{Y'}\right)^{2}}{\left(\frac{i}{S'}\right)^{3}}\right) \dot{v}' \\
+ \frac{i}{S'} \left[\left(\frac{i}{m_{i}}\left(\frac{i}{V_{i}}\right)\left(\frac{i}{V_{i}}\right)\right) v' + \frac{i}{i_{S'}}\frac{DV_{ud}}{Dt} \right] \delta v \\
+ \left[\frac{i}{m_{i}}\left(\frac{i}{V_{i}}\right)^{2}v'}{i_{S'}} \delta v \right]^{a_{i}} = 0, \tag{3.22 b}$$

Along with the boundary conditions at $^{1}y = 0$:

$$u(0,t) = v(0,t) = 0$$
 (essential), (3.23 a)

$$u''(0,t) = v''(0,t) = 0$$
 (natural), (3.23 b)

and at
$${}^{1}y = {}^{o}y_{t}$$
: $u({}^{o}y_{t}, t) = v({}^{o}y_{t}, t) = 0$ (essential), (3.24 a)

$$u''({}^{\circ}y_{i},t) = v''({}^{\circ}y_{i},t) = 0$$
 (natural), (3.24 b)

and
$$N_a = N_{aH}$$
 (essential), (3.24 c)

and the initial conditions at time t = 0:

$$u(^{T}y,\theta) = {^{T}u}, \ v(^{T}y,\theta) = {^{T}v},$$
 (3.25 a,b)

$$\dot{u}(^{1}y,0) = 0, \ \dot{v}(^{1}y,0) = 0,$$
 (3.25 c,d)

the system of partial differential equations (3.22 a-b) is the initial-boundary-value problem, which can be transformed to the system of ordinary differential equations by performing the following three steps of the finite element method.

Step 1. By separation of variables, the displacement vector is assumed as

$$\{\boldsymbol{d}\} = \{\boldsymbol{u} \quad \boldsymbol{v}\}^T = \left[\boldsymbol{N}(^T\boldsymbol{y})\right] \{\boldsymbol{d}_n(t)\}, \tag{3.26}$$

where the generalized coordinates of the nodal displacements of an element are

$$\{\boldsymbol{d}_{n}\} = \{u_{1} \quad u_{1}' \quad u_{1}'' \quad v_{1} \quad v_{1}' \quad v_{1}'' \mid u_{2} \quad u_{2}' \quad u_{2}'' \quad v_{2} \quad v_{2}' \quad v_{2}''\}^{T}, \tag{3.27}$$

and the shape function matrix at the displaced state is

$$[\mathbf{N}] = \begin{bmatrix} N_{51} & N_{52} & N_{53} & 0 & 0 & 0 & | N_{54} & N_{55} & N_{56} & 0 & 0 & 0 \\ 0 & 0 & 0 & N_{51} & N_{52} & N_{53} & | 0 & 0 & 0 & N_{54} & N_{55} & N_{56} \end{bmatrix} . (3.28)$$

Note that N_{5i} is the coefficients of the fifth order polynomial shape function.

Step 2. Substituting equation (3.26) into equations (3.22 a,b), the element equations can be obtained as

$$[\mathbf{m}^{(e)}]\{\ddot{\mathbf{d}}_n\} + ([\mathbf{c}^{(e)}] + [\mathbf{g}^{(e)}])\{\dot{\mathbf{d}}_n\} + [\mathbf{k}^{(e)}]\{\mathbf{d}_n\} = \{\mathbf{f}^{(e)}\},$$
(3.29)

where the element mass matrix is

$$\left[\mathbf{m}^{(e)}\right] = \int_{\alpha} \left\{ \left[\mathbf{N}\right]^{T} \binom{1}{s'} \binom{1}{m_{P}} + \binom{1}{m_{i}} + \binom{1}{c} C_{ao}^{*} \right\} \left[\begin{pmatrix} 1 & 0 \\ 0 & 1 \end{pmatrix} \right] \left[\mathbf{N}\right] \right\} d\alpha, \qquad (3.30 a)$$

the element hydrodynamic damping matrix is

$$\begin{bmatrix} \mathbf{c}^{(e)} \end{bmatrix} = \int_{\alpha} \left\{ [\mathbf{N}]^T \binom{1}{s'} \begin{bmatrix} {}^{I}C_{eqx}^* & {}^{I}C_{eqxy}^* \\ {}^{I}C_{eqxy}^* & {}^{I}C_{eqy}^* \end{bmatrix} [\mathbf{N}] \right\} d\alpha , \qquad (3.30 b)$$

the element gyroscopic matrix is

$$\begin{bmatrix} \mathbf{g}^{(e)} \end{bmatrix} = \int_{\alpha} \left\{ \begin{bmatrix} \mathbf{N} \end{bmatrix}^{T} m_{i} \binom{t}{V} \right\}_{i} \begin{bmatrix} 2 - \frac{\binom{t}{x'}}{\binom{t}{s'}^{2}} & -\frac{\binom{t}{x'}}{\binom{t}{s'}^{2}} \\ -\frac{\binom{t}{x'}}{\binom{t}{s'}^{2}} & 2 - \frac{\binom{t}{y'}}{\binom{t}{s'}^{2}} \end{bmatrix} \begin{bmatrix} \mathbf{N}' \end{bmatrix} \right\} d\alpha, \quad (3.30 \text{ c})$$

the element stiffness matrix is

$$\begin{bmatrix} \mathbf{k}^{(e)} \end{bmatrix} = \begin{bmatrix} \mathbf{k}_{b1}^{(e)} \end{bmatrix} + \begin{bmatrix} \mathbf{k}_{b2}^{(e)} \end{bmatrix} + \begin{bmatrix} \mathbf{k}_{N1}^{(e)} \end{bmatrix} + \begin{bmatrix} \mathbf{k}_{N2}^{(e)} \end{bmatrix}, \tag{3.30 d}$$

in which the bending stiffness matrix of the fourth order derivative is

$$\begin{bmatrix} \mathbf{k}_{bl}^{(e)} \end{bmatrix} = \int_{\alpha} \left\{ \begin{bmatrix} \mathbf{N}'' \end{bmatrix}^T \frac{{}^{t}B}{\left({}^{t}s'\right)^5} \begin{bmatrix} {}^{t}y' \end{pmatrix}^2 - {}^{t}x' \left({}^{t}y'\right) \\ -{}^{t}x' \left({}^{t}y'\right) & {}^{t}x' \right)^2 \end{bmatrix} \begin{bmatrix} \mathbf{N}'' \end{bmatrix} \right\} d\alpha , \qquad (3.30 e)$$

the bending stiffness matrix of the third order derivative is

$$\left[\mathbf{k}_{b2}^{(e)}\right] = \int_{\alpha} \left\{ \left[\mathbf{N}'\right]^{T} \frac{{}^{\prime}B({}^{\prime}\kappa)}{\left({}^{\prime}s'\right)^{4}} \left[\frac{2({}^{\prime}x')({}^{\prime}y')}{\left({}^{\prime}y'\right)^{2} - \left({}^{\prime}x'\right)^{2}} - 2({}^{\prime}x')({}^{\prime}y')} \right] \left[\mathbf{N}''\right] \right\} d\alpha, \qquad (3.30 f)$$

the axial stiffness matrix of the second order derivative is

$$\begin{bmatrix} \mathbf{k}_{NI}^{(e)} \end{bmatrix} = \int_{\alpha}^{\infty} \begin{bmatrix} \mathbf{N}' \end{bmatrix}^{T} \begin{pmatrix} \frac{{}^{\prime}N_{a}}{{}^{\prime}s'} \begin{bmatrix} 1 & 0 \\ 0 & 1 \end{bmatrix} - \frac{{}^{\prime}m_{i} ({}^{\prime}V)^{2}}{{}^{\prime}s'} \begin{bmatrix} 1 & 0 \\ 0 & 1 \end{bmatrix} \mathbf{N}' \end{bmatrix} d\alpha , \qquad (3.30 g)$$

$$+ \begin{bmatrix} \mathbf{N}' \end{bmatrix}^{T} \frac{E({}^{\prime}A_{P})}{({}^{\prime}s')^{3}} \begin{bmatrix} ({}^{\prime}x')^{2} & ({}^{\prime}x')({}^{\prime}y') \\ ({}^{\prime}x')({}^{\prime}y') & ({}^{\prime}y')^{2} \end{bmatrix} \mathbf{N}' \end{bmatrix}$$

the axial stiffness matrix of the first order derivative is

$$[\mathbf{k}_{N2}^{(e)}] = \int_{\alpha} \left\{ [\mathbf{N}]^T \left(\frac{{}^{I}m_i \left({}^{I}V_i \right) \left({}^{I}V_i' \right)}{\left({}^{I}s' \right)^2} \begin{bmatrix} 1 & 0 \\ 0 & 1 \end{bmatrix} \right) [\mathbf{N}'] \right\} d\alpha ,$$
 (3.30 h)

the element hydrodynamic excitation vector is

$$\{\mathbf{f}^{(e)}\} = \int_{\alpha} [\mathbf{N}]^{T} {\binom{1}{s'}} \begin{cases} {}^{I}C_{Dx}^{*}(2V_{c}V_{w} + V_{w}^{2}) + {}^{I}C_{M}^{*}\dot{V}_{w} - \frac{{}^{I}m_{i}({}^{I}x')}{{}^{I}s'} \frac{DV_{id}}{Dt} \\ {}^{I}C_{DxyI}^{*}(2V_{c}V_{w} + V_{w}^{2}) - \frac{{}^{I}m_{i}({}^{I}y')}{{}^{I}s'} \frac{DV_{id}}{Dt} \end{cases} d\alpha .$$
 (3.30 i)

Step 3. Assembling the element equations, the global system of finite element equations can be obtained as

$$[\mathbf{M}]\{\ddot{\mathbf{D}}_{n}\} + ([\mathbf{C}] + [\mathbf{G}])\{\dot{\mathbf{D}}_{n}\} + [\mathbf{K}]\{\mathbf{D}_{n}\} = \{\mathbf{F}\}, \tag{3.31}$$

where $\{\mathbf{D}_n\}, \{\dot{\mathbf{D}}_n\}, \{\mathbf{D}_n\}$ are the global nodal displacement, velocity, and acceleration vectors, respectively. In equation (3.31), the total mass matrix is

$$[\mathbf{M}] = \sum_{i=1}^{nelem} [\mathbf{m}^{(e)}], \qquad (3.32 a)$$

the total hydrodynamic damping matrix is

$$[\mathbf{C}] = \sum_{i=1}^{nelem} [\mathbf{c}^{(e)}], \tag{3.32 b}$$

the total gyroscopic matrix is

$$[\mathbf{G}] = \sum_{i=1}^{nelem} [\mathbf{g}^{(e)}], \qquad (3.32 c)$$

the total stiffness matrix is

$$[\mathbf{K}] = \sum_{i=1}^{nelem} [\mathbf{k}^{(e)}], \qquad (3.32 \text{ d})$$

the total hydrodynamic excitation vector is

$$[\mathbf{F}] = \sum_{i=1}^{nelem} [\mathbf{f}^{(e)}], \qquad (3.32 e)$$

and the global nodal displacement vector is

$$[\mathbf{D}_n] = \sum_{i=1}^{nelem} [\mathbf{d}_n], \tag{3.32 f}$$

in which *nelem* is the number of finite elements.

It is noteworthy that although the assumption of the vibrations with infinitesimal amplitude is adopted, equation (3.31) is still nonlinear. This is because of the nonlinear effects of the hydrodynamic damping and the gyroscopic forces appearing in the damping and the gyroscopic matrices.

To obtain the state space formulation, which is central to the development of nonlinear vibration control theory, the second order model of equation (3.31) must be transformed to the first order model. To achieve this, the following state vector is defined:

$$\{\mathbf{X}_n\} = \begin{cases} \mathbf{D}_n \\ \mathbf{V}_n \end{cases},\tag{3.33}$$

where

$$\{\mathbf{V}_n\} = \{\dot{\mathbf{D}}_n\}. \tag{3.34}$$

Substituting equation (3.34) into (3.31), one obtains

$$[\mathbf{M}]\{\dot{\mathbf{V}}_{n}\} + ([\mathbf{C}] + [\mathbf{G}])\{\mathbf{V}_{n}\} + [\mathbf{K}]\{\mathbf{D}_{n}\} = \{\mathbf{F}\}, \tag{3.35}$$

The system of equations (3.34) and (3.35) can be cast into the matrix form

$$\begin{bmatrix} \mathbf{I} & \mathbf{0} \\ \mathbf{0} & \mathbf{M} \end{bmatrix} \begin{bmatrix} \dot{\mathbf{D}}_n \\ \dot{\mathbf{V}}_n \end{bmatrix} + \begin{bmatrix} \mathbf{0} & -\mathbf{I} \\ \mathbf{K} & \mathbf{C} + \mathbf{G} \end{bmatrix} \begin{bmatrix} \mathbf{D}_n \\ \mathbf{V}_n \end{bmatrix} = \begin{bmatrix} \mathbf{0} \\ \mathbf{F} \end{bmatrix}. \tag{3.36}$$

Equation (3.36) can be manipulated in state space form

$$\{\dot{\mathbf{X}}_n\} = [\mathbf{A}]\{\mathbf{X}_n\} + \{\mathbf{B}\},$$
 (3.37)

where the coefficient matrix or state transition matrix is

$$[\mathbf{A}] = \begin{bmatrix} \mathbf{0} & \mathbf{I} \\ -\mathbf{M}^{-1}\mathbf{K} & -\mathbf{M}^{-1}(\mathbf{C} + \mathbf{G}) \end{bmatrix}, \tag{3.38 a}$$

and the deterministic input matrix is

$$\{\mathbf{B}\} = \begin{Bmatrix} \mathbf{0} \\ \mathbf{M}^{-1}\mathbf{F} \end{Bmatrix}. \tag{3.38 b}$$

The state equation (3.37) is used for the natural frequency analysis in section 3.3, and for the time history analysis in section 3.4.

3.3 NATURAL FREQUENCY ANALYSIS

For free vibrations, equation (3.37) is reduced to

$$\{\dot{\mathbf{X}}_n\} = [\mathbf{A}]\{\mathbf{X}_n\},\tag{3.39}$$

where

$$[\mathbf{A}] = \begin{bmatrix} \mathbf{0} & \mathbf{I} \\ -\mathbf{M}^{-1}\mathbf{K} & -\mathbf{M}^{-1}\mathbf{G} \end{bmatrix}. \tag{3.40}$$

Equation (3.39) has the harmonic solution in the exponential form

$$\{\mathbf{X}_n\} = e^{\lambda t} \{\mathbf{X}_{na}\},\tag{3.41}$$

where $\lambda = \alpha \pm i\omega$ is the complex eigenvalues, ω the natural frequency, and $\{X_{na}\}$ the vector of complex coefficients or initial modal weights.

Inserting equation (3.41) into (3.39) and dividing through by e^{λ} , the general algebraic eigenvalue problem is obtained as

$$[\mathbf{A}]\{\mathbf{X}_n\} = \lambda\{\mathbf{X}_n\},\tag{3.42}$$

in which the matrix [A] is the real, nonsymmetrical matrix. The Fortran-90 codes for implementing the eigenvalue problem of equation (3.42) has been developed based on the QR-algorithm (Press et al., 1992). The steps to the solution used in the codes are as follows:

- Step 1 Compute the element matrices, in which the procedures are as follows:
- Step 1.1 Form the element shape function matrix of equation (3.28).
- Step 1.2 Determine the element mass matrix of equation (3.30 a).
- Step 1.3 Determine the element gyroscopic matrix of equation (3.30 c).
- Step 1.4 Determine the element stiffness matrix of equation (3.30 d).
- Step 2 Assemble the element matrices to obtain the structural matrices of equations (3.32 a,c,d).
- Step 3 Impose the boundary conditions of equations (3.23) and (3.24) by utilizing the index matrix that identifies the dynamic degrees of freedom.
- Step 4 Form the coefficient matrix of equation (3.40).
- Step 5 Solve the eigenvalue problem of equation (3.42). This study uses the implicit double-shifted QR algorithm based on the EISPACK routine

HQR2 (Smith et al., 1976) to compute the eigenvalues and the eigenvectors.

Step 6 Save the numerical results of the eigenvalues and the eigenvectors in the result file.

3.4 NONLINEAR VIBRATION ANALYSIS

From equation (3.30 i), it is seen that the excitations inducing the nonlinear forced vibrations of the marine riser originate from the unsteady flow of ocean wave with velocity V_w and the unsteady flow of transported fluid with velocity V_{id} . In chapter 2, the expression of the ocean wave velocity V_w has been determined by using Airy's wave theory, as shown in section 2.6.1. However, the expression of V_{id} has not yet been mentioned. This is because the unsteady internal flow depends upon many factors such as: the variation of fluid density along the riser length; the unsteadiness of pump rate; the change of cross section of the riser due to the axial deformation as described in section 2.3. Consequently, the accurate expression of V_{id} closed to the real circumstances, is considerably more complicated and difficult to resolve by any theory. For simplicity, this study represents the unsteady internal flow velocity V_{id} as

$$V_{id} = V_{it}t + V_{ia}\cos\omega_i t , \qquad (3.43)$$

where V_{ii} is the linear velocity amplitude of internal flow, V_{ia} the wave velocity amplitude of internal flow, and ω_i the forcing frequency of internal flow.

From section 3.2, the initial-boundary-value problem of nonlinear vibrations with infinitesimal amplitudes of the marine riser is reduced to the initial-value problem of the state equation (3.37) in association with the initial conditions (3.25) by using the finite element method. This initial-value problem is highly nonlinear owing to the effects of nonlinear hydrodynamic damping. For implementing such an initial-value problem to be solved by numerical integration, the Fortran-90 computer code has been developed following the steps as shown below.

- Step 1 Compute the element matrices, in which the procedures are as steps 1.1 to 1.5:
- Step 1.1 Form the element shape function matrix of equation (3.28).
- Step 1.2 Determine the element mass matrix of equation (3.30 a).
- Step 1.3 Determine the element gyroscopic matrix of equation (3.30 c).
- Step 1.4 Determine the element stiffness matrix of equation (3.30 d).
- Step 1.5 Determine the element hydrodynamic damping matrix of equation (3.30 b) and the element hydrodynamic excitation vector of equation (3.30 i).
- Step 2 Assemble the element matrices to obtain the structural matrices of equations (3.32 a-e).
- Step 3 Impose the boundary conditions of equations (3.23) and (3.24) by utilizing the index matrix that identifies the dynamic degrees of freedom.
- Step 4 Form the coefficient matrix of equation (3.38 a) and the deterministic input matrix of equation (3.38 b).
- Step 5 Integrate the initial-value problem of equation (3.37) in association with the initial conditions (3.25) by the numerical integration. In this study, the Gear's stiff method using the backward differentiation formulas up to order five based on the subroutine DIFSUB (Bathe, 1996) are applied. The numerical values of the first derivatives of the state vector or the left-hand side of equation (3.37) are computed.
- Step 6 Save the numerical results of the dynamic degrees of freedom of the state vector in the result file.

4. RESULTS AND DISCUSSIONS

In this chapter, validation of the numerical results obtained from the solution procedures proposed in chapter 3 is demonstrated in section 4.1. The important results of the three-dimensional static analysis are concluded in section 4.2. The parametric studies are designated in section 4.3. Based on the numerical results of the parametric studies, the effects of axial deformation, and fluid transportation on behaviors of the pipes are explained further in sections 4.4, and 4.5, respectively.

4.1 VALIDATION OF NUMERICAL RESULTS

The accuracy of the solution can be verified in two ways: first, using the direct methods, and second, using the indirect approaches. The direct methods deal with monitoring and controlling the occurring numerical errors, while the indirect ones involve cross-checking with the solutions of the test cases reported in literature.

4.1.1 The Direct Methods

In nonlinear static analysis for which the equilibrium equation is $[{}^{I}\mathbf{K}]\{{}^{I}\mathbf{D}\} = \{{}^{I}\mathbf{R}\}$, Bathe (1996) showed that there are two kinds of errors to be controlled, namely the load error

$$\{\Delta^{T} \mathbf{R}\} = \{^{T} \mathbf{R}\} - [^{T} \mathbf{K}] \{^{T} \overline{\mathbf{D}}\}, \tag{4.1}$$

and the solution error

$$\{{}^{I}\mathbf{D}\} - \{{}^{I}\mathbf{\overline{D}}\} = [{}^{I}\mathbf{K}]^{-I}\{\Delta^{I}\mathbf{R}\}, \qquad (4.2)$$

where $\{^{\prime}\overline{\mathbf{D}}\}$ and $\{^{\prime}\mathbf{D}\}$ are the calculated and the exact degrees of freedom. He also demonstrated that the load error is usually much less than the solution error. Consequently, although the load error seems to indicate an accurate solution, the solution error may still be large, especially if $[^{\prime}\mathbf{K}]^{-\prime}$ is very large. In this study, for convenience the load error is kept very much small $\{\Delta^{\prime}\mathbf{R}\} \rightarrow \{\mathbf{0}\}$ in order to approach the solution error to zero. To achieve this, the Frobenius matrix norm of the load error, which has the scalar value

$$\left\|\Delta^{1}\mathbf{R}\right\|_{F}^{2} = \sum_{i=1}^{numdfs} \Delta^{1}R_{i}^{2}, \qquad (4.3)$$

is minimized to less than 10⁻¹².

In the natural frequency analysis for which the standard equation is $[A]{X_n} = \lambda{X_n}$, the performance index, which was first developed by the EISPACK project at Argonne National Laboratory (Smith et al., 1976), is employed to measure the performance of the EISPACK routine HQR2. The performance index is defined by

$$PI = \max_{1 \le i \le N} \frac{\|AX_{ni} - \lambda_i X_{ni}\|_1}{10\varepsilon \|A\|_1 \|X_{ni}\|_1},$$
(4.4)

where each pair of λ_i and X_{ni} is the eigenvalue and the corresponding eigenvector of the matrix [A] of order N, and ε the precision of arithmetic of the test machine. Note that the norm used in equation (4.4) is a modified form of the 1-norm, namely for the complex vector \mathbf{r} :

$$\left\|\mathbf{r}\right\|_{1} = \sum_{i=1}^{N} \left\{ \left| \operatorname{Re}(r_{i}) \right| + \left| \operatorname{Im}(r_{i}) \right| \right\}. \tag{4.5}$$

The performance of the EISPACK routine HQR2 in determining eigensolutions is excellent if PI < 1, good if $1 \le PI < 100$ and poor if $PI \ge 100$. In this study, all the performance indexes are found to be less than 10^{-3} , hence the excellent condition of the eigensolutions is definitely achieved.

In the nonlinear vibration analysis, the state space formulation is presented, thus the explicit time integration is preferred. However, the major drawback to the explicit methods is that they are conditionally stable, because the time step has a critical size. This shortcoming is overcome in this study by adopting the automatically adaptive time-step-size algorithm, which is included in the subroutine DIFSUB developed by Gear (1971). By using this algorithm, the time-step-size is automatically improved during the integration process so that the absolute error criterion:

$$\max_{i=1...N} (error_i) \le tol \tag{4.6}$$

is achieved. In this study, $tol = 10^{-3}$ is set forth, and the corresponding adaptive timestep-sizes are in the range 10^{-3} to 10^{-1} sec.

Table 4.1 Comparisons of In-Plane Natural Frequencies of Test Cases

	x_t									
	\overline{A} = Undeformed cross-sectional area E = Elastic modulus w_a suspended cable									
Case 1: the	Nondimension	nal l	Parameter $\frac{\overline{A}}{w_a}$	$\frac{E}{S}$	$\cong 5000, \frac{\sqrt{x_t^2}}{}$	+ . S	$\frac{\overline{y_t^2}}{} \cong 0.95, \Omega$			
Chord Inclination $oldsymbol{\phi}$	Mode No.				Interpolation (This Study*)				Quadratic Interpolation [105]	
7	(0)	4 Elements			0 Elements		0 Elements		Elements	
0°		$\rho_1(\Omega_1) = 0.62 (5.88)$		0.62 (5.87)		0.62 (5.87)		<u> </u>	60 (5.65)	
	$\omega_2(\Omega_2)$	0.92 (8.75)		0.92 (8.74)		0.92 (8.74)		0.92 (8.77)		
30°	$\omega_1(\Omega_1)$	(0.58 (6.00)		0.53 (5.43)		0.51 (5.29)		0.50 (5.17)	
	$\omega_2(\Omega_2)$	0	.98 (10.11)		0.85 (8.73)		0.81 (8.34)	0.	0.80 (8.17)	
60°	$\omega_1(\Omega_1)$ 0.3).30 (4.05)		0.27 (3.65)		0.26 (3.56)	0.	0.27 (3.65)	
	$\omega_2(\Omega_2)$).46 (6.19)			47 (6.30)		
Case 2: the	e Nondimension	nal l	Parameter $\frac{\overline{A}}{w_a}$	$\frac{E}{S}$	$\approx 2500, \frac{\sqrt{x_t^2}}{}$	+ . S	$\frac{\overline{y_t^2}}{2} \cong 0.98, \Omega$	$\Omega = 0$	$\omega \sqrt{\frac{S}{g}}$	
	~ ~	Fir	nite Element N	1eth	od		Initial-V			
Mode No.	Elements	8 Curve Elements (This Study*) 16 Straight-Figure Element [16]				05]	[107][Extrapolation Method		Continuous Method	
ω_1	0.793		0.809		0.795		0.80		0.811	
ω_2	1.148		1.185		1.155		1.16		1.175	
ω_3	1.620		1.680		1.627		1.63		1.653	
ω_4	1.984	2.090			1.998		1.99		2.027	

^{*} Including the effect of axial deformation

4.1.2 The Indirect Methods

The indirect methods involve comparisons of numerical results with the test cases. This study adopts the two test cases of the suspended cables reported in the papers by Henghold and Russell (1977), Gambhir, Barrington and Batchelor (1978), West, Geschwinder and Suhoski (1975) and West and Caramanico (1973). As shown in Table 4.1, the natural frequencies of the suspended cables calculated from the simplified version of this study are in good agreement with those obtained from other works. Therefore validity of the numerical results is confirmed.

Yet there are other informal checks that are carried out in this work. These include comparisons of the mode shapes of free vibrations of the marine pipes with the results reported by Pesce et al. (1999) and Chucheepsakul (1983); comparisons of the shapes of static equilibrium configurations and bending moment diagrams with the results of Bernitsas et al. (1985); checking the precision of the boundary conditions; checking that if subharmonic and superharmonic oscillations do not occur, the response frequencies should be closed to the hydrodynamic frequencies. The outcomes of these informal checks also manifest validity of the numerical results.

4.2 THREE-DIMENSIONAL STATIC ANALYSIS

This section presents the important results of three-dimensional static analysis of the deep-water risers. The properties of the riser used in the numerical applications are summarized in Table 4.2. The riser is subjected to a tidal current with an exponential velocity profile, Eq. (2.41), acting in the x-direction and a triangular profile in the z-direction as show in Figure 4.1. The velocity of the current at the surface is 0.75 m/s and 1.3 m/s, respectively. The displacement is computed in two different ways. First, the three-dimensional model described in the previous section is used to obtain the results. Second, the two-dimensional model is used to approximate the three-dimensional deformation by vectorial summation of the two-dimensional deformations in the x-y plane and z-y plane.

Table 4.2 Properties of the riser used in the three-dimensional nonlinear static analysis

Property	Value		
Undeformed external diameter of the riser	0.610 m		
Undeformed internal diameter of the riser	0.575 m		
Density of pipe	7850 kg/m^3		
Density of sea water	1025 kg/m^3		
Density of internal fluid	998.3 kg/m^3		
Elastic modulus	$2.07E+10^{11}$		
The ratio of the top tension to the effective weight (TTR)	1.1,1.5		
Sea depth (L)	2500 m		
In-plane offset	0 m		
Out-of-plane offset	0 m		
Normal hydrodynamic drag coefficient	0.7		
Tangential hydrodynamic drag coefficient	0.03		

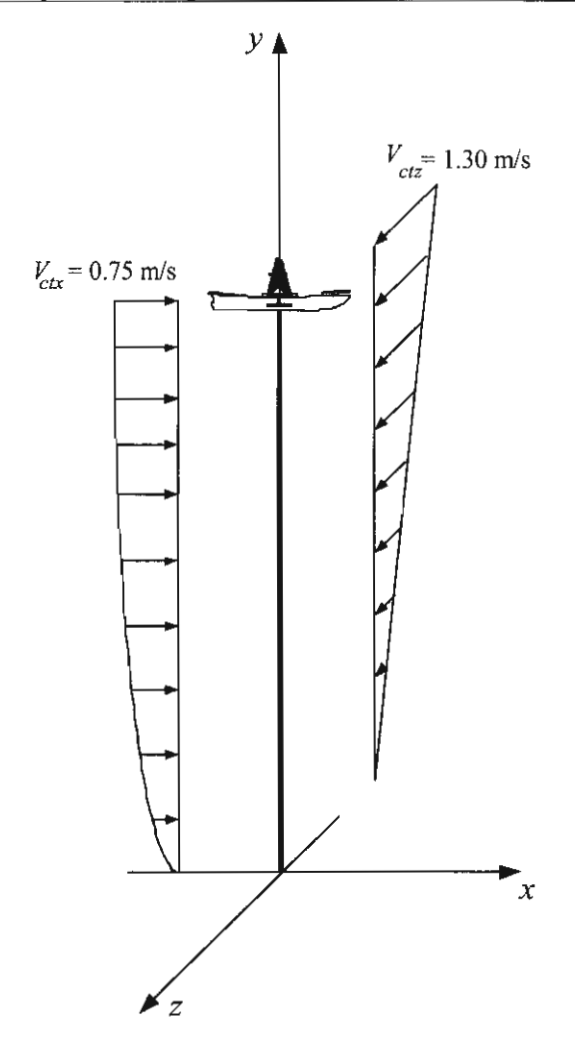


Figure 4.1 Deep-water riser subjected to the tidal and the triangular profile currents

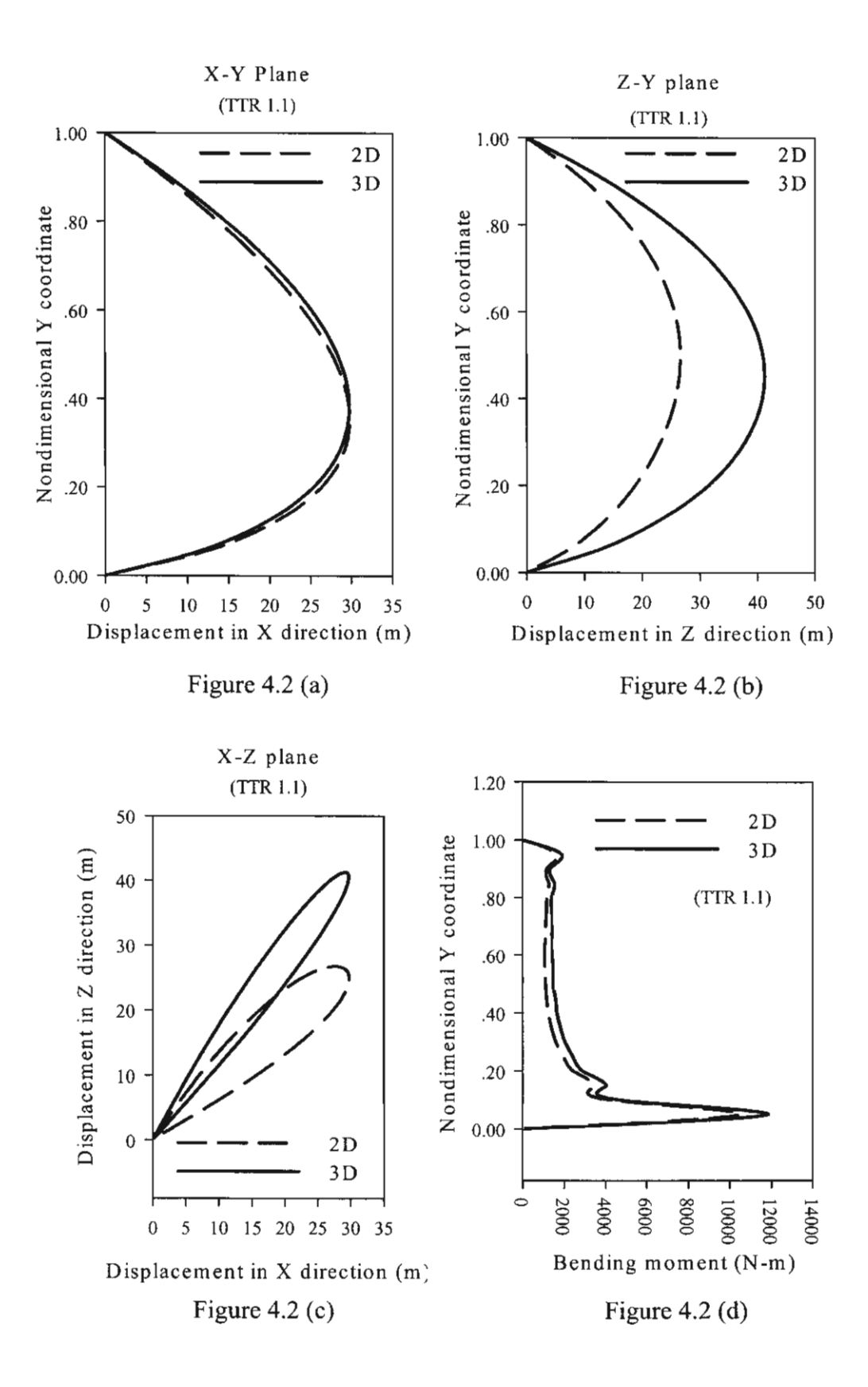


Figure 4.2 Static configurations and bending moment diagram of the deep-water riser subject to the tidal and the linear profile currents with TTR 1.1

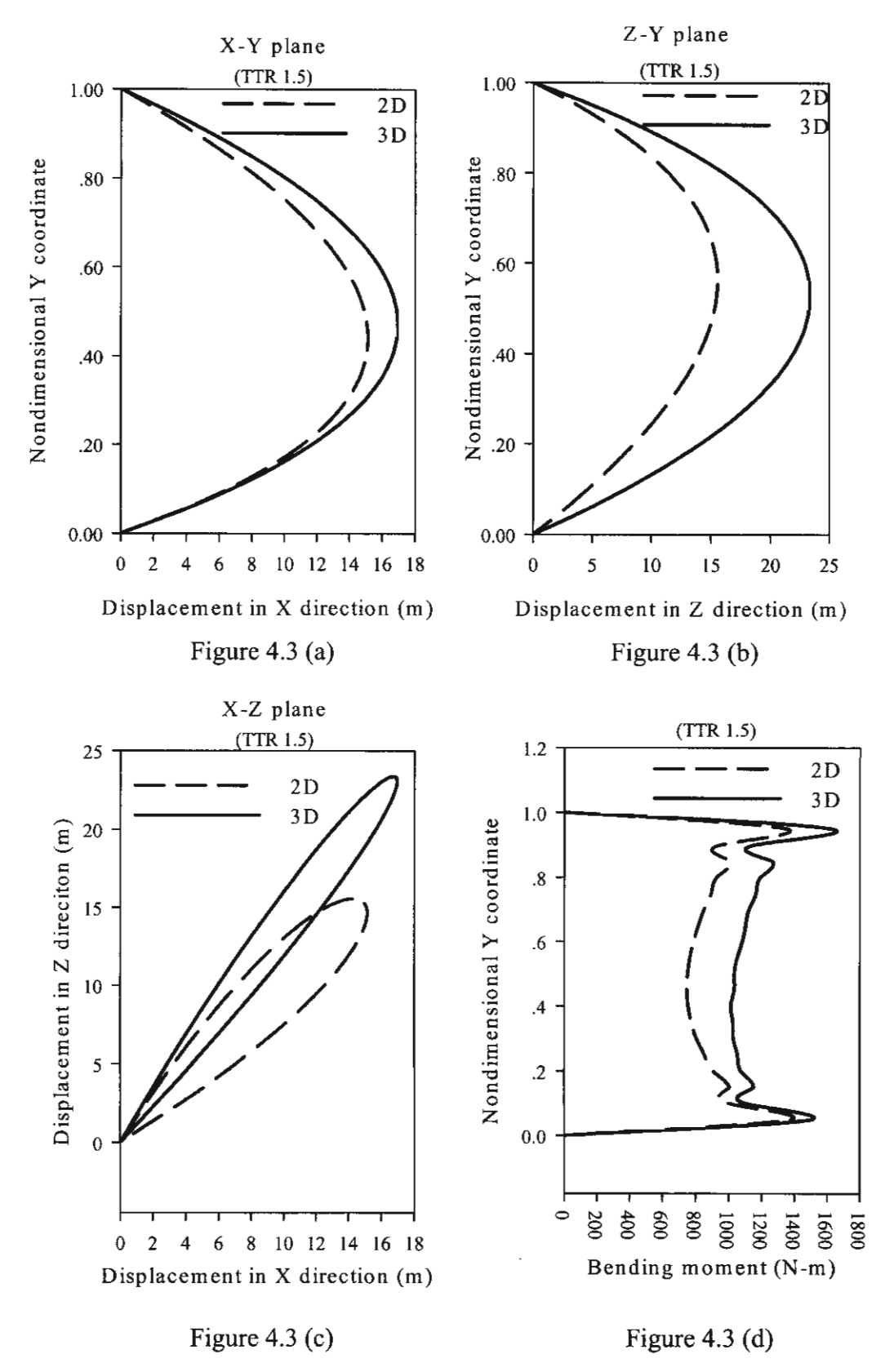


Figure 4.3 Static configurations and bending moment diagram of the deep-water riser subject to the tidal and the linear profile currents with TTR 1.5

Table 4.3 Displacement and bending moment comparison, between twodimensional and three-dimensional nonlinear analysis, of a riser subject to a tidal and a triangular current for TTR 1.1

TTR 1.1	Lateral in-plane displacement (m)		Lateral out-of-plane displacement (m)		Total Lateral Displacement $\sqrt{('x)' + ('z)'}$ (N-m)			Bending moment (N-m)		
Y/L	2-D	3-D	2-D	3-D	2-D	3-D	Diff	2-D	3-D	Diff
1.00	0.00	0.00	0.00	0.00	0.00	0.00	0.00	0.00	0.00	0.00
0.90	7.25	7.84	10.17	14.03	12.48	16.07	3.58	1173.91	1339.68	165.77
0.80	13.77	14.73	17.68	24.99	22.41	29.01	6.60	1176.02	1399.39	223.37
0.70	19.46	20.55	22.79	33.06	29.97	38.93	8.96	1113.45	1443.47	330.01
0.60	24.15	25.14	25.73	38.36	35.29	45.86	10.57	1077.77	1417.98	340.21
0.50	27.62	28.29	26.71	40.97	38.42	49.79	11.36	1104.93	1465.14	360.21
0.40	29.57	29.71	25.88	40.89	39.29	50.54	11.25	1247.05	1654.05	407.00
0.30	29.46	28.99	23.31	37.93	37.57	47.74	10.17	1606.53	2040.57	434.03
0.20	26.39	25.40	18.88	31.58	32.45	40.53	8.08	2424.71	2885.89	461.18
0.10	18.42	17.36	11.97	20.47	21.97	26.84	4.87	4265.35	4798.43	533.07
0.00	0.00	0.00	0.00	0.00	0.00	0.00	0.00	0.00	0.00	0.00

Table 4.4 Displacement and bending moment comparison, between twodimensional and three-dimensional nonlinear analysis, of a riser subject to a tidal and a triangular current for TTR 1.5

TTR 1.5	Lateral in-plane displacement (m)		Lateral out-of-plane displacement (m)		Total Lateral Displacement $\sqrt{('x)^2 + ('z)^2}$ (N-m)			Bending moment (N-m)		
Y/L	2-D	3-D	2-D	3-D	2-D	3-D	Diff	2-D	3-D	Diff
1.00	0.00	0.00	0.00	0.00	0.00	0.00	0.00	0.00	0.00	0.00
0.90	4.57	5.54	6.79	9.34	8.18	10.86	2.67	943.43	1146.53	203.09
0.80	8.43	10.09	11.47	16.13	14.23	19.02	4.79	924.88	1186.98	262.09
0.70	11.51	13.55	14.29	20.59	18.35	24.65	6.30	849.43	1120.26	270.83
0.60	13.71	15.86	15.50	22.92	20.69	27.87	7.18	786.38	1081.12	294.74
0.50	14.94	16.91	15.33	23.30	21.41	28.79	7.38	751.11	1032.66	281.54
0.40	15.04	16.63	14.00	21.90	20.55	27.50	6.95	754.36	1011.89	257.52
0.30	13.86	14.95	11.69	18.83	18.13	24.04	5.91	805.00	1027.03	222.03
0.20	11.15	11.73	8.56	14.15	14.06	18.38	4.32	904.88	1074.19	169.31
0.10	6.64	6.83	4.67	7.90	8.12	10.44	2.33	1001.06	1106.75	105.69
0.00	0.00	0.00	0.00	0.00	0.00	0.00	0.00	0.00	0.00	0.00

95

Figures 4.2 and 4.3 show the plot of the nonlinear static configurations and the bending moment diagram of the deep-water riser that are obtained from the approximate two-dimensional nonlinear analysis and three-dimensional nonlinear analysis for TTR = 1.1 and TTR = 1.5. The ratio of the top tension to the effective weight (TTR) is defined as

$$TTR = \frac{{}^{I}N_{t}}{{}^{o}w_{c}L} \tag{4.7}$$

Tables 4.3 and 4.4 show the numerical comparisons of the lateral displacement and bending moment between the two-dimensional and three-dimensional analyses of the deep-water risers for TTR = 1.1 and TTR = 1.5.

When the top tension is specified and the arc-length of the riser is varied with the magnitude of the large displacement. The lateral displacement and the bending moment computed by the three-dimensional model is higher than the displacement that computed by the two-dimensional model as shown in Figures 4.2 and 4.3. These results are due to the nature of nonlinearity in the model formulation. The linear combination or the superposition method of 2-D cases can not be applied to obtain the same results as those from the deep-water riser experiencing 3-D large displacement.

The increasing of the ratio of the top tension to the effective weight (TTR) reduces the lateral displacement and the bending moment as show in Tables 4.3 and 4.4. Moreover, the results in Tables 4.3 and Table 4.4 indicate that the difference of the lateral displacement and the bending moment between the two-dimensional and three-dimensional analysis are reduced when TTR is increased because the increasing top tension increases the axial deformation, thus reduce the effect of the large displacement. The discussion of the effect of the axial deformation and the effect of the internal flow velocity are discussed in the next section.

From the discussion above, it can be concluded that the coupling of the three-dimensional deformation affects on the large displacement and the bending moment when the in-plane and the out-of-plane loads occur in the same time. Therefore, the three-dimensional model formulation should be used in the general case.

4.3 PARAMETRIC STUDIES

The deep-water risers, which are the marine pipe under severe pressure environments, are employed as the specimen of the parametric studies. Their input parameters are given in Table 4.5. The details of the parametric studies are proposed in Table 4.6, where the applied top tension N_i , and the internal flow velocity ${}^{o}V_{i}$ are varied to demonstrate the effects of axial deformation, and fluid transportation on the behaviors of the marine pipes, respectively. The reasons for choosing the parameters N_i and ${}^{o}V_i$ for use in the parametric studies are that the axial strain $\varepsilon \propto N_i$ follows the constitutive relation; and the rate of fluid transportation may be represented by the internal flow velocity ${}^{o}V_i$.

Table 4.5 Input Parameters of the Deep-Water Riser Specimen

Parameter	Standard Value
Elastic modulus E (N/m²)	0.207x10 ¹²
External diameter of the pipe oD_e (m)	0.610
Internal diameter of the pipe oD_i (m)	0.575
Density of pipe material $ ho_p({ m kg/m^3})$	8337.9
Density of external fluid $ ho_e(ext{kg/m}^3)$	1025
Density of internal fluid $ ho_i$ (kg/m 3)	1438
Static in-plane offset ${}^{o}x_{i}$ (m) (see Fig.4.1)	100
Static out-of-plane offset $^{o}z_{i}$ (m) (see Fig.4.1)	0
$^{\circ}y_{i}$ (m) (see Fig.2.1a)	2000
Applied top tension N_i (N)	$0.7x10^{7}$
Normal drag coefficient C_{Dn}	2
Tangential drag coefficient C_{Dt}	0.1
Current velocity at mean sea level $V_{ct}\left(\mathrm{m/s}\right)$	0.2
Internal flow velocity ${}^{o}V_{i}$ (m/s)	20
Added mass coefficient C_a	1.5
Wave amplitude φ_a (m)	6
Wave frequency $\omega_{\rm w}$ (rad/sec)	0.6
Wave number k	0.03
Linear velocity amplitude of int. flow V_{it} (m/s)	0
Wave velocity amplitude of int. flow $V_{ia} (\text{m/s})$	0.2
Internal flow frequency ω_i (rad/sec)	0.05

Table 4.6 Parametric Studies

To Study the Effects of	The Values of Parameters in Table 4.2 are Reserve Constant Except Varying					
Axial deformation	$^{1}N_{t} = 10^{7}, 0.8 \times 10^{7}, 0.7 \times 10^{7}, 0.67 \times 10^{7}, 0.64 \times 10^{7}N$					
Fluid transportation	$^{o}V_{i} = 0, 5, 10, 15, 20 \text{ m/s}$					

4.4 EFFECTS OF AXIAL DEFORMATION ON BEHAVIORS OF THE MARINE PIPES

4.4.1 Effects of Axial Deformation on Nonlinear Static Behavior

From the parametric study of the axial deformation effects designated in section 4.3, the results are obtained as depicted in Figures 4.4-4.11. The effects of axial deformation on the nonlinear static behavior of the marine pipes are illustrated in Figures 4.4 and 4.5, and can be summarized as follows:

4.4.1.1 Axial deformation reduces the large deflections of the marine pipe. As seen in Figure 4.4, dropping the top tension, which induces a reduction of the axial deformation, increases the sag of the marine pipe. This result is not uncommon for a prestressed structure such as marine pipes. Diminishing degree of prestressing significantly reduces the axial stiffness of the prestressed structure. Consequently, the large deflections are raised.

4.4.1.2 Axial deformation affects behaviors of the marine pipe. The pipe subjected to the large axial deformation due to high pretension behaves as the taut pipe with low sag, whereas the low-tensioned pipe with low axial deformation behaves as the slack pipe with large sag. As shown in Figure 4.4, the pipe in the case where ${}^{1}N_{t} = 10^{7} N$ is taut, while the pipe subjected to ${}^{1}N_{t} = 6.4 \times 10^{6} N$ is largely slack, especially at the bottom portion ${}^{1}y = 0$ - 200 m. The vibration behaviors of the taut and the slack pipes are quite different, as will be discussed later.

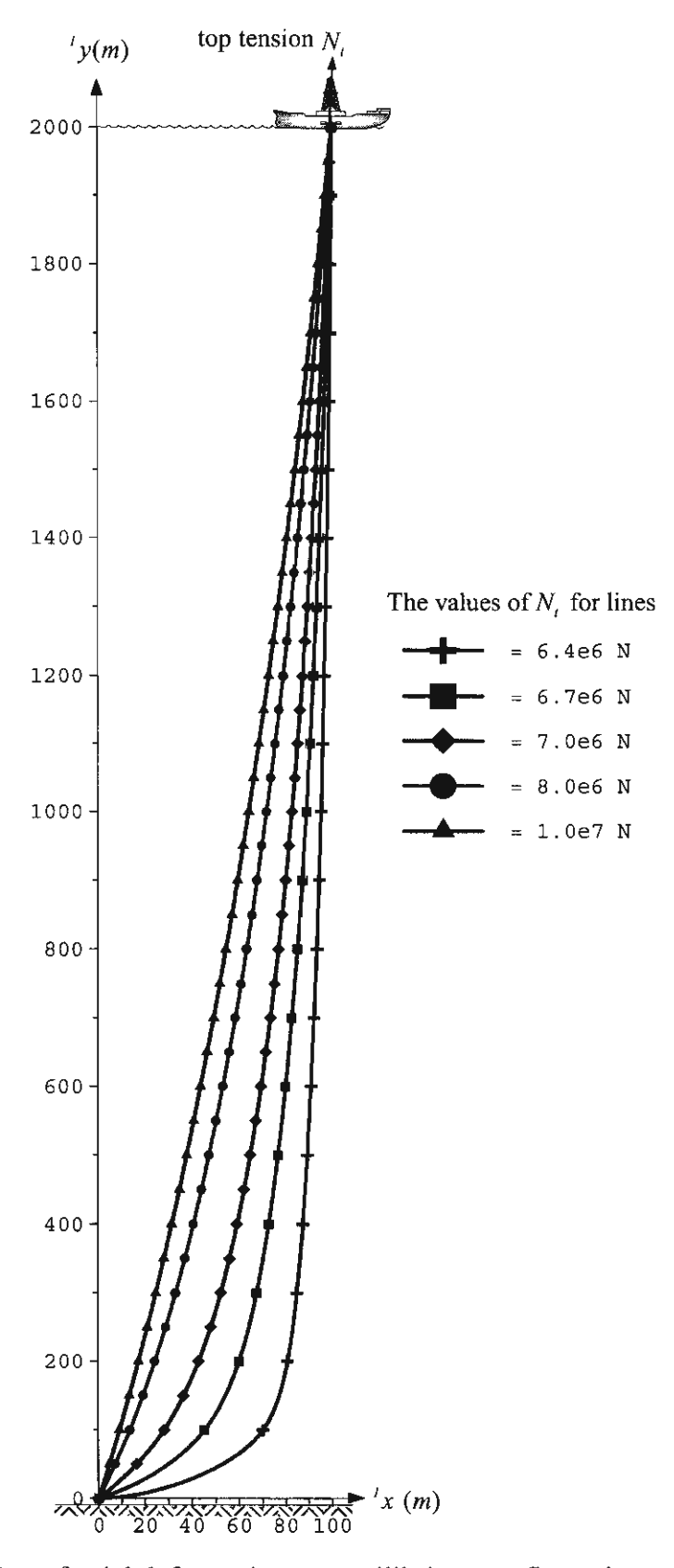


Figure 4.4 Effect of axial deformation on equilibrium configurations of the pipe

- 4.4.1.3 The allowable range of axial deformation indicates the design patterns of the marine pipe. In Figure 4.4, the effective design criterion belongs to the condition $0.7 \times 10^7 < {}^{1}N_{t} < 10^7 N$. The pipe is overdesigned if ${}^{1}N_{t} > 10^7 N$ is devised, and underdesigned if ${}^{1}N_{t} < 0.7 \times 10^7 N$ is adopted. Overdesign is uneconomical, while underdesign results in the divergence instability of the pipe.
- 4.4.1.4 Axial deformation reduces the rotations of the marine pipe particularly at the large sag region. As shown in Figure 4.5 (a), the pipe that is taut due to high axial deformation (${}^{I}N_{I} = 10^{7} N$), gains much less rotation of the bottom support than the pipe that is slack due to low axial deformation (${}^{I}N_{I} = 6.4 \times 10^{6} N$).
- 4.4.1.5 Axial deformation increases the axial strain in the marine pipe. Figure 4.5 (b) manifests this deduction. It is seen that the axial strains in the taut pipe with ${}^{1}N_{t} = 10^{7} N$ are all positive or tensile and higher than those of the slack pipe with ${}^{1}N_{t} = 6.4 \times 10^{6} N$. The axial strains of such a slack pipe are found to possess negative values at the bottom portion of the pipe.
- 4.4.1.6 Axial deformation augments the static stability of marine pipes. As previously found, with reductions of the top tension, the axial strain is reduced and can be negative at the bottom portion of the slack pipe. Following the constitutive equation, a negative axial strain signifies a negative apparent tension. The author found that when the top tension is decreased until ${}^{I}N_{I} < 6.4 \times 10^{6} N$ such a negative apparent tension will become large enough to embark the local buckling at the bottom portion of the pipe. It will be shown later that for ${}^{I}N_{I} < 6.4 \times 10^{6} N$ the natural frequency of the pipe converges to zero, and the pitchfork bifurcation thus occurs.
- 4.4.1.7 Axial deformation magnifies the true-wall and the apparent tensions in the marine pipe, as shown in Figure 4.5 (c). It should be note that for marine structures, the apparent tension is more important than the true-wall tension, because it is the total virtual tension appearing in marine structures.

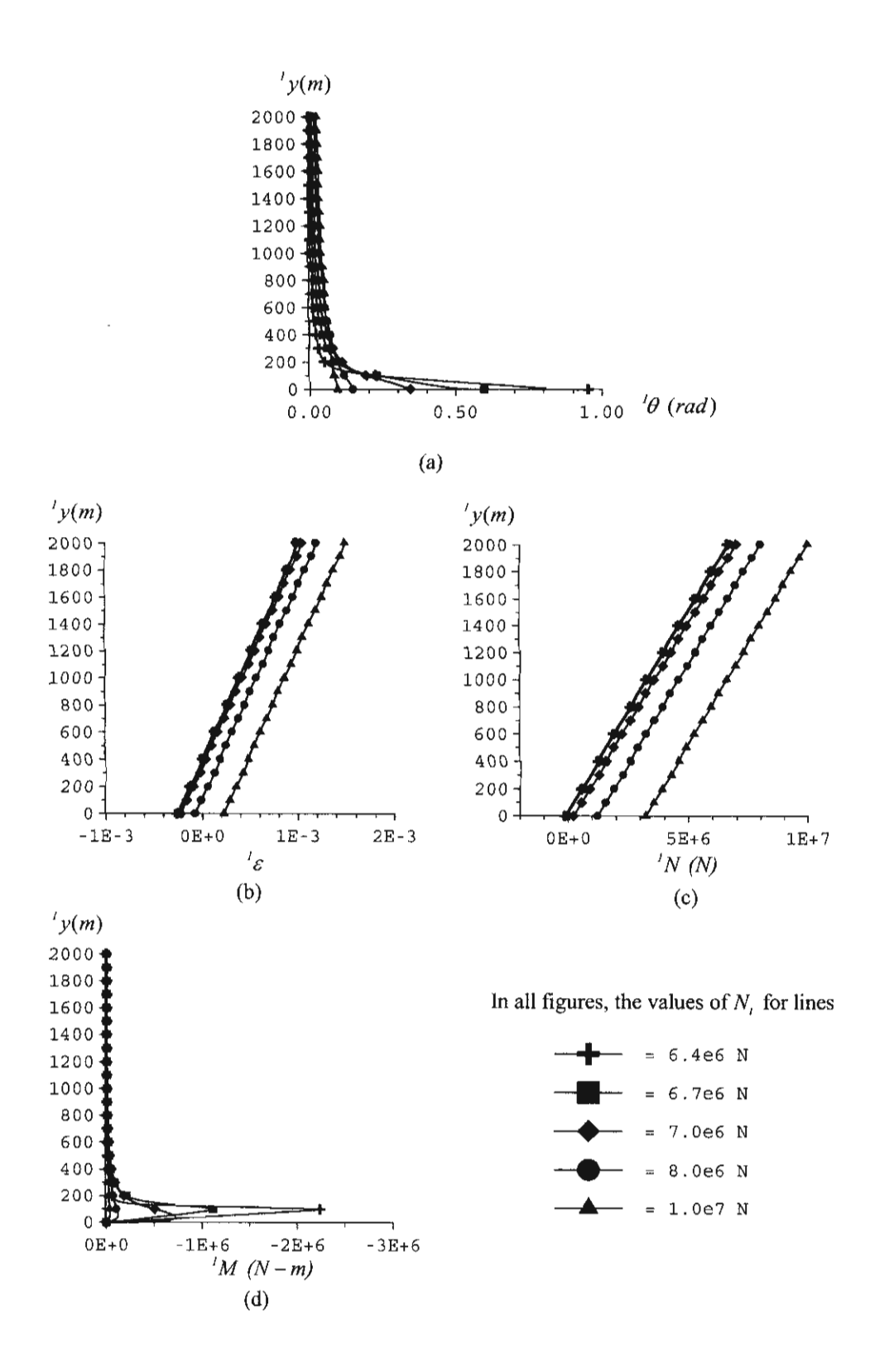


Figure 4.5 Effects of Axial Deformation on

(a) Rotations (b) Axial Strains

(c) True-Wall Axial Forces (d) Bending Moments

4.4.1.8 Axial deformation decreases the bending moments in the marine pipe especially at the large sag portion. This result is due to the effects of axial deformation on a reduction of the pipe's rotations as shown in Figure 4.5 (b). When the rotation θ decreases, the bending moment M will also diminish corresponding to the relationship

$$\kappa = \frac{1}{\Re} = \frac{d\theta}{ds} = \frac{M}{EI_P},\tag{4.8}$$

respectively. Figure 4.5 (d) asserts these results. It is found that the bending moment diagrams of the pipe that is taut due to high axial deformation (${}^{\prime}N_t = 10^{7} N$) are almost vertically straight, whereas those of the pipe that is slack due to low axial deformation (${}^{\prime}N_t = 6.4 \times 10^6 N$) have the curve parts magnificently growing at ${}^{\prime}y = 0$ - 200 m, where the slack pipe possesses large curvatures and large rotations. Therefore, in the design of the slack pipe, the bending stress and the shear stress should be carefully examined especially at the bottom part of the pipe. Sometimes the bending and shear stiffeners may be desired at that portion to eliminate the excessive conditions of large curvatures and bending moments, which may cause poor serviceability and localized damage to the pipe.

4.4.2 Effects of Axial Deformation on Natural Frequencies

The effects of axial deformation on the natural frequencies and the stability of the linearized system of the marine pipes are illustrated in Figures 4.6 - 4.8, and are summarized as follows:

4.4.2.1 Axial deformation raises the natural frequencies of the marine pipe. To display this effect, the eigencurves are plotted in the stiffness-frequency space as shown in Figure 4.6. It is revealed that the natural frequencies of the pipe are increased with an escalation of the top tension. The natural frequencies of the slack pipe with ${}^{\prime}N_{t} = 6.4 \times 10^{6} \, N$ are significantly lower than those of the taut pipe with ${}^{\prime}N_{t} = 10^{7} \, N$. As the top tension is reduced continuously, the eigencurves tend to intersect the top tension axis at the point, where the top tension possesses the critical values and the natural frequencies are zero. This implies that buckling of the pipe due to the effect of axial deformation is of static nature, and may be referred to as the divergence buckling.

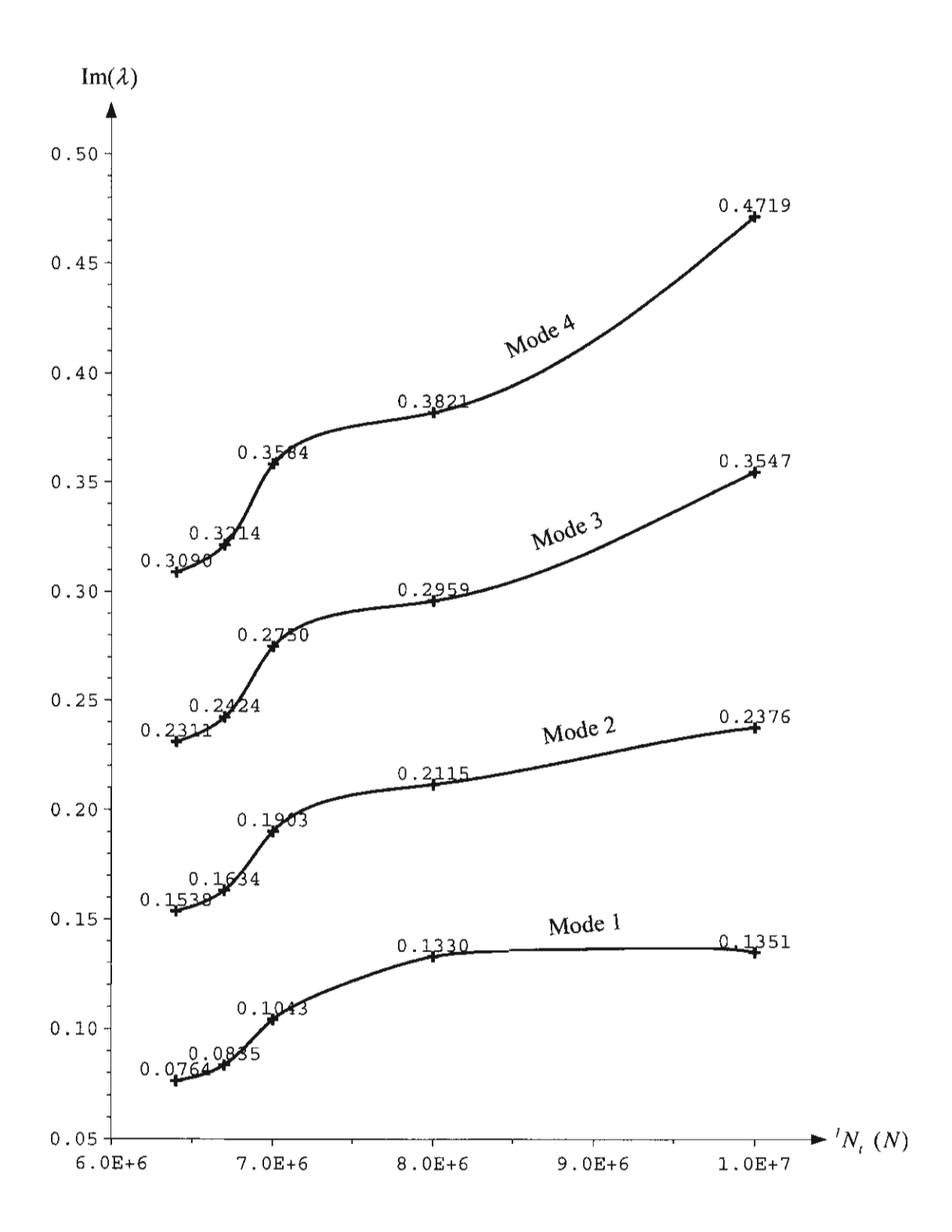


Figure 4.6 Effect of Axial Deformation on Natural Frequencies

4.4.2.2 Axial deformation boosts the dynamic stability of the linearized system of the marine pipe. To explain this effect, the complex plane of the Argand diagram is displayed in Figure 4.7. A continuous reduction of the axial deformation by incessantly diminishing the top tension motivates the pipe into experiencing 'static buckling' or 'divergence instability' at the Pitchfork bifurcation point, where the top tension has reached the critical value (Chucheepsakul and Monprapussorn, 2001). This behavior is explained as follows.

Before buckling, the complex eigenvalues λ have zero real part, no matter how much the top tension is varied. The constant reduction of the top tension yields a decrease in the natural frequencies of the pipe, which is imaginary part of the eigenvalues, along the vertical line $\text{Re}(\lambda) = 0$ to converge to zero. This type of the Argand diagram deals with the divergence instability via Pitchfork bifurcation. After buckling, pitchfork bifurcation would change the eigenvalues from wholly imaginary to become wholly real along the horizontal line $\text{Im}(\lambda) = 0$ as shown in Figure 4.7.

Based on the Liapunov indirect method, the stability of motion of the linearized system may be tested by examining the solutions of the linearized equations of motion with respect to the Liapunov stability definitions (Meirovitch, 1997). Such stability definitions can be interpreted into the complex eigenvalue analysis as follows.

For the complex eigenvalues $\lambda_j = \alpha_j + i\omega_j$, in which j = 1, 2, ..., 2 (numdfd), and numdfd is the dynamic degrees of freedom,

- (a) if $\forall \alpha_j = 0$, the system has stable motion, which is pure oscillation, and neither tends away nor moves to the equilibrium point as $t \to \infty$,
- (b) if $\forall \alpha_j < 0$, the system oscillates by asymptotically stable motion, which tends to the equilibrium point as $t \to \infty$,
- (c) if $\exists \alpha_j > 0$, the system exhibits unstable motion, which departs away from the equilibrium point as $t \to \infty$.

Note that the universal quantifier ' \forall ' means 'all of', and the existential quantifier ' \exists ' abbreviates 'some of'.

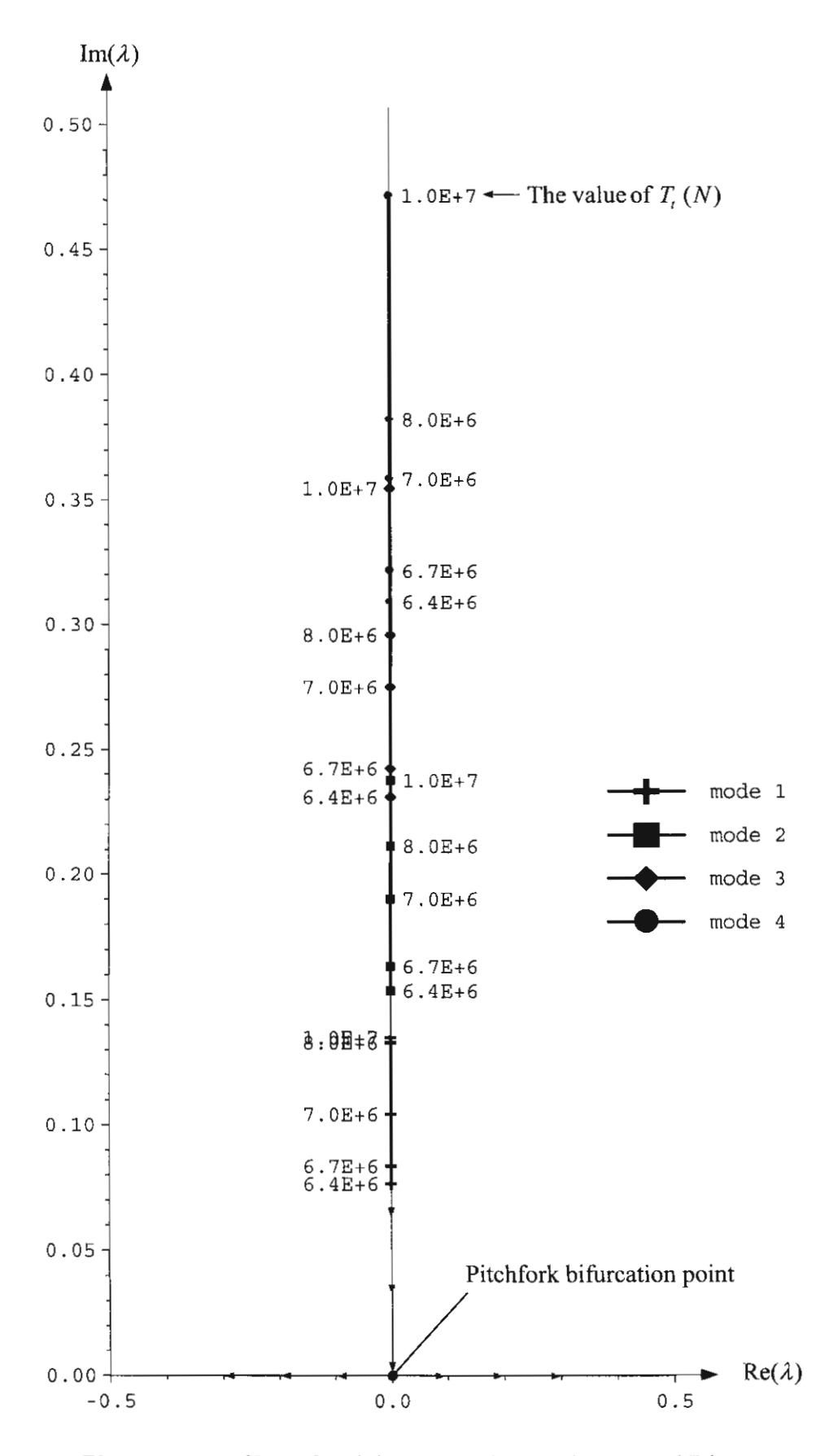


Figure 4.7 Effect of Axial Deformation on the Argand Diagrams

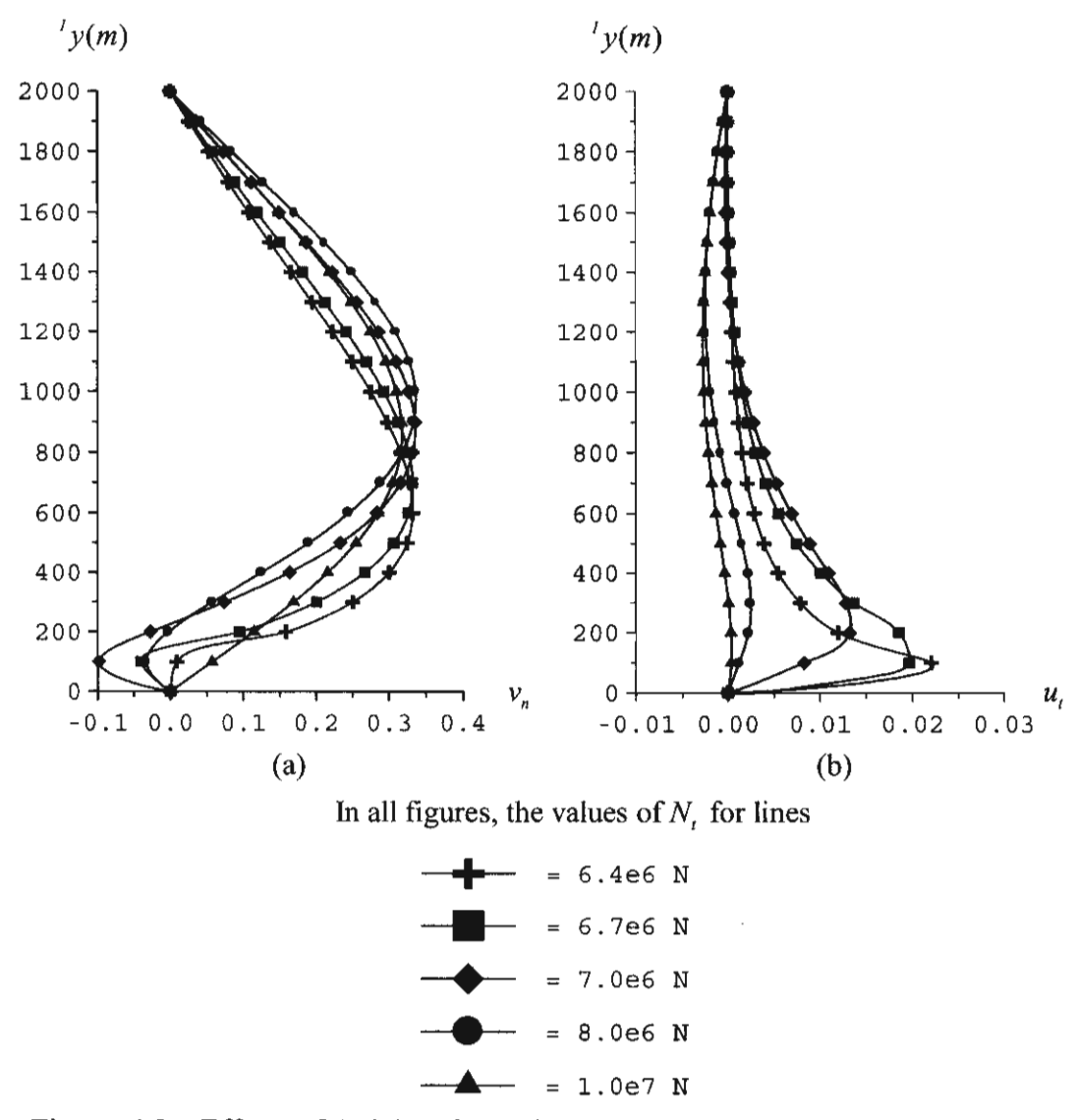


Figure 4.8 Effects of Axial Deformation on the Fundamental Mode Shapes of

(a) Normal Vibrations (b) Tangential Vibrations

The system is said to possess 'significant behavior' if its motion is either asymptotic stable or unstable, and is said to have 'critical behavior' if its motion is stable. The Russian mathematician and mechanician Liapunov (Meirovitch, 1997) indicated that if the linearized system exhibits significant behavior, the above stability criteria could be extended to the nonlinear system. However, if the linearized system displays critical behavior, then conclusions about the stability of the nonlinear system cannot be made accurately from the above stability criteria.

Adopting the stability criteria in the sense of Liapunov, the complex eigenvalues of the marine pipe as shown in Figure 4.7 agree with the condition (a), therefore free vibrations of the linearized system of the marine pipe possess stable oscillations and critical behavior. As a result, the stability of the linearized system cannot be guaranteed for the nonlinear system of the marine pipe. Instead, the stability of nonlinear vibrations of the marine pipe should be probed by the phase plane analysis based on the solutions of the nonlinear equations of motion, including the fully nonlinear hydrodynamic forces, as will be shown later.

4.4.2.3 Axial deformation affects the mode shapes of free vibrations of the marine pipe. Figures 4.8 (a), and 4.8 (b) demonstrate the effect on fundamental modes of free vibrations in the normal, and tangential directions, respectively. It is seen that the axial deformation has a significant effect on changing the mode shapes of normal and tangential free vibrations.

In Figure 4.8 (a), the fundamental mode shape of normal vibration of the pipe that is slack due to low axial deformation (${}^{1}N_{t} = 6.4 \times 10^{6} N$), has one more curvature than that of the pipe that is taut due to high axial deformation (${}^{1}N_{t} = 10^{7} N$) at the bottom portion (${}^{1}y = 0\text{-}200 \text{ m}$), where the pipe possesses a large sag. In Figure 4.8 (b), the slack pipe has maximum amplitudes of the tangential vibrations at the large sag portion of the pipe.

4.4.4 Effects of Axial Deformation on Nonlinear Vibration Behavior

The effects of axial deformation on the nonlinear forced vibrations of marine pipes are illustrated in Figures 4.9 - 4.11, and are summarized as follows:

4.4.4.1 Axial deformation decreases nonlinear responses of forced vibrations of the marine pipe. The nonlinear responses in a time period of 0-60 seconds of forced vibrations of the taut pipe with ${}^{I}N_{I} = 10^{7} N$ are plotted on the left-hand side of Figure 4.9, while those of the slack pipe with ${}^{I}N_{I} = 6.4 \times 10^{6} N$ are displayed on the right-hand side of the same figure. By comparing the left- and the right-hand side figures, it is evident that the slack pipe possesses much larger amplitudes of the normal, and tangential vibrations than the taut pipe.

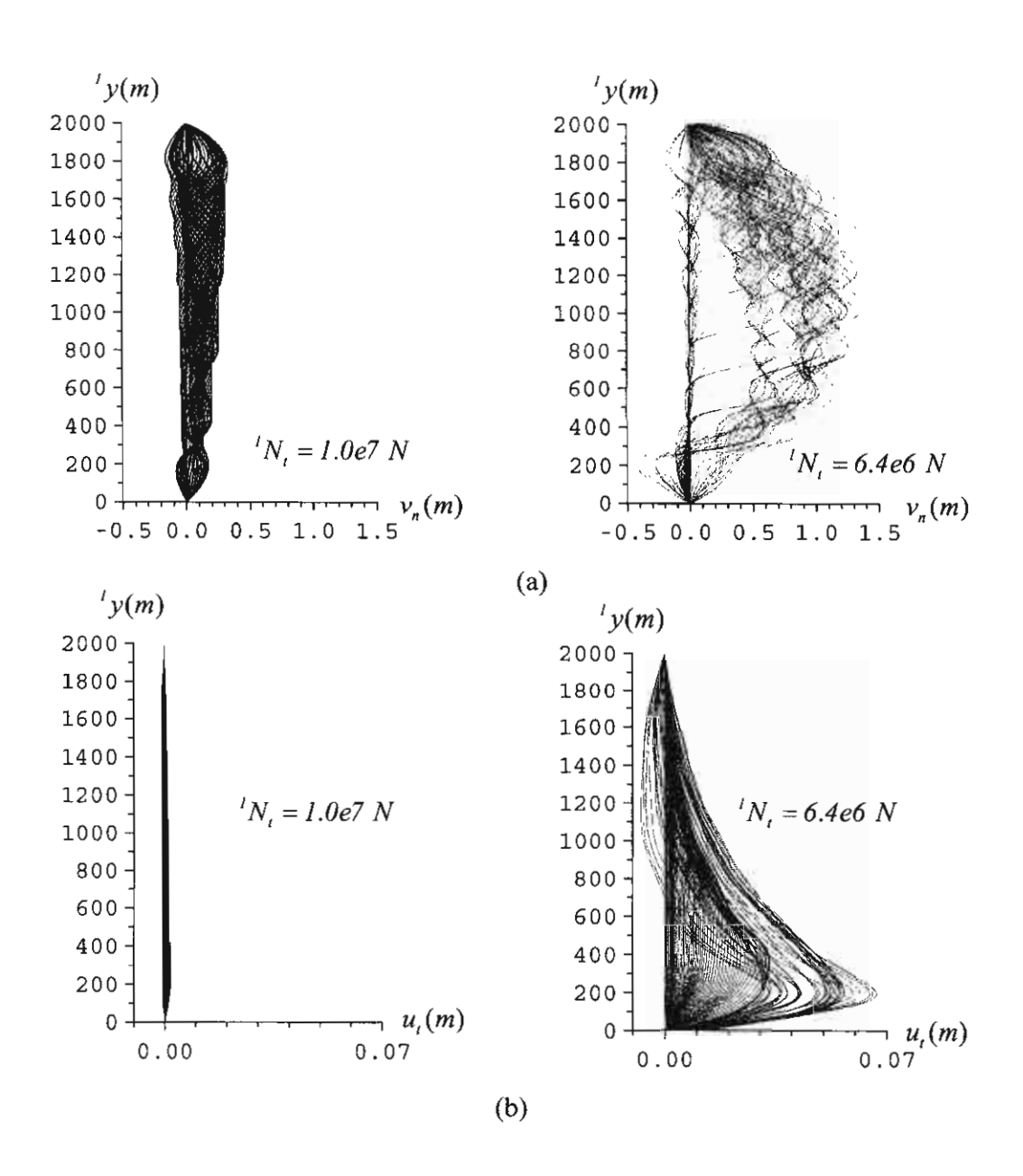


Figure 4.9 Nonlinear Responses in Time 0-60 Seconds of

(a) Normal Vibrations (b) Tangential Vibrations

4.4.4.2 Axial deformation affects the time histories of nonlinear vibrations of the marine pipe. Figures 4.10 (a), 4.10 (b) and 4.10 (c) demonstrate the time histories of the normal vibrations of the top part ($^{I}y = 1800$ m), of the middle part ($^{I}y = 1000$ m), and of the bottom part ($^{I}y = 400$ m) of the pipes, respectively. It is seen that the slack pipe possesses much larger amplitudes of the normal vibrations than the taut pipe.

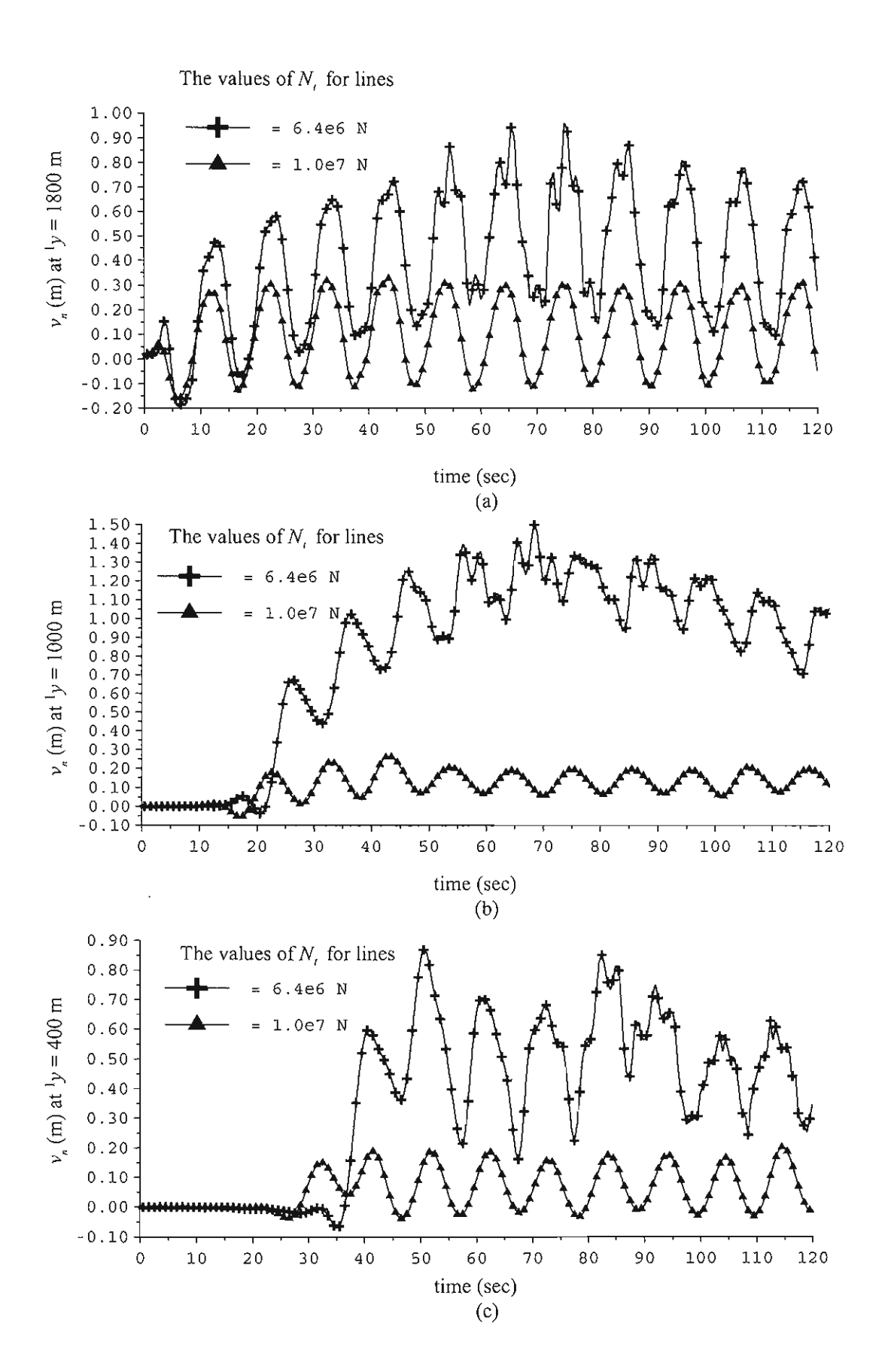


Figure 4.10 Effect of Axial Deformation on Time Histories of Normal Vibrations

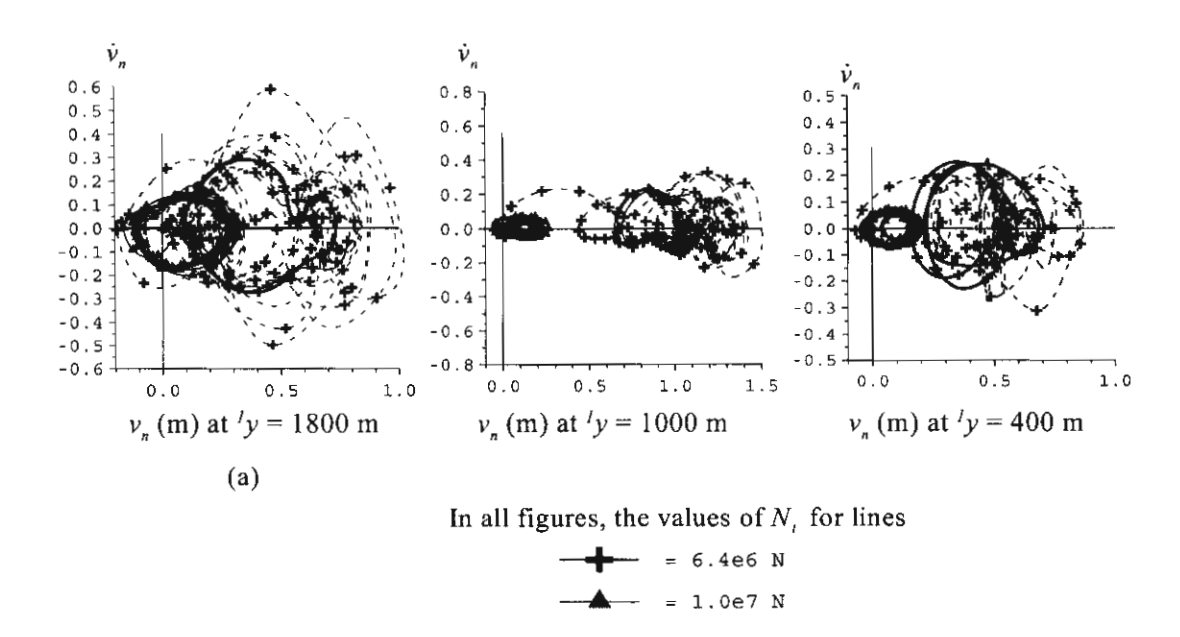


Figure 4.8 Effect of Axial Deformation on Trajectories of Normal Vibrations

Over a long-term period, the normal oscillations of all parts of the taut pipe are developed to steady motions, while all parts of the slack pipe exhibit unsteady normal vibrations. Unsteadiness of the normal vibrations of the slack pipe is remarkably great at the bottom part, where the slack pipe has a large curvature. It is noticed that the response frequencies of normal vibrations of all parts of the pipes $\approx 2\pi/10$ are close to the wave frequency 0.6. Therefore, the normal oscillations of the pipes are ordinary harmonic.

4.4.4.3 Axial deformation increases the stability of motion of the marine pipe. The trajectories of the normal vibrations of the top part ($^{I}y = 1800 \text{ m}$), of the middle part ($^{I}y = 1000 \text{ m}$) and of the bottom part ($^{I}y = 400 \text{ m}$) of the pipes are plotted in the phase planes as shown in Figures 4.11 (a), and 4.11 (b), respectively. The figures revealed that as a time period passes all trajectories, which start at the initial condition of the zero normal state speed and the zero normal displacement, tend to the closed curves (bold lines), which may be referred to as 'the limit cycle' (Meirovitch, 1997).

The stability of a limit cycle can be evaluated through the definitions of 'the orbital stability' or 'the stability in sense of Poincaré' (Meirovitch, 1997) as follows. Denoting the distance of a point \mathbf{x}_1 to a periodic orbit \mathbf{C} by

$$\operatorname{dist}(\mathbf{x}_{1}, \mathbf{C}) = \min\{\|\mathbf{x}_{1} - \mathbf{x}\|, \text{ for all } \mathbf{x} \in \mathbf{C}\}, \tag{4.9}$$

(a) if dist($\mathbf{x}(t_a)$, \mathbf{C}) < δ for $\delta > 0$ implicates an existence of any $\varepsilon > 0$ such that

$$\operatorname{dist}(\mathbf{x}(t), \mathbb{C}) < \varepsilon \text{ for all } t > t_{o},$$
 (4.10)

then the periodic orbit C is orbitally stable,

(b) if $\operatorname{dist}(\mathbf{x}(t_o), \mathbf{C}) < \delta$ for $\delta > 0$ implicates an existence of the condition

$$\operatorname{dist}(\mathbf{x}(t), \mathbf{C}) \to 0 \text{ as } t \to \infty,$$
 (4.11)

then the periodic orbit C is orbitally asymptotically stable,

(c) The periodic orbit C is orbitally unstable if it is not stable.

The physical meaning of the above definitions may be illuminated as follows. For a given closed trajectory \mathbb{C} , if every trajectory in the neighborhood of \mathbb{C} remains in the neighborhood of \mathbb{C} , the motion of the system is orbitally stable. If the trajectories approach \mathbb{C} as $t \to \infty$, the motion of the system is orbitally asymptotically stable. If the trajectories tend to leave the neighborhood of \mathbb{C} or approach \mathbb{C} as $t \to -\infty$, the motion of the system is orbitally unstable.

The concept of orbital stability can be extended to the nonclosed orbits of nonperiodic solutions as follows. For the two orbits C_1 and C_2 corresponding to the solutions x_1 and x_2 , which are close to each other at time t_o ,

- (a) if the orbits C_1 and C_2 remain close at all subsequent times $t > t_o$, the orbits C_1 and C_2 are orbitally stable,
- (b) if the orbits C_1 and C_2 converge to each other as $t \to \infty$, the orbits C_1 and C_2 are orbitally asymptotically stable,
- (c) if the orbits C_1 and C_2 tend away from each other or converge to each other as $t \to -\infty$, the orbits C_1 and C_2 are orbitally unstable.

Adopting the aforementioned concept of orbital stability, from Figures 4.11 (a), 4.11 (b) and 4.11 (c) it is found that the motions of all parts of the taut pipe are orbitally stable, because all the closed trajectories remain in the neighborhood of one another for all $t > t_o$, while those of the slack pipe are orbitally unstable on the grounds that the closed trajectories tend to leave the neighborhood of the others. This result indicates that the axial deformation augments the stability of motion of the pipe.

4.5 EFFECTS OF FLUID TRANSPORTATION ON BEHAVIORS OF THE MARINE PIPES

4.5.1 Effects of Fluid Transportation on Nonlinear Static Behavior

From the parametric study of the fluid transportation effects designated in section 4.3, the results are obtained as depicted in Figures 4.12 - 4.19. The effects of fluid transportation on the nonlinear static behavior of the marine pipes are illustrated in Figures 4.12 and 4.13, and are summarized as follows:

- 4.5.1.1 Fluid transportation increases large deflections of the marine pipe. As seen in Figure 4.12, when the transportation rate is raised by an increase of internal flow velocity, the sag of the marine pipe is enlarged.
- 4.5.1.2 Fluid transportation enlarges the rotations of the marine pipe, particularly in the large sag portion of the pipe. As shown in Figure 4.13(a), the pipe without fluid transportation has a lesser rotation of the bottom support than the pipe with internal flow velocity 20 m/s.
- 4.5.1.3 Fluid transportation has an insignificant effect on reducing axial strain in the marine pipe as shown in Figure 4.13(b), and thus slightly decreases the static stability of the pipe.
- 4.5.1.4 Fluid transportation has an insignificant effect on reducing the true-wall and the apparent tensions in the marine pipe as shown in Figure 4.18(d).
- 4.5.1.5 Fluid transportation amplifies bending moments in the marine pipe, especially at the large sag portion. Figure 4.13(c) illustrates this result. It is found that the bending moments of the pipe without fluid transportation are less than those of the pipe with a transportation rate of 20 m/s, especially at the bottom part of the pipe, where the pipe possesses large curvatures and large rotations.

4.5.2 Effects of Fluid Transportation on Natural Frequencies

The effects of fluid transportation on natural frequencies and the dynamic stability of the linearized system of the marine pipes are illustrated in Figures 4.14 - 4.16, and are summarized as follows:

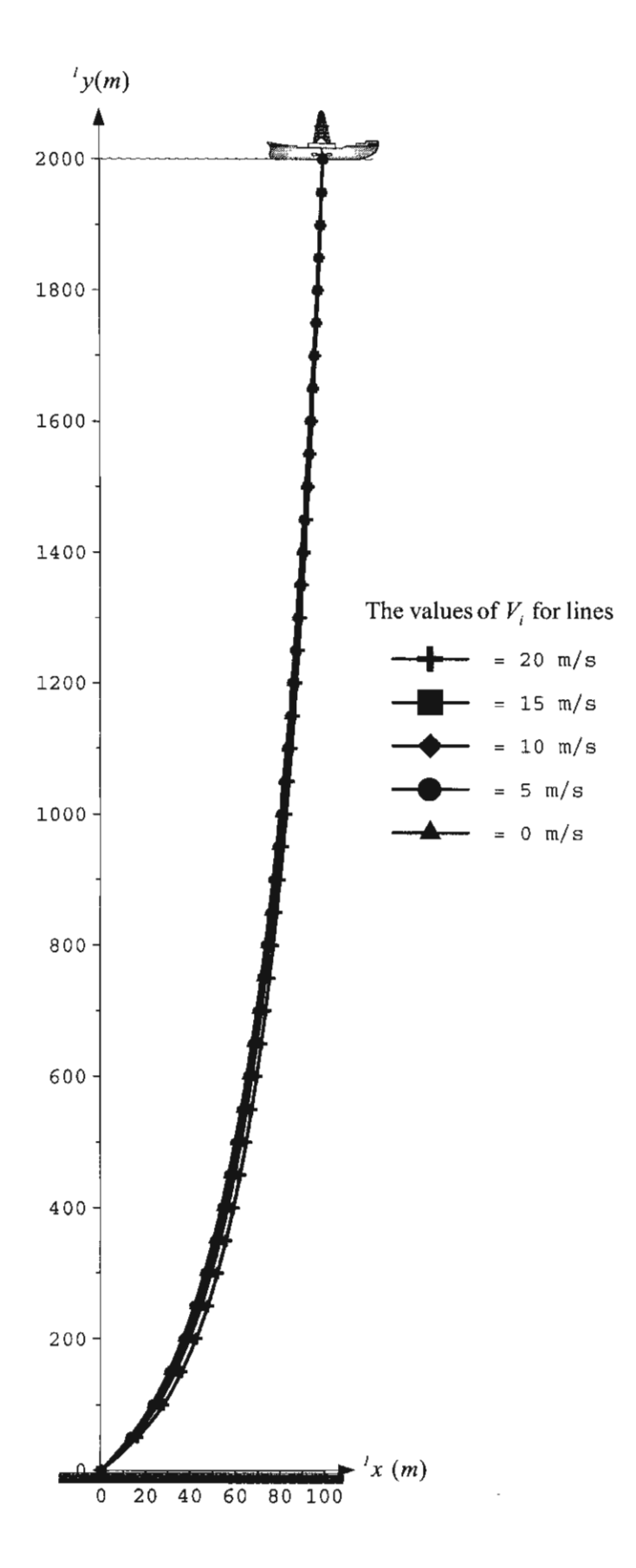


Figure 4.12 Effect of Fluid Transportation on Equilibrium Configurations of the Pipe

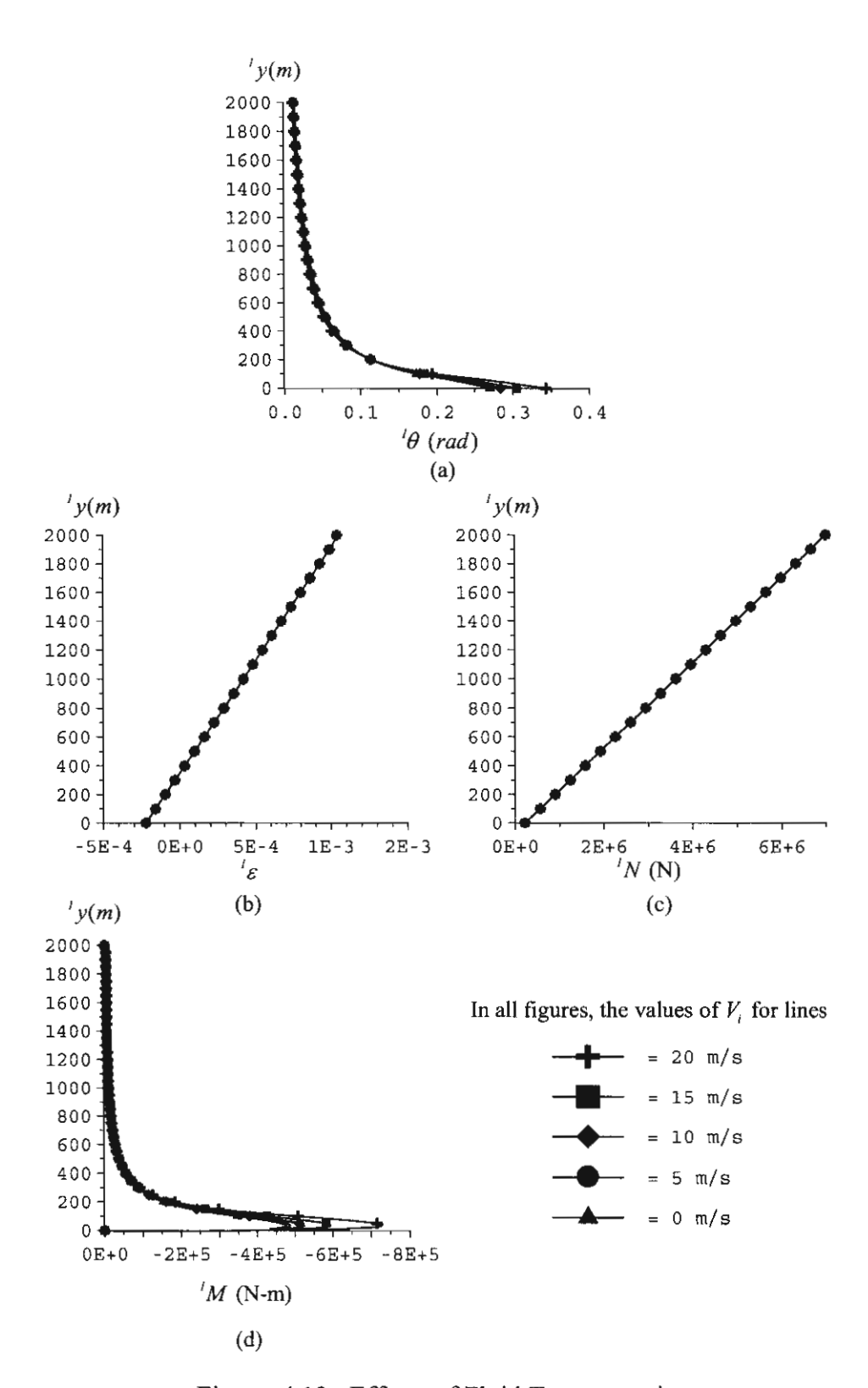


Figure 4.13 Effects of Fluid Transportation on

- (a) Rotations (b) Axial Strains
- (c) True-Wall Axial Forces (d) Bending Moments

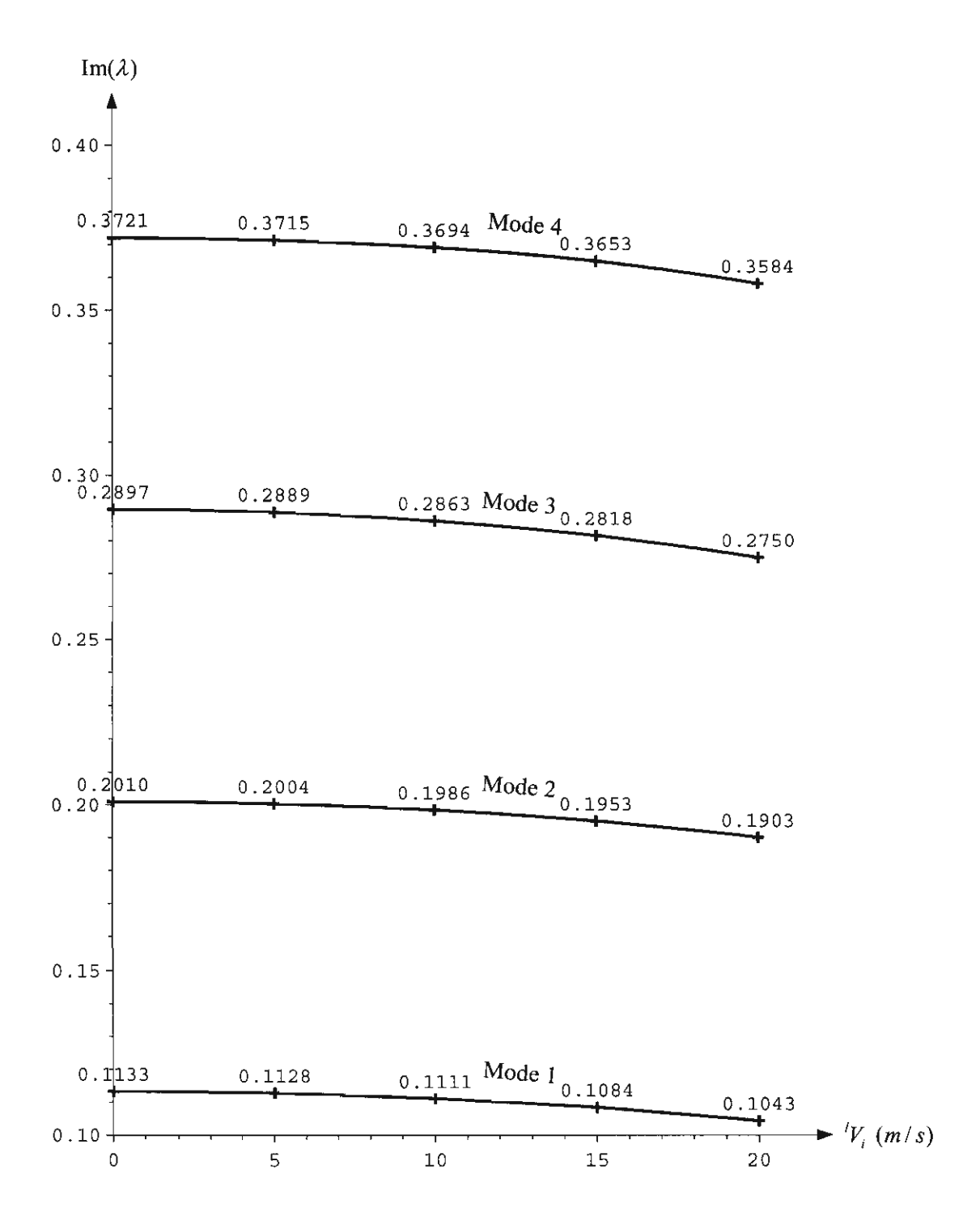


Figure 4.14 Effect of Fluid Transportation on Natural Frequencies

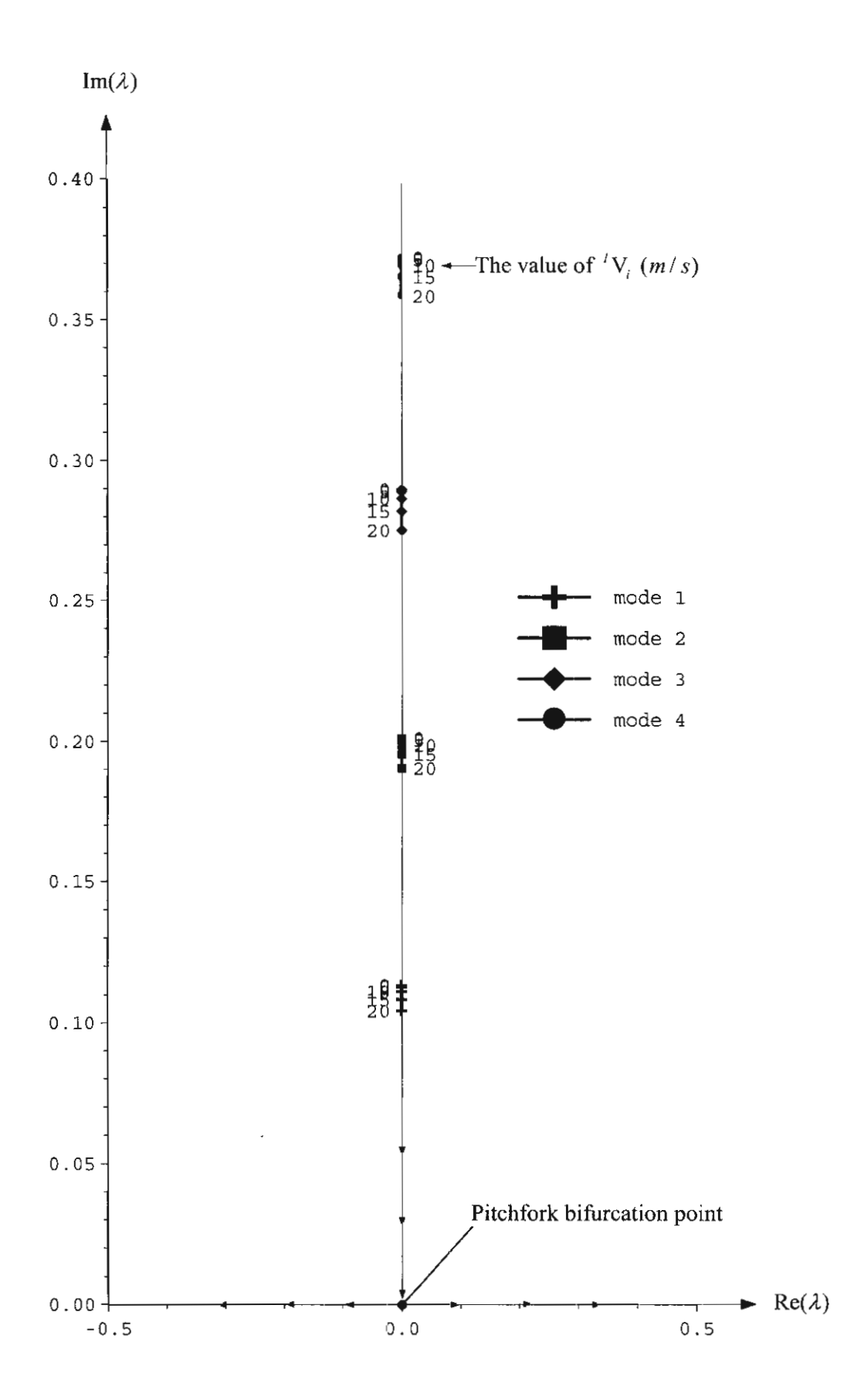


Figure 4.15 Effect of Fluid Transportation on the Argand Diagrams

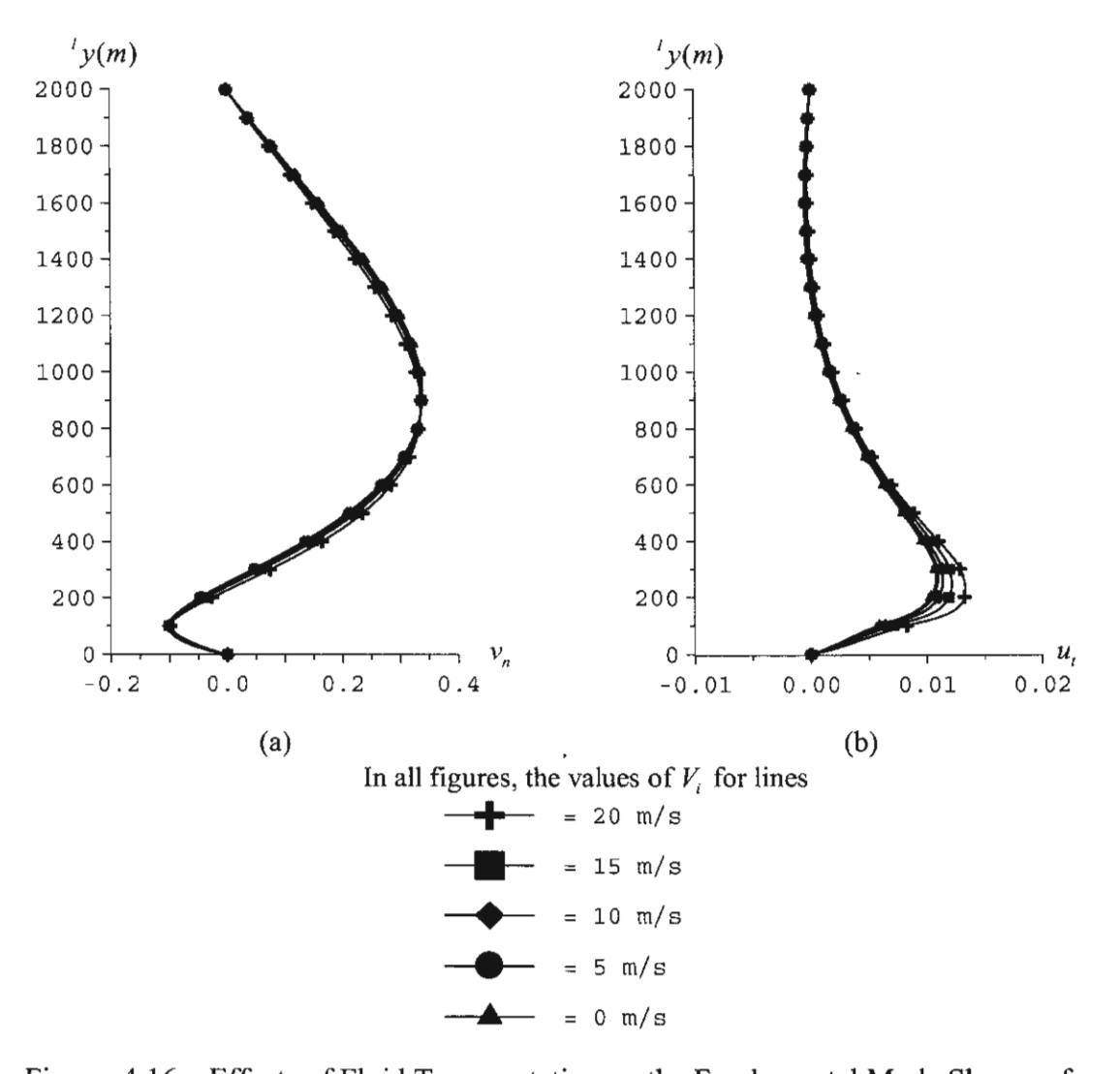


Figure 4.16 Effects of Fluid Transportation on the Fundamental Mode Shapes of

(a) Normal Vibrations (b) Tangential Vibrations

4.5.2.1 Fluid transportation diminishes natural frequencies of the marine pipe. As shown in Figure 4.14, the natural frequencies of the pipe decrease with an escalation of the internal flow velocity. When the internal flow velocity is increased continuously, the eigencurves tend to intersect the internal flow velocity axis at the point where the internal flow velocity possesses the critical values and the natural frequencies are zero. This implies that buckling of the pipe due to the effect of fluid transportation is of static nature, and may be referred to as divergence buckling.

4.5.2.2 Fluid transportation reduces the dynamic stability of the linearized system of the marine pipe. The complex plane of the Argand diagram is

displayed in Figure 4.15. It is found that a continuous augmentation of the internal flow velocity causes the pipe to experience 'the static buckling' or 'the divergence instability' at the Pitchfork bifurcation point, where the internal flow velocity possesses the critical value. Based on the Liapunov indirect method, the complex eigenvalues of the marine pipe as shown in Figure 4.15 have all zero real part, therefore free vibrations of the linearized system of the marine pipe possess stable oscillations and critical behavior.

4.5.2.3 Fluid transportation slightly affects the mode shapes of the free vibrations of the marine pipe in the normal, and tangential, directions as shown in Figures 4.16 (a), and 4.16 (b), respectively.

4.5.3 Effects of Fluid Transportation on Nonlinear Vibration Behavior

The effects of fluid transportation on nonlinear forced vibrations of the marine pipes are illustrated in Figures 4.17 - 4.19, and are summarized as follows:

- 4.5.3.1 Fluid transportation increases nonlinear responses of the forced vibrations of the marine pipe. The nonlinear responses in the time period 0-60 seconds of the forced vibrations of the pipe without fluid transportation are plotted on the left-hand side of Figure 4.17, while those of the pipe with a transportation rate of 20 m/s are displayed on the right-hand side of the same figure. By comparing the left- and the right-hand side figures, it is evident that the pipe with a transportation rate of 20 m/s possesses significantly larger amplitudes of the normal, tangential, and radial vibrations, than the pipe without fluid transportation.
- 4.5.3.2 Fluid transportation affects time histories of nonlinear vibrations of the marine pipe. Figures 4.18 (a), 4.18 (b) and 4.18 (c) demonstrate the time histories of the normal vibrations of the top part ($^{\prime}y = 1800$ m), of the middle part ($^{\prime}y = 1000$ m), and of the bottom part ($^{\prime}y = 400$ m) of the pipes, respectively. It is seen that the pipe with a transportation rate of 20 m/s possesses significantly larger amplitudes of the normal vibrations than the taut pipe without fluid transportation.
- 4.5.3.3 Fluid transportation reduces the stability of motion of the marine pipe. The trajectories of the normal vibrations of the top part ($^{1}y = 1800 \text{ m}$),

of the middle part ($^{1}y = 1000$ m), and of the bottom part ($^{1}y = 400$ m) of the pipes are plotted in the phase planes as shown in Figures 4.24(a), 4.24(b) and 4.24(c), respectively. In all the figures, the orbital motion of the trajectory of the pipe with a transportation rate of 20 m/s is more complex and unsteadier than that of the pipe without fluid transportation. This result indicates that the orbital stability of the pipe is reduced by the effect of fluid transportation.

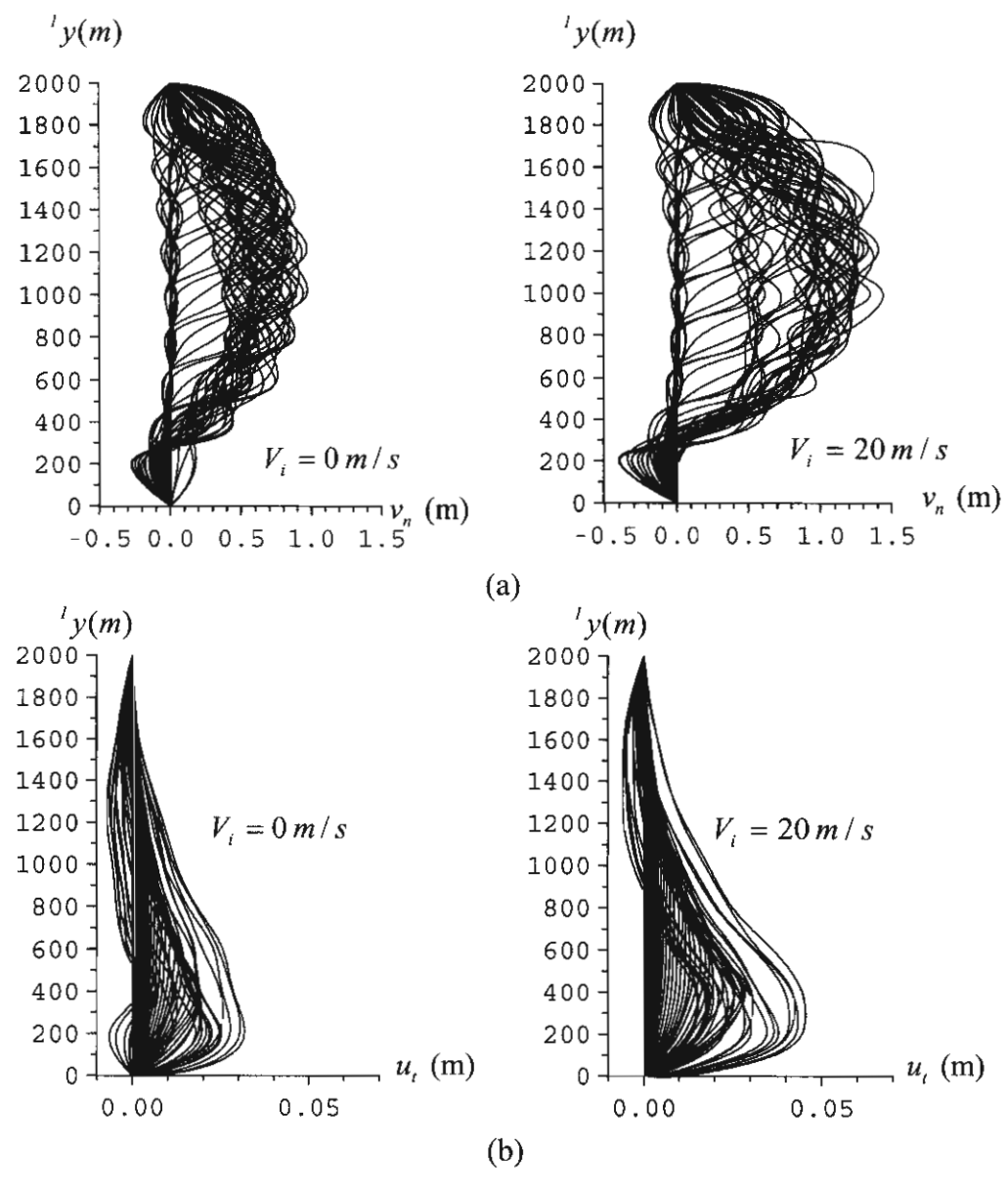


Figure 4.17 Nonlinear Responses in Time 0-60 Seconds of

(a) Normal Vibrations (b) Tangential Vibrations

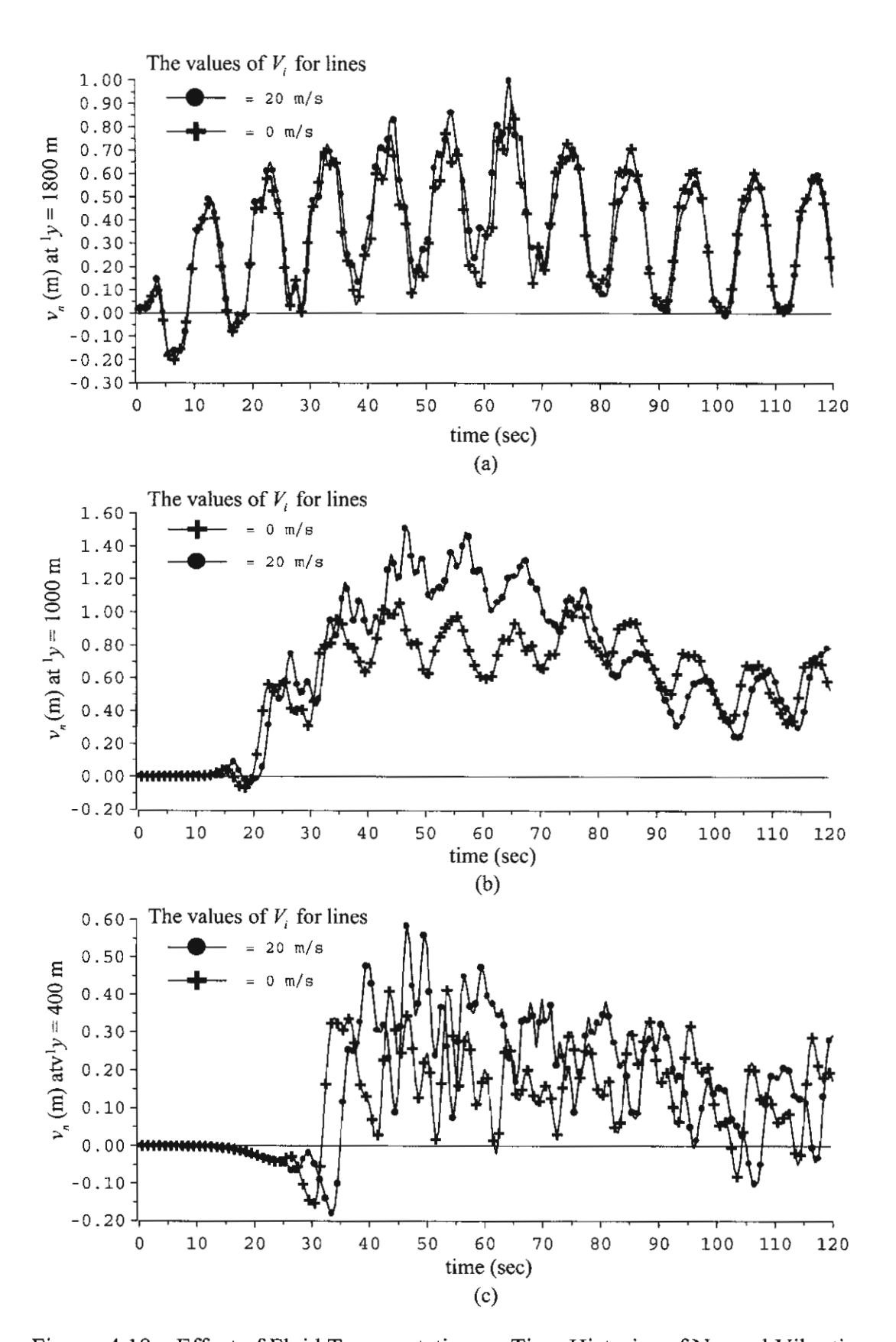


Figure 4.18 Effect of Fluid Transportation on Time Histories of Normal Vibrations

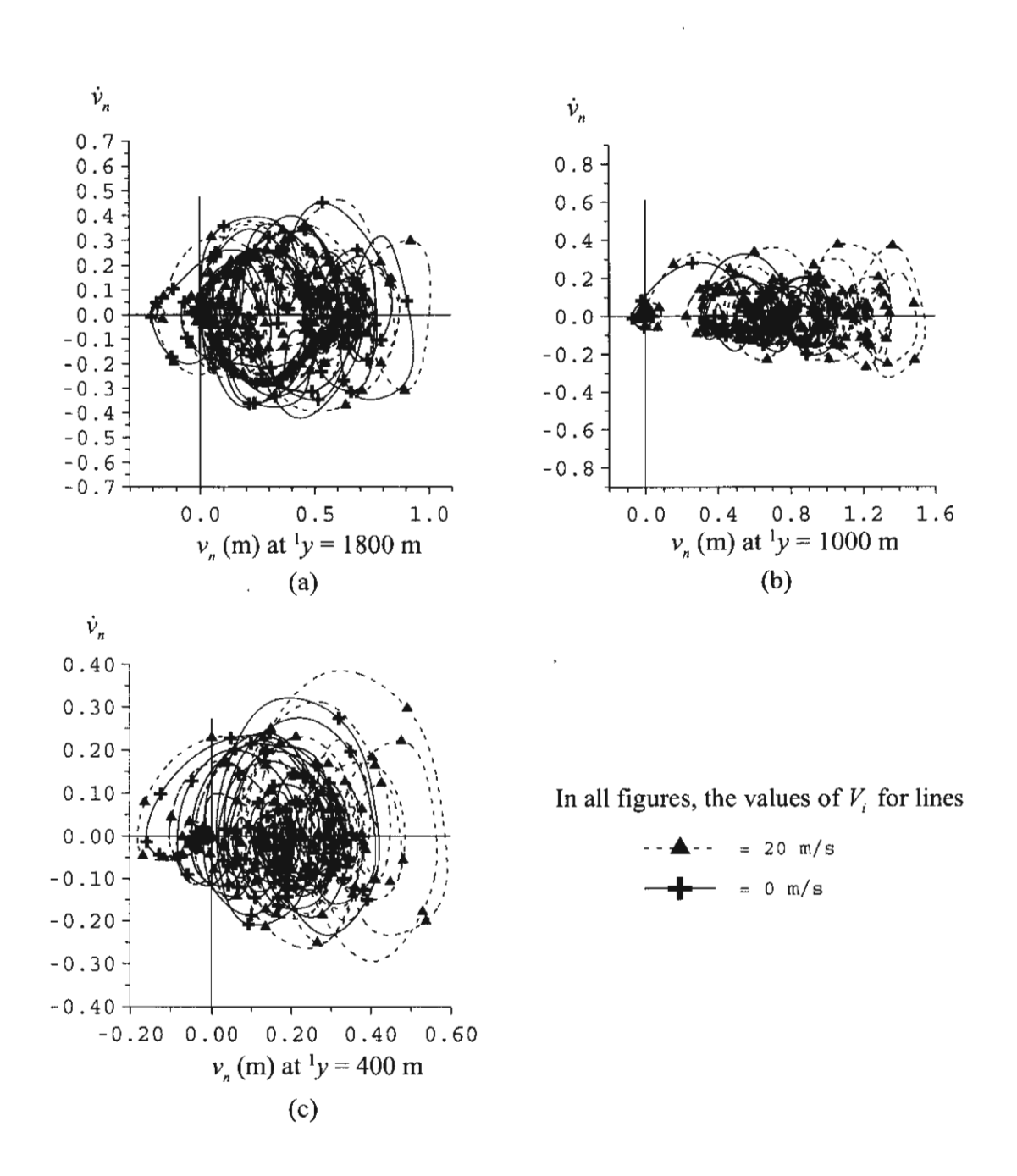


Figure 4.19 Effect of Fluid Transportation on Trajectories of Normal Vibrations

5. CONCLUSIONS

This research proposes the three-dimensional model formulation of an extensible marine risers/pipes transporting fluid. The combined action of the large axial deformation bending, torsion, and the internal flow are taken into account in the formulation. A number of original theories of extensible elastica and new formulation of riser/pipe transporting fluid have been developed in this research.

The original theories compose of the extensible elastica theorems and the apparent tension concept. The extensible elastica theorems are developed in three viewpoints; namely, the total Lagrangian, the updated Lagrangian, and the Eulerian descriptions. The apparent tension concept is introduced in order to cover the effect of the Poisson's ratio.

The three-dimensional model formulation of an extensible marine risers/pipes is developed via a variational approach based on the extensible elastica theory, the work-energy principle, and the kinematics theory of mass transported on the moving frame. The total virtual internal work of the risers/pipes consists of virtual strain energies due to large axial deformation, bending rigidity, and torsional deformations. The total virtual external work consists of virtual work done by effective weight of the risers/pipes, hydrodynamic loading, inertial forces of the risers/pipes and transported fluid. The vectorial summation of forces and moments is used to validate the variational formulation. The advantages of the present models relate to the flexibility offered in choice of the independent variable, and the possibility of applying them to numerous elastica problems, including some biomechanics applications.

The numerical examples of the three-dimensional static analysis and two —dimensional dynamic analysis have been presented by using the finite element method based on the updated Lagrangian formulation. The parametric studies are established and elaborated in order to explore the profound effects of axial deformation, and fluid transportation on behaviors of the pipe. It is found that the effects of axial deformations are very important to nonlinear static, nonlinear vibration behaviors, and static and dynamic stabilities of marine pipes. The effects of fluid transportation in present practice are found to be significant to nonlinear

nonlinear vibration behavior, but insignificant to nonlinear static behavior and natural frequencies of the pipe.

From the results of parametric studies, it can be concluded that axial deformation reduces large deflections and nonlinear responses of the pipe, and increases static and dynamic stabilities of the pipe. At the same time, fluid transportation yields the contrary effects. Consequently, if axial deformation of the pipe is designed too low, the pipe may be subjected to either poor serviceability or buckling due to insufficient stiffness. On the other hand, if fluid transportation is designed too high, the pipe may experience either poor serviceability or buckling due to overloading. Therefore, the designers are encouraged to examine these effects carefully in the design of the marine risers/pipes, especially for the design of the highly flexible pipes with large sag.

Finally, the mathematical models developed in this research work could be used as the basis of other research work and for the development of commercial programs for marine riser pipe analysis. It is hoped that this study will be of some value in the analysis and the design not only of marine risers/pipes, but also of any kind of long slender rods and pipes that pursue rigorous treatments of extensibility, and transported mass.

REFERENCES

- Ahmad, S. and Datta, T.K., 1989, "Dynamic Response of Marine Risers,"
 Engineering Structures, Vol. 11, pp. 179-188.
- Antman, S.S., 1991, "Nonlinear Problems of Elasticity," Applied Mathematical Sciences 107, Springer Verlag.
- 3. Atadan, A.S., Calisal, S.M., Modi, V.J. and Guo, Y., 1997, "Analytical and Numerical Analysis of the Dynamics of a Marine Riser Connected to a Floating Platform," Ocean Engineering, Vol. 24, No. 2, pp. 111-131.
- 4. Atanackovic, T.M., 1997, "Stability Theory of Elastic Rods," Series on Stability, Vibration and Control of Systems, World Scientific, Vol. 1.
- 5. Bar-Avi, P., 2000, "Dynamic Response of Risers Conveying Fluid," Journal of Offshore Mechanics and Arctic Engineering, Vol. 122, pp. 188-193.
- Bathe, K.J., Ozdemir, H. and Wilson, E.L., 1974, Static and Dynamic Geometric and Material Nonlinear Analysis, Report No. UCSESM 74-4, California, University of California, Berkeley.
- 7. Bathe, K.J., 1996, Finite Element Procedures, New Jersey, Prentice Hall.
- 8. Bennett, B.E. and Metcalf, M.E., 1977, "Nonlinear Dynamic Analysis of Coupled Axis and Lateral Motions of Marine Risers," **Offshore Technology Conference**, Vol. 1, pp. 2776-2782.
- Bernitsas, M.M., 1980, "Riser Top Tension and Riser Buckling Loads,"
 Computational Methods for Offshore Structures ASME, Vol. 1, pp. 101-109.
- Bernitsas, M.M., 1982, "A Three-Dimensional Nonlinear Large-Deflection Model for Dynamic Behavior of Risers, Pipelines, and Cables," Journal of Ship Research, Vol. 26, No. 1, pp. 59-64.
- Bernitsas, M.M., Kokarakis, J.E. and Imron, A., 1985, "Large Deformation Three-Dimensional Static Analysis of Deep Water Marine Risers," Applied Ocean Research, Vol. 7, No. 4, pp. 178-187.
- 12. Bernitsas, M.M. and Kokarakis, J.E., 1988, "Importance of Nonlinearities in Static Riser Analysis," **Applied Ocean Research**, Vol. 10, No. 1, pp. 2-9.
- 13. Bernitsas, M.M. and Vlahopoulous, N., 1989, "Three Dimensional Analysis of A Riser Bundle by A Substructuring and Incremental Finite Element

- Algorithm," International Journal for Numerical Methods in Engineering, Vol. 28, pp. 2517-2540.
- Burgess, J.J. and Triantafyllou, M.S., 1988, "The Elastic Frequencies of Cables,"
 Journal of Sound and Vibration, Vol. 120, pp. 153-165.
- 15. Burke, B.G., 1974, "An Analysis of Marine Risers for Deep Water," **Journal of etroleum Technology**, Vol. 14, pp. 455-465.
- Butler, H.L., Delfosse, C., Galef, A. and Thorn, B.J., 1967, "Numerical Analysis of a Beam Under Tension," Journal of Structural Division, Proceeding of ASCE, Vol. 76, No. 8, pp. 165-173.
- 17. Chakrabarti, S.K. and Frampton, R.E., 1982, "Review of Riser Analysis Techniques," **Applied Ocean Research**, Vol. 4, No. 2, pp. 73-90.
- Chen, Y.H. and Lin, F.M., 1989, "Drag-Force Linearization for Nonlinear Analysis of Marine Risers," Ocean Engineering, Vol. 16, No. 3, pp. 265-280.
- Chou, D.Y., Minner, W.F., Ragusa, L. and Ho, R.T., 1978, "Dynamic Analysis of Coupled OTEC Platform Cold Water Pipe System," Offshore Technology Conference, Vol. 1, pp. 3338-3345.
- 20. Chucheepsakul, S., 1983, "Large Displacement Analysis of a Marine Riser,"
 Doctor of Philosophy Dissertation, Civil Engineering Program, The
 University of Texas at Arlington.
- Chucheepsakul, S. and Huang, T., 1994, "Influence of Transported Mass on the Equilibrium Configuration of Risers," Proceeding of 4th International Offshore and Polar Engineering Conference, Vol. 2, pp. 246-249.
- 22. Chucheepsakul, S., Huang, T. and Laohaporjanat, P., 1995, "Effects of Axial Deformation on the Equilibrium Configurations of Marine Cables," Proceedings of 5th International Offshore and Polar Engineering Conference, Vol. 2, pp. 244-248.
- 23. Chucheepsakul, S. and Huang, T., 1997, "Effect of Axial Deformation on Natural Frequencies of Marine Cables," Proceedings of 7th International Offshore and Polar Engineering Conference, Vol. 2, pp. 131-136.
- 24. Chucheepsakul, S., Huang, T. and Monprapussorn, T., 1999, "Influence of Transported Fluid on Behavior of an Extensible Flexible Riser/Pipe,"

- Proceedings of 9th International Offshore and Polar Engineering Conference, Vol. 2, pp. 286-293.
- Chucheepsakul, S. and Monprapussorn, T., 2001, "Nonlinear Buckling of Marine Elastica Pipes Transporting Fluid," International Journal of Structural Stability and Dynamics, Vol. 1, No. 3, pp. 333-365.
- Chucheepsakul, S., Monprapussorn, T. and Huang, T., 2002, "Large Strain Formulations of Extensible Flexible Marine Pipes Transporting Fluid," to be published in Journal of Fluids and Structures.
- Chung, J.S. and Whitney, A.K., 1983, "Dynamic Vertical Stretching Oscillation of a Deep-Ocean Mining Pipe," Journal of Energy Resources Technology, ASME, Vol. 105, pp. 195-200.
- 28. Chung, J.S., Cheng, B.R. and Huttelmaier, H.P., 1994a, "Three-Dimensional Coupled Responses of a Vertical Deep-Ocean Pipe: Part I. Excitation at Pipe Ends and External Torsion," International Journal of Offshore and Polar Engineering, Vol. 4, No. 4, pp. 320-330.
- 29. Chung, J.S., Cheng, B.R. and Huttelmaier, H.P., 1994b, "Three-Dimensional Coupled Responses of a Vertical Deep-Ocean Pipe: Part II. Excitation at Pipe Top and External Torsion," International Journal of Offshore and Polar Engineering, Vol. 4, No. 4, pp. 331-339.
- Chung, J.S. and Cheng, B.R., 1996, "Effects of Elastic Joints on 3-D Nonlinear Responses of a Deep-Ocean Pipe," International Journal of Offshore and Polar Engineering, Vol. 6, No. 3, pp. 203-211.
- 31. Dareing, D.W. and Huang, T., 1979, "Marine Riser Vibration Response Determined by Modal Analysis," **Journal of Energy Resources Technology**, Vol. 101, No. 3, pp. 159-166.
- Doll, R.W. and Mote, C.D., 1976, "On the Dynamic Analysis of Curved and Twisted Cylinders Transporting Fluids," Journal of Pressure Vessel Technology, ASME, Vol. 98, pp. 143-150.
- 33. Ertas, A. and Kozik, T.J., 1987, "A Review of Approaches to Riser Modeling," **Journal of Energy Resources Technology**, Vol. 109, No. 3, pp. 155-160.

- 34. Etok, E.U. and Kirk, C.L., 1981, "Random Dynamic Response of a Tethered Buoyant Platform Production Riser," **Applied Ocean Research**, Vol. 3, No. 2, pp. 73-86.
- Felippa, C.A. and Chung, J.S., 1981, "Nonlinear Static Analysis of Deep Ocean Mining Pipe – Part 1: Modeling and Formulation," Journal of Energy Resources Technology, Vol. 103, No. 1, pp. 11-15.
- 36. Fischer, W. and Ludwig, M. 1966, "Design of Floating Vessel Drilling Risers," **Journal of Petroleum Technology**, Vol. 3, No. 1, pp. 272-283.
- 37. Fung, Y.C., 1965, Foundations of Solid Mechanics, New Jersey, Prentice-Hall.
- 38. Gambhir, M.L., Barrington, D.E. and Batchelor, V., 1978, "Parametric Study of Free Vibration of Sagged Cables," **Computers & Structures**, Vol. 8, No. 5, pp. 641-648.
- Gardner, T.N. and Kotch, M.A., 1976, "Dynamic Analysis of Risers and Caissons by the Element Method," Offshore Technology Conference, Vol. 1, pp. 2650-2655.
- 40. Gear, C.W., 1971, Numerical Initial Value Problems in Ordinary Differential Equations, New Jersey, Prentice Hall.
- 41. Gnone, E., Signorelli, P. and Giuliano, V., 1975, "Three-Dimensional Static and Dynamic Analysis of Deep-Water Sealines and Risers," **Offshore**Technology Conference, Vol. 1, pp. 2326-2331.
- 42. Goodman, T.R. and Breslin, J.P., 1976, "Static and Dynamics of Anchoring Cable in Waves," **Journal of Hydronautics**, Vol. 10, pp. 113-120.
- 43. Gosse, C.G. and Barksdale, G.L., 1969, "The Marine Riser a Procedure for Analysis," Offshore Technology Conference, Vol. 1, pp. 1080-1085.
- 44. Graham, R.D., Frost, M.A. and Wilhoit, J.C., 1965, "Analysis of the Motion of Deep-Water Drill Strings – Part 1: Forced Lateral Motion – and Part 2: Forced Rolling Motion," Journal of Engineering for Industry, Transaction of ASME, Vol. 10, No. 2, pp.137-147.
- 45. Gregory, R.W. and Païdoussis, M.P., 1966, "Unstable Oscillation of Tubular Cantilevers Conveying Fluid. I. Theory," **Proceedings of the Royal Society** (London) A, Vol. 293, pp. 512-537.

- 46. Hahn, G.D., She, M. and Carney, J.F., 1992, "Buckle Propagation in Submarine Pipelines," **ASCE Journal of Engineering Mechanics**, Vol. 118, No. 11, pp. 2191-2206.
- 47. Henghold, W.M. and Russell, J.J., 1977, "Free Vibrations of Cables in Three Dimensions," **Journal of Structural Division**, **ASCE**, Vol. 103, No. ST5, pp. 1127-1136.
- 48. Heuze, L.A.A., 1975, "A 4000 Ft Riser," **Offshore Technology Conference**, Vol. 1, pp. 2325-2329.
- 49. Holmes, P.J., 1978, "Pipes Supported at Both Ends Cannot Flutter," **Journal of Applied Mechanics**, **ASME**, Vol. 45, pp. 619-622.
- 50. Housner, G.W., 1952, "Bending Vibrations of a Pipe Line Containing Flowing Fluid," Journal of Applied Mechanics, ASME, Vol. 19, pp. 205-208.
- Huang, T. and Chucheepsakul, S., 1985, "Large Displacement Analysis of a Marine Riser," Journal of Energy Resources Technology, Vol. 107, No. 2, pp. 54-59.
- 52. Huang, T.S. and Leonard, J.W., 1990, "Lateral Stability of a Submarine Flexible Hoseline," **Ocean Engineering**, Vol. 17, No. 1, pp. 35-52.
- 53. Huang, T. and Kang, Q.L., 1991, "Three Dimensional Analysis of a Marine Riser with Large Displacements," International Journal of Offshore and Polar Engineering, Vol. 1, No. 4, pp. 300-306.
- 54. Huang, T., 1992, "A Static Equilibrium Formulation Including Axial Deformation for Marine Cables," Proceedings of 2nd International Offshore and Polar Engineering Conference, Vol. 2, pp. 252-255.
- 55. Huang, T., 1993, "Kinematics of Transported Mass Inside Risers and Pipes,"
 Proceeding of 3rd International Offshore and Polar Engineering
 Conference, Vol. 2, pp. 331-336.
- Huddleston, J.V., 1981, "Computer Analysis of Extensible Cables," Journal of Engineering Mechanics Division, ASCE, Vol. 107, pp. 27-37.
- 57. Huyse, L., Singh, M.C. and Maes, M.A., 1997, "A Static Drilling Riser Model Using Free Boundary Conditions," **Ocean Engineering**, Vol. 24, No. 5, pp. 431-444.

- 58. Irani, M.B., Modi, V.J. and Weit, F., 1987, "Riser Dynamics with Internal Flow and Nutation Damping," **Proceedings 6th International Offshore Mechanics and Arctic Engineering Symposium**, Vol. 3, pp. 119-125.
- 59. Jain, A.K., 1994, "Review of Flexible Risers and Articulated Storage Systems," Ocean Engineering, Vol. 21, No. 8, pp. 733-750.
- 60. Jones, M.R., 1975, Problem Affecting the Design of Drilling Risers, SPE paper 5268, London, Society of Petroleum Engineering.
- 61. Karamanos, S.A. and Tassoulas, J.L., 1991, "Stability of Inelastic Tubes Under External Pressure and Bending," **ASCE Journal of Engineering Mechanics**, Vol. 117, No. 12, pp. 2845-2861.
- 62. Kirk, C.L., Etok, E.U. and Cooper, M.T., 1979, "Dynamic and Static Analysis of a Marine Riser," **Applied Ocean Research**, Vol. 1, No. 3, pp. 95-105.
- 63. Kirk, C.L., 1985, "Dynamic Response of Marine Risers by Single Wave and Spectral Analysis Methods," **Applied Ocean Research**, Vol. 7, No. 1, pp. 2-13.
- 64. Kokarakis, J.E. and Bernitsas, M.M., 1987, "Nonlinear Three-Dimensional Dynamic Analysis of Marine Risers," **Journal of Energy Resources Technology**, Vol. 109, No. 5, pp. 105-111.
- 65. Kopecky, J.A., 1971, "Drilling Riser Stress Measurements," **Petroleum Engineering and Technology**, Vol. 14, No. 71, pp. 879-890.
- 66. Krolikowski, L.P. and Gray, T.A., 1980, "An Improved Linearization Technique for Frequency Domain Riser Analysis," **Offshore Technology Conference**, Vol. 1, pp. 3777-3783.
- 67. Larsen, C.M., 1976, "Marine Riser Analysis," Norwegian Maritime Research, Vol. 4, pp. 15-26.
- 68. Lin, H.P. and Perkins, N.C., 1995, "Free Vibration of Complex Cable/Mass System: Theory and Experiment," **Journal of Sound and Vibration**, Vol. 179, pp. 131-149.
- 69. Love, A.E.H., 1944, A Treatise on the Mathematical Theory of Elasticity, London, Cambridge University Press.
- 70. Maison, J.R. and Lea, J.F., 1977, "Sensitivity Analysis of Parameters Affecting Riser Performance," **Offshore Technology Conference**, Vol. 1, pp. 2918-2923.

- 71. Marine Computation Services International, 1989, FLEXCOM-3D Program Manuals, Galway, MCSI.
- 72. Meirovitch, L., 1997, Principles and Techniques of Vibrations, New Jersey, Prentice Hall.
- 73. Moe, G. and Chucheepsakul, S., 1988, "The Effect of Internal Flow on Marine Risers," Proceedings 7th International Offshore Mechanics and Arctic Engineering Symposium, Vol. 1, pp. 375-382
- 74. Moe, G., Stromsem, K.C. and Fylling, I., 1994, "Behavior of Risers with Internal Flow Under Various Boundary Conditions," **Proceeding of 4th International Offshore and Polar Engineering Conference**, Vol. 2, pp. 258-262.
- 75. More, J., Garbow, B.S. and Hillstrom, H., 1980, User guide for MINPACK-1, Illinois, Argonne National Laboratories.
- Morgan, G.W., 1972, Riser dynamic Analysis, Texas, Sun Oil Production Research Laboratory.
- 77. Morison, J.R., O'Brian, M.P., Johnson, J.W. and Schaaf, S.A., 1950, "The Force Exerted by Surface Waves on Piles," **Transaction of American Institute of Mining Metallic Engineering**, Vol. 189, pp. 149-154.
- 78. Munson, B.R., Young, D.F. and Okiishi, T.H., 1994, Fundamentals of Fluid Mechanics, Toronto, John Wiley.
- 79. National Engineering and Science Company, 1965, Structural Dynamic Analysis of the Riser and Drill String for Project Mohole, New York, NESCO, pp. 1-2.
- Natvig, B.J., 1980, "A Large Angle Large Displacement Analysis Method for Marine Risers," Computational Methods for Offshore Structures, ASME, Vol. 1, pp. 111-125.
- Ngiam, P.C.A., 1997, "Intrinsic Coordinate Elements for Large Deflection of Offshore Pipelines," Proceeding of 7th International Offshore and Polar Engineering Conference, Vol. 2, pp. 313-320.
- 82. O'Brien, P.J., McNamara, J.F. and Dunne, F.P.E., 1988, "Three Dimensional Nonlinear Motions of Risers and Offshore Loading Towers," Journal of Offshore Mechanic and Arctic Engineering, Vol. 110, pp. 232-237.
- 83. O'Brien, P.J. and McNamara, J.F., 1989, "Significant Characteristics of Three-Dimensional Riser Analysis," **Engineering Structures**, Vol. 11, pp. 223-233.

- 84. Oran, C., 1992, "Effect of Static Offset on TLP Modeling," **ASCE Journal of Engineering Mechanics**, Vol. 118, No. 1, pp. 74-91.
- 85. Owen, D.J. and Qin, J.J., 1987, "Nonlinear Dynamics of Flexible Risers by the Finite Element Method," **Proceedings 6th International Offshore Mechanics and Arctic Engineering Symposium**, Vol. 1, pp. 163-170.
- Païdoussis, M.P., 1970, "Dynamics of Tubular Cantilevers Conveying Fluid,"
 Journal of Mechanical Engineering Science, Vol. 12, pp. 85-103.
- 87. Païdoussis, M.P., 1998, Fluid-Structure Interactions, Slender Structures and Axial Flow, Vol. 1, New York, Academic Press.
- 88. Patel, H.M. and Seyed, F.B., 1989, "Internal Flow-Induced Behaviour of Flexible Risers," **Engineering Structures**, Vol. 11, No. 3, pp. 266-280.
- 89. Patel, M.H. and Seyed, F.B., 1995, "Review of Flexible Riser Modelling and Analysis Techniques," **Engineering Structures**, Vol. 17, No. 4, pp. 293-304.
- Patrikarakis, N.M. and Kriezis, G.A., 1987, "Linear Dynamics of Flexible Risers," Journal of Offshore Mechanics and Arctic Engineering, OMAE, vol. 109, pp. 254-262.
- Paulling, J.R., 1977, A Linearized Dynamic Analysis of the Coupled OTEC Cold-Water Pipe and HMB-1 Barge System, New York, Morris Guralnick Associates.
- 92. Pesce, C.P., Fujarra, A.L.C., Simos, A.N. and Tannuri, E.A., 1999, "Analytical and Closed Form Solutions for Deep Water Riser-Like Eigenvalue Problem,"
 Proceedings of 9th International Offshore and Polar Engineering
 Conference, Vol. 2, pp. 255-264.
- Press, W.H., Teukolsky, S.A., Vettering, W.T. and Flannery, B.P., 1992,
 Numerical Recipes in Fortran, 2nd ed., New York, Cambridge University Press.
- 94. Safai, V.H., 1983, "Nonlinear Dynamic Analysis of Deep Water Risers,"

 Applied Ocean Research, Vol. 5, No. 4, pp. 215-225.
- Sexton, R.M. and Agbezuge, L.K., 1976, "Random Wave and Vessel Motion Effects on Drilling Riser Dynamics," Offshore Technology Conference, Vol. 1, pp. 2650-2658.
- Seyed, F.B. and Patel, H.M., 1992, "Mathematics of Flexible Risers Including Pressure and Internal Flow Effects," Marine Structures, Vol. 5, pp. 121-150.

- 97. Shames, I.H., 1992, Mechanics of Fluids, Singapore, McGraw-Hill.
- 98. Shih, B. and Tadjbakhsh, I.G., 1984, "Small-Amplitude Vibrations of Extensible Cables," **ASCE Journal of Engineering Mechanics**, Vol. 110, pp. 569-576.
- Smith, B.T., Boyle, J.M., Dongarra, J.J., Garbow, B.S., Ikebe, Y., Klema, V.C. and Moler, C.B., 1976, Matrix Eigensystem Routines - EISPACK Guide, New York, Springer-Verlag.
- 100. Spanos, P.D., Tein, W.Y. and Ghanem, R., 1990, "Frequency Domain Analysis of Marine Risers with Time Dependent Tension," **Applied Ocean Research**, Vol. 12, No. 4, pp. 200-210.
- 101. Sparks, C.P., 1984, "The Influence of Tension, Pressure and Weight on Pipe and Riser Deformations and Stresses," Journal of Energy Resources Technology, ASME, Vol. 106, pp. 46-54.
- 102. St. Denis, M. and Armijo, L., 1955, "On Dynamic Analysis of the Mohole Riser," Proceeding of Ocean Science and Ocean Engineering Conference, Vol. 1, pp. 325-330.
- 103. Thampi, S.K. and Niedzwecki, J.M., 1992, "Parametric and External Excitation of Marine Risers," ASCE Journal of Engineering Mechanics, Vol. 118, No. 5, pp. 942-960.
- 104. Thompson, J.M.T. and Lunn, T.S., 1981, "Static Elastica Formulations of a Pipe Conveying Fluid," **Journal of Sound and Vibration**, Vol. 77, pp. 127-132.
- 105. Tidwell, D.R. and Ilfrey, W.T., 1971, "Developments in Marine Drilling Riser Technology," Petroleum Engineering and Technology, Vol. 14, No. 69, pp. 272-283.
- 106. Tikhonov, V.S., Safronov, A., Kamyshev, M.A. and Figarov, N.G., 1996, "Numerical Analysis of Pipeline Dynamics in Seabed Laying," International Journal of Offshore and Polar Engineering, Vol. 6, No. 3, pp. 212-218.
- Timoshenko, S.P. and Goodier, J.N., 1982, Theory of Elasticity, Singapore, McGraw-Hill.
- 108. Tjavaras, A.A. and Triantafyllou, M.S., 1996, "Shock Waves in Curved Synthetic Cables," ASCE Journal of Engineering Mechanics, Vol. 122, pp. 308-315.